Declaration

I hereby certify that this material, which I now submit for assessment on the programme of study leading to the award of Doctor of Philosophy is entirely my own work, that I have exercised reasonable care to ensure that the work is original, and does not to the best of my knowledge breach any law of copyright, and has not been taken from the work of others save and to the extent that such work has been cited and acknowledged within the text of my work

Zarah Walsh

ID No.: 51083791

Date: 30/03/10

Acknowledgements

First and foremost I would like to thank my supervisors Dr. Mirek Macka and Prof. Brett Paull for all their help and support throughout the course of my PhD. These past three years have been a great experience.

Dr. Silvija Abele, it was a pleasure to work with you, thank you for all your help, support and guidance throughout these past three years. Thank you also for introducing the very helpful chocolate/coffee breaks, they work wonders on the stress levels!

Thanks must also go to Dr. Silvia Scarmagnani and Dr. Fernando Benito Lopez for the long collaboration on spiropyran based stationary phases which make up Chapter 3 and the great friendship.

Additionally Dr. Nameer Alhashimy is acknowledged for his contribution to this chapter, with the synthesis of the spiropyran dyes for the preliminary experiments.

I must also thank my colleague Dr. Damian Connolly for his immense knowledge of all things chromatography related and his willingness to share this with me when it was needed.

Dr. Fu-Qiang Nie is also acknowledged for the fabrication of numerous PMMA micro-fluidic chips for the EOF experiments conducted in Chapter 4 and for excellent thoughts for the day!

I would like to thank Dr. František Švec for allowing me to spend some time in his lab at the Lawrence Berkeley National Laboratory, a large portion of the results in Chapter 4 and the entirety of the data in Chapter 5 was obtained during my stay in Berkeley. I would also like to thank my colleagues in the LBNL, Dr. Pavel Levkin, Dr. Jana Křenkova and Dr. Marian Snauko, for their assistance during my stay.

Another portion of the data obtained in Chapter 4 comes from a research trip to Masaryk University, Czech Republic. I would like to thank Prof. Petr Klán and Dr. Dominik

Dedication

To my Parents,

This thesis is dedicated to you for everything you have given me and done for me throughout my life. Without your support and encouragement I would not have been able to get this far.

There is so much to thank you for, thank you for 'carrying me', guiding me and encouraging me to steer clear of Home Ec. and do Science instead....probably the best thing you ever told me to do!

Most of all thank you for letting me be me and encouraging me to follow my dreams, even if I never would become a prima ballerina!

Table of Contents

Abstract

This thesis is entitled 'Exotic Monoliths', which has been defined, in the context of this thesis, as monoliths; (1) synthesised by methods not previously described in the literature, (2) synthesised from commonly used silica or organic polymer materials but whose surface has been modified with a novel material such as dyes, nano-particles and biologically active compounds, and (3) synthesised from materials which are not based on silica or organic polymers, such as zirconia or titania. The first two of these definitions have been the main focus for this thesis.

The thesis itself comprises five chapters. Chapter 1 presents an introduction to polymer monolith stationary phases and a detailed summary of the many different methods of synthesis. The surface modification of the monoliths and their applications in separation science, along with a short comparison with particle packed columns and introduction to some more novel inorganic monoliths is also presented.

Following on from this, Chapter 2 shows the preliminary work carried out on synthesising monoliths in capillary. Presented in this chapter is an investigation of thermally initiated polymerisation in standard 100 μm i.d. capillary and in larger diameter fused silica and PEEK capillary moulds. Photo-initiated polymerisation using both conventional UV lamps and light emitting diodes is also investigated, along with a novel application of LED synthesised monoliths, i.e. using short plugs of monoliths as retaining frits for column packing. Finally a short study of the ability to reproduce literature methods of surface modification by successfully grafting a layer of methacrylic acid and 2-aminoethyl methacrylate on the surface of a monolithic scaffold is shown.

Chapter 3 presents the research carried out on the modification of organic polymer monoliths with photochromic dyes and the synthesis of monoliths directly from modified photochromic dyes with a polymerisable double bond. A novel application of these photochromic monoliths is their use as photo-switchable electroosmotic pumps allowing eluent flow to be controlled by light in micro-fluidic devices, which is also

presented in this chapter. It is shown that by switching the wavelength of irradiation from visible to ultraviolet an increase or decrease, respectively, in the flow rate can be observed.

The final two chapters, 4 and 5, present novel methods of monolith synthesis using light emitting diodes in the visible region. Chapter 4 looks at the polymerisation of methacrylate monomers within polyimide coated moulds using red light while Chapter 5 looks at the polymerisation of styrenic monomers in poly(tetrafluoroethylene) coated capillaries using blue light emitting diode arrays. In both cases the characterisation and application of the synthesised monoliths is presented showing that they are suited to use in separation science. The suitability of this method to polymerise monoliths in chips moulds was also shown, as was the ability of the initiation system activated by red light to be used for the photo-initiated grafting of chromophoric monomers.

A final section entitled 'General Conclusions and Outlook' provides a summary of the thesis and areas for further work.

Aims of this Project

The aims of this project were four-fold consisting of;

1. the investigation of alternative methods of photo-initiating the polymerisation of monolithic materials using light emitting diodes with a view to the polymerisation of styrenic monomers and the polymerisation of monoliths within polyimide coated capillary,

2. the investigation of new types of surface modification, in particular the immobilisation of dyes on the surface of monolithic scaffolds,

3. the investigation of monoliths synthesised from unusual starting materials other than standard organic monomers, in particular dye monomers, and

4. the investigation of novel applications of monolithic materials such as the use of monolith plugs as retaining frits or as electroosmotic pumps.

In addition to these main aims the characterisation and application of these stationary phases post-synthesis were important to the outcome of the project.

The final chapter (General Conclusions and Outlook) summarises how these aims were approached, their success and some work for the future.

List of Abbreviations and Table of Monomer Structures

AA   amino acid

ACE   acetone

ACN   acetonitrile

AEMA   2-aminoethyl methacrylate

AES   atomic emission spectroscopy

AIBN   2,2'-azobisisobutyronitrile

AMPS   2-acrylamido-2-methyl-1-propane sulphonic acid

BuMA   butyl methacrylate

BP   benzophenone

BSA   bovine serum albumin

BSE   back-scattered electrons

C⁴D $\;$ capacitively coupled contactless conductivity detection

CE   capillary electrophoresis

CEC   capillary electrochromatography

COC   cyclic olefin copolymer

CQ   *S*-(+)-camphorquinone

CSP   1',3'-dihydro-1',3',3'-trimethyl-6-nitrospiro-[2H-1]-benzopyran-2,2'-(2H)-indole (commercial spiropyran)

CyB   3-butyl-2-[5-(1,3-dihydro-3,3-dimethyl-1-propyl-2H-indol-2-ylidene)-penta-1,3-dienyl]-1,1-dimethyl-1H-benzo[e]-indolium triphenyl butyl borate

Abbreviations and Monomer Structures

CytC	cytochrome C
DMPAP	2,2-dimethoxy-2-phenylacetophenone
DVB	divinylbenzene
EDAB	ethyl 4-dimethylaminobenzoate
EDC	1-ethyl-3-[3-dimethylaminopropyl]carbodiimide hydrochloride
EDMA	ethylene dimethacrylate
EDX	energy dispersive X-rays
EOF	electroosmotic flow
EOP	electroosmotic pump
EtOH	ethanol
FS	fused silica
GC	gas chromatography
GC-FID	gas chromatography-flame ionisation detection
GMA	glycidyl methacrylate
HEMA	2-hydroxyethyl methacrylate
HPLC	high performance liquid chromatography
I784	Irgacure 784 (bis-(eta-5-2,4-cyclopentadien-1-yl)-bis-[2,6-difluoro-3-(1H-pyrrol-1-yl)-phenyl]titanium)
ICP	inductively coupled plasma
i.d.	internal diameter
IR	infrared

13
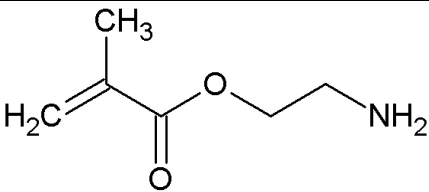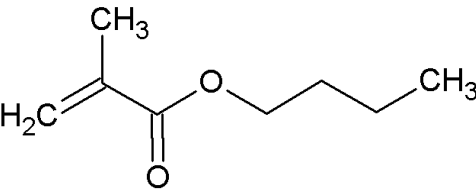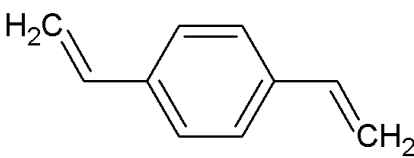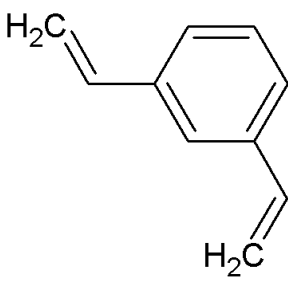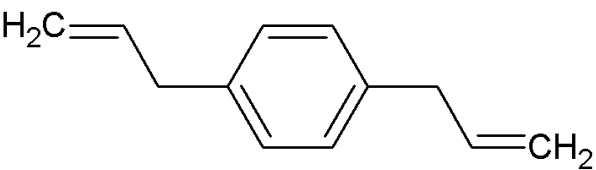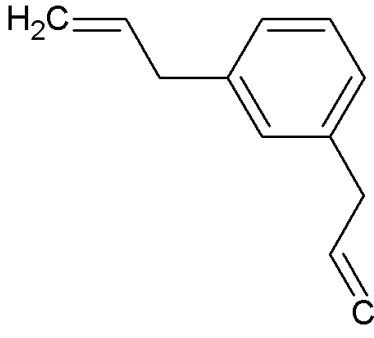
Abbreviations and Monomer Structures

LC   liquid chromatography

LD   laser diode

LED   light emitting diode

LaMA   lauryl methacrylate

MAA   methacrylic acid

MC   merocyanine

MeOH   methanol

MES   2-(*N*-morpholino)ethanesulphonic acid

META   [2-(methacryloyloxy)ethyl]-trimethylammonium chloride

MK   Michler's ketone (4,4'-*bis*(dimethylamino)benzophenone)

MMA   methyl methacrylate

MPAP   α-methoxy-α-phenylacetophenone

MPPB   *N*-methoxy-4-phenylpyridinium tetrafluoroborate

NIR   near infrared

o.d.   outer diameter

PDMS   poly(dimethylsiloxane)

PEEK   poly(ether ether ketone)

PI   poly(imide)

PMMA   poly(methyl methacrylate)

poly(BuMA-*co*-EDMA)   poly(butyl methacrylate-*co*-ethylene dimethacrylate)

poly(GMA-*co*-EDMA)   poly(glycidyl methacrylate-*co*-ethylene dimethacrylate)
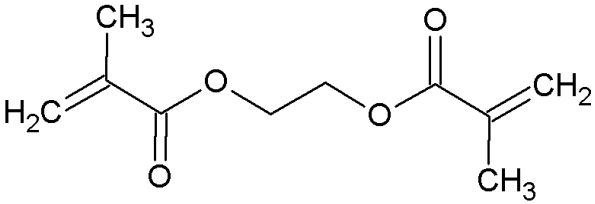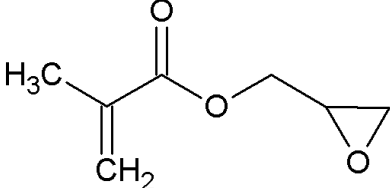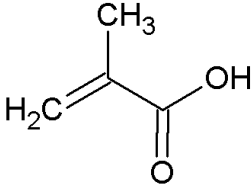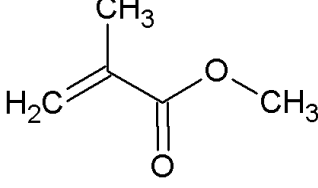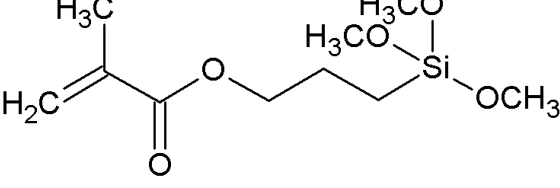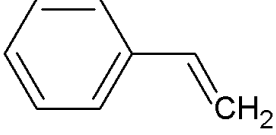
poly(MMA-*co*-EDMA)   poly(methyl methacrylate-*co*-ethylene dimethacrylate)

poly(S-*co*-DVB)   poly(styrene-*co*-divinylbenzene)

poly(SPM-*co*-DVB)   poly(spiropyran monomer-*co*-ethylene dimethacrylate)

PSDVB   poly(styrene-*co*-divinylbenzene)

PTFE   poly(tetrafluoroethylene)

S   styrene

SE   secondary electrons

SEM   scanning electron microscopy

SP   spiropyran

SPCOOH   1'-(3-carboxypropyl)-3',3'-dimethyl-6-nitrospiro-[2H-1]-benzopyran-2,2'-
indoline

SP-C18   1'-(hexadecyl)-3',3'-dimethyl-6-nitrospiro-[2H-1]-benzopyran-2,2'-
indoline

SPM   1'-(9-decenyl)-3',3'-dimethyl-6-nitrospiro-[2H-1]-benzopyran-2,2'-
indoline (monomeric spiropyran)

SPOH   1'-(propan-3-ol)-3',3'-dimethyl-6-nitrospiro-[2H-1]-benzopyran-2,2'-
indoline

TMPTMA   trimethylolpropane trimethacrylate

TMSPM   3-(trimethoxysilyl)propyl methacrylate

UV   ultraviolet

Vis   visible light

Table 0.1: *The chemical structure, chemical name and abbreviation of monomers used in this thesis for polymerisations are described below*

Structure	Name	Abbreviation
	2-aminoethyl methacrylate	AEMA
	butyl methacrylate	BuMA
	1,4-divinylbenzene	DVB
	1,3-divinylbenzene	1,3-DVB
	1,4-diethylvinylbenzene	1,4-DEVB
	1,3-diethylvinylbenzene	1,3-DEVB

16

	ethylene dimethacrylate	EDMA
	glycidyl methacrylate	GMA
	methacrylic acid	MAA
	methyl methacrylate	MMA
	3-(trimethoxysilyl)- propyl methacrylate	TMSPM
	styrene	S

1. Literature Review – Organic Polymer Monoliths: Synthesis, Modification and Application in Separation Science

1.1 Historical Development of Monoliths

The word monolith comes from the Greek 'μονο' (mono) meaning 'single' and 'λιτηοσ' (lithos) meaning 'stone'. In chromatographic terms, the word monolith describes a rigid, continuous, macroporous rod generally made from organic polymers or silica based materials. The monolithic rods are usually encased in outer tubing, such as fused silica capillary, stainless steel or poly(ether ether ketone) (PEEK), for protection and then used for the separation of analytes in liquid chromatography (LC), gas chromatography (GC) and capillary electrochromatography (CEC). The shape, pore size and surface chemistry can be modified and tailored to a specific separation.

While they have been called many things over the years, such as macroporous polymer membranes and porous silica rods, monolithic stationary phases have had a long development process to get to the point at which they are known today. In the 1960s Kubín *et al.* [1] synthesised what is believed to be the starting point of the development of monolithic stationary phases, a methacrylate based monolithic hydrogel as a stationary phase for size-exclusion chromatography, however the efficiency of these as stationary phases was very low [2]. These hydrogels were followed in the 1970s by foams [3, 4] and in the 1980s by compressed chromatographic beds [5]. In 1992, Svec and Fréchet published the first work on rigid macroporous rods, the first of what we now call monolithic stationary phases and shortly after the use of monolithic disks, or 'Convective Interaction Media' (CIM disks), was also described in the literature [6, 7]. Most recently, work was carried out by Nakanishi and Soga [8] and Minakuchi and co-workers [9] into the development of these monolithic stationary phases from silica materials.

Monolithic stationary phases are relatively new, compared to chromatography in general, which is 107 years old [10]. In the short time since monolithic stationary phases

started appearing in the literature, they have made quite an impact on separation science. Using search terms TS=monolith* and TS=separat*, it can be seen there has been a steadily increasing number of publications related to monolithic materials each year (Fig. 1.1) with, on average, 370 publications per year for the last 4 years, a trend that is hopefully to improve or at least continue for years to come.
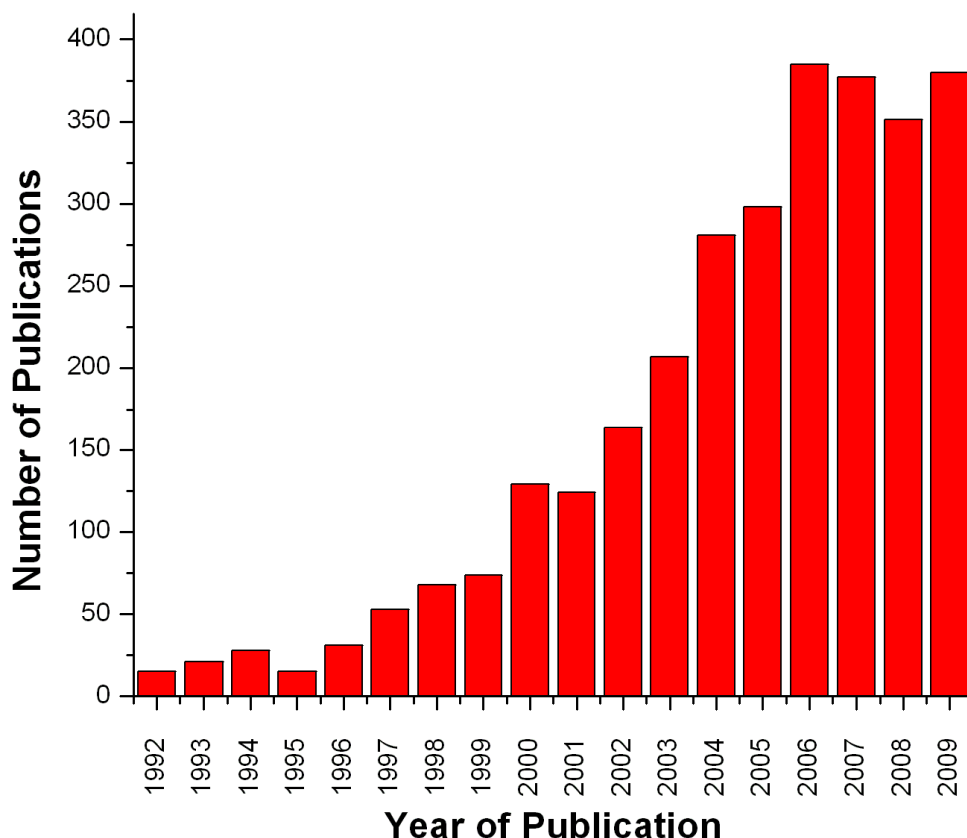
Figure 1.1: *Graph of the number of publications per year from Web of Science (www.isiknowledge.com) using search terms TS=monolith* and TS=separate*, searched: January 10th 2010*

Commercially silica monoliths are the most common monolithic stationary phase with several companies producing their own versions, such as Merck's 'Chromolith^TM' and Phenomenex's 'Onyx^TM' columns. They boast high surface areas in the region of 200-300 g/m^2, making the separation of both small and large molecules possible, and a well studied surface chemistry making them easily modified for different separations. They do, however, have several disadvantages such as dissolution of the stationary phase in

certain buffers, e.g. phosphate buffer, and in basic media [11] and relatively long preparation times (over 3 days) [9]. Organic monoliths present a useful alternative to silica, despite lesser interest commercially. They offer a wide range of different surface chemistries, which are easily tailored by wet and photo-chemical processes, stability over pH extremes and shorter synthesis times compared to silica. Their disadvantage is their lower surface area, which makes the small molecule separation difficult, however this is changing with many groups showing elegant modifications to the monolith surface allowing small molecule separation [12, 13]. For these reasons the focus of this thesis is centred on organic monoliths, their methods of synthesis, properties, methods of functionalisation and applications and this is reflected in this review Chapter.

1.2 Monoliths *vs.* Conventional Packed Columns

Monolithic stationary phases consist of inter-linked porous globules around an inter-connected series of macro- and micro-pores. Compared to particle-packed columns the surface area of organic polymer monoliths is relatively low, however silica monoliths have been known to have higher surface areas often in the region of 200-300 m^2/g. Silica monoliths have a third type of pore, meso-pores, which contribute to their large surface area.

The presence of the macro-pores provides good flow through properties at low back pressures. Additionally, they have excellent mass transfer properties meaning they do not suffer from stagnation of the sample and mobile phase in the pores of the monolith, which helps to improve column efficiency [14]. A scanning electron micrograph of a poly(styrene-*co*-divinylbenzene) [poly(S-*co*-DVB)] monolith is shown in Fig. 1.2, which shows the globular porous structure of the organic polymer monolithic stationary phase.
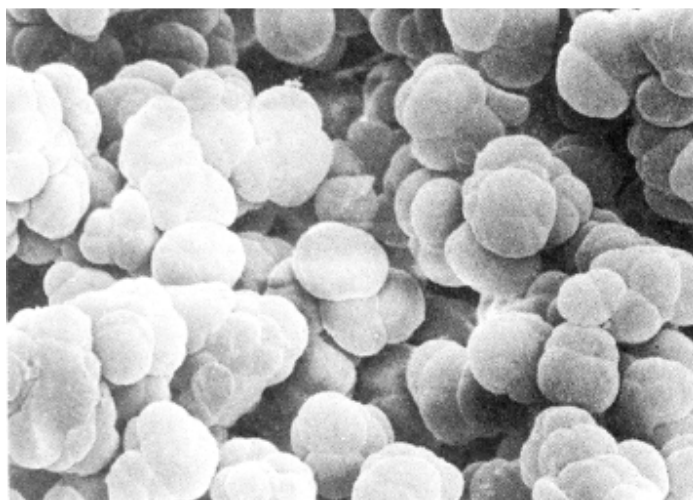
Figure 1.2: *Scanning electron micrograph of a section of a poly(styrene-co-divinylbenzene) monolithic polymer synthesised by thermally initiated polymerisation, reprinted from Wang et al. [15]*

Before the introduction of monolithic materials, and even after, the most commonly used columns for liquid chromatography were particle packed columns. In using monolithic stationary phases, however, some of the disadvantages of particle packed columns, or the areas where monoliths represent an improvement in stationary phase technology, have been brought to light.

To increase the separation efficiency of packed columns, the diameter of the packing material can be reduced. By reducing the particle diameter the surface area of the stationary phase is increased meaning that the area on which the analytes can be retained is also increased [16]. The problem with decreasing the size of the particles is that this decreases the size of the inter-particular voids and increases the flow resistance over the length of the column.

In certain cases, particularly in the use of sub-µm particles such as demonstrated by MacNair and co-workers [16], the use of ultra high performance LC systems is usually necessary as conventional systems cannot generate the required pressures to pump through these densely packed columns. If the pumping system cannot handle the pressure generated by the column and causes the column to repeatedly disconnect from

the injection valve under pressure, damage to the column, such as the creation of voids in the packing, can result.

For industrial applications, companies are interested in fast separations. Faster separations need higher flow rates, which can cause a reduction in the stationary phase efficiency due to inefficient/incomplete mass transfer between the mobile and stationary phase [14]. Additionally, at higher flow rates pressure can also be a limiting factor in the separations.

Due to the inter-linked network of macro-pores in monolithic stationary phases, higher flow rates can be achieved while still maintaining lower back pressures. Additionally, the network of micro- and macro-pores contribute to more efficient mass transfer as all the mobile phase flows through the uniquely created structure, eliminating stagnation of the sample and eluent [17] while also providing a relatively large surface area giving high separation efficiency [18]. In silica monoliths the network of meso-pores is the main contributor to the large surface area.

An additional advantage of monoliths over particle-packed columns is their ability to be localised within the mould without the need for retaining frits [17]. This is particularly useful in micro-fluidics applications where short plugs of stationary phase in a channel may be required for valves [19] or sample pre-concentration [20]. *In situ* photo-initiated polymerisation is a simple way to achieve a well designed plug of stationary phase compared to channel tapering or the insertion of frits in the channel to fix the particles in place.

On-column detection is another area where the synthesis of stationary phases *in situ* can be more useful than packed columns, such as described by O'Ríordáin *et al.* [21]. Removal of the retaining frits in order to place the detector on the particle packed capillary can cause voids in the column packing, which will ultimately destroy the efficiency of the column. Lack of retaining frits mean that on-column detection is easily carried out on monoliths synthesised in capillary without any detrimental effect on the efficiency of the stationary phase.

The combination of monoliths and particle packed stationary phases is also possible and has been described in the literature by Peters *et al.* [22]. In their work they synthesised monolithic plugs in capillary as retaining frits for particle packing. This shows a very useful application for monoliths in separation science, which could prove to be very advantageous combining the qualities of particle packed columns, such as high column efficiency, with the qualities of monoliths, such as specific stationary phase locations and easy on-column detection.

Despite the dominance of particle packed columns, monoliths are used extensively in separation science for bio-molecule separations [23], extractions [24] and pre-concentrations [25]. Some of the more novel applications are for use as valves [26] and electroosmotic pumps [27, 28] in micro-fluidic devices.

1.3 Polymerisation Reaction Mechanisms

Polymers are defined as macromolecules, of a relatively high molecular mass, which are made up of smaller molecules called monomers [29]. Polymers can be linear, branched or cross-linked [30]. Monolithic stationary phases are commonly cross-linked polymers as this provides them with their rigid, macroporous structure which can have large surface areas [31], can resist high pressures, relatively high temperatures (> 200°C) [32] and extremes of pH [33].

Polymers are generally divided into two groups based on their polymerisation mechanism; the method of classification of polymers was suggested in 1929 by Carothers and later modified by Flory [30].

The first of the two classes are condensation polymerisations, also known as step-growth polymerisation, where small molecules like water are excluded from the polymer with every addition to the chain and so the polymer becomes condensed. The second class is addition (chain-growth) polymerisation, in which monomer chains bind at a reactive site to form polymer chain without any loss from the original units. In general monolithic polymers are obtained by chain-growth polymerisations [34], however there are some examples such as urea-formaldehyde monoliths which are synthesised by condensation polymerisation [35].

Due to the clear dominance of monoliths formed by addition polymerisation, and the fact that all monoliths synthesised during the course of this research project are addition polymers, this type of polymerisation will be the focus in this section.

There are five main types of addition polymerisation techniques; bulk, dispersion, emulsion, solution and suspension polymerisation [34]. According to Svec and Fréchet [34], only dispersion, emulsion and suspension polymerisations are useful for the synthesis of monolithic materials as these methods tend to produce spherical particles unlike bulk and solution polymerisation techniques.

In emulsion polymerisation a hydrophobic monomer is dispersed in an aqueous phase containing a surfactant above its critical micelle concentration (CMC) and water soluble initiator. The surfactant solubilises the monomer and the polymerisation is carried out when a free radical enters the micelle [30, 34].

Dispersion polymerisation, however, necessitates that the monomers and initiators should be soluble in an organic solvent, when the polymer chains begin to grow they will be insoluble in the original solvent and will start to drop out of solution [34].

Finally, in suspension polymerisation a monomer is suspended in a solvent in which a free radical initiator has already been dissolved. A disperse organic phase then forms consisting of spherical droplets, which become more solid and interconnected as the reaction proceeds [30, 34]. The growing chains remain soluble in the remaining monomer, however, they are insoluble in the solvent [36], the final polymer must be precipitated from the monomer when the polymerisation has terminated. If all the monomer is used up in the reaction then the polymer will begin to precipitate in the porogenic solvent. Suspension polymerisation is the most common technique used to synthesise monolithic scaffolds.

In addition to the different polymerisation techniques, there are also different initiation mechanisms. The most common initiating mechanism for addition polymers is free radical initiation [37]. Anionic [38, 39], cationic [40, 41], reversible addition-fragmentation transfer (RAFT) [42, 43] and ring-opening metathesis [44, 45] are also mentioned in the literature but are far less common.

Free radical addition polymerisation is composed of three steps; initiation, propagation and termination. During initiation an unpaired electron is generated on the initiator, which reacts with the double bond of an alkenic monomer to create a chain carrier. This chain carrier should have enough energy to attack another monomer in the same way to generate a macromolecular chain, in what is known as the propagation stage. The termination stage occurs with the meeting of two radicals to create an electron pair, or the exhaustion of the monomer or initiator supply, and the propagation of chains cease [37].

During a cationic polymerisation the monomers undergo electrophilic attack by a carbenium ion and the most common initiators are Lewis acids, while in anionic polymerisations monomers undergo nucleophilic attack by a carbanion. In the case of anionic polymerisations alkyl amides would be common initiators [37]. RAFT polymerisation is a type of living radical polymerisation, which uses thiocarbonylthio compounds to initiate the polymerisation by a reversible chain-transfer process; it can be used with a large number of monomers and porogens and usually gives polymers with complex architectures, such as graft and brush copolymers [46]. This method has been mentioned in the literature as being useful for the synthesis of molecularly imprinted polymer monoliths [47, 48]. Lastly, ring-opening metathesis polymerisation, or ROMP, is another living polymerisation mechanism. The initiation of the polymerisation is transition metal catalysed, which allows a high level of control over the polymerisation kinetics, the polymer structure and the polymer properties. There are two different types of catalyst used for the initiation of ROMP; these are either Schrock catalysts or Grubbs-type initiators. Buchmeiser and co-workers have shown that this initiation mechanism is suited to both the polymerisation of monolithic stationary phases and the subsequent surface modification of the scaffold [49, 50].

The majority of monomers, such as styrenes, (meth)acrylates, (meth)acrylamides and halogenated alkenes, for example, can undergo radical initiated polymerisation [51], it is unusual for monomers to only be able to undergo either cationic or anionic polymerisation such as 1,1'-dialkylolefin and vinyl ethers [37]. Within this thesis radical initiation is the only type shown in detail as, without a doubt, free radical suspension

polymerisation is the most common method for the synthesis of monolithic stationary phases [52, 53].

There are also a number of different ways to provide the energy needed to start the decomposition of the initiator, which in turn starts the polymerisation reaction. The most commonly used sources are heat [6] and ultraviolet light [54, 55]. Several other sources including γ-radiation [56], microwaves [57], electron beam [58] and visible light [59] have also been described in the literature but are significantly less common. These methods are analysed in more detail in the following section and the experimental work done as part of this thesis on the development of visible light initiated polymerisation using light emitting diodes is presented in the experimental section (Chapter 4 and Chapter 5).

The morphology of the monolithic polymer is determined by a combination of each component of the pre-polymer solution and the mould in which the solution is placed. The pore size is dependent on the porogenic solvent and the rate of the reaction. In thermally initiated polymerisation, for example, the higher the temperature of the reaction, the faster the reaction proceeds and therefore the smaller the pores will be in the final monolithic structure [36].

1.4 Methods of Initiation

1.4.1 Thermally Initiated Polymerisations and Their Limitations

The first examples of what are now commonly called monolithic stationary phases were produced by thermally initiated free radical suspension polymerisation in 1992 [6, 15]. Further investigation and application of these novel monolithic stationary phases was presented by Wang *et al.* the following year [15]. In this work the copolymerisation of styrene (S) and divinylbenzene (DVB) using 2,2'-azobisisobutyronitrile (AIBN) was used as the initiator, which decomposes in the temperature range 60-90°C (Fig. 1.3).
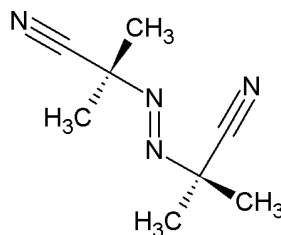
Figure 1.3: *Structure of 2,2-azobisisobutyronitrile (AIBN)*

AIBN is by far the most frequently used free radical initiator reported in the literature however there are also reports of the use of benzoyl peroxide [60] although these are less common. An example of the morphology of the polymer monoliths formed by thermally initiated polymerisation using AIBN as the initiator is shown in Fig. 1.2.

In brief the synthesis procedure is as follows; the pre-polymer solution is prepared, sonicated and degassed and filled into a pre-treated mould. The mould is then hermetically sealed and placed in a thermostatted water bath at a certain temperature for a fixed period of time. The time and temperature of the polymerisation are dependent on the initiator used, along with the desired morphology and filling of the capillary as porous layer open tubular (PLOT) monoliths, for example, will need less time (and monomer content in the pre-polymer solution), than full monoliths. After the necessary time has passed the mould is removed from the water bath and attached to a pump. A washing solvent, such as methanol or acetonitrile but never water, is used to remove traces of initiator and porogen from the pores of the polymer. Water is not used as should the reaction not go to completion water will make the polymer chains drop out of solution in the pores and cause them to be blocked.

In addition to the ease of synthesis, thermally initiated polymerisations can be carried out in any type of mould as long as it can withstand the temperature necessary to start the decomposition of the initiator. There are, however, some disadvantages to the technique particularly the lack of control over the area in which the polymer is formed.

As mentioned above, the size of the pores does generally depend on the temperature at which the polymerisation was carried out [56]. The higher the temperature of the polymerisation, the smaller will be the pores in the resulting monolith. Buchmeiser

suggests this is because increasing the temperature increases the number of growing polymer chains in the same amount of space. As there are so many chains growing, there is not the same space for them to grow and therefore both the chains and the resulting monolith pores tend to be smaller [36].

Another disadvantage of thermal polymerisations is that they generally require long polymerisation times, for example a standard thermal polymerisation using AIBN as the initiator takes approximately 20-24 h at 60°C, judging from the standard polymerisation times described in the literature [61-64]. Raising the temperature to 70°C shortens the half-life of the initiator to 5.7 h, while heating to 110°C shortens this further to 3.2 min [36]. While this will shorten the polymerisation, the boiling points of the porogens and monomers and the required pore size have to be taken into account and a compromise has to be made between the desired polymer structure and a reasonable polymerisation time. This compromise usually results in the longer polymerisation time being chosen as the polymer structure is the important outcome of the reaction.

1.4.2 Photo-initiated Polymerisations

The principal disadvantages of thermally initiated polymerisations in monolith synthesis are the long reaction time and the lack of spatial control during polymer formation. Photo-initiated polymerisation provides a solution to these problems [55]. Using photo-initiated polymerisation the location of the monolith within a mould can be controlled by the use of simple photo-masks [55, 65], which stop the photons from the light source from falling on certain areas of the pre-polymer solution within the mould. Additionally the polymerisation reaction times are significantly reduced, polymerisations being completed in the region of tens of minutes as opposed to hours in the case of thermally initiated polymerisation [55].

1.4.2.1 Initiators for Photo-Induced Polymerisations

So far the majority of organic monolithic materials synthesised by photo-initiated polymerisation have used light from the ultraviolet region of the electromagnetic spectrum to activate the initiator. While there are a large number of different photo-initiators available for use in the UV region of the spectrum, the majority of papers

describe the use of derivatives of benzo-and aceto-phenone, which both absorb strongly in the UV region to produce radical species.

Here a few of the most common examples will be presented. Viklund *et al.* demonstrated the first photo-initiated polymerisation of a monolithic stationary phase in UV-transparent capillary [55]. In this work they optimised the synthesis of poly(glycidyl methacrylate-*co*-trimethylolpropane trimethacrylate) [poly(GMA-*co*-TMPTMA)] using an experimental design programme. To initiate the polymerisation α-methoxy-α-phenylacetophenone (MPAP, Fig. 1.4) was used and the mixture was irradiated at 365 nm to start the decomposition of the initiator to radicals. This radical is a Norrish Type I radical generator meaning that on absorbing light in the region 300-400 nm, there is an simple cleavage at the C=O to generate a benzyl and a ketyl radical [66].
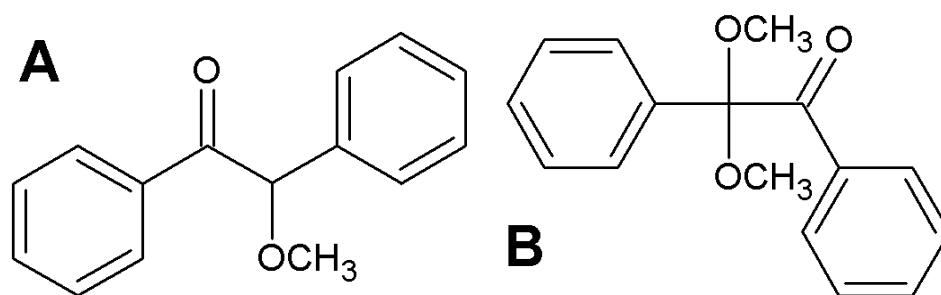
Figure 1.4: *Structure of (A) α-methoxy-α-phenylacetophenone (MPAP) and (B) 2,2'-dimethoxy-phenylacetophenone (DMPAP)*

Certainly one of the most common photo-initiators is 2,2'-dimethoxy-phenylacetophenone (DMPAP, Fig. 1.4). DMPAP is also a Norrish Type I photo-initiator, however with a maximum absorbance at 254 nm, slightly outside the normal range. This initiator is commonly used to initiate the polymerisation of hydrophobic methacrylate monomers such as butyl methacrylate (BuMA) [67-69].

Abele *et al.* have described the use of Michler's ketone (4,4'-*bis*(dimethylamino)benzophenone) (Fig. 1.5) to initiate the polymerisation of the more reactive methacrylates such as poly(glycidyl methacrylate-*co*-ethylene dimethacrylate) [poly(GMA-*co*-EDMA)] [65].
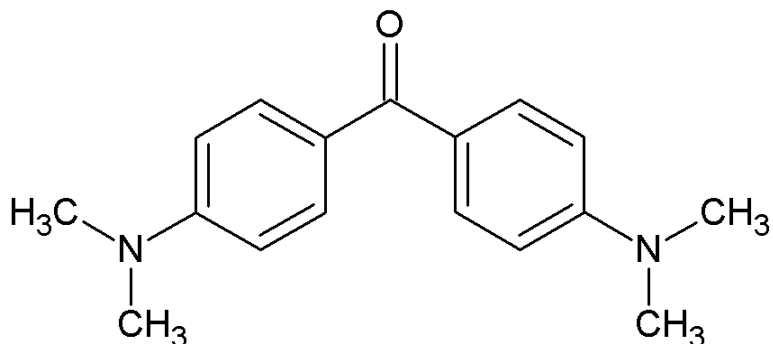
Figure 1.5: *Structure of Michler's Ketone (4,4'-bis(dimethylamino)benzophenone)*

As a benzophenone derivative, Michler's ketone is a Norrish Type II initiator, as described by Aoki *et al.* [66]. The absorbance of Type II initiators is usually in the near UV and into the blue region of the spectrum. This type of cleavage involves intra-molecular abstraction of the gamma hydrogen resulting in a diradical which then either undergoes rearrangement to a stable form or is cleaved to form an enol and an alkene [70].

Abele *et al.*, while working with Michler's Ketone, have also noted the effect of matching the emission maximum of the light source (in their case the LED) with the absorbance maximum of the initiator. This was found to play an important role in the efficiency of the reaction as well as the ability to control the location of the polymer within the capillary and chip [65].

AIBN, the commonly used thermal initiator is also often used to initiate polymerisations using light instead of heat to start the decomposition into radicals. AIBN has an absorbance maximum at 365 nm and therefore can undergo UV-light initiated polymerisation. There are several examples of this in the literature [53, 71, 72]. For example Yu and co-workers showed several examples of the polymerisation of a variety of methacrylate monoliths in micro-fluidic chips for applications in on-chip separations [53, 71].

Although there are several advantages to using UV light to initiate polymerisation of monolithic stationary phases such as spatial control, there are two main disadvantages. Firstly, only UV-transparent moulds can be used to carry out the photo-initiated

polymerisation reaction. UV-absorbing moulds such as polyimide coated capillary cannot be used, therefore the most common moulds used for UV initiated polymerisations are PTFE coated fused silica capillaries [73-75], poly(methyl methacrylate) (PMMA) [76], cyclic olefin copolymer (COC) [26] and glass micro-fluidic chips [77]. Secondly, UV absorbing monomers such as styrene or DVB cannot be polymerised with this method of initiation due to competition between the monomers and the initiators for light emitted from the irradiation source.

For these two reasons it was eventually necessary to start investigating the potential of longer wavelengths to initiate polymerisations, which would enable the photo-initiated polymerisation of UV-absorbing monomers or within UV-absorbing moulds.

Dulay *et al.* were the first to describe the photo-initiated polymerisation of monolithic materials in fused silica capillary using visible light [59]. They carried out this polymerisation within polyimide coated fused silica capillary demonstrating that polymerisation is now possible in more durable non-UV transparent moulds. Using a cationic polymerisation mechanism they carried out the synthesis of a silica sol-gel monolith using *bis*-(eta-5-2,4-cyclopentadien-1-yl)-*bis*-[2,6-difluoro-3-(1H-pyrrol-1-yl)-phenyl]titanium (Irgacure 784) as the photo-sensitiser and diphenyliodonium chloride as the initiator. The initiator was activated by photo-induced electron transfer at 470 nm from the sensitiser, which in turn attacked the monomer chains to initiate and propagate the chain growth. Photo-induced electron transfer is the most common method of inducing radical formation in a molecule indirectly. A molecule, called the photo-sensitiser, is selected which absorbs at a specific wavelength. Once irradiated at this wavelength, an excited electron can jump from an occupied orbital in the sensitiser to an unoccupied orbital of a closely located acceptor molecule causing the formation of either a radical-ion pair or a charge-transfer complex [70, 78]. In the example mentioned here and all the examples described in the experimental part of this thesis it is a radical-ion pair that is formed, and the radical then goes on to initiate the polymerisation of the monomers in solution. These ideas of photo-initiated polymerisation of monolithic stationary phases in the visible region are further studied in Chapters 4 and 5 of this thesis.

1.4.2.2. Light Sources for Photo-initiated Polymerisations

Since the first publication detailing the use of light to initiate the polymerisation of monolithic stationary phases [55], conventional light sources such as mercury lamps, deuterium lamps, but in particular, fluorescent lamps have been used most often. While they are evidently very useful, considering the number of publications detailing their use, they also have a number of disadvantages. Fluorescent lamps have a rather short operational life, somewhere in the region 2,000 – 10,000 h [79] and require the use of filters to be able to produce the correct emission wavelength [80]. Additionally, they are fragile and breakage of the external glass means the light source will no longer be usable, they are also expensive to replace and dispose of due to non-environmentally friendly components (particularly in the case of Hg lamps) [80].

Recently light emitting diodes (LEDs) are being used in place of conventional light sources due to their small size, negligible heat generation, robustness, low cost, long lifetime and quasi-monochromatic light output while still retaining comparable efficiency relative to conventional light sources [80].

In 1962 Hall *et al.* [81] published a paper on infrared light emitting diodes (LEDs), the first of a new kind of solid-state light source. Later the same year Holonyak and Bevacqua developed the red LED [82]. It was over a decade before papers began to appear detailing work done to create light emitting diodes which were capable of emitting blue light [83]. These devices were the precursors to the blue LEDs in use today the first of which were synthesised by Amano *et al.* [84] in 1990, followed by Haase *et al.* [85] in 1991. Work carried out by Rutz [86] in 1976 details the first example of ultraviolet electroluminescence from an aluminium nitride (AlN) semi-conductor which is the basis for the development of ultraviolet emitting diodes.

While LEDs have always had a steady interest in the field of optics and photonics, in the last decade their popularity outside of this field has also been on the increase. The uses of LEDs are quite diverse from indicator lights in electronic circuits [87] to replacing standard tungsten/deuterium lamps in detectors for analytical applications [88, 89]. An increasingly popular use of LEDs is in dentistry where LED based curing units consisting of ordered arrays of 470 nm LEDs are used to cure polymeric resins as

fillings for dental cavities [90-95]. Their use is growing due to their higher efficiency and more reproducible light output compared to conventional light curing units [96].

More recently, McDermott *et al.* [80] have used UV LEDs to synthesise polymer in bulk, while the Abele and co-workers report the synthesis of monolithic polymers within PTFE coated fused silica capillaries using UV LEDs as the initiating light source (Fig. 1.6) [65], which shows the great potential and ease of use of LEDs for the synthesis of monolithic stationary phases.
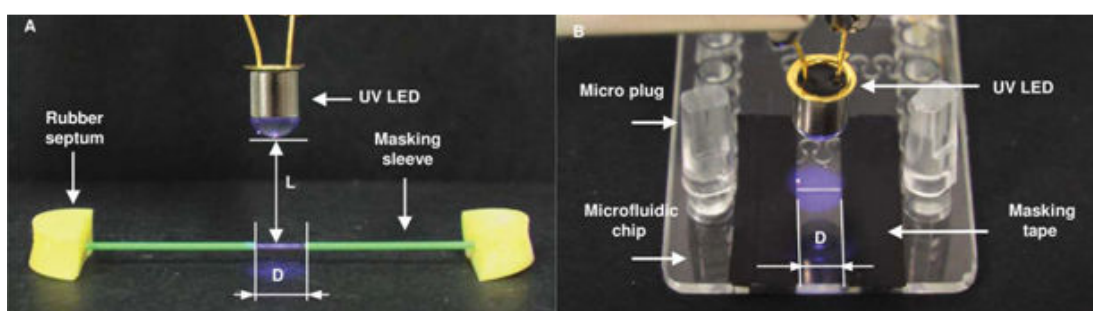
Figure 1.6: *Set-up of photo-initiated polymerisation of methacrylate monoliths within (A) PTFE coated fused silica capillaries and (B) cyclic olefin copolymer (COC) micro-fluidic chips, using light emitting diodes as the light source to induce polymerisation, reprinted from Abele et al. [65].*

1.4.3. Polymerisations Initiated by Ionising Radiation

Recently polymerisation initiated by different forms of ionising radiation, in particular by electron beam [58, 97-99] and gamma radiation [100, 101], has been described in the literature.

This method has not become extremely popular just yet with a literature search for monoliths and electron beam turning up four hits and for gamma radiation showing only two hits; however, there are many advantages to these methods of polymerisation which have yet to be fully explored.

Zhang *et al.* [100] and Bandari *et al.* [97] explain that using both these types of ionising radiation that no initiator is required, the radiation generates radicals directly on the monomers. This tends to make the distribution of radicals more homogeneous along the

length of the column, assuming the radiation is applied evenly to the whole column. The lack of initiator simplifies the pre-polymer solution as there is no need to select initiators which are soluble in the choice of porogens and monomers.

A further advantage of this method of initiation is that the radiation can penetrate any of the commonly used moulds, and therefore, unlike for photo-initiated polymerisations, the mould does not need to be transparent.

The disadvantages, however, are similar to those for thermally initiated polymerisations, in that the location of the polymer within the mould cannot be spatially controlled. Once there is radiation applied, polymer will be formed all along the mould.

1.4.4. Polymerisations Initiated by Non-Ionising Radiation

Initiation of polymerisation by non-ionising radiation, that is, by microwave initiation, for example, has also been described in the literature recently [57, 102, 103].

Using microwaves to induce polymerisation means that the use of an initiator is necessary as the non-ionising radiation will not generate radicals on the monomers. AIBN, a common thermal initiator, is also used as a radical initiator in microwave induced polymerisation.

The polymerisation times reported for microwave initiated polymerisation range from 10 min [103] to 15 s [57]. They certainly provide an advantage over the long polymerisation times recorded for thermally initiated polymerisation; however they do suffer the same problem of lack of spatial control of the forming polymer as thermal polymerisation.

Another issue of microwave induced polymerisation is the reproducibility problem. Using domestic microwave ovens is common practice for microwave induced reactions, not only for monolith synthesis, however the microwave generation within the chamber is not homogeneous. Due to this inhomogeneity multi-mode cavities or "hotspots", that is areas where the microwave radiation is more intense than other areas, are formed which is the cause of poor reproducibility [104]. For monolith synthesis this can mean inhomogeneous stationary phases, which of course should be avoided. It is therefore

necessary to use a well-calibrated micro-wave reactor in order to obtained reproducible microwave initiated monolithic stationary phases, although this is not always the case [57].

1.4.5. Moulds for Monolith Synthesis

Without a doubt the most common moulds for monolith synthesis are polyimide and poly(tetrafluoroethylene) coated fused silica capillaries [25, 105, 106]. From the literature it can be seen that most monolithic polymers are synthesised in fused silica capillaries of internal diameters from 10 to 150 μm for applications in CEC and LC.

Initially monoliths were often synthesised in stainless steel capillaries as described by Svec in the first paper on monolith synthesis [6] and their use is still relatively common [107, 108]. While Luo *et al.* [107] and Svec *et al.* [6] report the use of large diameter steel moulds, large bore stainless steel, and indeed large bore fused silica capillaries, can be disadvantageous for monolith synthesis. For thermally initiated polymerisations in particular they can cause inhomogeneous polymer formation due to less efficient heat dissipation in larger diameter moulds [2], care must be taken to ensure more efficient heat dissipation to improve the quality of the resulting monoliths. It is likely that there would also be issues with light transmission through large diameter transparent moulds as the polymerisation progresses, due to light scattering from the polymer particles dropping out of solution.

While stainless steel moulds are still used, a large number of different moulds have been noted in the literature, each having their own effect to different extents on the dynamics of the polymerisation.

In the late 1980s Tennikova *et al.* developed porous monolithic disks approximately 20 mm in diameter and 1-2 mm in length which they used for High Performance Membrane Chromatography (HPMC) [7, 109]. These are held in specially designed large diameter PEEK cartridges designed by the group of Josić and optimised by the group of Štrancar, and are now known as Convective Interaction Media, or CIM disks [110].

In recent years the use of micro-fluidic chips for monolith synthesis has become more common with a large number of applications for monoliths in this format, such as valves

[19], sample pre-concentration [20] and the traditional CEC and LC separations [111, 112]. There have been numerous publications describing monolith synthesis within COC, PMMA, glass and more recently specially designed Agilent polyimide micro-fluidic chips [111, 113-115].

Finally there have also been reports of the synthesis of monolith polymers in syringe barrels [116], pipette tips [117] and 96-well plates [118], showing that with the appropriate surface modification, selection of a suitable initiation method and adjustment to polymerisation time or temperature, the possibility is there to create monoliths in almost any type of mould.

1.5. Synthesis of Functional Monoliths

In addition to the commonly used hydrophobic monoliths such as poly(BuMA-*co*-EDMA), poly(lauryl methacrylate-*co*-EDMA) [poly(LaMA-*co*-EDMA)] and poly(S-*co*-DVB), there are a large range of functional monomers which are often copolymerised with a cross-linking agent to create a functional monolith, the simplest example of which is the synthesis of poly(GMA-*co*-EDMA). Copolymerisation of three functional monomers (of which one is cross-linker) would result in terpolymers with some specific functionality; additionally functional monomers can also be polymerised on the surface of an existing monolithic scaffold in a process known as grafting.

1.5.1. Copolymerisations with Cross-Linkers

Looking firstly at some simple copolymerisation of functional monomers with cross-linkers, lots of different functionalities can be achieved.

Beiler *et al.* [56] copolymerised 2-hydroxyethyl methacrylate (HEMA) and EDMA by gamma radiation induced addition polymerisation to obtain a monolith which has a hydrophilic character for the separation of amino acids.

Poly(methacrylic acid-*co*-EDMA) monoliths were synthesised by Thabano *et al.* as weak cation exchangers used for the separation of neurotransmitters by capillary electrophoresis [119]. Wei *et al.* also synthesised the same type of monoliths but in this

case they were used for the separation of ephedrine and pseudoephedrine from biological fluids [120].

The most common functional monolith is poly(GMA-*co*-EDMA), which is often used as a starting point for further functionalisation of the monoliths, due to the ease with which the surface chemistry can be modified. The high reactivity of the epoxy ring in GMA allows the ring to be opened, creating a negatively charged site in basic media and a diol in acidic media. This can then be further functionalised by means of wet chemistry, for example, Potter *et al.* [61] have modified a poly(GMA-*co*-EDMA) monolith by flushing the column with *p*-hydroxyphenylboronic acid in basic media to allow the phenylboronic acid to stick to the surface. The attached phenylboronic acid sites can then be used to retain carbohydrates through their 1,3-*cis*-vicinal diol groups [61].

Using a similar approach, Dong *et al.* have prepared a zwitterionic stationary phase by taking a poly(GMA-*co*-EDMA) monolithic scaffold, filling the pores with a solution of lysine, which attack the epoxy ring and bind to the surface creating a stationary phase which can be cationic or anionic depending on the pH of the environment [121].

1.5.2. Terpolymerisations

Synthesising terpolymers (polymers of three monomers) is another common method of incorporating functional monomers into a monolithic scaffold to create some alternative surface chemistries. Lämmerhofer *et al.* [64, 122] synthesised a terpolymer of poly(*O*-9-(*tert*-butylcarbamoyl)-11-[2-(methacryoyloxy)ethylthio]-10,11-dihydroquinone-*co*-2-HEMA-*co*-EDMA) to create an efficient enantioselective stationary phase by thermally initiated polymerisation. This terpolymer which includes a chiral monomer, a hydrophilic monomer and a cross-linker, respectively, was used for the separation of a model racemate (*R,S*)-*N*-3,5-dinitrobenzoylleucine by capillary electrochromatography. This group also synthesised a terpolymer of poly(2-dimethyl aminoethyl methacrylate-*co*-2-HEMA-*co*-EDMA) by both thermal and ultraviolet initiated polymerisation to obtain a hydrophilic weak anion exchange monolith which was then alkylated *in situ* to give a strong anion exchange monolith [63]. These strong anion exchange monoliths were then used for the separation of various 2-substituted propionic acid drugs using CEC.

Peters *et al.* showed the optimisation of the synthesis of a terpolymer of 2-acrylamido-2-methyl-1-propane sulphonic acid (AMPS), BuMA and EDMA to give a strong cation exchange terpolymer monolith, poly(AMPS-*co*-BuMA-*co*-EDMA) [22]. Adu *et al.* subsequently showed the use of such strong cation exchange monoliths for the separation of therapeutic peptides by CEC [62].

1.5.3. Grafting of Functional Monomers

Another approach documented in the literature by which to obtain functional monoliths is the grafting of a layer of a functional monomer onto a pre-existing monolithic scaffold. There are many publications dealing with grafting for various applications.

Wei *et al.* [123] have described the preparation of a pH responsive monolith by thermally grafting a layer of methacrylic acid (MAA) onto the surface of a poly(GMA-*co*-EDMA). They achieved a layer of MAA by first hydrolysing the surface with sulphuric acid. Following this an aqueous solution of methacrylic acid and potassium peroxydisulphate, a radical initiator, was prepared and flushed through the column for 4 h at 60°C.

Despite the relatively short reaction times, compared to thermally initiated polymerisations in general, this method still suffers from the disadvantage that the grafted area cannot be controlled. For this reason photo-initiated polymerisation is now the most common method of grafting a functional monomer onto the surface of a pre-existing monolithic scaffold.

As regards initiators for photo-initiated grafting, the most common initiator is benzophenone, Fig. 1.7. The radical formed from benzophenone has quite a short lifetime in solution but can generate an energy rich surface radical under irradiation at 254 nm. A solution of the initiator is made and filled into a pre-existing monolithic scaffold; the initiator is then excited at the correct wavelength, in this case 254 nm. Benzophenone generates radicals by a process known as hydrogen abstraction from the surface it is important that the solvent used to dissolve the initiator has few or no abstractable hydrogen atoms. Additionally, it is important that the solvent and the initiator do not absorb in the same region. For these reasons a common solvent for

dissolution of the benzophenone in order to generate surface radicals is a 3:1 mixture of *t*-butanol:water [68].

When the benzophenone is irradiated it abstracts hydrogen and the diphenylketyl radical becomes attached at the point of abstraction (Fig.1.7). If the hydrogen is abstracted from the surface the radical will be a surface radical, which is the ideal situation. If the radical is formed on a solvent molecule there is a risk of radical being removed from the capillary during the washing stage, hence the importance in choosing the correct solvent. After irradiation the capillary is flushed with organic solvent to remove unreacted initiator and any solvent radicals that may have formed. A solution of the monomer to be grafted is then prepared and the capillary is filled and sealed. The solution is irradiated again at the optimum wavelength which causes cleavage of the diphenylketyl radical allowing the monomer chains to be attached to the polymer surface due to attack of the methacrylate group by cleaved bonds on the polymer surface [124]. This process can be done in one step by mixing the monomer and initiator together, however sometimes polymer can form in solution rather than on the surface which can cause blockage of the capillary.
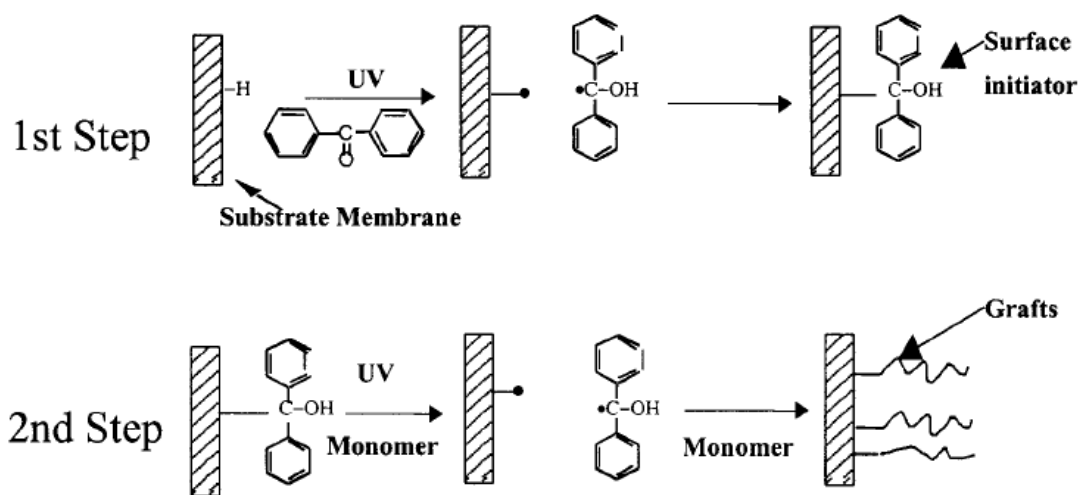
Figure 1.7: *Generation of surface radicals from benzophenone on polymer monoliths for subsequent photo-initiated grafting a functional monomer, reproduced from Ma et al. [124]*

Rohr *et al.* have grafted a layer of the anionic monomer AMPS onto a poly(BuMA-*co*-EDMA) monolithic scaffold in order to impart some strong cation exchange functionality [68]. In this paper they also examined the effectiveness of the graft and the ability to graft onto specific sections of the monolith by grafting on a layer of 4,4-dimethyl-2-vinylazlactone and then flushing through a solution of rhodamine 6G. 4,4-Dimethyl-2-vinylazlactone forms a covalent bond with any amine which come in contact with it, rhodamine 6G is a strongly coloured fluorescent dye which contains a tertiary amine. When the dye is flushed through the monolith it binds to the areas which have been grafted with 4,4-dimethyl-2-vinylazlactone and therefore it is easy to visualise the grafted area. It was seen that the grafted region could be very accurately controlled by the application of simple photo-masks.

Connolly *et al.* have prepared poly(GMA-*co*-EDMA) monoliths functionalised with a layer of [2-(methacryloyloxy)ethyl]-trimethylammonium chloride (META) for the separation of small inorganic anions [13]. This paper also outlines a method for the visualisation of the grafted area so that its sharpness can be verified. This visualisation involves the use of a capacitively coupled contactless conductivity detector (C^4D) which is moved along the column at regular intervals, significant changes in the conductivity indicate areas of inhomogeneity. This technique was first described by Gillespie [125] for examining coating homogeneity on capillary stationary phases.

As has been seen through the previous sections there are many ways to synthesise organic polymer monoliths and still more ways to modify the surface chemistry once the monoliths have been synthesised. In the next section the synthesis of monoliths from inorganic materials and the modification of standard organic polymer and silica monoliths with unusual materials such as dyes, metal nano-particles, metallic layers and biological materials will be presented.

1.6. Exotic Monoliths

Rigid macroporous organic polymer and silica monoliths are the most extensively used monolithic stationary phases for chromatography and electrochromatography today and excellent reviews have been published on these materials [2, 126-136].

In the context of monolithic stationary phases, 'Exotic monoliths' have been defined in the context of this work in two ways; firstly they encompass monoliths which are made from organic polymer or silica materials but have had the surface modified by some more unusual material such as dyes, biological stains, metal nano-layers or biologically active compounds and secondly, monolithic materials which are made from non-standard materials such as metal oxides and not from silica or organic polymer materials are also classified as exotic monoliths.

While there are examples of these types of stationary phases in the literature, they are not as thoroughly explored as the standard silica or organic polymer monolithic stationary phases or monoliths surface modified with other silica or organic monomers.

While there are a large number of stationary phase modifications that can be discussed, as this thesis is particularly concerned with functionalised organic polymer stationary phases, materials similar to these will be discussed in detail below.

1.6.1. Application of Dyes in the Modification of Monolithic Stationary Phases and Packed Columns

Affinity chromatography is a method of separating biochemical mixtures based on molecular recognition [137], it uses specific interactions such as those between antibodies and antigens or enzymes and substrates to purify biological samples. Dye-ligand affinity chromatography uses dyes immobilised on the surface of a stationary phase to selectively interact with an analyte causing retention of this analyte on the surface.

In the past the majority of stationary phases used for dye-ligand affinity chromatography were particle packed or membranous stationary phases, generally from agarose or cellulose materials although sometimes from silica or other organic polymers. These membranous cellulose and agarose stationary phases are also considered to be monolithic due to their inter-connected fibres and continuous porous nature [138]. In these applications chlorotriazine or 'Reactive' dyes appear to be the most commonly used and this is likely due to the fact that many of the stationary phases are polysaccharide based and reactive dyes are most commonly used in the textile industry

to dye cellulosic fibres. They are immobilised on the polysaccharide stationary phase, such as cellulose or agarose, because they have either a chlorotriazine group or an activated double bond which will attack hydroxyl groups on the surface of the stationary phase and form a covalent bond. This is carried out in basic media at temperatures between 40-80°C.

While there are a large number of dyes used in this type of chromatography only the most common examples will be mentioned here. By far the most commonly used dye is Reactive blue 2, also known as Cibacron blue F3GA (Fig. 1.8).
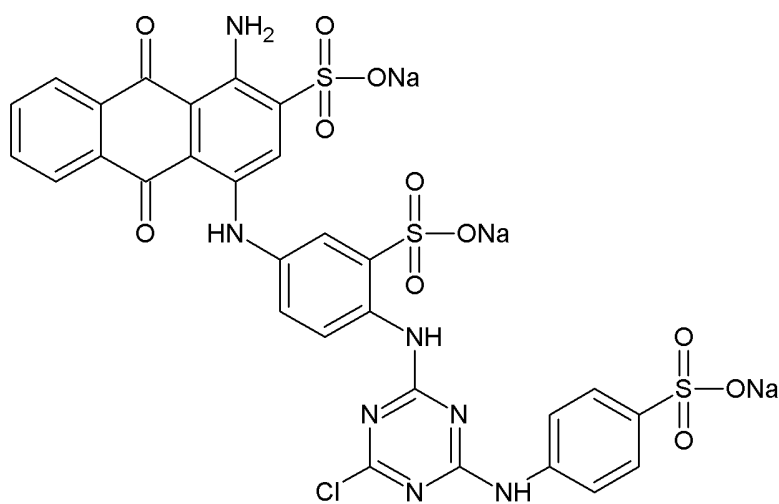
Figure 1.8: *Structure of Reactive blue 2*

There are a large number of examples of the use of this dye in the literature. In general this dye is immobilised on cellulosic stationary phases [139], however there are reported examples of the use of magnetic poly(2-hydroxyethyl methacrylate) beads [140, 141], poly(methyl methacrylate) beads [142], magnetic poly(methyl methacrylate) nano-spheres [143], poly(vinyl alcohol) coated poly(styrene-*co*-divinylbenzene) beads [144, 145], a macroporous chitosan/silica hybrid scaffold [146] and zinc and poly(vinyl alcohol) modified poly(tetrafluoroethylene) membranous Sepharose capillaries [74].

Immobilised on these various different scaffolds the Reactive blue 2 has been used for human serum albumin adsorption, retention and separation [74, 140, 142, 144], protein affinity separations [143], as a support for column based protein refolding [146],

purification of high M_R glutenin subunits from wheat flour [139] and lysozyme adsorption [145].

Reactive brown 10 (Fig. 1.9) also appears frequently in the literature and is mainly used for the adsorption, purification and separation of lysozyme from egg white [147-149].
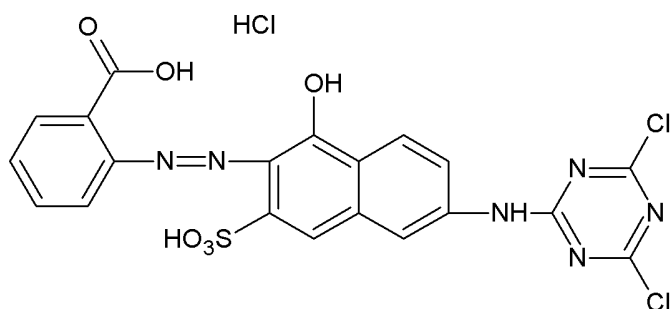
Figure 1.9: *Structure of Reactive brown 10*

This dye has also been immobilised on a variety of substrates including poly(HEMA) membranes [147], poly(ethylene terephthalate) fibres grafted with methacrylamide [148] and poly(HEMA) and poly(HEMA)/chitosan [149], in addition to commonly used cellulosic fibres.

Reactive green 19 (Fig. 1.10) is a very versatile reactive dye being used in a number of different applications including; the separation of secreted alkaline phosphatase from CHO cell culture and *aspergillus Niger* [150], the isolation of G-DNA structures [151] and the separation and purification of lysozyme [152] from egg white.
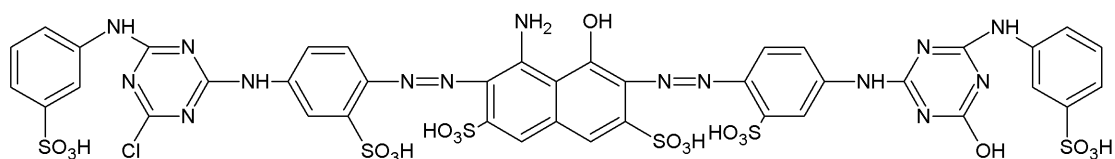
Figure 1.10: *Structure of Reactive green 19*

For these applications Reactive green 19 is commonly immobilised on Sepharose [150], agarose [151] or poly(HEMA)-chitosan membranes [152].

Lastly, Reactive red 120 (Fig. 1.11) is a popular red stain used for lysozyme adsorption and purification [153, 154], the purification of high M_R glutenin subunits from wheat

flour [155] and for human serum albumin retention [144]. In addition to agarose [155], this dye is generally immobilised on either copper incorporated poly(HEMA) hydrogels [153], poly(vinyl alcohol) coated-poly(S-*co*-DVB) [144] or poly(HEMA) and HEMA-chitosan membranes [154] for these applications.
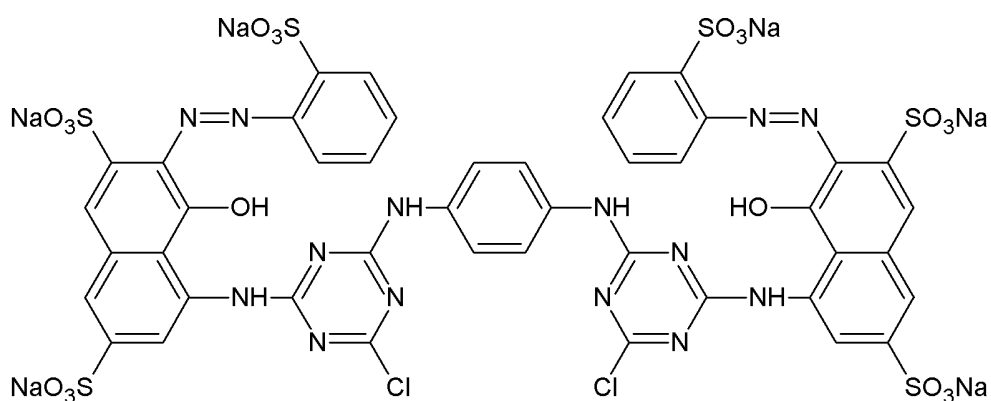
Figure 1.11: *Structure of Reactive red 120*

There are few examples of silica and organic polymer monolithic stationary phases for dye-ligand affinity chromatography, one particular example is that of the research of Sun *et al.* [35] who immobilised Reactive blue 4 on the surface of a urea-formaldehyde monolith and then used this for protein isolation. In their paper they showed the ability of the column to retain human serum albumin, lysozyme and ovalbumin and separate bovine serum albumin from newborn calf serum. It was remarked in a recent review [133] that the efficiency of the column would have been greater if the stationary phase had been based on agarose in place of urea-formaldehyde as reactive dyes bind covalently to polysaccharides without having to undergo extreme reaction conditions. It is likely that more examples will appear in the future due to the usefulness of monolithic materials in the separation of bio-molecules.

While there are a large number of papers discussing the use of reactive dyes as stationary phase coatings for affinity chromatography, there are relatively few examples in the literature reporting on the use of other types of dyes in separations applications. Nakagama *et al.* [156] synthesised an azobenzene modified cyclodextrin stationary phase which was partially responsive to light and partially thermo-responsive. This stationary phase was then examined for the separation of perylene and pentacene by

light and thermo modified retention mechanisms. While this stationary phase could not be made to retain and release materials simply by light irradiation it helped to prove the concept that it is possible to control retention and elution mechanisms by methods other than solvent polarity and column temperature.

Work with the photochromic dye spiropyran (SP) has made a major part of this thesis and these results are reported in Chapter 3.

Spiropyrans are a family of organic dyes known for their photochromic, thermochromic and solvatochromic properties among others. The thermochromic properties of the spiropyrans were discovered in 1921, however it wasn't until 1952 that the photochromic properties were discovered by Fischer and Hirshberg [157, 158]. Since this discovery the spiropyrans have found many uses in light responsive ophthalmic lenses [159], molecular switches [160], optical memory [161, 162], non-silver high resolution photography [158], metal ion sensors [163] and photovoltaic and holographic systems [158].

The definition of photochromism is that it is a chemical process caused by electromagnetic radiation, where a molecule changes reversibly between two states having separate absorption spectra and so different colours [164]. The process is caused either by changing the wavelength of the source of the irradiation or by switching it on and off.

The two forms of the spiropyran molecule are the passive spiropyran form (SP), which is uncharged and colourless, and the active merocyanine form (MC), which is zwitterionic and intensely coloured. The switch is triggered by irradiation at different wavelengths of light, UV light producing the MC form while visible light produces the SP form as can be seen in Fig. 1.12.
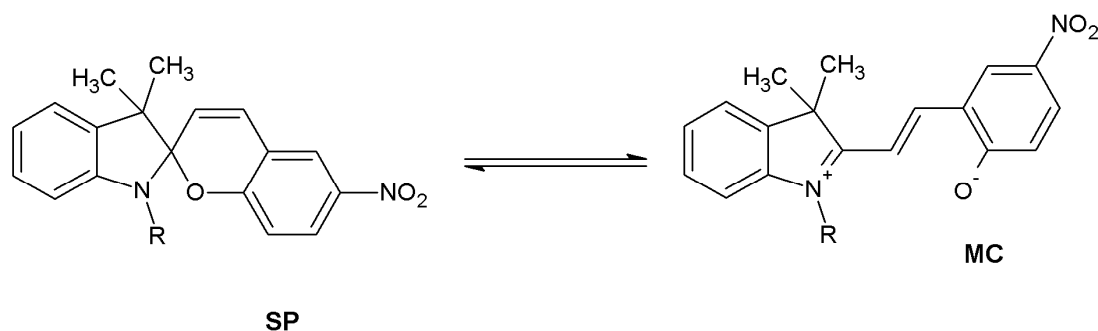
Figure 1.12: *Switching mechanism of a generic spiropyran molecule from the SP form to the MC form*

Spiropyrans have been extensively studied in the literature and have dedicated chapters in several books relating to dyes and colour chemistry [158, 159, 164], however the majority of this information involves the dye in solution or trapped in polymer films. Although the spiropyrans are thermochromic (heating causes the appearance of the intense red/pink MC form) [158], solvatochromic (MC form is red/pink in polar solvents and blue in non-polar solvents) [165, 166], acidochromic (MC form is yellow in the presence of acids) and electrochromic (electro-reduction and photolysis (photoelectrochromism) can cause the appearance of the MC) [167], research is mainly focused on the photochromic properties of the molecule.

The main usage of the spiropyrans in the literature is as photo-switchable chelating ligands. It has been stated as far back as 1965 that the merocyanine form has chelating abilities [158, 165, 168]. The MC form can act as a chelating ligand for both divalent metal ions [169-171] and amino acids [168]. The metals that have the strongest complexation with the MC form are the transition metal ions in particular, Cu^{2+} and Co^{2+}.

While it has been stated that spiropyrans do not complex well with monovalent metal ions, it has been reported that attaching a crown-ether group to the dye molecule significantly improves its ability to complex with Li^+, Na^+ and K^+ [172]. Filley *et al.* [173] have synthesised a *bis*-spiropyran to improve the complexation of the spiropyrans with non-transition divalent metal ions, Ca^{2+} and Mg^{2+}, 8-fold. In all cases retention and

release of metal ions was controlled by irradiation of the molecule with different wavelengths of light.

There is potential for further development of this technique of photo-controlled retention and release to make it more suitable to applications in chromatography, in particular pre-concentration and sample clean-up, where the target analytes could be held on the stationary phase using light until all contaminants of the sample have been eluted at which point the target analyte could then be released from the surface.

1.6.2. Monoliths Modified with Biologically Active Compounds

Currently one of the most interesting applications of surface modified monoliths is the immobilisation of biologically active compounds on the surface for a range of different applications. The most commonly described applications are the use of protein immobilised monoliths for affinity chromatography and enzyme grafted monoliths as enzymatic reactors for the digestion of proteins.

Bedair *et al.* [174] presented the modification of poly(GMA-*co*-EDMA) and poly(GMA-*co*-EDMA-*co*-[2-(methacryloyloxy)ethyl]trimethyl ammonium chloride]) monoliths with both two different lectins, concavalin A and wheat germ agglutenin, for Lectin Affinity Chromatography. This was achieved by first hydrolysing the epoxide functionality to a diol and then oxidising it to an aldehyde. This aldehyde can bind to the primary amines in the protein, which is then flushed through the column. This step is followed by the reduction of the primary amines to secondary amines and conversion of any remaining aldehydes to alcohols. They showed that these monoliths had a strong affinity for glycoproteins and glycans allowing them to effectively concentrate glycoconjugates. By adding a second dimension, a reversed phase column, they were then able to separate the concentrated glycoconjugates from one another.

Using a similar method to Bedair *et al.* [174], which they have noted in this publication is a Schiff Base method, Mallik *et al.* [175] have immobilised human serum albumin onto poly(GMA-*co*-EDMA) monolithic stationary phases. While they have examined different methods of immobilisation, the Schiff base method allowed for the largest concentration of HSA to be immobilised on the column. This protein affinity column

was then used for the chiral separation of enantiomers such as *R/S* warfarin and D/L-tryptophan. They noted that for the separation of the warfarin enantiomers the column efficiency was greater than that noted for silica monoliths with HSA immobilisation.

Looking now at enzymatic reactors, it can be seen that a large number of different enzymes can be immobilised on the surface of monoliths for different protein digestions, however, by far the most common is trypsin.

Křenkova *et al.* [176] showed the use of trypsin immobilised poly(GMA-*co*-EDMA) monoliths for protein digestion. They achieved enzyme modified columns by simply equilibrating the column with an immobilisation buffer, then flushing the column with a solution of the immobilisation buffer containing trypsin and benzamidine for 4 h and finally flushing the column with the immobilisation buffer containing NaCl to remove non-specifically adsorbed enzyme. They showed that complete digestion of cytochrome C was achieved in 30 s at 25°C with a sequence coverage of 80% determined by mass spectrometry compared to 3 h at 37°C when the same digestion is done in solution. In later work by Křenkova *et al.* [177] they showed an improvement to the immobilisation procedure, which involved photo-grafting a layer of 4-vinyl-2,2-dimethylazlactone onto the poly(GMA-*co*-EDMA) monolith to increase the immobilisation capability as amines present in the enzyme will covalently bind to 4-vinyl-2,2-dimethylazlactone. They then showed that these new trypsin immobilised monoliths could digest human immunoglobulin G in 6 min at 25°C to the same extent as solution digestion at 37°C carried out for 24 h.

Logan *et al.* [178] have also reported the multi-enzyme grafting onto poly(butyl methacrylate-*co*-ethylene dimethacrylate) monoliths. To prepare the column they first grafted a layer of poly(ethylene glycol) methacrylate to prevent non-specific interaction between the enzyme and the stationary phase then, using photo-masks they grafted a 1 cm section of the monolith with 2-vinyl-4,4-dimethylazlactone. This step was followed by flushing with a solution of the enzyme, which binds to the surface through the amine groups. To extinguish the binding capabilities of any excess azlactone functionalities the column was then flushed with ethanolamine. This procedure was repeated to immobilise two or three different enzymes, invertase, glucose oxidase or horseradish peroxidase, on

each monolithic reactor. They suggest that these multi-enzyme reactors would be useful in miniaturised diagnostic assays and the investigation of metabolic pathways for example.

While these applications are the most commonly reported in the literature the grafting of peptides [179], antibodies [180], polysaccharides [181] and aptamers [182], among others, have also been reported. In all cases reference here the polymers were co- or ter-polymers containing glycidyl methacrylate and ethylene dimethacrylate, in the case of the polysaccharide binding a polymer identical to that described by Bedair *et al.* [174] above was used. The immobilisation of all the different biological compounds seems to be carried out in one of two ways, either by a method similar to that of Křenkova *et al.* [176] described previously, or by first modifying the epoxy ring with an amine functionality before flushing the columns with solutions of the amine containing biologically active compounds. Applications range from affinity chromatography purification of human blood coagulation factor VIII in the case of peptide bound columns [179] to protein purification and separation from serum in the case of aptamer modified columns [182], with numerous others besides.

These monoliths modified with biologically active compounds have a variety of applications in the field of biochemistry and biotechnology and pave the way for further investigation of the miniaturisation of bio-separations, analysis and assays.

1.6.3. Monoliths Modified with Organic and Inorganic Nano-particles

As has been described previously there are a number of methods by which to modify the surface of organic polymer monoliths, with other organic polymers or biologically active compounds, for example. This section presents the work done by several different groups on the immobilisation of both organic and inorganic nano-particles on the surface of organic polymer monoliths for a variety of separations applications.

Hutchinson *et al.* [183] describe the immobilisation of latex nano-particles on methacrylate monoliths. These latex coated columns were achieved by first incorporating AMPS into the pre-polymer solution to obtain a terpolymer, poly(BuMA-*co*-AMPS-*co*-EDMA), which, as mentioned in previous sections, contains cation-

exchange sites thanks to the AMPS. After the synthesis of this monolith a suspension of quaternary ammonium functionalised polymeric latex particles were flushed through the column until all the cationic sites were covered with latex particles. These latex coated monoliths were then used for the on-line pre-concentration of organic anions prior to separation by capillary electrophoresis.

Daņiļēvičs *et al.* [184] have also reported the surface immobilisation of nano-particles on methacrylate monoliths. In their work they report the immobilisation of gold nano-particles on the surface of poly(GMA-*co*-EDMA) monoliths by first hydrolysing the monolith surface to produce anionic sites and then flushing through coatings of alternate solutions of cationic and anionic polymers before flushing through a solution of gold nano-particles in water. They estimate that their stationary phases should be suitable for the separation of thiol containing proteins and peptides, due to the affinity of gold for thiol functionalities.

In addition to surface immobilisation, embedding is another technique reported in the literature to achieve monoliths functionalised by inorganic nano-particles. Yao *et al.* [185] have described the synthesis of a super-macroporous monolithic cryogel, a monolith synthesised at temperatures below zero, synthesised from ternary mixture of acrylamide, *N,N′*-methylene-*bis*-acrylamide and allyl glycidyl ether monomers. Into the pre-polymer solution was added a surfactant stabilised suspension of magnetite nano-particles (Fe_3O_4) and was incorporated into the polymer matrix during the polymerisation procedure. They reported that the addition of these magnetite nano-particles improved the protein absorption capacity of the stationary phase compared to similar cryogels reported in the literature from tests carried out with bovine serum albumin (BSA).

Rainer *et al.* [186] have reported the incorporation of titanium dioxide and zirconium dioxide in poly(divinylbenzene) monoliths synthesised in pipette tips. They achieved this by mixing a certain weight of the dry nano-particles into the polymerisation mixture, which was then put into the pipette tips and thermally polymerised. These monolithic pipette tips were then used for the selective enrichment of phosphorylated

peptides from tryptic digests, and a higher selectivity compared to standard immobilised metal affinity chromatography was observed.

1.7 Conclusions

From the literature examples presented in this chapter it can be seen that monolith synthesis is a large and varied field.

In addition to the numerous sources of energy used to initiate the polymerisation, such as heat, light and microwaves, there are also a variety of initiation methods including free radical, anionic and RAFT mechanisms.

Different surface chemistries can also be obtained by selection of the appropriate monomers, while porosity is determined by the selection of porogens, the chosen polymerisation method and the duration of the polymerisation reaction. Further interesting chemistries can be obtained by modifying the surface of the monolith with other synthetic monomers, or more exotically with dyes, stains, nano-particles or biologically active compounds.

Adding these to the number of different moulds available for the synthesis of monolithic stationary phases, it is clear that the monolith can be tailored to the desired application of the user. This diversity makes monoliths quite important in the field of separation science.

2. Monoliths in Capillaries – General Studies

2.1. Introduction

As mentioned in Chapter 1, monoliths are cross-linked chain polymers synthesised by suspension polymerisation. The majority of monolith syntheses, and all those discussed within this thesis, are free radical initiation mechanisms, which rely on the generation of free radicals by the initiator to propagate chain growth.

Several different mechanisms are known from the literature by which to initiate the polymerisation of monolithic stationary phases; cationic, anionic RAFT, ring-opening metathesis and free radical initiation mechanisms, the free radical initiation mechanism being the most common for the synthesis of organic polymer monoliths [37]. Additionally, there are a number of different methods of supplying energy to the system in order to start the decomposition of the initiator to radicals. Polymerisations initiated by heat [6], light [55], microwave irradiation [57] and gamma radiation [56] have all been described in the literature, however the most common energy source used to initiate polymerisations remains heat, with photo-initiated polymerisation a close second.

Thermally initiated polymerisations are quite simple to perform, however the polymerisation time is long and there is no control over the location of the polymer within the mould. Photo-initiated polymerisation on the other hand allows full control of the location of the polymer and the polymerisation time is rather short. As ultraviolet (UV) radiation is mainly used to carry out the polymerisation, it is important that both the mould and the pre-polymer solution are UV transparent otherwise polymerisation cannot occur. This excludes standard polyimide coated fused silica capillary as a mould due to the fact that it absorbs very strongly below 550 nm as can be seen in Fig. 2.1.
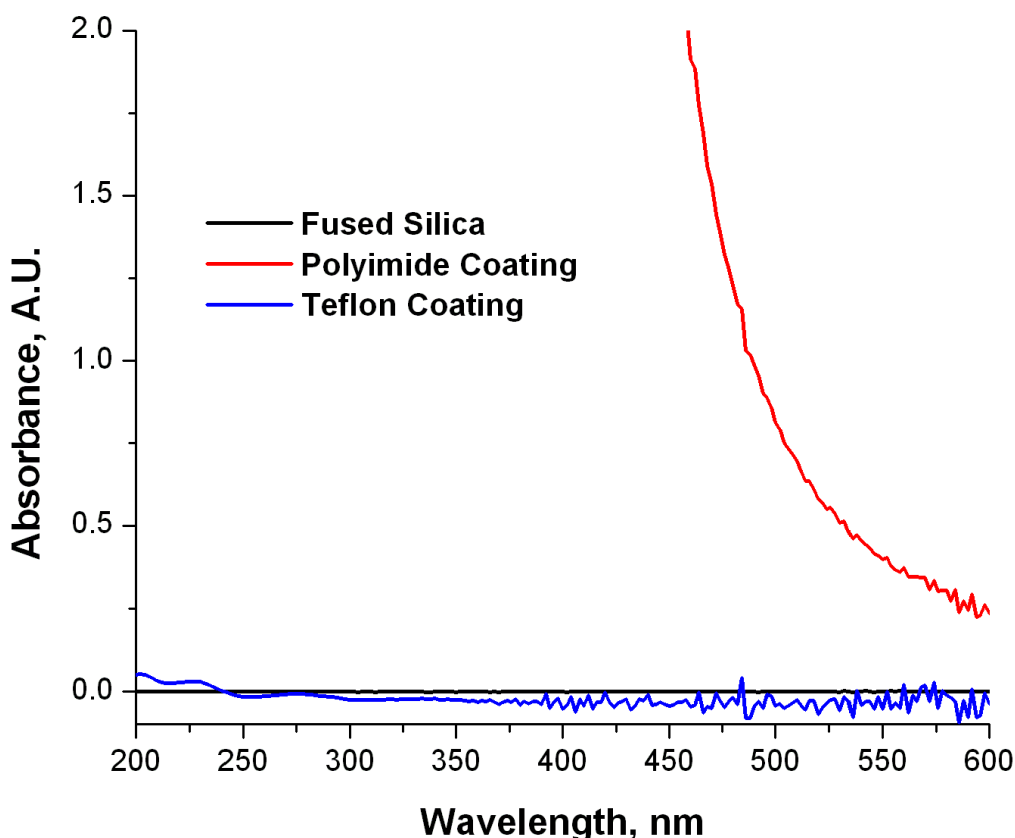
Figure 2.1: *Spectra of fused silica capillary with the protective coating removed, polyimide coated fused silica capillary and poly(tetrafluoroethylene) coated fused silica capillary. All capillaries have an internal diameter of 100 µm, an external diameter of 375 µm and 335 µm with and without coating, respectively. Measurements were performed on an Agilent CE instrument with the capillary filled with deionised water.*

Before any new methods of initiation of the polymerisation of monolithic stationary phases could be developed at a later point in the research project, it was necessary to first investigate both of these types of polymerisation and the moulds which can be used.

In addition to the investigation of the moulds and initiators, some study was also carried out on how other experimental factors such as polymerisation time, porogenic solvent, monomers and monomer concentration can affect the outcome of the polymerisation reaction.

The synthesis of functional monoliths or the functionalisation of existing monolithic scaffolds is also an area with great potential. Perfecting the ability to immobilise a variety of different functional groups within a monolithic polymer or on the pore surface allows the user to perform a range of separations with functional groups particularly selected for a specific analysis. For chromatography this means better and faster separations with improved efficiency and reproducibility. The synthesis of these functional monoliths and functionalised monoliths was also examined and is presented in this section.

In this chapter gaining control over the known methods of polymer monolith synthesis as described in the literature, particularly thermal and photo-initiated polymerisation methods was the main focus. Once knowledge of these procedures had been gained, investigation of the use of different porogens, monomers and moulds, and examination of how the resulting monolith is changed by varying these parameters was carried out. With photo-initiated polymerisation the use of alternative light sources to initiate the polymerisation was also studied. Other applications of photo-initiated polymerisations such as photo-initiated grafting and the synthesis of monolithic frits for column packing are also investigated.

2.1.1. Aims

The aims of the work carried out in this chapter were;

1. to investigate literature methods for the thermally initiated synthesis of methacrylate and styrenic monoliths and show that these can be easily reproduced and modified to suit this project,

2. to study thermally initiated polymerisation in non-standard moulds,

3. to investigate literature methods for the photo-initiated synthesis of methacrylate monoliths and show that these can be easily reproduced and modified to suit this project,

4. to study the use of light emitting diodes in place of conventional UV lamps for photo-initiated polymerisation,

5. to investigate the ability to use short monolithic plugs as retaining frits for a new low-pressure method of column packing,

6. to study the ability to effectively graft layers of monomers onto pre-existing monolith scaffolds.

2.2. Experimental

2.2.1. Reagents

1,4-Butanediol (ReagentPlus, 99%), 1-decanol (Reagent grade, 99%), 2,2'-azobisisobutyronitrile (98%, AIBN), 2.2-dimethoxy-2-phenylacetophenone (99%, DMPAP), 2-aminoethyl methacrylate hydrochloride (90%, AEMA), 3-(trimethoxysilyl)propyl methacrylate (> 98%, TMSPM), 4,4'-*bis*(dimethylamino)benzophenone (98%, Michler's ketone, MK), benzophenone (99%, BP), bovine serum albumin (BSA), butyl methacrylate (99%, BuMA), cyclohexanol (Reagent grade, 99%), cytochrome C from bovine heart, divinylbenzene (80%, DVB), dodecanol (Reagent grade, 98%), ethylene dimethacrylate (98%, EDMA), formic acid (ACS Reagent 88%), glycidyl methacrylate (97%, GMA), ovalbumin from chicken egg white, methacrylic acid (99%, MAA), methanol (HPLC grade), myoglobin from equine skeletal muscle, ribonuclease A from bovine pancreas, styrene (>99%, S), *t*-butanol (HPLC grade, 99.5%) and toluene (Reagent grade) were all purchased from Sigma-Aldrich Chemical Co. (Wicklow, Ireland) and were used as received.

HPLC grade acetone and acetonitrile were purchased from LabScan (Gliwice, Poland) and UV-spectrometric grade ethanol was obtained from Lennox Laboratory Supplies (Dublin, Ireland).

The structures, names and common abbreviations of the monomers used in this work are shown in Table 0.1.

2.2.2. Materials

Polyimide and poly(tetrafluoroethylene) (PTFE) coated fused silica capillaries were purchased from Polymicro Technologies (Phoenix, AZ, USA).

Poly ether ether ketone (PEEK) tubing, micro-tight sleeves, fluorinated ethylene propylene (FEP) sleeves, ferrules, nuts, adaptors, unions, luer fittings and T-pieces were purchased from Upchurch Scientific (Oak Harbor, WA, USA).

Rubber septa were obtained from Sigma-Aldrich Chemical Co (Wicklow, Ireland), black vinyl insulating tape was purchased from 3M (Austin, TX, USA) and glass syringes were obtained from Hamilton (Bonaduz, Switzerland).

2.2.3. Instrumentation

A capacitively coupled contactless conductivity detector (C^4D) with a 375 µm sensor head was obtained from Innovative Sensor Technologies (Vienna, Austria) and used for lateral conductivity profiling.

A Bransonic 5510 ultrasonic bath from Branson (Danbury, CT, USA) was used to ensure dissolution of all pre-polymer solutions and removal of dissolved oxygen which can interfere with the generation of radical in the polymerisation reaction.

A Clifton thermostatted water bath from Bennett Scientific Ltd., (UK) was used for thermally initiated polymerisations. For photo-initiated polymerisations either light emitting diodes (LEDs) or a conventional UV curing unit were used. LEDs, 365 nm, 375 nm and white, were purchased from Roithner Laser Technik (Vienna, Austria) and a 255 nm deep UV LED was obtained from Sensor Electronic Technology (SC, USA). The UV light curing unit, an X1-1000 UV cross-linker, was purchased from Spectroline (New York, NY, USA).

An Ultimate-3000 Nano-LC with Famos micro-autosampler, obtained from Dionex Corporation (Sunnyvale, CA, USA), was used for the separation of test compounds on the synthesised monolithic stationary phases. A S-3000N variable pressure scanning electron microscope and a S-3400 VP-SEM, both from Hitachi (Tokyo, Japan), were used to image monoliths in capillary.

A Labview Synchronized Video Microscope (SVM-340) was also used to image monoliths in capillary at lower magnification; this was purchased from National Instruments Corporation (Austin, TX, USA).

Flushing the capillaries was done with a peristaltic pump from Lambda Technologies (Brno, Czech Republic), a syringe pump from KD Scientific (Holliston, MA, USA), an

LC-10AD HPLC pump from Shimadzu (Kyoto, Japan) or a K-120 HPLC pump from Knauer (Berlin, Germany).

2.2.4. Procedures

2.2.4.1. Pre-treatment of the walls of fused silica capillaries

Two different silanisation procedures were used during the course of this thesis. The first procedure was described by Okanda and El Rassi [187] and involved flushing the capillary with 1 M NaOH for 30 min, following by 0.1 M HCl for a further 30 min before flushing with deionised water for 30 min. After flushing with water the capillary was dried under nitrogen for 30 min and then filled with a sonicated 50:50 mixture of TMSPM:acetone. The ends were sealed with rubber septa and the capillary was placed in a water bath at 60°C for 20 h.

The second procedure was described by Křenkova *et al.* [177]. In this procedure a length of fused silica capillary was cut and flushed with acetone to clean the inner walls of the capillary. After drying the capillary with nitrogen, the cavity was flushed with a 0.2 M solution of sodium hydroxide for 30 min until the pH of the eluent is basic. The column was then flushed with water for 30 min until the pH returned to neutral. 0.2 M HCl was then flushed through the column for 30 min until the pH was acidic followed by water to return the pH to neutral.

Acetic acid in ethanol at pH 5 was then flushed through the column before flushing a solution of 20% 3-(trimethoxysilyl)propyl methacrylate (TMSPM) in ethanol at pH 5 for 90 min. The TMSPM/ethanol solution was then removed from the column by flushing with acetone and drying under nitrogen. The capillary was end-capped and then allowed to sit overnight for the polycondensation reaction to proceed.

2.2.4.2. Synthesis of poly(glycidyl methacrylate-*co*-ethylene dimethacrylate) monoliths) by thermally initiated polymerisation

Svec and Fréchet have previously described the thermally initiated synthesis of poly(GMA-*co*-EDMA) [6], the procedure used throughout this thesis is a modified version of the original which is described in this section.

40 µl (0.29 mmol) GMA monomer and 40 µl (0.21 mmol) EDMA cross-linker were added to an Eppendorf tube. Along with the monomer and cross-linker, approximately 0.63-1.66 mg of 2,2'-azobisisobutyronitrile (AIBN) was added. Approximately 1-2% of AIBN per weight of monomers is necessary to start the polymerisation reaction. A binary porogenic solvent was used consisting of 40 µl micro-porogen (generally cyclohexanol or 1,4-butanediol) and 80 µl macro-porogen (generally 1-decanol or dodecanol). The total volume of the reaction mixture was 200 µl. The vial containing the pre-polymer solution was sonicated for 20 min to ensure dissolution of all components of the reaction mixture and to remove dissolved oxygen from the solution. A pre-treated polyimide coated fused silica capillary with 100 µm i.d. was filled with the reaction mixture, the ends of the capillary were sealed with rubber septa and the capillary was placed in a water bath at 60°C for 20 h. After the reaction was complete the capillary was taken out of the water bath and 1-2 mm was cut from each end of the capillary to remove any blockages caused by the rubber septa. Methanol was used to flush any remaining porogens from the pores of the monolith and the monolith was then dried with nitrogen. The synthesised monoliths were white and had good flow through properties when flushed with methanol at 10 µl/min.

2.2.4.3. Synthesis of poly(styrene-*co*-divinylbenzene) monoliths by thermally initiated polymerisation

Poly(S-*co*-DVB) monoliths were synthesised containing varying percentages of monomers, following a method loosely based on the procedure for the thermally initiated synthesis of poly(S-*co*-DVB) described by Wang *et al.* [15].

The general procedure is described as follows; 35 µl (0.31 mmol) styrene monomer and 35 µl (0.25 mmol) DVB cross-linker were mixed in a vial. Along with the monomer and cross-linker, approximately 0.64mg (1% of the weight of the monomers) of AIBN was added to initiate the polymerisation. Two different porogens were used, in one batch 130 µl of 1-decanol was added to the mixture as porogenic solvent and in the second batch 23 µl acetonitrile, 46 µl 1-propanol and 61 µl 1-decanol were used as the porogenic solvent. The reaction mixture was sonicated for 20 min and then purged with nitrogen before being filled into a pre-treated polyimide coated capillary and placed in a water

bath for 20 h at 60-70°C. After polymerisation the monolith was washed and dried as described previously. The synthesised monolith was white and had good flow through properties when flushed with MeOH at 10 µl/min.

2.2.4.4. Synthesis of poly(glycidyl methacrylate-*co*-ethylene dimethacrylate) monoliths by photo-initiated polymerisation at 365 nm

The procedure used for the synthesis of methacrylate monoliths using UV LEDs is similar to the procedure described by Abele *et al.* [65].

In this procedure, 60 µl (0.44 mmol) GMA and 60 µl (0.32 mmol) EDMA were added to a sample vial, along with 1.26-2.52 mg (1-2%) Michler's Ketone (MK). MK is a free radical photo-initiator which is activated in the ultraviolet region at 365 nm. A binary porogenic solvent was used consisting of 186 µl cyclohexanol and 94 µl 1-decanol. The reaction solution was sonicated for 10 min to allow all components to mix thoroughly and then purged with nitrogen.

A pre-treated PTFE-coated fused silica capillary was filled with the reaction mixture, the ends of the capillary were sealed with rubber septa and black electrical tape was used to mask parts of the capillary so that the monolith formation could be spatially controlled within the mould. The exposed areas were irradiated with a 365 nm light emitting diode (LED) for 20 min with the LED current set at 20 mA and the LED positioned perpendicular to the capillary at a distance of 5 mm.

The synthesised monoliths were flushed with MeOH to remove any excess porogen and then dried with nitrogen flow. After flushing with solvent white plugs of monolith were observed in the capillary corresponding to the un-masked sections of the mould.

2.2.4.5. Synthesis of poly(butyl methacrylate-*co*-ethylene dimethacrylate) monoliths by photo-initiated polymerisation at 254 nm using a conventional UV curing unit

Poly(BuMA-*co*-EDMA) monoliths were synthesised using a procedure similar to that described by Pucci *et al.* [67]. 36 µl (0.23 mmol) BuMA and 24 µl (0.13 mmol) EDMA were mixed in a sample vial. Along with the monomer and cross-linker, 0.57-1.14 mg

(1-2%) of DMPAP was added to initiate the polymerisation. A binary porogen was used consisting of 93 µl 1-decanol and 47 µl cyclohexanol.

The reaction mixture was sonicated for 20 min to dissolve the initiator and remove any dissolved oxygen before being filled into pre-treated PTFE-coated fused silica capillaries. The capillaries were placed in the X1-1000 UV cross-linker directly under the UV lamps which are calibrated at 254 nm. The capillaries were subjected to two doses of irradiation with the lamp set to deliver 1 J/cm^2 each time.

The product of this synthesis was flushed with MeOH at 10 µl/min to remove any excess porogens from the pores of the monolith.

2.2.4.6. Synthesis of poly(butyl methacrylate-*co*-ethylene dimethacrylate) monoliths by photo-initiated polymerisation at 254 nm using a light emitting diode

Using a similar procedure to that described in Section 2.2.4.5, poly(BuMA-*co*-EDMA) monoliths were synthesised using light emitting diodes as the initiating light source in place of a conventional UV curing unit.

A solution of total volume of 200 µl was made up, consisting of 48 µl (0.31 mmol) BuMA, 32 µl (0.24 mmol) EDMA and 120 µl of decanol as the porogenic solvent. Approximately 0.77 mg of DMPAP was added to initiate the polymerisation. The reaction mixture was sonicated for 20 min to dissolve the initiator and remove any dissolved oxygen before being filled into pre-treated PTFE-coated fused silica capillaries.

Using rubber septa as a photo-mask a length of capillary 3-5 mm long was exposed to UV light from a 255 nm LED (forward current = 20 mA) to initiate the *in situ* polymerisation. The LED was placed perpendicular to the capillary at a distance of 1 mm and the polymerisation allowed to proceed for 1 h. After this time, the capillary was flushed with methanol in order to remove any unreacted components of the polymerisation mixture. The resulting polymeric monolith typically has a pore size of around 1-2 µm judging from SEM images (Fig 2.21).

2.2.4.7. 2-Step grafting of methacrylate monomers on monolithic scaffolds

Using a procedure similar to that introduced by Ma *et al.* [124] and modified for monolith grafting by Rohr *et al.* [68], 1.38 mg of benzophenone was added to 5 ml of a 3:1 mixture of *t*-butanol:water and the solution was sonicated for 30 min to ensure complete dissolution of the initiator and removal of any dissolved oxygen present. Once the initiator was fully dissolved the solution was filled into pre-synthesised poly(BuMA-*co*-EDMA) monoliths (Section 2.2.4.5) in PTFE-coated fused silica capillary and the ends were sealed with rubber septa.

The capillaries were then subjected to 3 J/cm^2 of irradiation from a UV-Spectrolinker calibrated at 254 nm. This process generates surface radicals which will then react with the monomers used in the next step to immobilise them on the surface of the monolith.

2.2.4.7.1. Grafting of methacrylic acid onto the monolith surface

A 15% w/v solution of MAA in methanol was prepared containing 148 µl (1.75 mmol) of the monomer in 1 ml of methanol. This solution was filled into a pre-synthesised monolith which had been previously modified (as in Section 2.2.4.7) to obtain surface radicals in the pores of the monolith. The ends of the capillaries were sealed with rubber septa and then given a further 3 J/cm^2 of irradiation at 254 nm from the calibrated UV-Spectrolinker. After irradiation the monolith was flushed with ethanol to remove any unreacted components.

2.2.4.7.2. Grafting of 2-aminoethyl methacrylate onto the monolith surface

This procedure is the same as described in the previous section except the 15% w/v solution of reactive monomer contained 148.83 mg (0.9 mmol) AEMA in 1 ml methanol instead of MAA.

2.2.4.8. Characterisation of the monoliths in capillary

2.2.4.8.1. Scanning Electron Microscopy

Lengths of monolith filled capillary of approximately 8 mm were cut from different places along the capillary. These pieces were then held upright with the surface to be imaged facing upwards. Before imaging the capillaries were sputter coated with a thin layer of gold to reduce surface charge effects generated by the non-conducting polymer.

Generation of surface charge can distort the quality of the image. The sputtered capillaries were held in a specially designed by a post-doc in this group, which consisted of an SEM stub with 7 capillary sized holes in it where the capillaries could be placed so that more than one capillary could be imaged in one session.

2.2.4.8.2. Flow resistance measurements

The resistance to flow of the monolithic columns was measured using a Knauer S-120 HPLC pump with 100% deionised water with as the eluent. The flow measurements were carried out over a specific range, which depended on the permeability of the monoliths, in a step-wise manner.

2.2.4.8.3. Lateral conductivity profiling

An on-column C^4D cell was placed on the capillary, which was connected to a pump continuously flushing water through it, and moved down the length of the filled capillary at 1 mm increments, as shown in Fig. 2.2. The conductivity value was recorded at each interval. While the stationary phase bears no charge, voids in the columns result in an increase in conductivity. The capillaries were flushed constantly with water during the measurement.
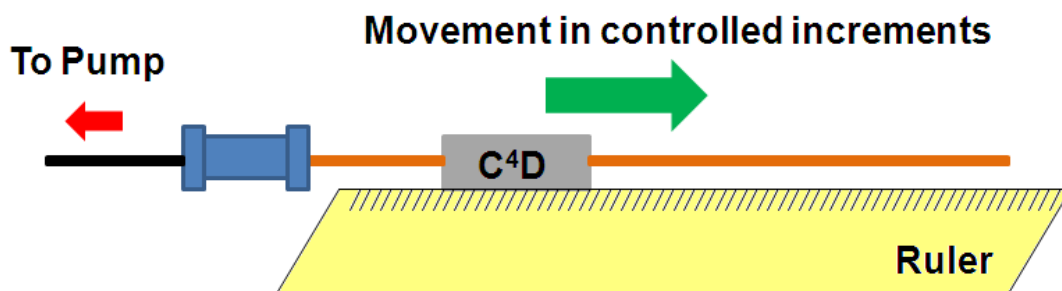
Figure 2.2: *Schematic of the lateral conductivity profiling performed with the aid of an on-column capacitively coupled contactless conductivity detector.*

2.2.4.8.4. Separation of proteins

Analyses were carried out at a flow rate of approximately 1 μl/min, with an injected sample volume of 50 nl and a detection wavelength of 210 nm. The gradient elution profile consisted of 0.1% formic acid in water (mobile phase A) for 1 min, 5 min to go

from 0-60% mobile phase B in A (0.1% formic acid in acetonitrile), 10 min hold, return to A in 5 min followed by 5 min conditioning before the next injection. Each separation was run three times on each column.

2.3. Results and Discussion

2.3.1. Pre-treatment of capillaries

Before any polymerisation can be carried out in fused silica capillaries, regardless of the method of initiation and the initiation energy source, the walls of the capillary must be treated in order to bind to the growing polymer chains. There are a large number of methods described in the literature for the pre-treatment of the capillary walls but throughout this thesis only two different methods have been used, those described by Okanda *et al.* [187] and Křenková *et al.* [177].

Pre-treatment of the walls of the capillary ensure the creation of a layer of molecular 'anchors' to which the growing polymer chains attach and the monolith then grows from the wall outwards. Good wall attachment gives the monolith greater mechanical stability, which is particularly important to prevent the monoliths being pushed out of the mould when pressures are applied when connected as part of a chromatographic set-up. If the monolith is well adhered to the walls the presence of voids is less likely which can cause problems for chromatographic analyses such as peak tailing [31]. The most commonly used silanising agent described in the literature is 3-(trimethoxysilyl)propyl methacrylate (TMSPM), Fig. 2.3, this is also used in this work to prepare the walls of all capillaries before polymerisation is carried out within the internal channels.
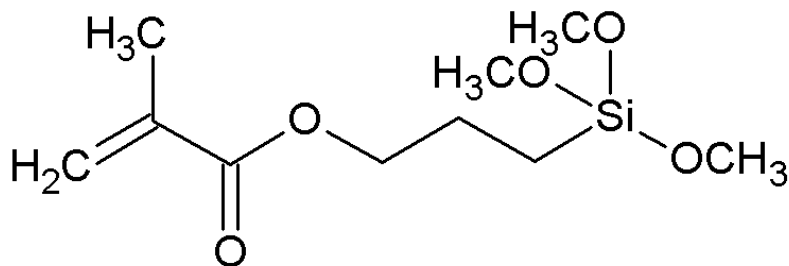
Figure 2.3: *Structure of the silanising agent 3-(trimethoxysilyl)propyl methacrylate (TMSPM)*

TMSPM has two active sites, on one end there is a silane group which binds to the silanol groups which are exposed on the surface of the fused silica capillary during the silanisation procedure. The other end of the molecule has a methacrylate group which is susceptible to attack by radical species during the polymerisation reaction in order to allow polymer chains to grow from the walls of the capillary. This mechanism ensures that the monolith is well anchored to the walls.

2.3.2. Thermally initiated polymerisations

The procedures outlined in the experimental section above were determined to be the best and most reproducible methods found in the literature for the synthesis of both poly(GMA-*co*-EDMA) and poly(S-*co*-DVB) monoliths, however, they were often modified to produce monoliths which were more tailored to our specific needs particularly in the case of the methacrylate monoliths, a number of other porogenic mixtures were studied and evaluated by scanning electron microscopy (SEM). From the literature [36] a number of potential porogens were identified, such as methanol, toluene, 1,4-butanediol, cyclohexanol, decanol, tetrahydrofuran (THF) and dodecanol. Due to their extremes of polarity methanol and toluene are useful as micro-porogens, producing very small globules which give the monolith a higher surface area. 1,4-Butanediol and cyclohexanol are also common micro-porogens, although the micro-globules they produce are generally larger than those formed by methanol or THF. Finally decanol and dodecanol are described in the literature [36] as macro-porogens, meaning they will produce a monolith with large pores thus giving the structure higher

permeability and better flow through properties. It was decided to perform some investigations with these porogens to ensure the same conclusions were reached as described in the literature. The examples shown below were made using a GMA-EDMA pre-polymer solution. Fig. 2.4 shows an example of the pore structure when only one porogen is used, in this case the macro-porogen decanol.
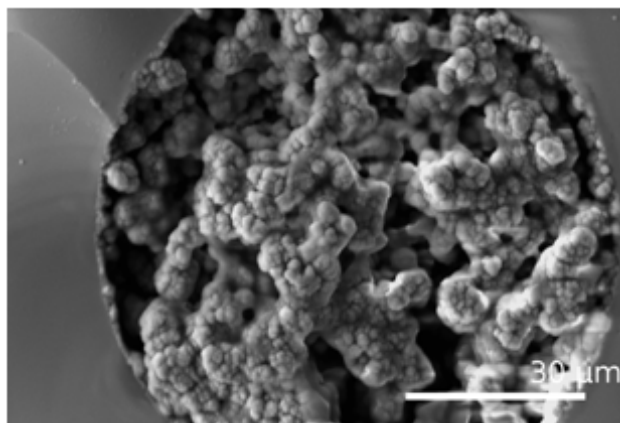
Figure 2.4: *Scanning electron micrograph of a poly(GMA-co-EDMA) monolith where a single porogen, 1-decanol, was used in the pre-polymer solution.*

GMA and EDMA are of intermediate polarity which means that only a solvent of intermediate polarity will effectively solvate the growing polymer chains allowing the growth of large globules and flow-through pores. Extremely polar or non-polar solvents, for example toluene, will cause early phase separation meaning the globules will not have a chance to swell in the monomer solution and will be relatively small, as will the flow through pores creating very dense monoliths. The opposite is observed when a macro-porogen, such as decanol, is used and this is clearly seen in Fig. 2.4. Whereas toluene will produce a monolith of low permeability, decanol gives a monolithic structure with large globules and flow-through pores. Fig. 2.5 shows the structure of monoliths when a binary porogen mixture was used. There was more variety in the pore structure in this case. This allows for tailoring the pore structure for a specific application. Fig. 2.5A, B and E shows the combination of a strongly polar/intermediate polarity solvent (Fig. 2.5A) and a strongly non-polar/intermediate polarity solvent (Fig. 2.5B, E), in both the cases the structure is not the most desirable.
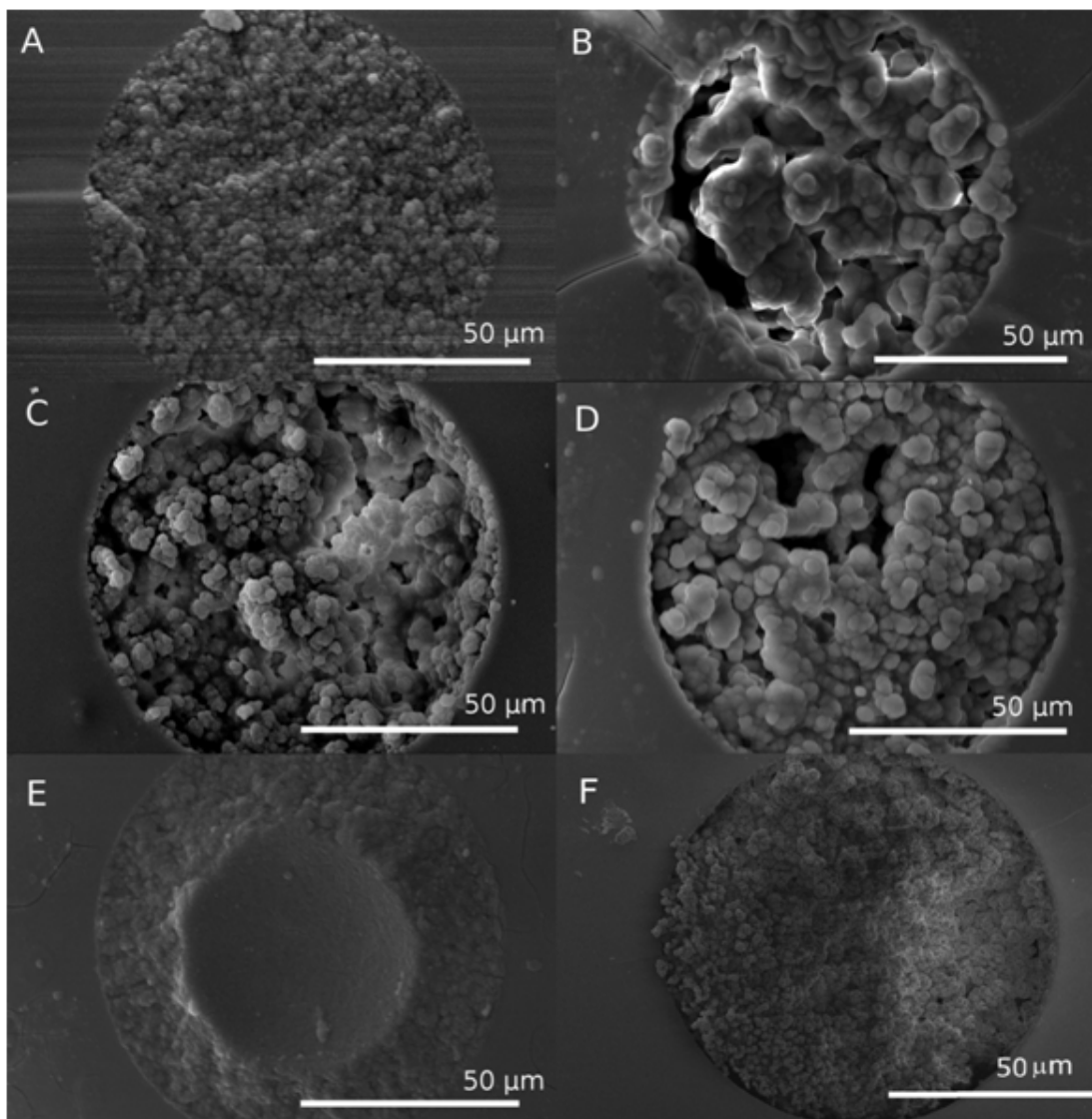
Figure 2.5: *Scanning electron micrograph of poly(GMA-co-EDMA) where a binary porogen was used in the pre-polymer solution, (A) 50% methanol/50% 1-decanol, (B) 40%toluene/60% 1-decanol, (C) 40% 1,4-butanediol/60% 1-decanol, (D) 40% 1,4-butanediol/60% dodecanol (E) 40% toluene/60% dodecanol and (F) 40% cyclohexanol/60% 1-decanol*

The combination of methanol/1-decanol and toluene/dodecanol produced extremely small pores, it appeared that the methanol and toluene in these cases had a stronger effect in the pre-polymer solution than decanol or dodecanol, on the other hand, the mixture of toluene and decanol produced extremely large globules. These large globules

will have a lower surface area due to large particle size; therefore will be less efficient in chromatographic separations. Monoliths with smaller particles will have a larger surface area but higher back pressures, therefore a compromise should be made between surface area and back pressure. This trade-off is the use of two intermediate polarity solvents, one of a more polar character and the other of a more non-polar character, but no extremes of polarity. Examples of this type of porogen system are shown in Fig. 2.5C, Fig. 2.5D and Fig. 2.5F. These images show the use of a mixture of 1,4-butanediol/1-decanol (40:60, C), 1,4-butanediol/dodecanol (40:60, D), and cyclohexanol/1-decanol (40:60, F). Each image shows a monolith with a good porous structure, intermediate size globules and good-flow through pores which make application in separation science easier due to the good mass transfer and low back pressures produced by these characteristics. For the synthesis of methacrylate monoliths the cyclohexanol/1-decanol mixture was used most often throughout this research project. In the case of the styrenic monoliths, it is known from the literature that a mixture of tetrahydrofuran/1-decanol is commonly used as porogenic solvents for the synthesis of poly(S-*co*-DVB) monoliths. It was decided to experiment a little with the porogenic solvent and use also a range of single and ternary solvents also. The results of characterisation experiments presented here show only the use of 1-decanol as a single porogen or a mixture of acetonitrile/1-propanol/1-decanol as a ternary porogenic solvent. The scanning electron micrographs in Fig. 2.6 show the difference in pore structure when a single or ternary porogen was used. In Fig. 2.6A the globules are evenly sized and relatively large in the range of 2 µm and higher, in Fig. 2.6B on the other hand the globules and pores are much smaller, in the nanometre range, meaning the surface area of this monolith is higher suggesting higher column efficiency.
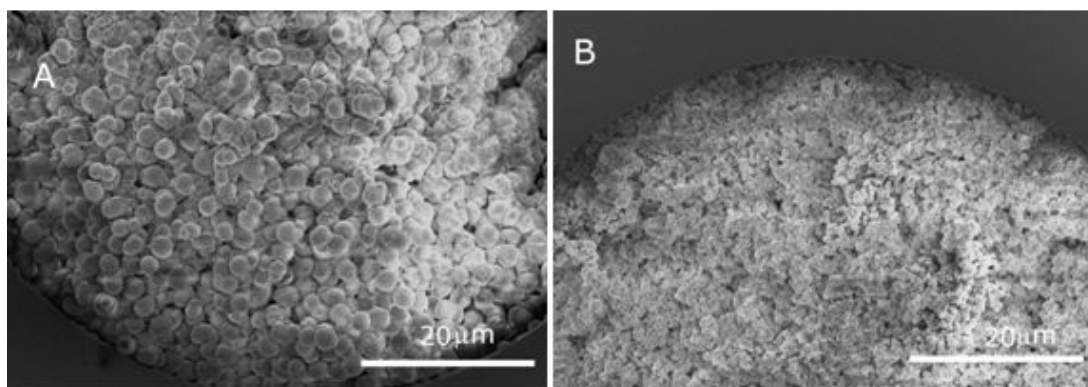
Figure 2.6: *Scanning electron micrograph of poly(S-co-DVB) where (a) 1-decanol and (b) a tertiary mixture of acetonitrile, 1-propanol and 1-decanol were used as the porogen in the pre-polymer solution.*

A batch of poly(GMA-*co*-EDMA) and poly(S-*co*-DVB) monoliths were produced according to the procedures outlined in Sections 2.2.4.2 and 2.2.4.3, respectively, and some further characterisation was carried out to show that they are reproducible, homogeneous and suitable for application in separation science. The most common method of determining reproducibility was to measure the pressure generated by the column on the pump when a solvent is pumped through it. After connecting the monoliths to the HPLC system the flow was increased and decreased in 1 µl/min increments and the pressure generated by the columns was recorded.
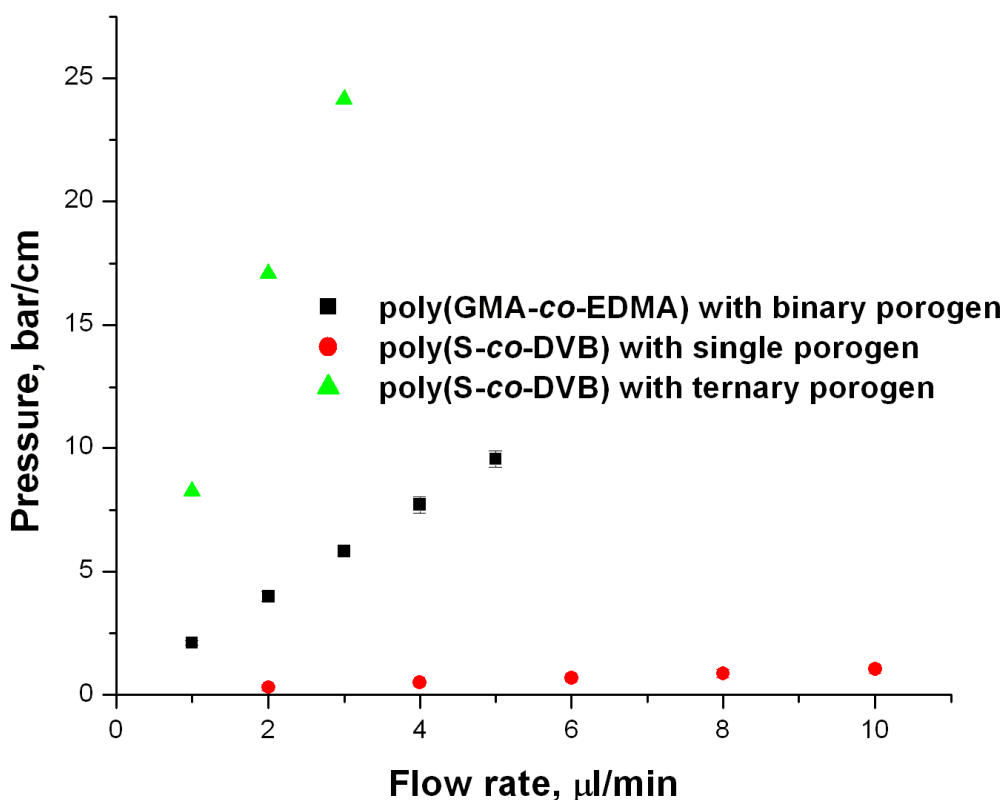
Figure 2.7: *Plot of flow rate (µl/min) vs. back pressure (bar/cm) for a batch (n=3) of poly(S-co-DVB) monoliths with 1-decanol as porogen, a batch (n=3) of poly(GMA-co-EDMA) monoliths with cyclohexanol/1-decanol as porogen and a single poly(S-co-DVB) monolith with acetonitrile/1-propanol/1-decaol as porogen using 0.1% formic acid in water as the eluent.*

Fig. 2.7 shows a plot of the average pressure from three separate poly(GMA-*co*-EDMA) monolithic stationary phases synthesised in the same manner. As can be seen the deviation between the pressures from replicate columns is low, represented by small error bars, indicating that the monolith synthesis is very reproducible. At each flow rate the relative standard deviation (RSD) is less than 5%, which is well within the acceptable error range allowing the claim that the synthesis is very reproducible. To show the effect of the difference in pore size in the styrenic monoliths when the different porogens were used the back pressure was measured. The monolith where 1-decanol was used as the porogen can be measured in the range 2-10 µl/min easily with the maximum pressure at 10 µl/min not exceeded 2 bar/cm. In the case of the monolith

where the ternary porogen was used at 3 µl/min the maximum pressure already exceeds 24 bar/cm, showing that the monolith is denser and also illustrating that decreasing the particle size increases the back pressure.

The next stage of the characterisation is to measure the homogeneity along the length of the capillary. Determination of homogeneity was done by using a technique known as lateral conductivity profiling using a capacitively coupled contactless conductivity detector (C^4D). This technique was described by Gillespie *et al.* [125] as a non-destructive method by which to evaluate the homogeneity of the monolith within a mould. Here it has been used to determine if the growth of the polymer within the mould is the same along the length of the column. An example of the lateral conductivity profiling of the thermally synthesised poly(GMA-*co*-EDMA) monoliths is shown in Fig. 2.8.
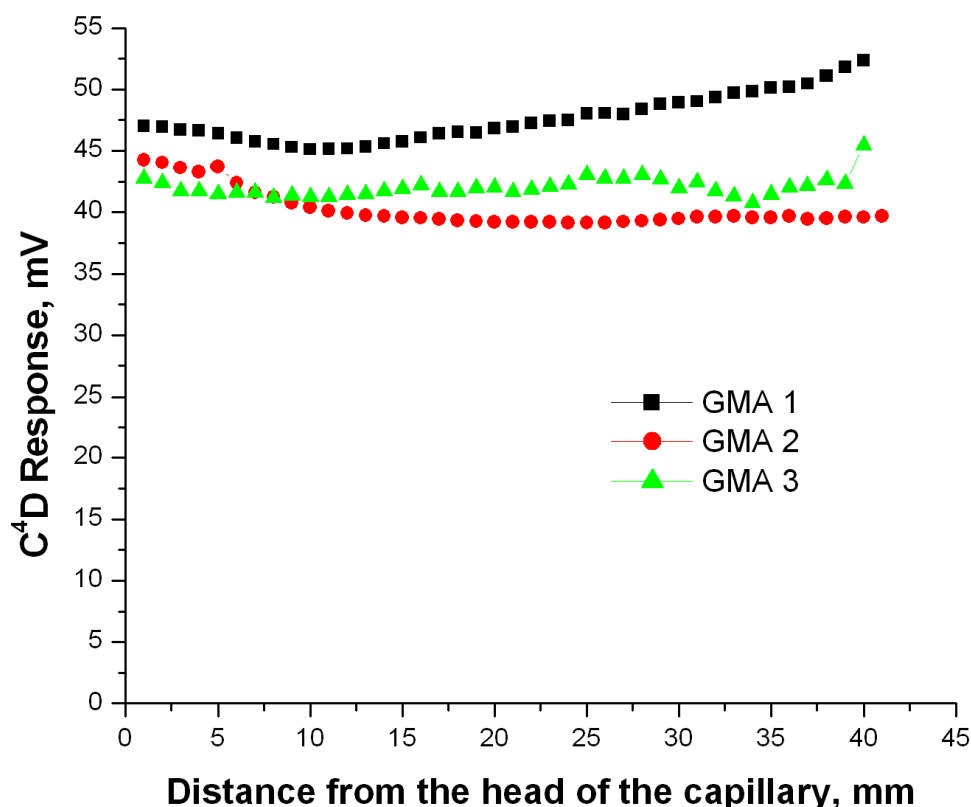
Figure 2.8: *Plot of distance from the head of the capillary (mm) vs. detector response (mV) for poly(GMA-co-EDMA) monoliths with cyclohexanol/1-decanol as porogen using deionised water as the eluent.*

The RSD along the length of the columns is 4.1%, 3.7% and 1.9% for columns 1, 2 and 3, respectively, and within the batch the overall value is 8.8%, which is well within the acceptable range for gauging reproducibility. It can, therefore, be said that the columns are reproducibly homogeneous. Lateral conductivity profiling was also carried out on the two different poly(S-*co*-DVB) monoliths to be sure of homogeneity along the length of the column and the results are shown in Fig. 2.9. In both cases deionised water is flushed through the monolith during the measurement. The profiling for the monolith synthesised with a single porogen is shown in Fig. 2.9, here it can be seen that for the most part the columns are quite homogeneous with a RSD for column 1 of 2.8% and column 3 of 0.7%, however there seems to be a patch of higher density in column 2 as towards the end of the column there is a significant drop in the conductivity. In the case

71

of the monolith synthesised with a ternary porogen, Fig. 2.9, it can be seen that this monolith is also very homogeneous with RSD along the column only 0.6%. The mV response from the detector is at a higher level for this monolith, despite the detector settings being the same as for the previous measurements as the monolith is less dense which seems to cause an increase in conductivity, which is in contrast to the pressure measurements recorded previously (Fig. 2.7). The higher density is also evident from the SEM images above (Fig. 2.6), therefore while the monolith appears to be quite homogeneous it is possible that this measurement has been subject to some experimental error as it doesn't correlate with the high density of the monolith seen from other characterisation procedure. The very well resolved protein separation in Fig. 2.10, on the poly(S-*co*-DVB) monolith formed using acetonitrile.1-propanol/1-decanol as the porogen, also indicates a high surface area, which is obtained by smaller micro-globules resulting in higher back pressure.
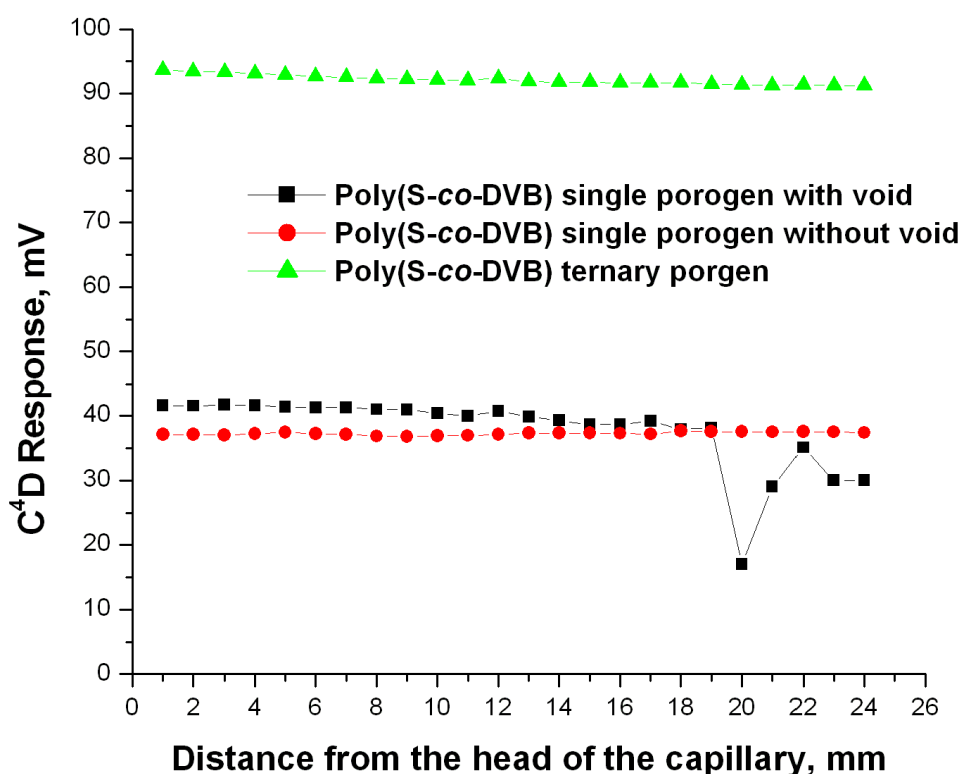
Figure 2.9: *Plot of distance from the head of the capillary (mm) vs. detector response (mV) for poly(S-co-DVB) monoliths using deionised water as the eluent.*

All of these characterisation methods combine to show that the monoliths synthesised by this method are reproducible and homogeneous, exactly what is desired when developing a method for stationary phase synthesis. For the final stage of the characterisation of the monolithic stationary phase, the separation of a mixture of model proteins was carried out. As an example a 0.1 mg/ml solution of ribonuclease A, cytochrome C, myoglobin and ovalbumin were injected onto a poly(S-*co*-DVB) stationary phase, synthesised with the ternary porogen, and separated by a gradient elution profile. The water content decreases from 100% 0.1% formic acid (FA) in water to 40% 0.1% FA in water with the 0.1% FA in acetonitrile content increasing from 0% to 60% over 10 min. This concentration is held constant over 10 min and then allowed to return to the original concentrations over 5 min. An example of the separation is shown in Fig. 2.10.
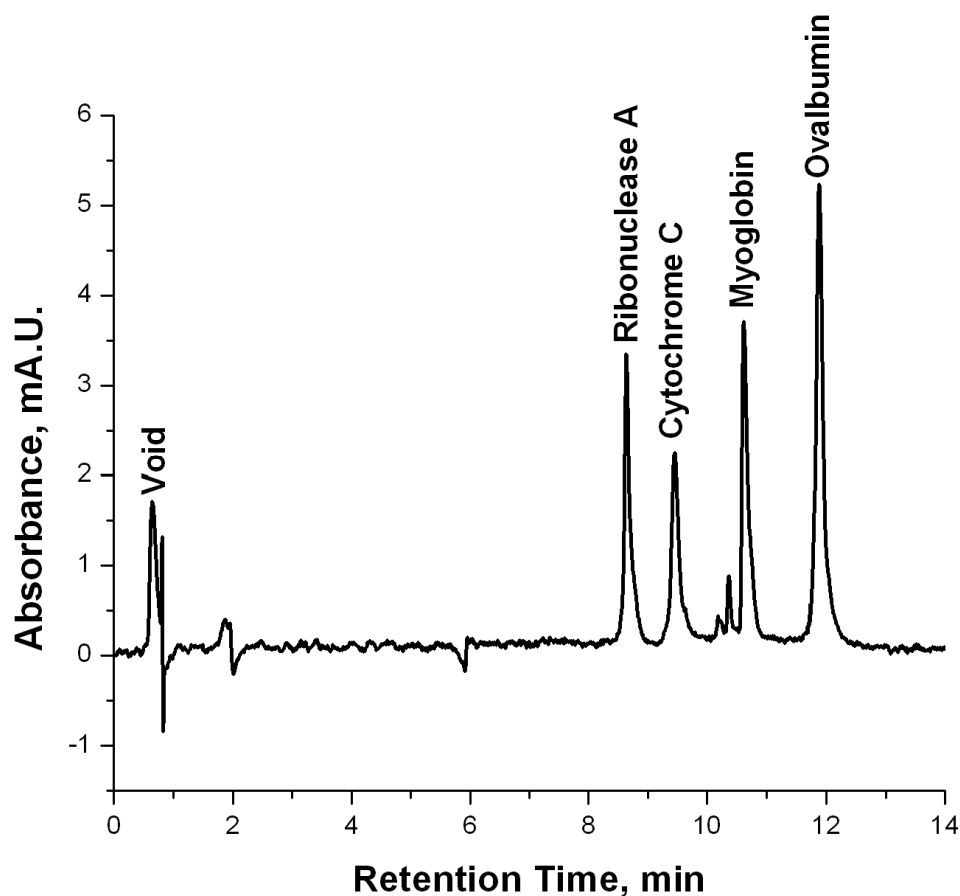
Figure 2.10: *Separation of a mixture of proteins on a poly(S-co-DVB) monolith synthesised by thermally induced polymerisation. Porogens: ACN/1-propanol/1-decanol. Column length: 6.5 cm. Column i.d.: 100 µm. Gradient: 100-40% 0.1% FA in water and 0-60% 0.1% FA in ACN over 10 min. Flow rate: 1 µ//min, Detection: 210 nm*

Thanks to the ternary porogen comprising acetonitrile and 1-propanol in addition to the 1-decanol macro-porogen the size of the globules in the monolith structure is very small (< 1 µm, Fig. 2.6B) giving the monolith a greater surface area, which increases with decreasing globule size. This higher surface area is evident in the quality of the separation in Fig.2.10, the peaks are very sharp with no asymmetry, tailing or spreading. In a later Section (Section 2.3.3.1) a comparison is made with protein separations on monoliths with lower surface area and the difference in separation quality is quite evident (Fig. 2.17)

For these columns, the average resolutions are 4.6 for the ribonuclease A/cytochrome C peaks, 6 for the cytochrome C/myoglobin peaks and 6.7 for the myoglobin/ovalbumin peaks. These values are well above the baseline resolution value of 1.5 indicating excellent resolution of the peaks by this stationary phase. The monolith synthesised using a single macro-porogen, likely has a lower surface area as the globules are approximately 2 µm (Fig. 2.6A), combined with the column being only approximately 6 cm meant that the resolution was very bad and so the separation is not shown here. The smaller pores and increased surface area of the ternary porogen monolith make it a very efficient stationary phase verified by the high resolution between the peaks.

2.3.2.1. Examination of different moulds

While polymerisation in capillaries of 10-150 µm internal diameter is the most common type of monolith synthesis, it can also be necessary to polymerise monoliths in a variety of larger moulds for certain specific purposes. In particular the synthesis of monoliths for higher throughput analysis would be a reason to synthesise polymeric stationary phases in larger bore tubing. While examining thermally initiated polymerisation the use of larger diameter moulds was also investigated. Presented in this section is the synthesis of poly(GMA-*co*-EDMA) monoliths in 700 µm i.d. fused silica capillary and poly(GMA-*co*-EDMA) and poly (S-*co*-DVB) monoliths in poly(ether ether ketone) (PEEK) tubing of a variety of internal diameters.

Fig. 2.11 shows an example of a poly(GMA-*co*-EDMA) monolith formed in the 700 µm internal diameter capillary. The synthesis procedure in this capillary was quite problematic, which started during the silanisation step. After the capillary was filled with the silanisation agent (Section 2.2.4.1) the ends were sealed with rubber septa. Due to the large diameter of the tubing the septa did not hermetically seal the ends and during the silanisation step the solution began to leak from the capillary. The large tubing diameter also makes the capillary more brittle therefore the septum cannot be forced onto the capillary to make a tighter seal as this will potentially break the capillary. To ensure that there were enough methacrylate groups on the surface to allow good anchorage of the polymer to the walls the last stage of the silanisation procedure was repeated twice. When the second treatment step was completed the capillary was

filled with the monolith mixture and allowed to polymerise for 48 h. From the SEM image (Fig. 2.11) the monolith appears to have filled the capillary quite well and the polymer seems to be well adhered to the walls of the mould.
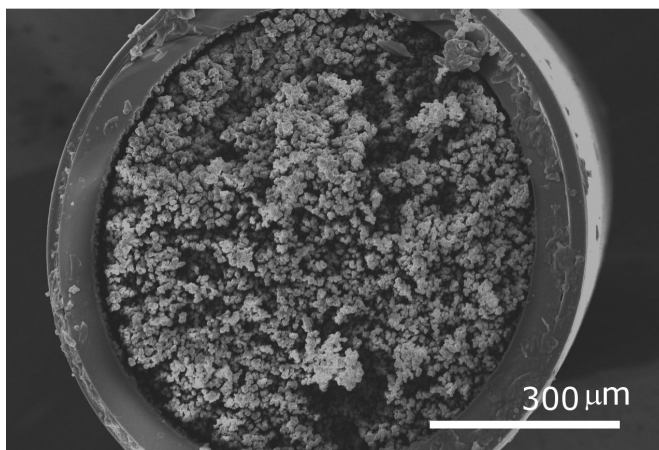
Figure 2.11: *Scanning electron micrograph of a poly(GMA-co-EDMA) monolith in 700 µm internal diameter polyimide coated fused silica capillary.*

From visual examination of the length of the capillary however, this is not the case as several voids were observed within the polymer. What was observed here has also been noted in the literature [2]. According to the literature large diameter moulds dissipate the heat generated during the polymerisation reaction very slowly which results in monoliths of random porosity, which was observed here.

As the monolith formation was not as controllable as in smaller diameter moulds it was decided to decrease the diameter of the tubing used. As there is little variety in the sizes of fused silica capillary available commercially over 150 µm internal diameter, the use of PEEK tubing was also attempted in this study as it comes in a larger variety of diameters. Despite this advantage, there is one particular disadvantage, in that the walls of the tubing are very difficult to modify and therefore it is not easy to attach the monolith to the internal walls. This problem resulted in the monoliths not attaching well to the walls and being pushed out of the mould once a certain pressure had been reached, usually over 100 bar. This effect can be seen in Fig. 2.12. Fig. 2.12A shows a poly(GMA-*co*-EDMA) monolith in 250 µm i.d. PEEK tubing, which has not attached to the walls during polymerisation due to high resistance of the surface to chemical attack.

Fig. 2.12B shows a poly(S-*co*-DVB) monolith which has been pushed out of the 150 µm internal diameter PEEK tubing when attached to the pump due to insufficient wall attachment.
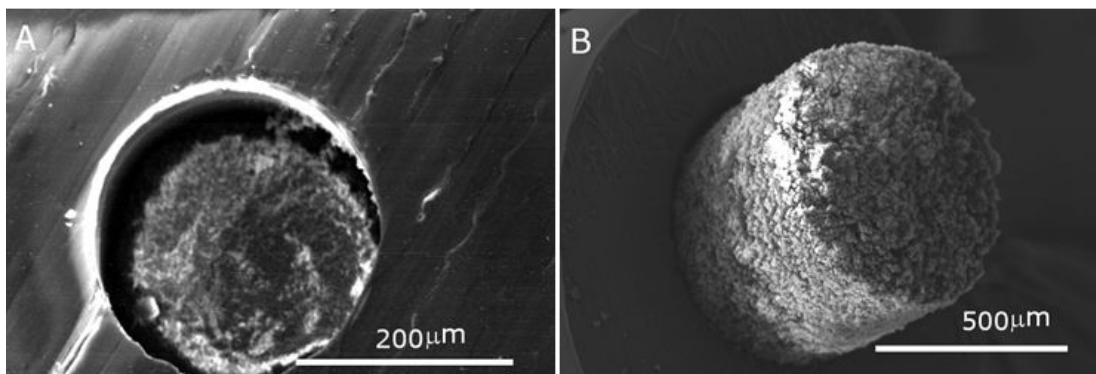
Figure 2.12: *Scanning electron micrograph of (A) a poly(GMA-co-EDMA) monolith in 250 µm internal diameter PEEK tubing and (B) a poly(S-co-DVB) monolith being pushed out of 100 µm internal diameter PEEK tubing.*

Due to the large number of problems experienced when examining larger diameter moulds it was decided that future work would be carried out in capillary moulds where heat and light dissipation is far more efficient leading to more reproducible and homogeneous monolithic stationary phases.

2.3.3. UV-light initiated polymerisation

Once the synthesis of both poly(GMA-*co*-EDMA) and poly(S-*co*-DVB) monoliths had been investigated, the next stage was to examine the synthesis of monolithic stationary phases using UV light initiated polymerisation. The change of initiation method is desirable as, although the reproducibility and homogeneity of the monoliths synthesised using thermally initiated polymerisations is very good, there is no control over their location within the mould. There are many applications where it is necessary to control the location of the synthesis of the polymer within the mould some of which will be discussed in this thesis, for example monolithic frits and monolithic materials in micro-fluidic chips. To study the photo-initiated polymerisation two different types of light sources have been used, a commercially available ultraviolet light source with a calibrated emission at 254 nm and light emitting diodes, one emitting at 254 nm and a

second at 365 nm. LEDs are often used in place of conventional light sources due to their small size, negligible heat generation, robustness, low cost, long lifetime and quasi-monochromatic light output while still retaining comparable efficiency relative to conventional light sources [80].

Using this method of initiation, only the polymerisation of methacrylate monomers could be studied due to the absorbance of styrenic monomers in the ultraviolet region of the spectrum. This can be seen in Fig. 2.13, which shows the absorbance spectra of a 0.51 M solution of styrene and a 0.41 M solution of DVB overlaid with the emission spectra of a 254 nm and a 365 nm LED. It can be seen that the emission spectrum of the 254 nm LED is totally surpassed by the absorbance of the monomers and that of the 365 nm LED is very close to the two absorbance spectra of the monomers. As the monomer solutions used here for absorbance spectroscopy are approximately 20% of the concentration normally used in the polymerisation mixture, it is fair to say that at the necessary, increased concentration of monomers, there will be interference between the absorbance of the monomer and any initiator chosen to absorb at 365 nm.
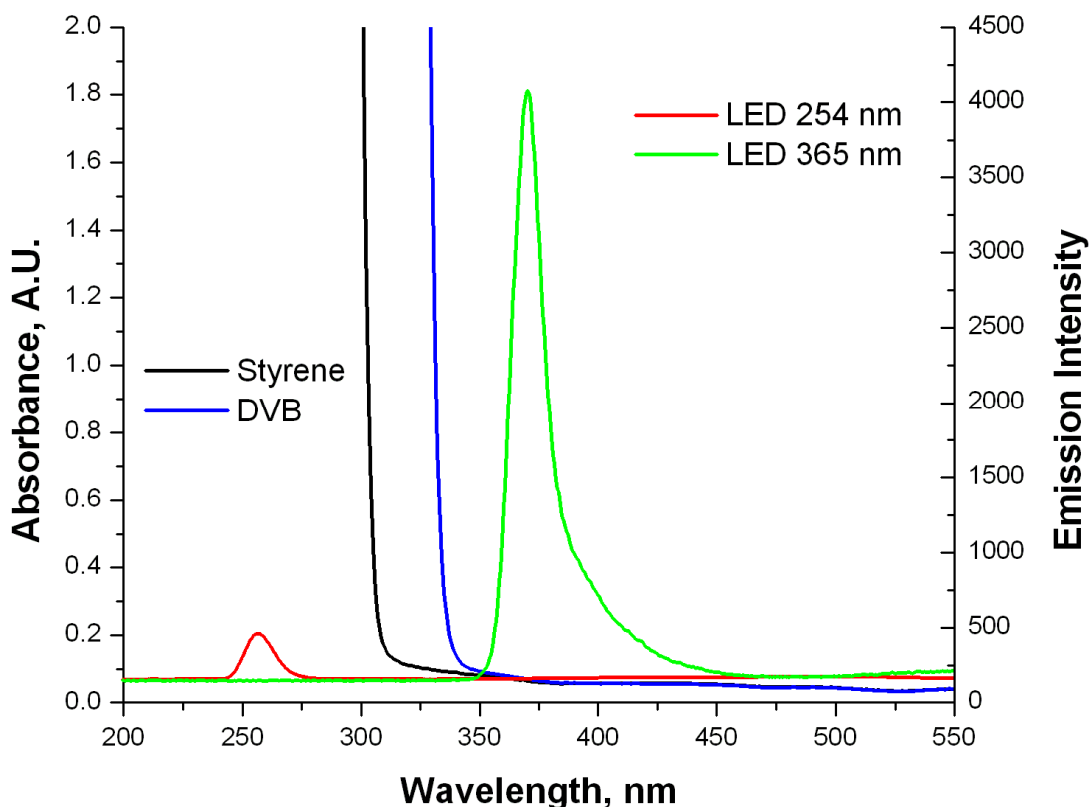
Figure 2.13: *Plot of wavelength (nm) vs. absorbance (A.U.) of 0.51 M S and 0.41 M DVB solutions overlaid with a plot of wavelength (nm) vs. emission (A.U.) for a 254 nm and 365 nm LED*

Most methacrylate monomers, on the other hand, absorb around 200-210 nm and therefore do not interfere with the absorbance of initiators activated by 254 nm or 365 nm light.

2.3.3.1. Commercially available light sources

Poly(BuMA-*co*-EDMA) monoliths were synthesised using a commercially available light source with calibrated emission at 254 nm as the energy source to initiate polymerisation. In original experiments 40% monomer was used in the pre-polymer solution and the capillaries were given a dose of 1 J/cm^2, however the resulting monoliths were extremely permeable and not useful at all in separations applications. Increasing the radiation dose to 2 J/cm^2 caused the problem of having monolithic materials that were too dense to pump through. Keeping the radiation dose at 2 J/cm^2

and reducing the % of monomer in the pre-polymer solution to 30% caused the formation of well-polymerised dense yet permeable monolithic stationary phases. A scanning electron micrograph of one of the formed monoliths is shown in Fig. 2.14.
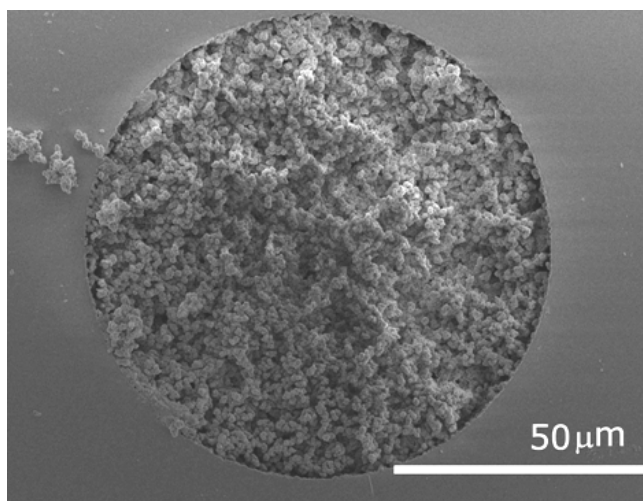
Figure 2.14: *Scanning electron micrograph of a poly(BuMA-co-EDMA) monolith synthesised by light initiated polymerisation at 254 nm with an X1-1000 Spectrolinker calibrated light source*

As can be seen from the image the monolith has the characteristic globular porous structure of polymer monoliths, it is well-filled and completely attached to the walls. The globules are relatively large and the flow-through pores are large enough to allow for low back-pressures across the column. To confirm that the back pressure across the column is within a suitable range and that the back pressures across a batch of columns are reproducibly similar, flow resistance measurements were taken using a HPLC pump. Fig. 2.15 shows the average flow resistance measurements of a batch of 10 columns, the % RSD between the columns is 10%, within the acceptable range for reproducibility. From the back pressure measurements it is clear to see that the monolith synthesis using this calibrated light source is reproducible.
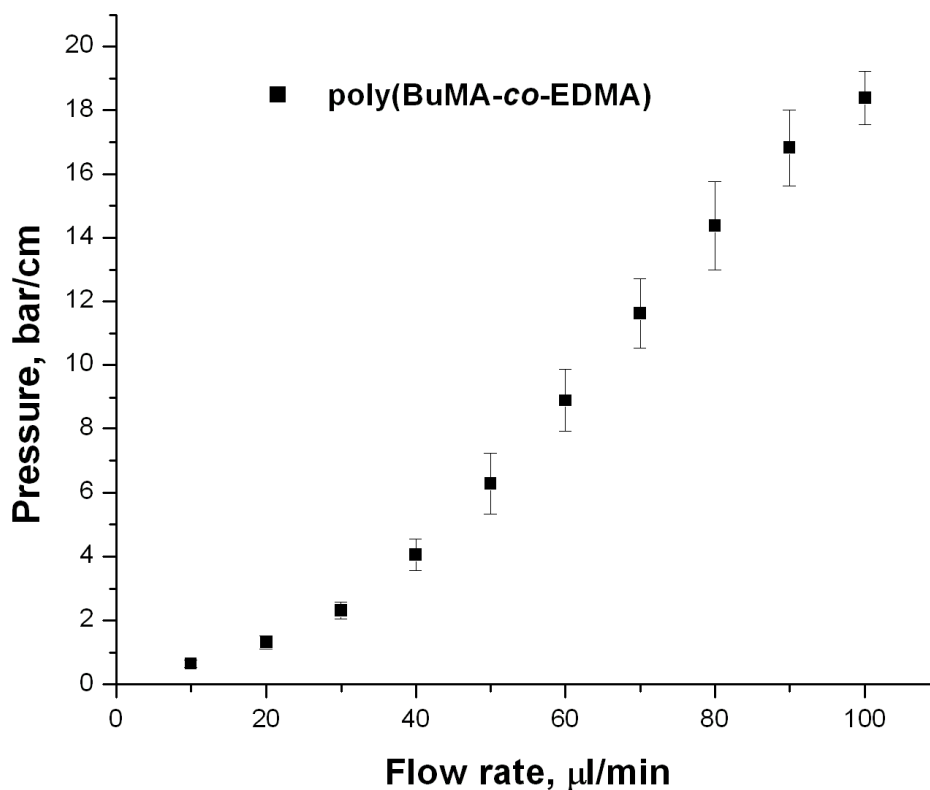
Figure 2.15: *Plot of flow rate (μl/min) vs. pressure (bar/cm) for an average of 10 poly (BuMA-co-EDMA) monoliths synthesised by light initiated polymerisation at 254 nm with an X1-1000 Spectrolinker calibrated light source*

It was also important to determine whether this method produced homogeneous monolithic stationary phases. The C^4D sensor head was placed on the capillary and moved along it in 2 mm increments. After each movement the detector response, in mV, was allowed to stabilise for approximately 2 min before moving the head again. These values were then plotted against the distance from the head of the column, which allows the homogeneity of the surface to be observed. The same 10 monoliths as were used for Fig. 2.15 were used for this experiment and the results are shown in Fig. 2.16.
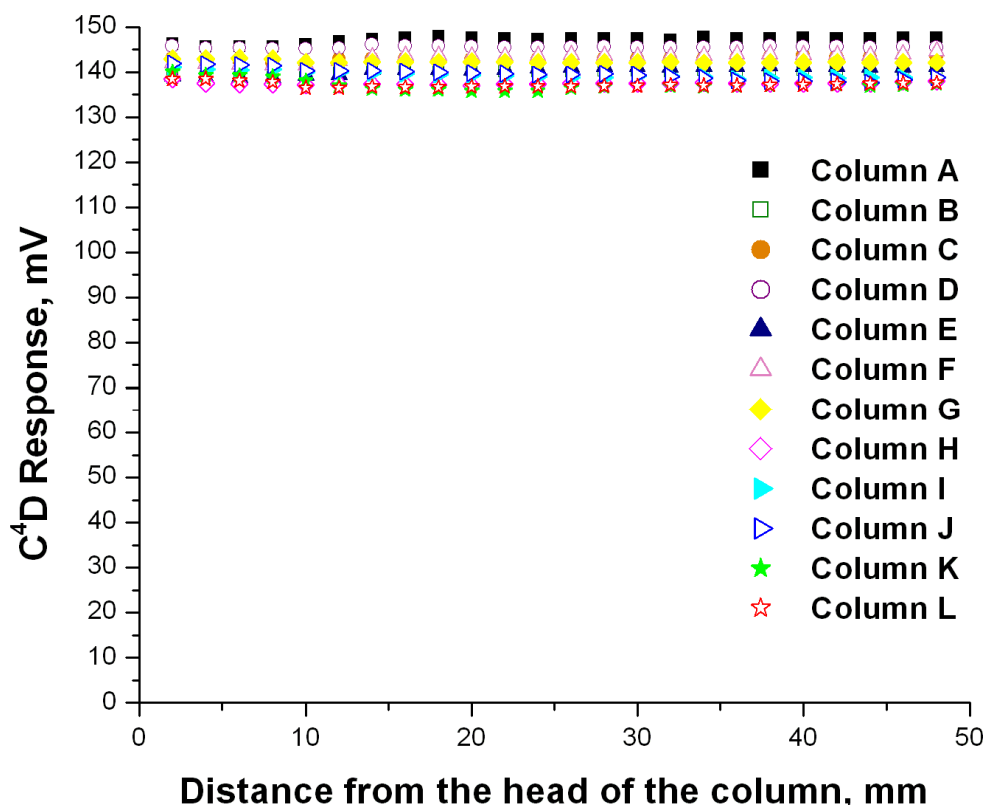
Figure 2.16: *Plot of distance from the head of the column (mm) vs. detector response (mV) for 10 different poly(BuMA-co-EDMA) monoliths synthesised by light initiated polymerisation at 254 nm with an X1-1000 Spectrolinker calibrated light source*

It was found from examining each profile individually that the % RSD for a single column was never greater than 0.9% and for all ten columns together the value was 2.12%, showing excellent homogeneity along the length of the columns and excellent reproducible formation of homogeneous stationary phases.

While they have been shown to be homogeneous and their synthesis is reproducible the most important feature is whether they can be applied as stationary phases in separations applications. The final test of this stationary phase was to inject a standard mixture of proteins onto the column to see if these stationary phases are suitable for applications in chromatography. As poly(BuMA-*co*-EDMA) is mildly hydrophobic it is often used for the separation of proteins in a mixture. Knowing this a mixture of two proteins, cytochrome C from bovine heart and bovine serum albumin, of known concentration

(0.01 mg/ml) was injected onto the column and eluted under a gradient elution profile using water and acetonitrile, each containing 0.1% formic acid, as the two mobile phases. The gradient profile changed from 0% to 60% acetonitrile in 5 min, held at this % for 10 min and then returned to 100% water in 5 min. The results of the separation are shown in Fig. 2.17.
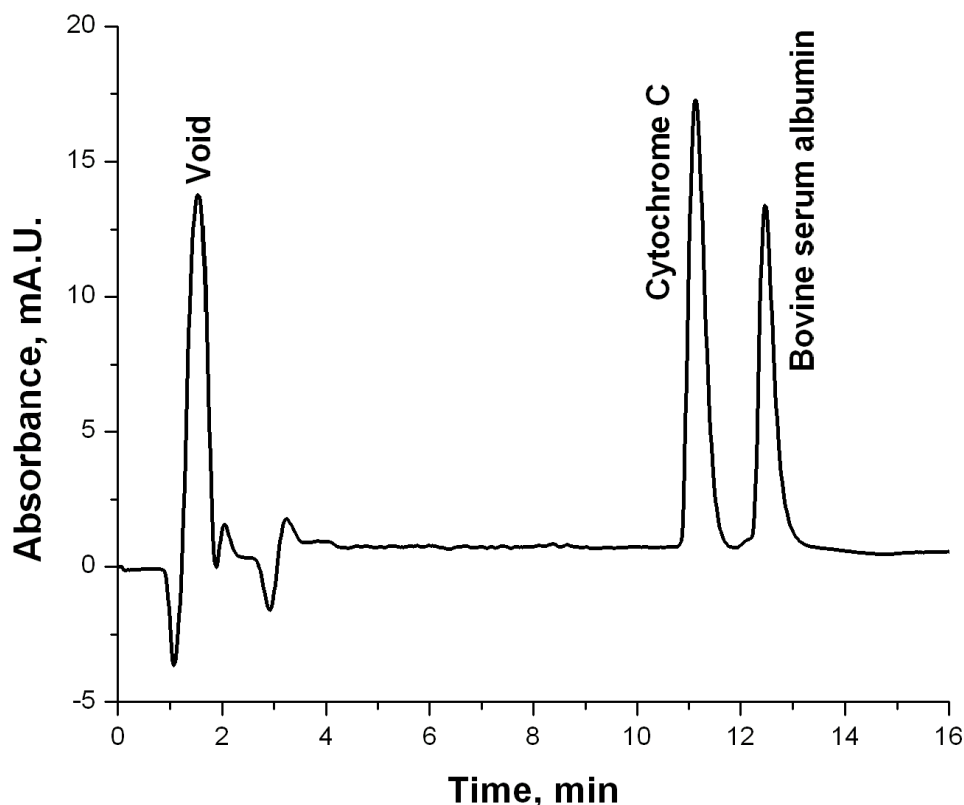
Figure 2.17: *Separation of a 0.01 mg/ml mixture of cytochrome C and bovine serum albumin on a poly(BuMA-co-EDMA) monoliths synthesised by light initiated polymerisation at 254 nm with an X1-1000 Spectrolinker calibrated light source. Column parameters: 100 μm i.d., 7 cm; Separation parameters: 1 μl/min, detection at 210 nm, gradient of 100-40% 0.1% FA in water and 0-60% 0.1% FA in ACN*

Although only two proteins were used in the mixture, they are very well separated from one another with an average resolution of 2.35 calculated from 6 runs on two different columns synthesised by the same procedure. This is well above the value of 1.5 which indicates baseline resolution and is the indicator of a good separation. Despite the high

resolution, comparing this separation to that in Fig. 2.10 shows some striking differences. Under similar gradient conditions and with the same sample volume and concentration, the peaks are much broader for this poly(BuMA-*co*-EDMA) separation than for the poly(S-*co*-DVB) separation shown previously (Fig. 2.10). Looking back at Fig. 2.14, the globule size of the monolith can be estimated to be approximately 2 μm. The globule size of the poly(S-*co*-DVB) monolith was estimated to be less than 1 μm from Fig. 2.6B. As the globule size between the two monoliths has more than doubled, the surface area will certainly have decreased, mass transfer will be affected and the peaks as a result are broader, as seen above (Fig.2.17). This shows the importance of creating monoliths with high surface areas as the quality of the separation is improved.

It can be seen from the above characterisation that it was possible to reproduce the synthesis of poly(BuMA-*co*-EDMA) monoliths from procedures described in the literature and that these monoliths were of a sufficient quality as to be useful for the separation of a standard mixture of proteins.

2.3.3.2. Light emitting diodes (LEDs)

Using the commercially available light source was necessary to develop skills in photo-initiated polymerisation as well as investigating new pre-polymer solution compositions and their effect on the resulting monolith. The next stage was to investigate the use of more unconventional light sources. This involved the use of LEDs to synthesise monolithic polymers in capillary. While using the large calibrated UV light source was useful when long columns were necessary, making short monolithic plugs was more difficult due to the wave-guiding nature of PTFE-coated fused silica capillary. Due to a phenomenon called total internal reflection, depicted in Fig. 2.18, if light strikes the PTFE coating of the capillary at the correct angle, known as the critical angle, the light will travel through the PTFE and fused silica and be reflected back towards the PTFE layer.
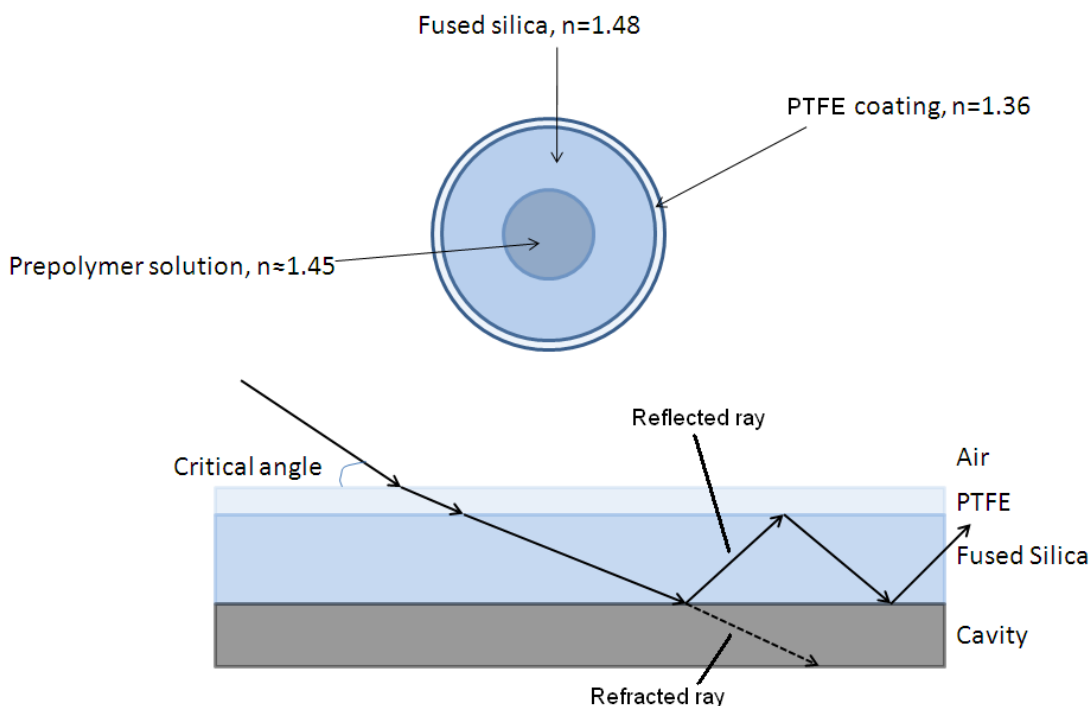
Figure 2.18: *Schematic explaining the phenomenon of total internal reflection.*

As the PTFE (n = 1.36) has a lower refractive index than the fused silica (n = 1.48) the light will not be able to return across the boundary between the two layers and so will be reflected back into the fused silica, effectively becoming trapped in the fused silica layer until the energy of the light wave dissipates. On each reflection some of the wave will be lost into the cavity and this will contribute to the dissipation of energy. The reason this causes such a problem when making short monolithic plugs with a large calibrated light source is because light is emitted in all directions from the bulb (multi-directional) and therefore it is possible that some light will strike at exactly the right angle to pass underneath the photo-masking and cause this total internal reflection to occur. This under-illumination causes the formation of long lengths of monolith under the mask which are very diffuse and inhomogeneous in nature and render the monolithic plug useless. To combat this problem LEDs were used. LEDs, especially in the UV region, emit light of a lower intensity than the conventional UV light sources. Additionally the light from the LEDs is known as mono-directional as there is a cone of emittance (Fig. 2.19) within which all the light is distributed, therefore using LEDs there is far less stray light.
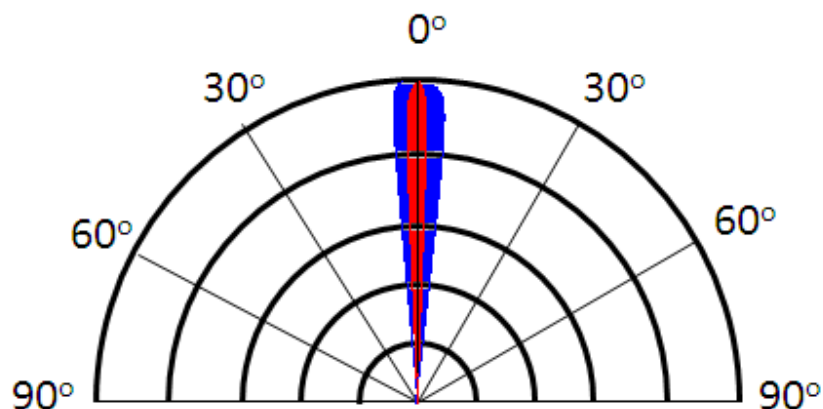
Figure 2.19: *Diagram of the cone of emittance of a two different LEDs, the red cone represents the 255 nm LED and the blue cone the 365 nm LED.*

Due to a reduction in stray light, masking of the capillary is far more effective, less light is able to illuminate the area under the masking and the edges tend to be much sharper. As the masking is more effective the area, within which the plugs are formed, is much more controllable. It must be noted, however, that the LED should not be placed too close to the capillary as under-illumination and wave-guiding can once again become a problem as can be seen in Fig. 2.20.
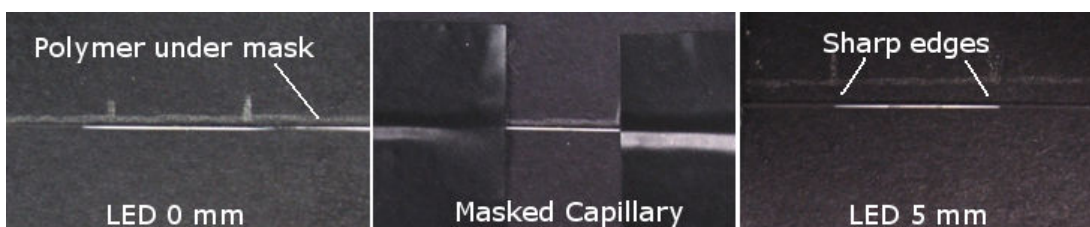
Figure 2.20: *Images showing the result of the photo-initiated polymerisation of poly(GMA-co-EDMA) using a 365 nm LED where the original window size was 10 mm (centre), and the LED was positioned 0 mm from the capillary (left) and 5 mm from the capillary (right) during polymerisation*

For this work, the synthesis of both poly(GMA-*co*-EDMA) and poly(BuMA-*co*-EDMA) short monolithic plugs using Michler's Ketone and a 365 nm LED and 2,2-dimethoxy-2-phenylacetophenone and a 254 nm LED, respectively, were examined. While

poly(GMA-*co*-EDMA) can be synthesised using initiation at both 255 nm and 365 nm [65], poly(BuMA-*co*-EDMA) polymerises more efficiently at 255 nm and this has also been seen in the literature. Matching the wavelength of absorbance of the initiator to the wavelength of emission of a light source was mentioned in a recent publication by Abele *et al.* [65] as a method of maximising the light absorbing of the initiator and thereby increasing the efficiency of the radical generation and polymer synthesis. During this research this principle has been followed, therefore MK which has an absorbance maximum at 365 nm is used with the 365 nm LED while DMPAP is used with the 255 nm LED as this is the wavelength of its absorbance maximum. Using LEDs along with photo-masking allows the creation of very small plugs of monolith 3-5 mm in length. It was decided to optimise these short plugs of monolith for use as monolithic frits for column packing.

Monolithic frits as a replacement for the conventional stainless steel frits have many advantages. Stainless steel frits, which are used due to the high pressures reached during column packing, are quite costly and bulky. Their size and the problems involved with removing and replacing them repeatedly, such as voids forming in the packing material, means that on-column detection is not possible or is at least permanent. Due to the pre-treatment step performed on the column before polymerisation is carried out, monolithic frits have excellent mechanical stability meaning that they can withstand extremely high back pressures comparable to the stainless steel frits. In addition, monolithic frits with differing pore size, tailored to the size of the packing beads, are easily and reproducibly synthesised at a low cost.

The idea of using monoliths as retaining frits for column packing has previously been described in the literature [72, 188, 189]. While high pressure column packing is well described in the literature as the optimal method of column packing, producing homogeneous, well packed columns, there are some limitations. The main disadvantage being the need for specialised equipment, that is, a high pressure column packer. In addition there is the large amount of time needed to pressurise the system, pack the column and depressurise the system. This low pressure method allows also for a

homogeneous packing, high pressures are not required so the overall packing time and the use of specialised packing equipment is not necessary.

From the SEM images in Fig. 2.21, it can be seen that the polymerisation of both poly(GMA-*co*-EDMA) and poly(BuMA-*co*-EDMA) works equally well as a fully filled monolithic capillaries were obtained. Poly(GMA-*co*-EDMA) monoliths, however, have quite reactive surfaces due to the epoxy group, and therefore can interfere in a number of different types of separations. The final application of these packed columns was for metal ion retention with which the poly(GMA-*co*-EDMA) could interfere. As it is important that this does not occur, poly(BuMA-*co*-EDMA) monoliths were chosen for all column packing experiments.
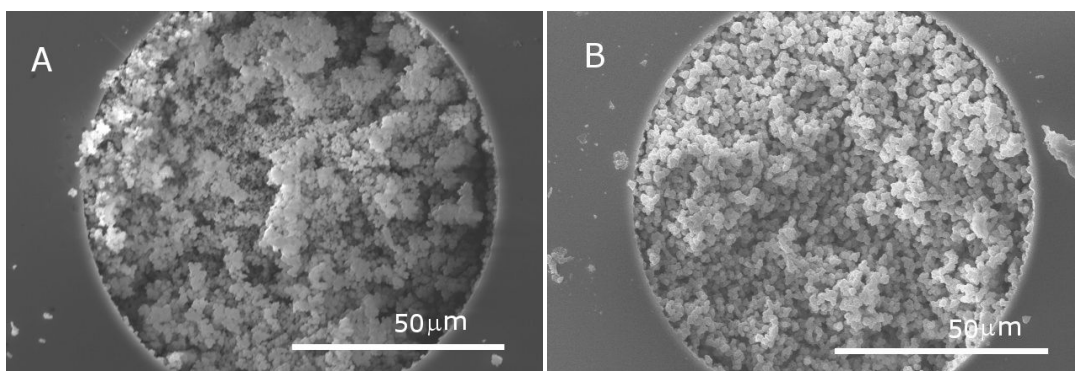
Figure 2.21: *Scanning electron micrographs of (A) poly(GMA-co-EDMA) synthesised by UV-initiated polymerisation with a 365 nm LED and (B) poly(BuMA-co-EDMA) synthesised by UV-initiated polymerisation with 255 nm LED*

To pack the columns a suspension of the COOH-functionalised PS packing beads, 2 µm in diameter, was made in methanol. Using a peristaltic pump the beads were filled into a packing loop and the ends were sealed with micro-tight adapters with stoppers. Using a micro-tight adapter the packing loop was connected to the outlet of the HPLC pump, as shown in Fig. 2.22. A 100 µm i.d. capillary with a poly(BuMA-*co*-EDMA) monolith as a frit was connected to the system after the loop to complete the packing set-up.
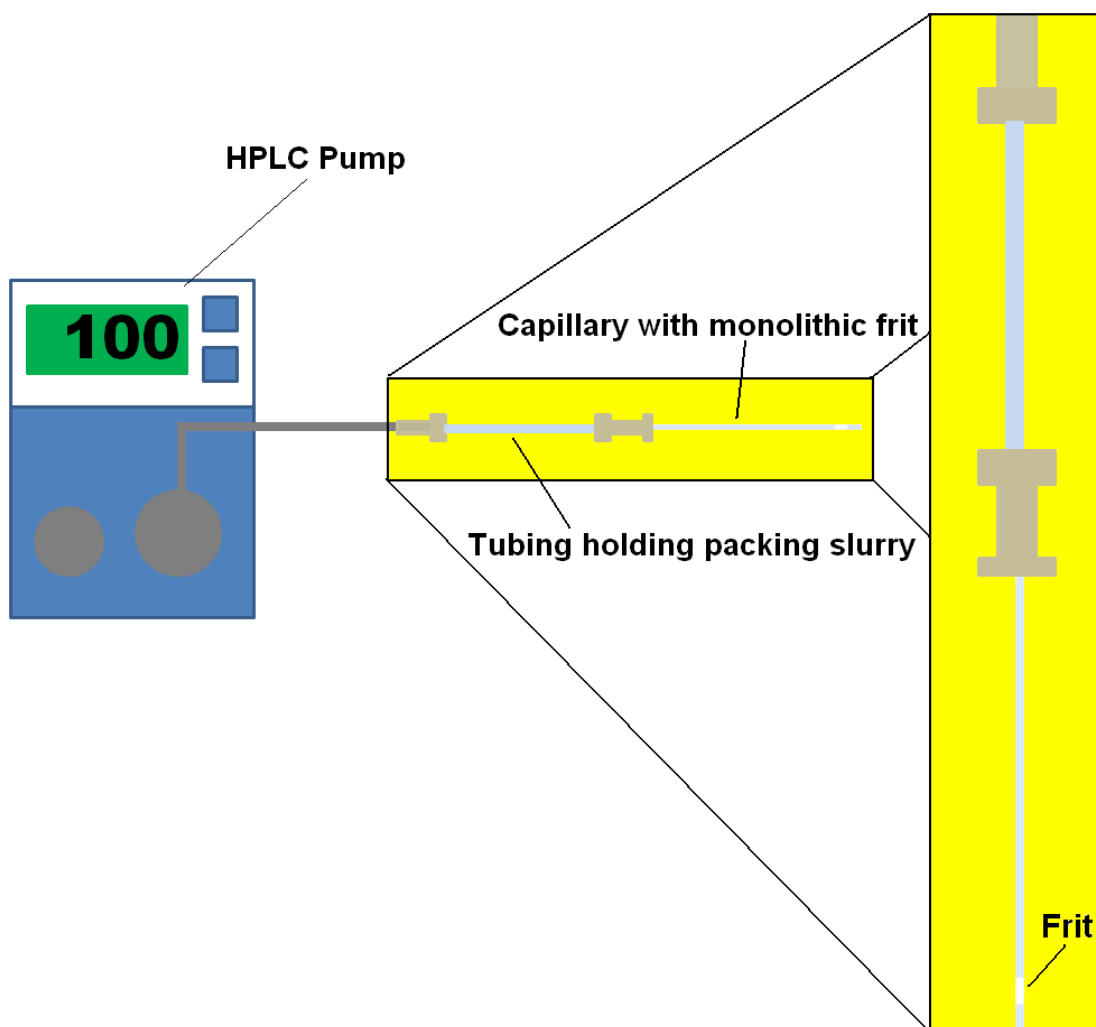
Figure 2.22: *(Right) Schematic of packing system consisting of an HPLC pump, Teflon[®] tubing holding the packing slurry, essentially the column packer and a capillary containing a monolithic frit attached to the set-up for packing, (Left) Schematic on the left the column packing tubing and connection to the capillary containing the monolithic frit*

Flow was started at a low flow rate of approximately 5 μl/min and the loop was agitated continuously as the eluent from the pump pushed the packing beads into the column to prevent the packing material from becoming lodged in the tubing. The loop was also orientated vertically to further reduce the chance of the beads sticking in the tubing before entering the capillary to be packed. Packing was carried out at approximately 100

bar, as the packing continued and the back pressure of the column increased the packing flow rate was dropped to maintain the original packing pressure.

Once packing was complete the loop was removed from the set-up and the eluent was pumped through the packed column at a higher flow rate (approx 10-20 μl/min) in order to create a more dense packing and eliminate voids.

Fig. 2.23 shows the lateral conductivity profile of a column after packing with 2 µm COOH-functionalised poly(styrene) beads.
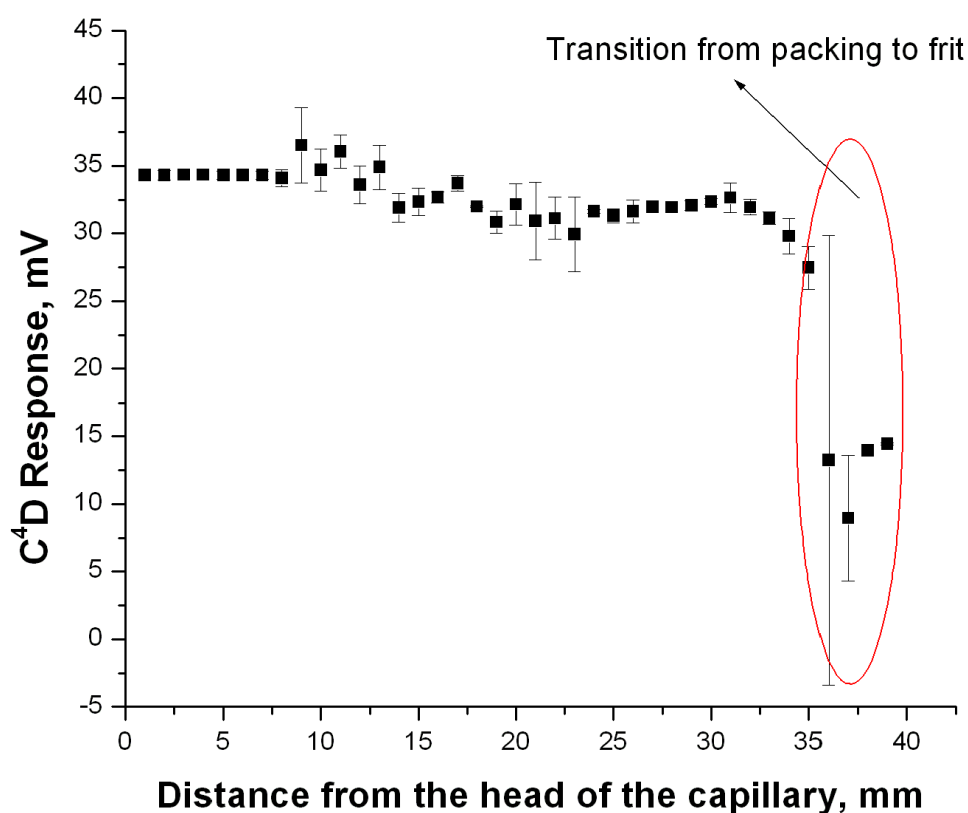
Figure 2.23: *Plot of distance from the head of the capillary (mm) vs. response from the detector (mV) for a capillary packed with 2 µm COOH functionalised poly(styrene) beads against a 3 mm poly(BuMA-co-EDMA) frit, eluent is deionised water.*

It can be seen from the profile shown in Fig. 2.23 that there is little fluctuation in the conductivity along the length of the measured packed area, the RSD for the values measured is 6.3% which is within the acceptable error range. These factors indicate that

the packing is very homogeneous along the length of column measured and that this method can produce columns of a sufficiently high standard of homogeneity. A drop in the measured conductivity can be seen after 35 mm have been measured which shows the transition from the packed area to the monolithic frit. The frit having no surface charge and being of a lower permeability, in order to be able to retain the packing material, produces a lower response from the detector. The drop then levels off also showing that the frit is also homogeneously formed.

The ultimate application for this method was to pack spiropyran functionalised silica micro-beads with a diameter of 5 µm into a capillary column, which could then be used with an on-column reflectance detector, this means that the frits have to be inside the column rather than on the end. The monolith possesses pores of 1-2 µm in diameter which is excellent for retaining the beads 5 µm, eliminating the possibility of beads leaking from the column. Fig. 2.24 shows an image of capillary after the packing has been completed. The beads used for the packing fluoresce under UV light thanks to the spiropyran surface functionalisation and therefore it is easy to see the definition between the packed beads and the monolithic frit.
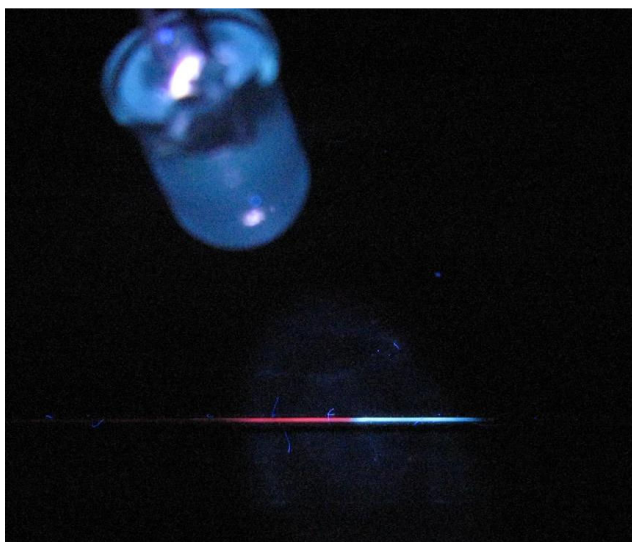
Figure 2.24: *Photograph of a 100 µm internal diameter PTFE coated capillary with a poly(BuMA-co-EDMA) monolithic frit (white) against which 5 µm spiropyran functionalised silica beads (pink) have been packed.*

Due to the metal chelating abilities of the spiropyrans, which will be discussed in more detail in Chapter 3, these packed columns with monolithic frits were used for on-column photo-induced retention and release of metal ions. This work has been published in the e-Journal of Surface Science and Nanotechnology [190].

Photo-induced polymerisation of monolithic columns is a quick, simple, low cost method of generating frits for column packing. Using a high concentration of monomer it is possible to obtain a monolith with relatively small flow through pores which allows even the smaller 0.4 μm beads to be packed easily without leakage of the beads through the pores. Low pressure packing is an excellent alternative to high pressure column packing giving homogeneously packed columns in shorter times and for reduced costs. Costs are dramatically reduced for low pressure packing as no specialised packing equipment is necessary, with the exception of a HPLC pump.

2.3.4. Functionalisation of monolithic scaffolds

One of the most commonly used functional monoliths is poly(GMA-*co*-EDMA), however one issue with the synthesis of functional monoliths in a one-step procedure, that is by direct copolymerisation of a functional monomer and a cross-linker, is that some of the functionality can be trapped in the bulk of the monolith and become inaccessible to the solvent matrix. One method for combating this problem is to use a technique called photo-grafting to polymerise a layer of a functional monomer directly on the pore surface. This ensures that all of the functional groups can interact with the surrounding environment. An additional benefit of this type of functionalisation is that, due to its light activated nature, the location where this functional layer is placed can be easily controlled by the use of photo-masks.

From the literature [68, 124, 191, 192] it was found that benzophenone, a radical initiator with a substantially shorter radical lifetime than the common initiators described previously is more suited to surface grafting. Upon irradiation at 255 nm benzophenone abstracts a hydrogen from a donor molecule and forms a diphenylketyl radical. As the monolithic material is the most abundant source of abstractable hydrogen, particularly when more hydrophobic monoliths are used such as poly(BuMA-*co*-EDMA), the radical will abstract a H from the pore surface and become attached

generating surface radicals allowing the polymer chains to grow directly at the pore surface. Using a solvent for the photo-grafting process which is not susceptible to H abstraction, such as *t*-butanol/water (3:1), increases the chances of surface radical formation. As does conducting the grafting as a two-step process, keeping the monomer and the initiator separate so that the initiator cannot abstract H from the monomers only from the existing monolith surface.

Functionalisation of monolithic stationary phases was investigated for use in the experiments related to the work carried out in Chapter 3 where it was necessary to graft a layer of a functional monomer on the surface of a monolith in order to immobilise a layer of a photochromic dye. For this application it was necessary to have either –COOH groups or –NH$_2$ groups on the surface, therefore the photo-grafting of methacrylic acid and 2-aminoethyl methacrylate onto the pore surface of a poly(BuMA-*co*-EDMA) monolith was attempted. Functionalisation was carried out using both LEDs and commercial light sources to initiate the grafting reaction. While LEDs are useful if the area to be functionalised is in the region of 3-5 mm, as the area irradiated by the LEDs is approximately this size, for longer sections of grafting it is necessary to use a larger light source such as the commercially available light source described previously. The grafting experiments carried out in this section were done using a commercial UV-light. In order to prevent under illumination and foggy edges on the graft, rubber septa were used to mask the edges of the area to be exposed as the rubber septa absorb the light before it can propagate along the fused silica capillary allowing the grafted area to spread. The graft was characterised by lateral conductivity profiling as in previous sections and the results are shown in Fig. 2.25.
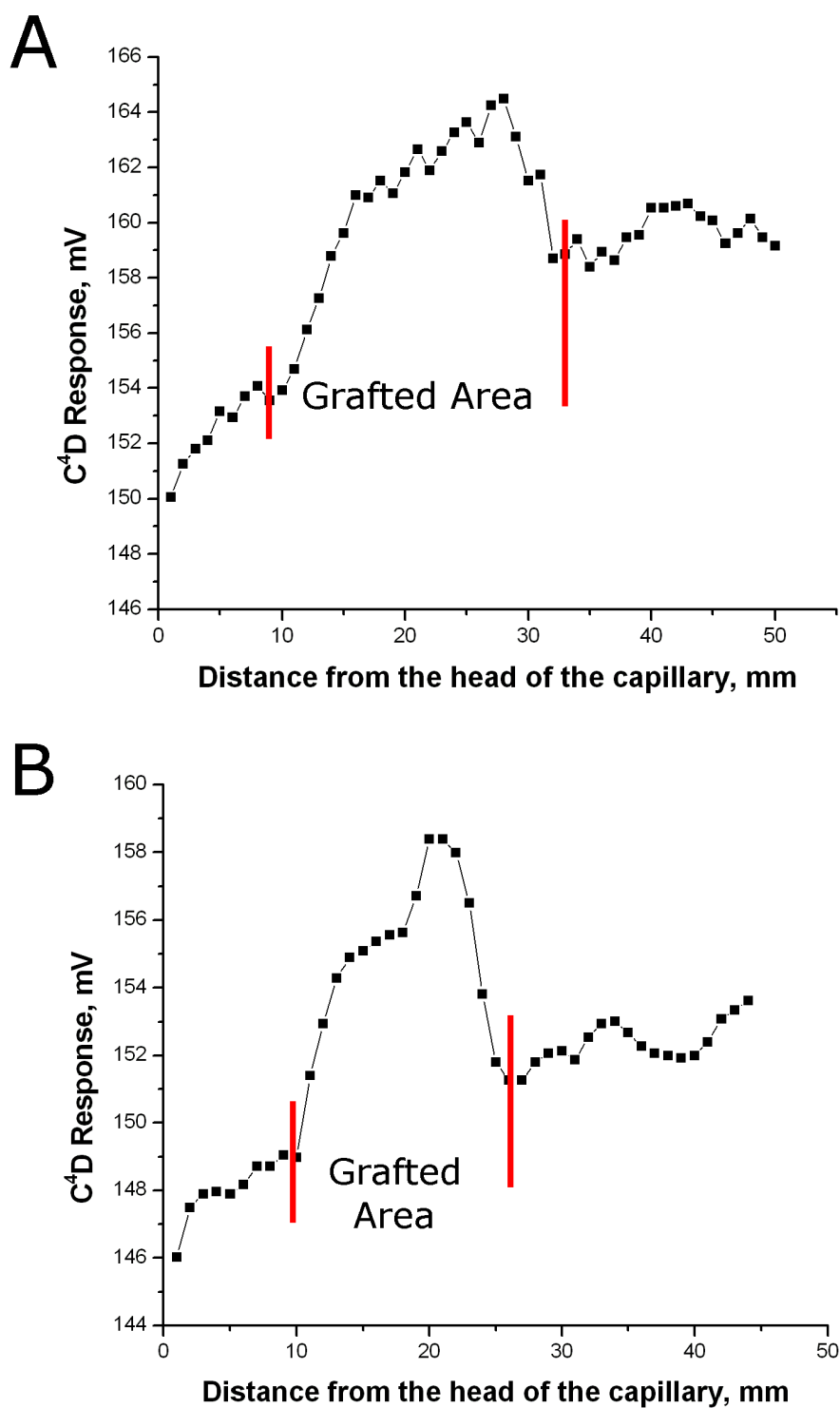
Figure 2.25: *Lateral conductivity profiles of poly(BuMA-co-EDMA) monoliths after photo-initiated grafting of a 15% w/w solution of (A) 2-aminoethyl methacrylate and (B) methacrylic acid*

The area where the graft has been carried out shows an increase in the baseline conductivity values. In both cases there is a relatively sharp increase and decrease in conductivity at the start and end of the grafted areas showing little trailing, indicating that this method has been quite successful. This method of surface functionalisation has been further employed in Chapter 3 as a part of a method to immobilise dyes onto monolithic materials. This will be discussed in more detail further on.

2.4. Conclusions

It is generally accepted that the inner walls of the mould should be pre-treated with binding some type of molecular anchor before monoliths can be prepared within the channels. In the case of fused silica capillaries this is done by preparing the channels with TMSPM, this allows the polymer to grow from the walls and ensures that the polymer is not pushed out of the mould when pressure is applied. In the case of the PEEK tubing no pre-treatment was carried out and the monolith was pushed out of the mould under pressure. This shows the importance of this step in the general monolith synthesis procedure if high-quality stationary phases are to be obtained.

According to the literature thermally initiated polymerisation is the most common method of producing monolithic stationary phases. The methods in the literature have been examined and studies have been carried out varying the porogen mixture and the mould size in order to understand the effect that this has on the resulting monolith. These columns have then been characterised in a variety of different manners including lateral conductivity profiling, which has been shown to be useful in detecting inhomogeneity in monolith formation. Thermally initiated polymer monoliths were characterised to show their excellent homogeneity, reproducibility and their applicability for the separation of large molecules.

After studying the fundamental parameters of monolith synthesis while examining thermally initiated polymerisations, the next stage was to look at light initiated polymerisations as this method gives far more control over the location and size of the final monolith. Once again some reproduction of literature techniques was required to ensure that the necessary knowledge of photo-initiated polymerisations had been acquired. This focussed on the polymerisation of monolithic stationary phases in

capillary using a commercial UV light source. Once this had been carried out, the use of light emitting diodes as initiating sources was examined. The ability of LEDs to efficiently produce short plugs (3-5 mm) of monolith allowed them to be used as monolithic frits for column-packing. Such monoliths were synthesised and using a low pressure column packing set-up spiropyran functionalised and COOH PS beads were packed. This low pressure, low cost method of column packing has been shown to give homogeneously packed capillary columns without the need for high-cost equipment. These columns perform to a high standard without the disadvantages of long packing time and high-cost, allowing on-column detection of packed capillary columns which is not generally possible.

Lastly the functionalisation of the surface of monolithic materials was studied. The use of photochemical surface modification was reproduced from the literature and shown to work very well for the immobilisation of functional monomers on the surface of the monolithic stationary phases. This functionalisation was done by photo-chemical means which allowed the functionalisation of selected areas of the monolith. Of course, functionalisation can be carried out on the entire length of monolith if that is required. This method is very important as it allows the surface chemistry of the monolith to be tailored specifically to a particular interaction, thereby optimising the efficiency of the stationary phase. Immobilisation of materials on the pore surface also ensures more of the active functional groups are available for interaction, which polymerisation in the bulk can sometimes restrict. This method will be put to further use in Chapter 3 where it will be used as a method of immobilising photochromic dyes on the surface of monolithic materials for applications in electrochromatography and micro-fluidics.

3. Spiropyran Modified Monolithic Stationary Phases

3.1. Introduction

The spiropyrans are a well-known family of organic dyes. They were first discovered in 1952 by Fischer and Hirshberg [157] and are known to change their properties in response to light [158], heat [158], solvent polarity [165], metal complexation [170, 193] and pH [166]. The dyes exist in two forms; an uncharged, colourless spiropyran (SP) and an intensely coloured, zwitterionic merocyanine (MC), in addition to the zwitterionic form some of the MC form exists as an uncharged quininoid form. The structure of these forms of the dye is shown in Fig. 3.1.
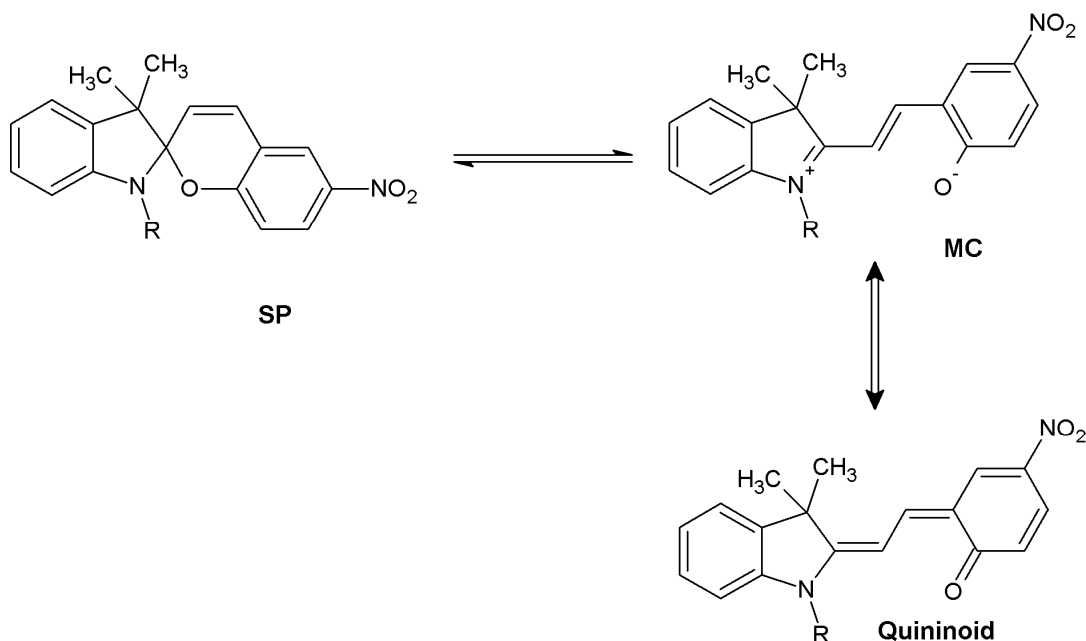
Figure 3.1: *Schematic of the most common structures of the two forms of the spiropyran molecule, the MC form exists both as a zwitterion and as an uncharged quininoid form*

The most commonly exploited property of these molecules is their photochromism, which has allowed them to find applications in light sensitive media such as photo-sensitive ophthalmic lenses and optical recording media [194-196]. Chromism is defined as the chemical process by which a molecule can switch between two different forms, having different absorbance spectra, in response to a stimulus [164]. The

97

photochromism of the spiropyrans, that is the conformational and polarity changes induced by light irradiation, is of primary importance in this work particularly in the final section where the development of a photo-dynamically controllable electroosmotic pumping system is described.

The conversion between the SP and the MC form is carried out with ultraviolet (UV) and visible light. Irradiation of the molecule with UV light at approximately 375 nm produces the zwitterionic MC form, while the white light returns the molecule to the uncharged SP form. The λ_{max} of absorbance of the spiropyran in the visible region is approximately 540 nm (depending on the specific derivative of the molecule), however, it was found through the course of this research that white light instead of green light produces a faster reconversion to the SP form [193]. This switching process is entirely reversible over a large number of irradiations [197] although the exact number depends on several factors such as the stability of the particular spiropyran, the intensity of the light source and the presence of oxygen as the dye is susceptible to photo-bleaching, that is irreversible cleavage of the pyran ring [158]. Byrne *et al.* [170] noted that the period of time over which the molecule is stable can be increased by binding it to or incorporating it within some type of polymeric support rather than leaving it free in solution. This is likely due to the fact that, when immobilised, the chances of aggregation of the molecule in solution are reduced and so the dye switches more freely [198]. Scarmagnani *et al.* [193] observed that there is a minimum distance to be maintained between the spiropyran and the support in order to prevent the surface interactions from interfering with the switching efficiency, they showed that a chain length of 8-methylene groups provides enough separation from the surface to allow effective switching between the two forms of the molecule.

Conversion experiments conducted with light emitting diodes (LEDs), chosen for their high intensity, quasi monochromatic light output and negligible heat generation [80, 88], showed that more than 100 switches could be performed when the spiropyran was immobilised on polymeric beads before a decrease in the switching intensity could be detected [193]. Moreover, spiropyran moieties have recently been immobilised by Benito-López *et al.* [199] in the channels of polydimethylsiloxane (PDMS) micro-

fluidic chips as a photonically controlled, self-indicating system for metal ion accumulation and release.

In this work a carboxylated spiropyran derivative, 1',(3-carboxypropyl)-3',3'-dimethyl-6-nitrospiro[2H-1]-benzopyran-2,2'-indoline [SPCOOH] and a derivative with a long vinyl chain, 1',(9-decenyl)-3',3'-dimethyl-6-nitrospiro[2H-1]-benzopyran-2,2'-indoline [SPM], were synthesised from procedures by Garcia *et al.* [200] and McCoy *et al.* [201], respectively. The carboxylated derivative, SPCOOH, was used to modify monolith surfaces while the monomeric derivative, SPM, was incorporated into a polymeric monolith by copolymerising it with a common cross-linker, divinylbenzene, to produce a rigid, macroporous, photochromic monolith. The first sections detail the preliminary work carried out using spiropyran solutions and bulk polymers, this is followed by detailed descriptions of the modification and synthesis of the monolithic materials. Three different methods of immobilising and incorporating the spiropyrans on/within the monolith were examined; (1) immobilisation of the spiropyran on the pores of a monolithic scaffold by electrostatic interaction, (2) immobilisation of the dye on the monolith by covalent linkage and (3) copolymerisation of a monomeric derivative of the dye with a cross-linking monomer to achieve a monolithic dye polymer. The final section presents the application of certain modified monolithic stationary phases as photo-controllable electroosmotic pumps with photo-controllable flow rates.

3.1.1. Aims

The aims for the work detailed in this section are;

1. to examine the binding of different spiropyrans to metal ions in solution,
2. to study the retention of metal ions on the spiropyrans which have been immobilised on polymeric supports by electrostatic or hydrophobic interactions,
3. to investigate different methods of immobilisation of spiropyrans on monolithic scaffolds,
4. to determine whether the synthesis of monoliths directly from spiropyran monomers is possible,

5. to find an application for these different photochromic monoliths, synthesised directly from photochromic monomers and obtained by the immobilisation of photochromic dyes on the monolith surface, in separation science.

3.2. Experimental

3.2.1. Reagents

The following reagents were employed in the experiments conducted in this chapter; 1,8-diaminooctane, 1',3'-dihydro-1',3',3'-trimethyl-6-nitrospiro[2H-1-benzopyran-2,2'-(2H)-indole], 1-bromo-dec-9-ene, 1-decanol (Reagent grade, 99%), 1-ethyl-3-[3-dimethylaminopropyl]carbodiimide hydrochloride (EDC), 2-(*N*-morpholino)-ethanesulphonic acid (MES), 2,2'-azobisisobutyronitrile (98%, AIBN), 2,2'-dimethoxy-2-phenylacetophenone (99%, DMPAP), 2,3,3-trimethylindoline, 2-aminoethyl methacrylate (90%, AEMA), 3-(trimethoxysilyl)propyl methacrylate (>98%, TMSPM), 5-nitrosalicylaldehyde, acetone (HPLC grade), benzophenone (99%, BP), butyl methacrylate (99%, BuMA), chloroform (UV spectrophotometric grade), cobalt (II) nitrate, copper (II) nitrate, cyclohexanol (Reagent grade, 99%), divinylbenzene (80%, DVB), ethylene dimethacrylate (98%, EDMA), glycidyl methacrylate (97%, GMA), hydrochloric acid, methacrylic acid (99%, MAA), methanol (HPLC grade), quaternary salt of 1-(3-carbomethoxypropyl)-3,3-dimethyl-2-methylene-indoline, sodium hydroxide, styrene (>99%, S), *t*-butanol (HPLC grade, 99.5%) and tetrahydrofuran (HPLC grade). All were purchased from Sigma-Aldrich Chemical Co. (Wicklow, Ireland) and used as received.

UV-spectrophotometric grade ethanol was obtained from Lennox Laboratory Supplies (Dublin, Ireland).

Deionised water was obtained from a Milli-Q water filtration system.

3.2.2. Materials

Poly(tetrafluoroethylene) coated fused silica capillary with an internal diameter of 100 μm was purchased from Polymicro Technologies. The internal walls of the capillary

were treated using the procedure described in Section 2.2.4.1 from the paper by Okanda *et al.* [187].

Pressure sensitive adhesive (PSA, ARcare 8890) and sheets of poly(methyl methacrylate) were purchased from Adhesives Research Ltd. (Limerick, Ireland). 5 min epoxy resin was purchased from Bondloc (Worcestershire, UK).

400 μm i.d. poly ether ether ketone (PEEK) tubing and a nano-flow sensor to monitor eluent flow rate from the electroosmotic pump were obtained from Upchurch Scientific (Oak Harbor, WA, USA).

375 nm and white (400-750 nm) LEDs were purchased from Roithner Laser Technik (Vienna, Austria). Power supplies for the LEDs were made in-house.

3.2.3. Instrumentation

A liquid chromatography set-up consisting of a pump working in the flow range 10 μl - 10 ml (Applied Biosystems, Foster City, CA, USA), a manual injector with a 5 μl loop (Rheodyne, Oak Harbor, WA, USA) and a capacitively coupled contactless conductivity detector (Istech, Vienna, Austria) were employed in this work.

A peristaltic pump from Lambda Technologies (Brno, Czech Republic) was used for all solution flushings in the following procedures.

Voltage was generated for the electroosmotic pump (EOP) using a 0-30 kV high voltage power supply from Unimicro Technologies (Pleasanton, CA, USA).

3.2.4. Procedures

3.2.4.1. Solution and Bulk Polymer Experiments: Synthesis of 1'-(3-carboxypropyl)-3',3'-dimethyl-4-nitrospiro[2H-1]-benzopyran-2,2'-indoline [SPCOOH]

The 1',(3-carboxypropyl)-3',3'-dimethyl-6-nitrospiro[2H-1]-benzopyran-2,2'-indoline was synthesised from a procedure described by García *et al.* [200] by a collaborator (S.Scarmagnani). In brief, equimolar amounts of 5-nitrosalicylaldehyde and the quaternary salt of 1-(3-carbomethoxypropyl)-3,3-dimethyl-2-methylene-indoline were

mixed in ethanol and refluxed for 6 h. The dark purple product was cooled in an ice bath, filtered and then washed with ethanol. The product was recrystallised several times from ethanol to obtain 1'-(3-carboxypropyl)-3',3'-dimethyl-6-nitrospiro[2H-1]benzopyran-2,2'-indoline [SPCOOH]. This product was then dissolved in tetrahydrofuran and stirred at room temperature for 24 h with an excess of 10% NaOH. The solution was then acidified with dilute HCl. The product was extracted with chloroform which was then removed by low pressure distillation. Column chromatography using 10% methanol in chloroform yielded the pure 1',(3-carboxypropyl)-3',3'-dimethyl-6-nitrospiro[2H-1]-benzopyran-2,2'-indoline (Fig. 3.2).
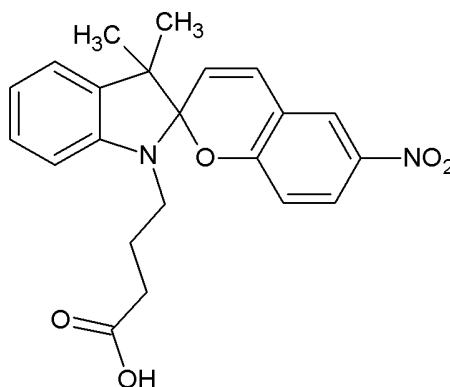
Figure 3.2: *Structure of the carboxylated spiropyran, 1',(3-carboxypropyl)-3',3'-dimethyl-6-nitrospiro[2H-1]-benzopyran-2,2'-indoline [SPCOOH]*

3.2.4.2. Solution and Bulk Polymer Experiments: Spectral determination of the complexation between the spiropyran in solution and selected test analytes

The spectra of the complexation of the merocyanine form with $Cu(NO_3)_2$ and $Co(NO_3)_2$ were taken in ethanol. For each experiment the spiropyran was dissolved in ethanol and kept in the dark overnight so that the equilibrium state between the two forms could be reached. During the experiment the solution of dye was irradiated for 2 min with a UV BondWand at 365 nm and then the spectrum was taken in the region 200-800 nm. 300 µl of a solution of one of the test compounds of a known concentration was added to the solution of dye and the spectrum was taken again. The spectra were taken at a range of different concentrations of the analyte and this data was plotted and is presented in

Section 3.3.1. To validate the results the experiments were performed with two different spiropyran derivatives, the first is the commercially available derivative, 1',3'-dihydro-1',3',3'-trimethyl-6-nitrospiro[2H-1-benzopyran-2,2'-(2H)-indole] [CSP] and the second the carboxylated derivative, SPCOOH, synthesised in the laboratory.

3.2.4.3. Solution and Bulk Polymer Experiments: Coating of the poly(S-*co*-DVB) bulk polymer with SPCOOH

The spiropyran was immobilised by mixing 0.5 g of finely ground bulk poly(S-*co*-DVB) polymer, prepared using the procedure described in Section 2.2.4.3, with 1 ml of a solution of 1 mM SPCOOH in ethanol. The solution was vortexed for 2 h and then centrifuged to remove the SPCOOH solution. After centrifugation the polymer was washed with methanol to remove the excess SPCOOH and then dried under nitrogen.

3.2.4.4. Solution and Bulk Polymer Experiments: Retention/release of Cu^{2+} on the SPCOOH coated poly(styrene-*co*-divinylbenzene) bulk polymer

Finally, a short proof of concept study was carried out to determine how well the spiropyran immobilised on the surface of the polymer could retain and release metal ions in a flow through set-up. In order to carry out this experiment some of the spiropyran coated poly(S-*co*-DVB) bulk polymer was first packed into solid phase extraction (SPE) cartridges. The selected SPE cartridges have a silica-C18 packing, this was chosen as this packing will have affinity for the spiropyran molecule but not for the metal ions. This means that if the spiropyran coating starts to elute it will be retained on the packing in the cartridges so it can be observed while the metal ions should not be retained on anything but the spiropyran coating. The experimental set-up is shown schematically in Fig. 3.3.
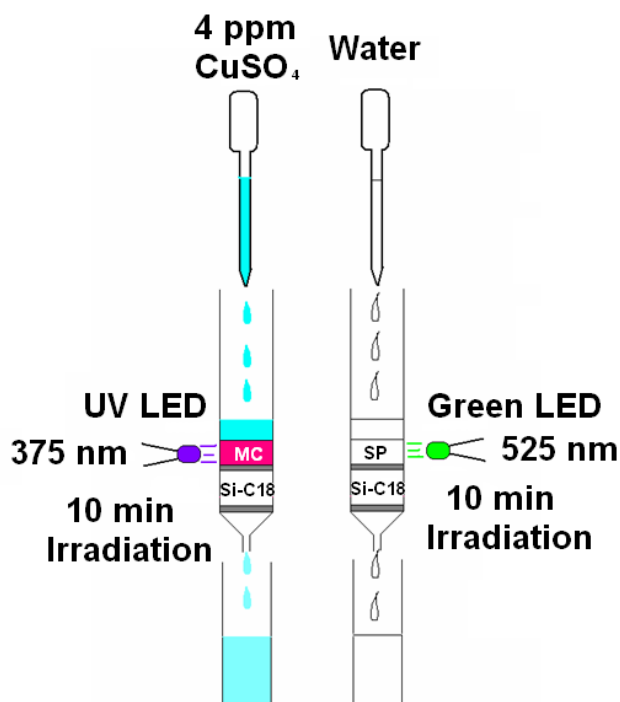
Figure 3.3: *Schematic of the experimental set-up used to prove the concept of a photo-responsive stationary phase*

After packing into the cartridge the stationary phase was irradiated at approximately 375 nm to produce the merocyanine form and then a 4 ppm aqueous solution of Cu^{2+} from copper sulphate was passed through the material. The material was irradiated again at 375 nm and then flushed with water to remove any unbound Cu^{2+} ions. Both times the eluent was collected and labelled.

In the second step the material was irradiated with visible light at 525 nm until the material appeared white (approximately 10 min) and the SP form was regenerated. The material was then flushed with water a second time to remove any Cu^{2+} which had been released from the stationary phase. Once again the eluent was collected and labelled. The eluent was then analysed by inductively coupled plasma-atomic emission spectroscopy.

3.2.4.5. Immobilisation of spiropyran by electrostatic interaction: Synthesis and coating of poly(styrene-*co*-divinylbenzene) monoliths with 1',(3-carboxypropyl)-3',3'-dimethyl-6-nitrospiro[2H-1]-benzopyran-2,2'-indoline [SPCOOH]

A poly(S-*co*-DVB) monolith was synthesised in 100 µm poly(tetrafluoroethylene)-coated fused silica capillary by the procedure described in Section 2.2.4.3. A solution containing 6 mg/ml (15 mM) SPCOOH in ethanol was made up and sonicated to ensure dissolution of the dye. The manual injector was used to introduce the dye onto the poly(S-*co*-DVB) column with the pump flushing ethanol through the system throughout the injection. The conductivity detector was used first to observe the breakthrough point at which the monolith was coated to saturation and then to characterise the switch between the two forms of the dye on the monolith surface.

3.2.4.6. Immobilisation of spiropyran by covalent linkage: Preparation of the scaffold

Before the immobilisation of the dye to the monolith surface could take place it was necessary to synthesise the monolith scaffold. A batch of poly(butyl methacrylate-*co*-ethylene dimethacrylate) [poly(BuMA-*co*-EDMA)] monoliths were synthesised as described in Section 2.2.4.5. These were then divided into two groups; both groups underwent surface modification by the two-step photo-grafting procedure presented in Section 2.2.4.7. Group I obtained a layer of methacrylic acid (MAA) and Group II were modified with a layer of 2-aminoethyl methacrylate (AEMA). Using these two different types of photo-grafted monolith as the starting point, the carboxylated spiropyran was immobilised on the surface by two different routes.

3.2.4.7. Immobilisation of spiropyran by covalent linkage: Immobilisation of spiropyrans through grafted carboxylic acid groups of MAA (Route I)

After the carboxylic acid groups were grafted on the surface of the poly(BuMA-*co*-EDMA) monoliths (as described in Section 2.2.4.7), the column was flushed with methanol to remove all traces of the 15% w/v MAA in methanol grafting solution. After washing with methanol the column was flushed with 0.1 M 2-(*N*-morpholino)-ethanesulphonic acid (MES) buffer at pH 4.6 overnight to ensure dissociation of the

carboxylic acid groups which have been grafted on the surface. This method is relatively long, taking 6 days in total to produce the spiropyran modified column, additionally there are 6 steps involved in producing the monolith, the first two being the synthesis of the scaffold and the grafting of the layer of MAA, the four subsequent steps are described below.

3.2.4.7.1. Amination of the monolith surface with 1-ethyl-3-[3-dimethylaminopropyl]carbodiimide hydrochloride (EDC)

A solution of 10 mg 1-ethyl-3-[3-dimethylaminopropyl]carbodiimide hydrochloride (EDC) in 0.1 M MES buffer was flushed through the MAA-modified monolith at room temperature for 24 h. As can be seen from the scheme in Fig. 3.4, this process removes the H from the acid group and the EDC attaches itself to the molecule.
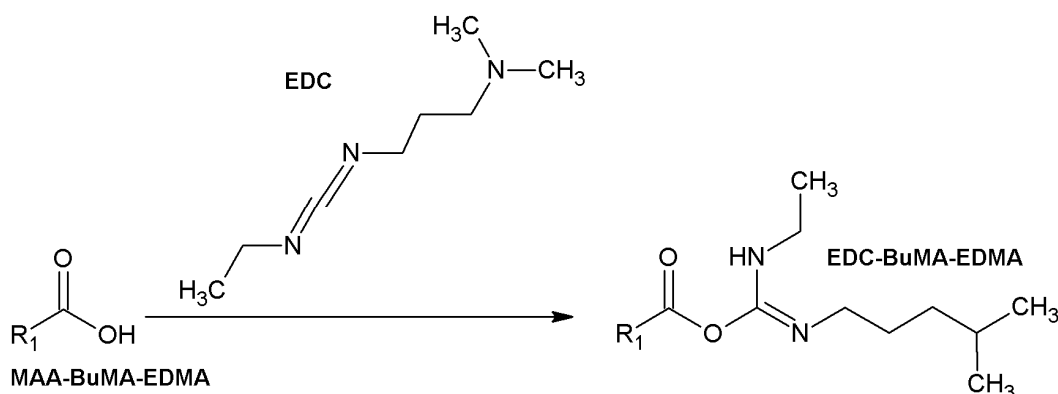
Figure 3.4: *Amination of MAA modified poly(BuMA-co-EDMA) monolith using EDC.*

3.2.4.7.2. Attachment of the 1,8-diaminooctane linker

After 24 h the flushing solution is replaced with a solution of 1,8-diaminooctane in 0.1 M MES buffer. This molecule acts as a spacer between the surface and the spiropyran. This reaction was allowed to continue for 24 h at room temperature. In this stage the EDC molecule which has attached to the alcohol group is displaced by the amine linker, which then forms a covalent bond to the surface (Fig. 3.5).
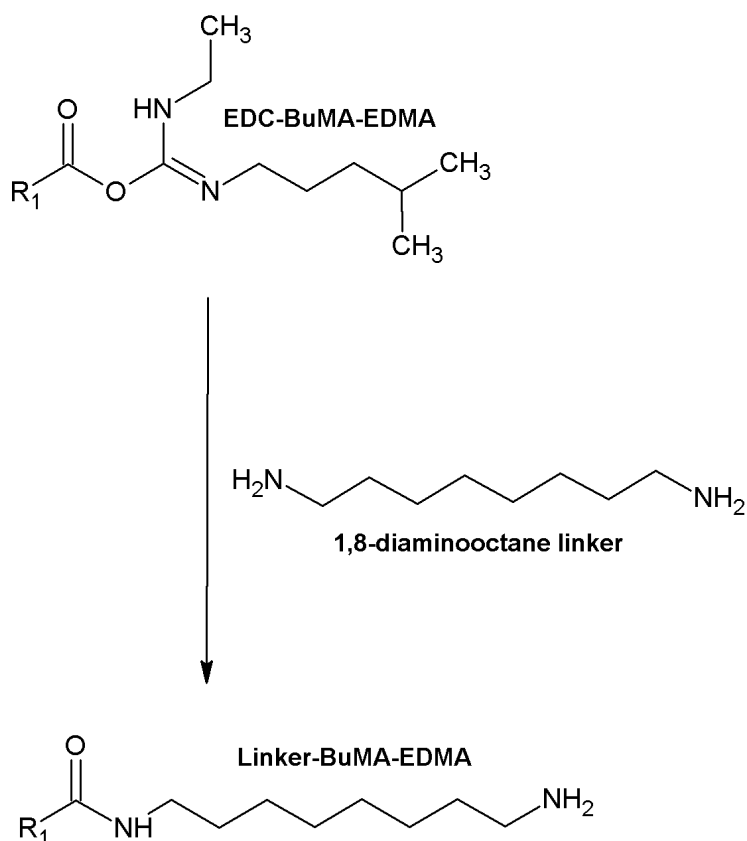
Figure 3.5: *Reaction of 1,8-diaminooctane with aminated monolith surface BuMA-EDMA-EDC.*

3.2.4.7.3. Amination of the spiropyran

Before the spiropyran can be covalently bound to the surface the -OH of its carboxylic group must be modified so that it will become a good leaving group. This is done in the same way as the surface was modified, by removing the H of the hydroxyl group and replacing it with the EDC. When the molecule comes in contact with an amine group of the EDC, the acyl group will be displaced in favour of the amine, allowing the two parts to form a covalent linkage (Fig. 3.6). A concentrated solution containing 16 mg (41 µmol) spiropyran dye was made up in 3 ml ethanol, to this approximately 32 mg (167 µmol) EDC was added (the EDC is in four-fold excess to ensure complete amination of the SPCOOH). These two reactants were left to react together for 1 h in the dark while the solution was stirred continuously.
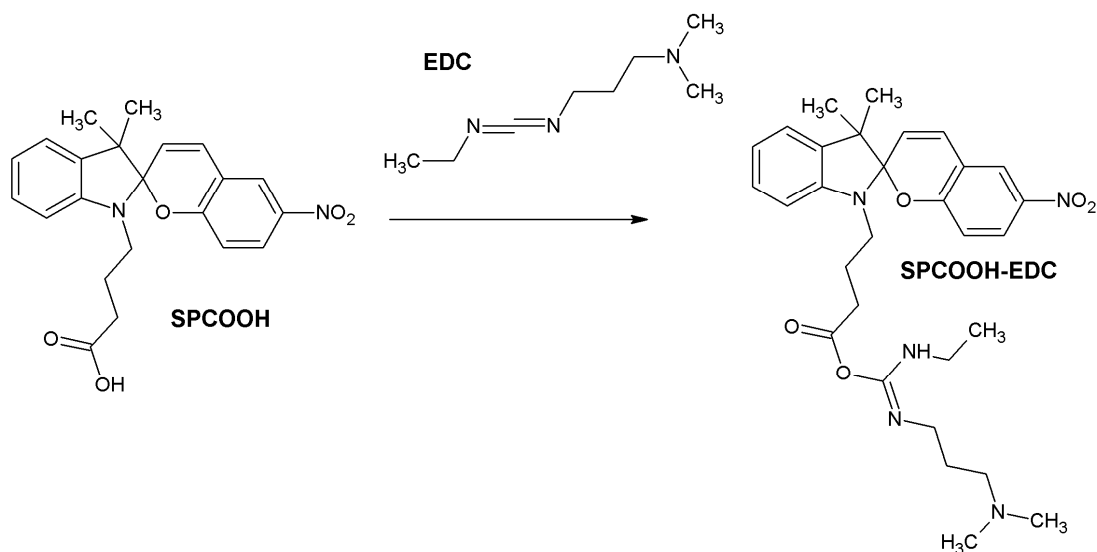
Figure 3.6: *Amination of the –COOH group of SPCOOH with EDC*

3.2.4.7.4. Immobilisation of the spiropyran on the surface of the monolith

The solution of EDC-modified SPCOOH is flushed through the linker-modified monolith for 72 h to ensure complete reaction of the dye with the surface. As the 13.5 mM solution of SPCOOH-EDC is flushed through the column the EDC modified groups are lost in favour of the amine on the surface of the monolith and the spiropyran is covalently bound to the pore surface (Fig. 3.7). As a result the monolith appears pink.
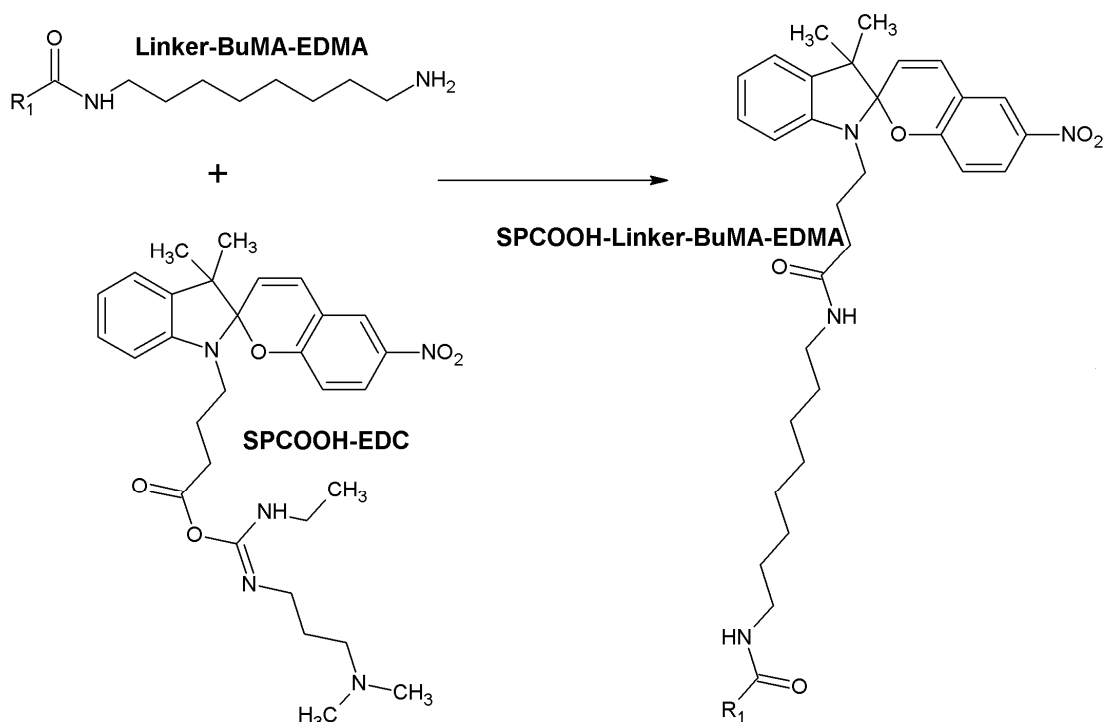
Figure 3.7: *Covalent linkage of SP: reaction of linker-modified poly(BuMA-co-EDMA) monolith with SPCOOH-EDC.*

After immobilisation of the spiropyran the column was flushed with ethanol for 48 h to remove any excess dye. The amide linkage is very strong and attempts to remove it from the surface by repeated flushing with polar solvents have been unsuccessful as the pink colour of the merocyanine form of the dye is clearly visible on the surface of the monolith even after flushing.

3.2.4.8. Immobilisation of spiropyran by covalent linkage: Immobilisation through grafted amine groups of AEMA (Route II)

After the monolith synthesis and the grafting of the layer of 2-aminoethyl methacrylate (AEMA) was complete (Section 2.2.4.7) the monolith was flushed overnight with ethanol to ensure removal of all traces of the grafting solution. As a result an amine-modified poly(BuMA-*co*-EDMA) monolith was obtained. Unlike the procedure outlined in Section 3.2.4.7 the modification of the monolithic surface with EDC and subsequent attachment of 1,8-diaminooctane to the surface are unnecessary as the amine groups are already on the surface of the monolith from the grafting reaction with AEMA.

The aminated spiropyran, SPCOOH-EDC (Section 3.2.4.7.3), solution was flushed through the NH_2-modified monolith for 12 h at room temperature. The last stage was to wash the column for 72 h with ethanol. This washing stage proved the strength of the immobilisation as after this length of washing time the spiropyran still remained on the surface of the monolith, indicated by the presence of the strong pink colour of the MC form after UV irradiation. The reaction of the EDC modified spiropyran and the aminated monolith can be seen in Fig. 3.8.
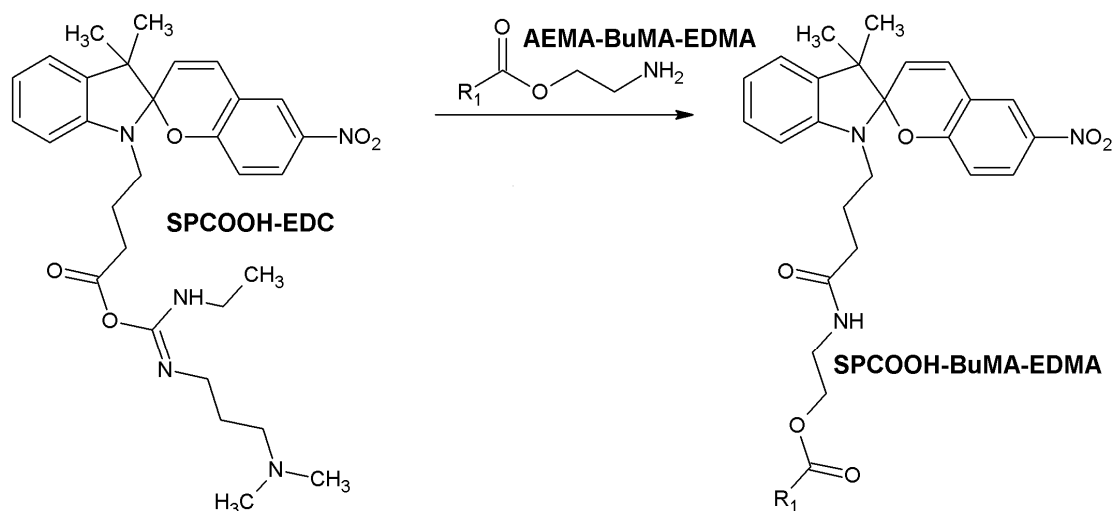
Figure 3.8: *Reaction of aminated spiropyran SPCOOH-EDC with NH_2-modified poly(BuMA-co-EDMA) monolith*

3.2.4.9. Incorporation of spiropyrans in monolithic materials by copolymerisation: Synthesis of a spiropyran monomer [SPM]

A monomeric spiropyran, 1',(9-decenyl)-3',3'-dimethyl-6-nitrospiro[2H-1]-benzopyran-2,2'-(2H)-indoline [SPM], containing a long carbon chain with a vinyl group on the pyrrole ring, Fig. 3.9, which is suitable for subsequent copolymerisation with a divinylbenzene monomer, was synthesised in a two-step procedure by a collaborator on this project (S. Scarmagnani). Firstly, a N-alkylation of the 2,3,3-trimethylindoline with a 1-bromo-dec-9-ene was carried out followed by hydroxide treatment of the product and a coupling with 5-nitrosalicylaldehyde as outlined in a procedure by McCoy *et al.* [201]. The reaction temperature was always kept below 80°C to prevent thermally initiated polymerisation of the monomeric spiropyran.

110
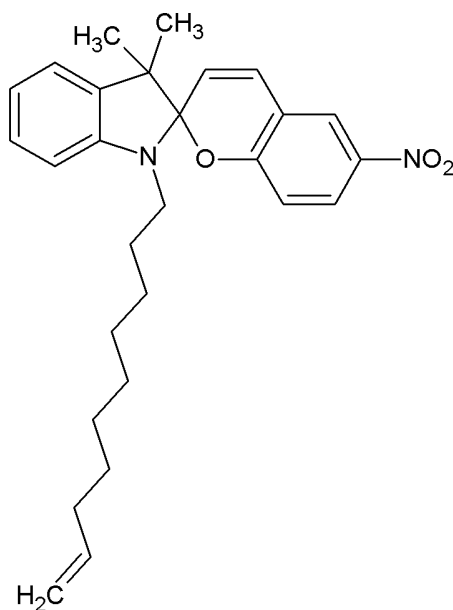
Figure 3.9: *Structure of the monomeric spiropyran 1',(9-decenyl)-3',3'-dimethyl-6-nitrospiro[2H-1]-benzopyran-2,2'-indoline (SPM)*

3.2.4.10. Incorporation of spiropyrans in monolithic materials by copolymerisation: Synthesis of poly (spiropyran-*co*-divinylbenzene)

A 110 μl solution containing 40 μl divinylbenzene, 6 mg of the spiropyran monomer, SPM, 70 μl of 1-decanol and 0.42 mg of the initiator AIBN was sonicated, purged with nitrogen and then filled by capillary action into pre-silanised PTFE coated fused silica capillaries (treated as per Section 2.2.4.1). Using a rubber septum attached to a weight, the capillaries were immersed in the water bath vertically in order to promote a more homogeneous and dense growth of polymer. The polymer was allowed to form over 5 days at 60°C. After polymerisation the columns were flushed with methanol for 30 min to remove porogens and unreacted initiator.

3.2.4.11. Application of spiropyran modified monoliths as photo-dynamically controllable electroosmotic pumps: Synthesis of poly (styrene-*co*-divinylbenzene)

A 200 μl solution containing 40 μl styrene, 40 μl divinylbenzene, 120 μl 1-decanol and 0.73 mg of the initiator AIBN was sonicated, purged with nitrogen and then filled by capillary action into PTFE-coated fused silica capillaries treated using the procedure

described in Section 2.2.4.1. They were then polymerised in the same way as the poly(spiropyran-*co*-divinylbenzene) monoliths described previously with the exception that the polymerisation time was 20 h.

3.2.4.12. Application of spiropyran modified monoliths as photo-dynamically controllable electroosmotic pumps: Fabrication of the micro-fluidic chip platform

Channels in the micro-fluidic chip were first designed using 3D Excalibur software (Progressive Software Corp., USA) and then fabricated by direct micro-milling (Datron 3D M6, Datron Technology Ltd., Milton Keynes, UK) by a post-doctoral researcher in our group (F-Q. Nie). A chip 20 mm x 30 mm x 5 mm with channels 8 mm x 0.4 mm x 0.4 mm was produced by him as described in his previous publications [27, 28].

The PMMA sheets were washed thoroughly with ethanol after milling to remove traces of dust and excess PMMA and capillaries within which the photochromic monoliths were contained were encased in the channels. In order to compare the response of a non-switchable monolith with the photochromic monoliths, a poly(S-*co*-DVB) monolith was synthesised and encased in one of the channels of the chip. The capillaries were held in place in the channel using a drop of 5 min epoxy glue before the channels were covered with a layer of pressure sensitive adhesive (PSA) and a second, unmilled sheet of PMMA. The whole chip was placed in a vice for several minutes to ensure that the chip was well sealed and would not leak. 1 cm lengths of PEEK tubing were used as inlet and outlet tubing and were connected from the inlet/outlet to 1.5 ml Eppendorf tubes which served as solvent reservoirs. Schematic of the set up is shown in Fig. 3.10.
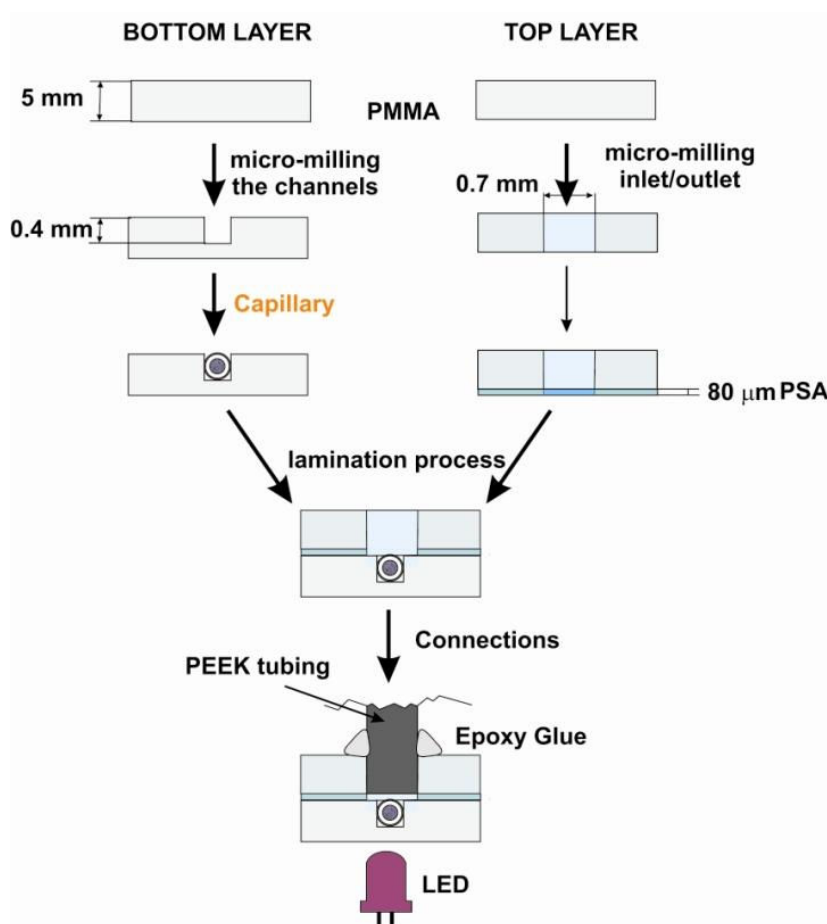
Figure 3.10: *Schematic of the micro-fluidic device fabrication, schematic courtesy of F. Benito-López.*

3.2.4.13. Application of spiropyran modified monoliths as photo-dynamically controllable electroosmotic pumps: Measurement of the electroosmotic flow (EOF)

Channels and reservoirs of the electroosmotic pump were filled with either 2 mM MES-histidine buffer or 1 mM HCl, the first being a common electrophoresis low conductivity buffer and the second chosen specifically to protonate the spiropyran and generate charge on the SP form and a stable positive charge on the MC form of the molecule. The electrodes were immersed in the electrolyte, a field of 0-125 kV/m or 0-250 kV/m (depending on the stability of the current) was applied across the channels and finally the flow rate of the eluent from the channel was measured using a nano-flow sensor. All the experiments were carried out in the dark with the outlet tubing positioned

at the same height as the reservoirs so that there was no difference in pressure between the outlet and the inlet. The EOF was measured when the monolith was switched by LED to each of the two forms of the spiropyran.

3.2.4.14. Characterisation of the spiropyran modified monoliths

Before any experiments were attempted with these photochromic monolithic materials characterisation of the stationary phase was necessary. The photochromic monolithic scaffold itself was characterised by optical and scanning electron microscopy (SEM). A SVM-340 Synchronized Video Microscope (Labsmith, USA) and an electron microscope S-3000N VP-SEM (Hitachi, Japan) were used for visualisation.

The presence of the spiropyran was verified by reflective absorbance spectroscopy for which a purposely designed capillary holder for reflectance measurement was fabricated in black acrylonitrile-butadiene-styrene (ABS) copolymer with a Stratasys 3D printer (Eden Prairie, MN, USA). The two parts of the holder (the probe case and the capillary case, Fig. 3.11) were designed using a standard CAD/CAM software package (ProEngineer from PTC, Needham, MA, USA) by collaborators on this project C. Slater and C. Fay.
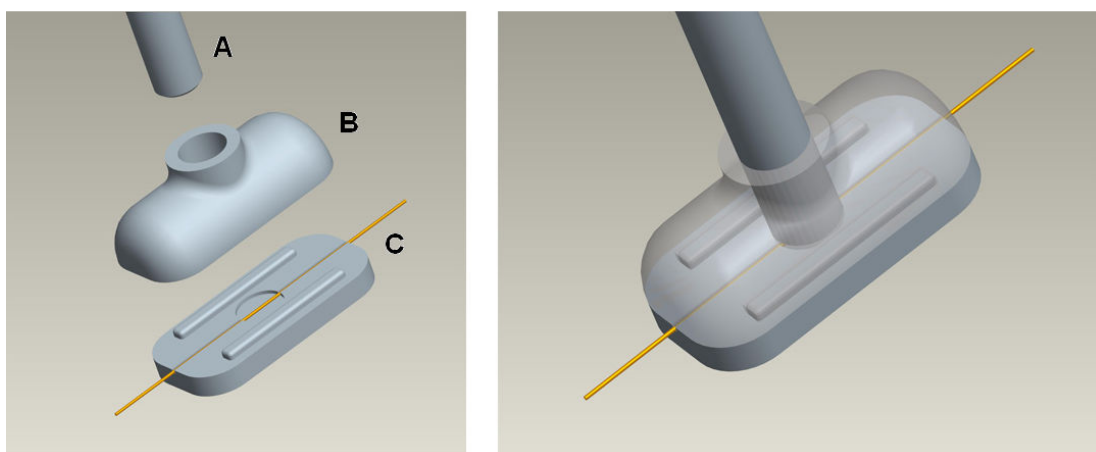
Figure 3.11: *Schematic of the probe/capillary holder used to carry out Reflective Absorbance Spectroscopy measurements on capillary as designed and fabricated by C. Slater and C. Fay, where (A) is the reflectance probe, (B) is the top section/probe holder and (C) is the bottom section/capillary holder. Schematic courtesy of C. Fay.*

Reflectance UV-Vis spectra were recorded using a S2000® spectrometer combined with a FCR-7UV200-2 reflection probe (7x200 μm cores) which was connected to a DH-2000-FSH, deuterium (215-400 nm) and halogen (400-1700 nm) light source, using a PTFE-based reflectance standard WS-1-SL to standardise measurements at 100% reflectance [202, 203]. All spectrometric instrumentation was purchased from Ocean Optics Inc. (Eerbeek, Netherlands). The resulting spectra are relative measurements processed by the Ocean Optics software against the previously recorded reference spectrum, which was recorded in the dark at the same distance from the probe as the sample [202-204].

3.3. Results and Discussion

3.3.1. Solution and bulk polymer experiments

From the literature it is known that the spiropyran has an affinity for a number of different analytes such as divalent metals (e.g. Cu^{2+}, Co^{2+}, Zn^{2+}) [170, 193, 199], amino acids (e.g. glycine) [168] and protonated molecules (e.g. HCl) [166, 205]. If the analyte has just one type of charge, that is positive or negative such as metal ions, they will only complex with one of the available charges on the MC form. In the case of zwitterionic analytes, such as amino acids, they will occupy both of the charged sites during complexation. This means it will be more difficult to expel the analyte during ring-closure to the SP form, possibly taking much longer than the time needed to expel the metal ions. In chromatography slow release of analytes from the stationary phase will result in broad and even overlapping peaks, therefore it was decided to avoid working with amino acids during the course of this work and concentrate initially on divalent metal ions.

To examine how the spiropyran reacts with the metals some preliminary experiments were done with solutions of metals and with two spiropyrans in the MC form in solution. Once the analyte had been selected it was necessary to find a method by which the spiropyran could be immobilised on a polymer material such as a polymer stationary phase. These preliminary experiments were carried out using bulk poly(S-*co*-DVB)

synthesised from the same mixtures as standard monolithic columns, such as those described in Section 2.2.4.3.

By taking the spectra of the species formed by the complexation of the merocyanine form of both dyes – commercial SP [CSP] and SPCOOH - with a range of analytes it is aimed to determine the binding constant of the merocyanine form for the test analyte. Ideally, this should be relatively high so that there is a good chance of the analyte being retained by the dye; however it should not be too high so that it would be difficult to force the release of the analyte by the dye, as in the case of amino acids. Additionally, it would also be important to be able to see the complexation, that is, a colour change that would appear when complexation with metal ions occurs, this would indicate that the analyte had really been bound to the stationary phase. The criteria for the selection of the optimum analyte are based on a relatively high binding constant and a significant colour change during complexation.

Fig. 3.12 and Fig. 3.13 below show the UV-Vis absorbance spectra of the merocyanine form of both the commercial spiropyran, CSP, and the carboxylated derivative SPCOOH, respectively, when mixed with solutions of differing concentrations of $Cu(NO_3)_2$ (top) and $Co(NO_3)_2$ (bottom) in ethanol.
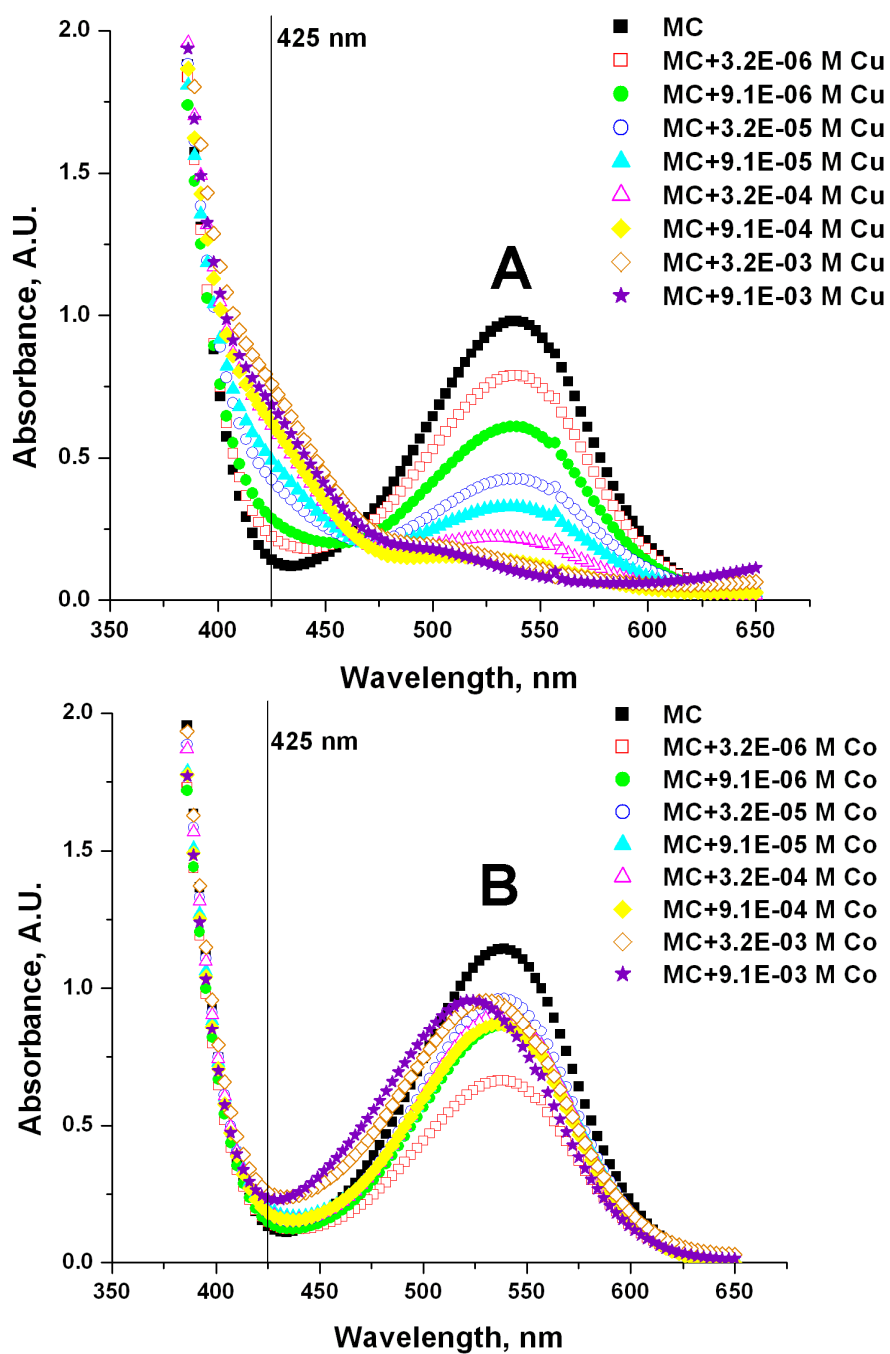
Figure 3.12: *Absorbance spectra of a commercially available spiropyran derivative, CSP, when increasing concentrations of Cu^{2+} (A) and Co^{2+} (B) are added to a 9.1 x 10^{-4} M solution of MC in EtOH*
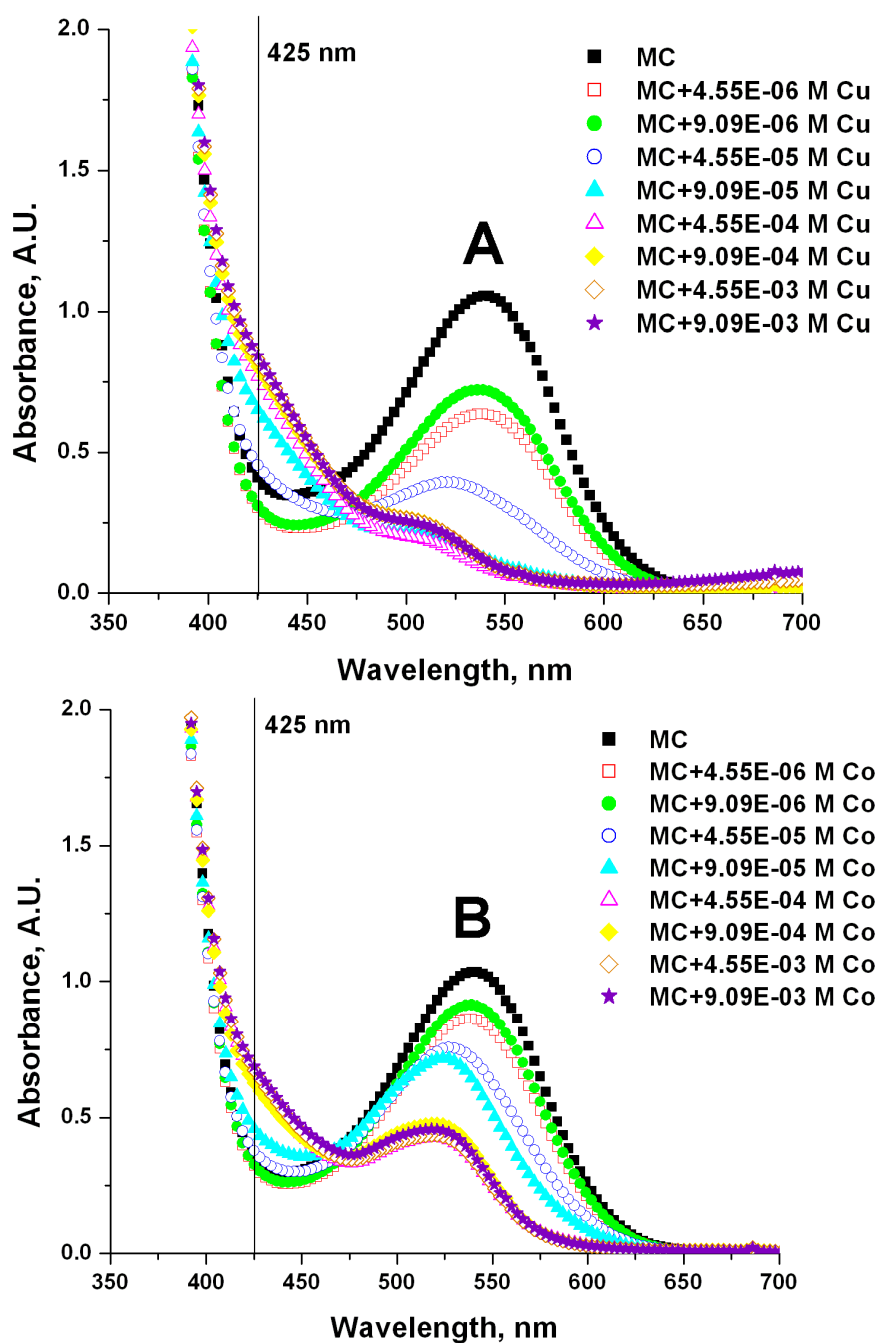
Figure 3.13: *Absorbance spectra of a carboxylated spiropyran derivative, SPCOOH, when increasing concentrations of Cu^{2+} (A) and Co^{2+} (B) are added to a 9.1 x 10^{-4} M solution of MC in EtOH*

As is clearly seen from the four sets of spectra the complexation is more pronounced when the copper is added to the solution of the MC form than when cobalt is added. In

the cobalt complexation spectra the merocyanine peak at approximately 540 nm never completely disappears while in the copper complexation spectra the 540 nm peak is significantly reduced while the peaks at 510 nm and 425 nm, which indicate the appearance of the complexed form, become more pronounced.

These spectra were then used to determine the binding constant of the merocyanine form for the two different metals. In all cases the complexation of the merocyanine form causes the appearance of a band at approximately 425 nm, this is the λ_{max} of absorbance of the complexed form. In order to calculate the binding constant K, some assumptions must first be made, namely that the divalent metal complexes with the zwitterionic spiropyran ligand in a ratio of 2:1. If this is the case then the equation for the binding constant, K, as described by Shao *et al.* [169], is as shown below (Eq. 3.1);

$$K = \frac{[ML_2]}{[M^{2+}][L]^2} \qquad (3.1)$$

Where $[ML_2]$, $[M^{2+}]$ and $[L]$ are the concentrations of the complex, metal ions and ligand in the solution, respectively. As all of the ligand may not be used to complex with the metal ions there is also a need to introduce another term, α, which is the ratio between the concentration of the free ligand, $[L]$, and the initial concentration of the ligand, $[L_I]$ (Eq. 3.2);

$$\alpha = \frac{[L]}{[L_I]} \qquad (3.2)$$

Knowing this, it is possible to reformulate the expression for [L] as (Eq. 3.3);

$$1 - \alpha = 2\left(\frac{[ML_2]}{[L_I]}\right) \qquad (3.3)$$

Yang *et al.* [206] have previously defined $[M^{n+}]$ as (Eq. 3.4);

$$[M^{n+}] = \frac{1}{2K} \times \frac{1}{[L_I]^{n-1}} \times \frac{1-\alpha}{\alpha^2} \qquad (3.4)$$

And, therefore, binding constant K could be expressed as (Eq. 3.5);

$$K = \frac{1 - \alpha}{2[M^{2+}] \times [L_I] \times \alpha^2} \qquad (3.5)$$

To calculate α it is necessary to know the maximum absorbance of the M^{2+}-MC complex at a given concentration of the M^{2+} (A_c), the absorbance of the MC form with no M^{2+} present (A_{min}) and the absorbance of the M^{2+}-MC complex at the maximum concentration of M^{2+} (A_{max}), all at the same wavelength which is the wavelength of maximum absorbance of the complex. The modified equation for α is given as (Eq. 3.6);

$$\alpha = \frac{A_c - A_{max}}{A_{min} - A_{max}} \qquad (3.6)$$

The binding constant can be determined from a plot of the log of the concentration of the metal ion $[M^{2+}]$ *vs.* α, by fitting a theoretical line to the data points based on an estimated value of K. The estimation is very simple and is done by selecting a value for K at random and then fitting the line of theoretical points obtained to the experimental data, the process is continued until the line gives the best to the experimental data. This means that K is an approximate value.

Looking first at the plot made by overlaying the theoretical binding constant data over the experimental data for the commercially available spiropyran derivative, CSP, (Fig. 3.14) it can be seen that the experimental data fit well to the assumption that the complexation occurs in a ratio of 2:1 (MC:M^{2+}). From estimating the value of K the binding constant has been found to be log K=7.48 for Co^{2+} and log K=7.54 for Cu^{2+}. It can therefore be seen that the merocyanine form has a stronger affinity for the copper ions than for the cobalt, although the difference using this derivative is slight. Shao *et al.* [169] reported a value for K for Cu^{2+} of 6.8, which is lower than the value obtained here, however they reported the use of a different spiropyran derivative, 1'-(methyl)-3',3'-dimethyl-6-tert-butyl-8-dimethylaminoethyl-[2H-1]benzopyran-2',2'-indoline, and therefore the values cannot be expected to be identical. They are, however, within the same order of magnitude indicating good correlation of the theoretical and experimental data.
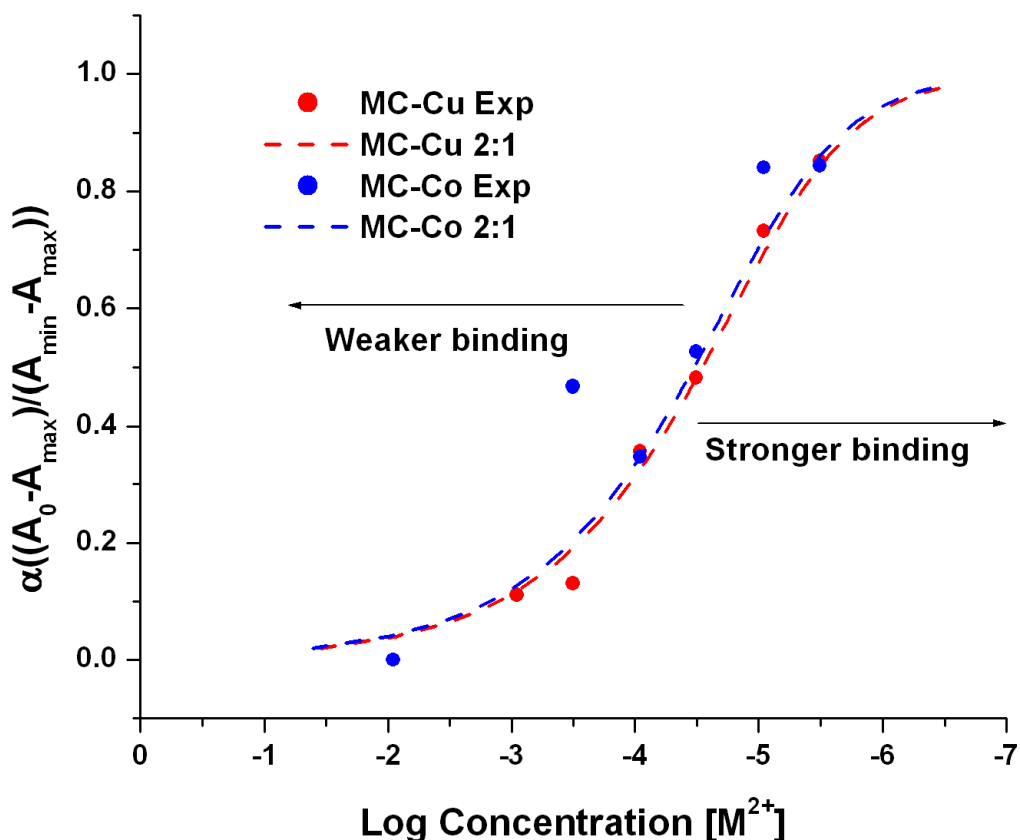
Figure 3.14: *Plot of the experimental and theoretical log of the concentration of metal ions added to the 9.1 x 10^{-4} M CSP solution in EtOH vs. α for Cu^{2+} (red) and Co^{2+} (blue)*

Looking next to the carboxylated derivative SPCOOH which was intended for use for the rest of this work the same calculations were performed and a plot was generated (Fig. 3.15) which showed the experimental data obtained from absorbance spectra and the theoretical data obtained by assuming the complexation ratio was 2:1 ($MC:M^{2+}$). It was found by observing the fit of the two lines that the two sets of data are not a good fit for one another and therefore a second set of theoretical data was obtained using the assumption that the MC form and the metal ions complex in the ratio 1:1 (Fig. 3.15).
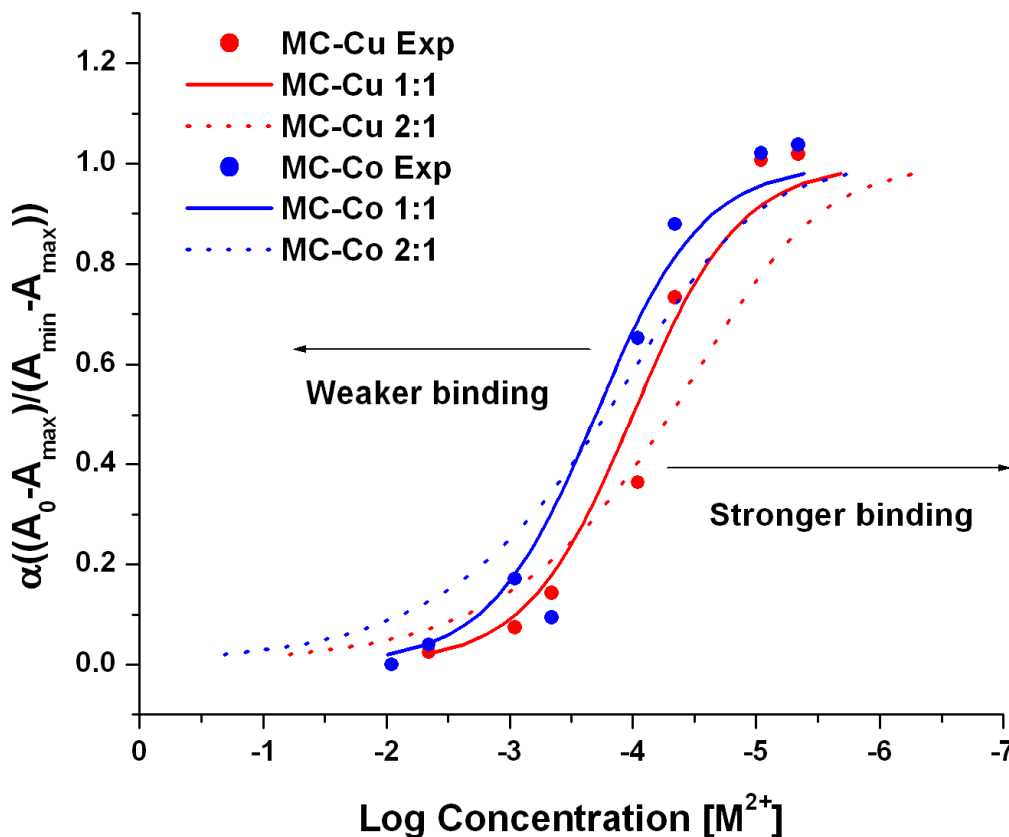
Figure 3.15: *Plot of the experimental and theoretical log of the concentration of metal ions added to the 9.1 x 10^{-4} M SPCOOH solution in EtOH vs. α for Cu^{2+} (red) and Co^{2+} (blue)*

It can be seen from the Fig. 3.15 that the best fitting curve is that where the MC-M^{2+} ratio is 1:1. This indicates that only one metal ion binds with each spiropyran in the solution. This can be explained by the fact that our test spiropyran was the carboxylated derivative and the –COOH group on the molecule can also act as a binding site for the metal ions. As the experiment was performed in solution, the –COOH group is free to complex with the metal ions in solution, to remove this interaction it is necessary to bind the spiropyran to the surface of the monolith using this carboxylic acid group, as described by Byrne *et al.* [170].

The binding constant given as the Log of K, which based on the theoretical fitting line data of the 1:1 complexation ratio, was estimated to be 4 for Cu^{2+} and 3.7 for Co^{2+} for

the carboxylated merocyanine form. The values are approximately half those observed for the same concentration of the CSP, indicating again the 1:1 binding.

Again the value for Log K for Cu^{2+} differs from the values shown by Shao *et al.* [169]. Using different spiropyran derivatives, in different concentrations or in different solvents can change the binding efficiency.

Knowing that the Cu^{2+} ions show a higher binding affinity for the spiropyran it was then necessary to determine the best method by which to immobilise the spiropyran molecule on the stationary phase material.

Some polymeric materials were then synthesised in bulk, these were poly(glycidyl methacrylate-*co*-ethylene dimethacrylate) [poly(GMA-*co*-EDMA)] and poly(styrene-*co*-divinylbenzene) [(poly(S-*co*-DVB)]. The procedures used for their synthesis are as described in Sections 2.2.4.2 and 2.2.4.3, respectively.

For this part of the work simple experiments were performed with immobilisation of the spiropyran onto bulk polymer by electrostatic interactions to determine whether this is a viable method for obtaining spiropyran coated stationary phases.

While the spiropyran binds to the methacrylate copolymer poly(GMA-*co*-EDMA), the fact that the epoxy group is so reactive that it can easily cleave and create a charged site on the surface is a problem for the development of the spiropyran modified stationary phase. With the presence of a charged site on the surface, the metal ions could bind to this instead of the spiropyran and there would be no light driven elution of these bound ions therefore it would counteract the usefulness of a light controlled stationary phase.

The styrenic copolymer poly(S-*co*-DVB) has no surface epoxy-groups and is hydrophobic in nature meaning the spiropyran, which is also hydrophobic due to the aromatic rings, can stick on the surface by hydrophobic interaction. Fig. 3.16 shows the switching of the spiropyran coated polymer after the first washing of the polymer. The polymers were washed by placing the solid in an Eppendorf tube with 1 ml of methanol, sonicating and vortexing the mixture before centrifuging to remove the solvent and drying in a column oven at 60°C. The polymer was irradiated completely with a 375 nm

UV LED for 2 min to produce the MC form; the polymer was then irradiated through a mask with a green LED at 525 nm to produce the spiropyran form.
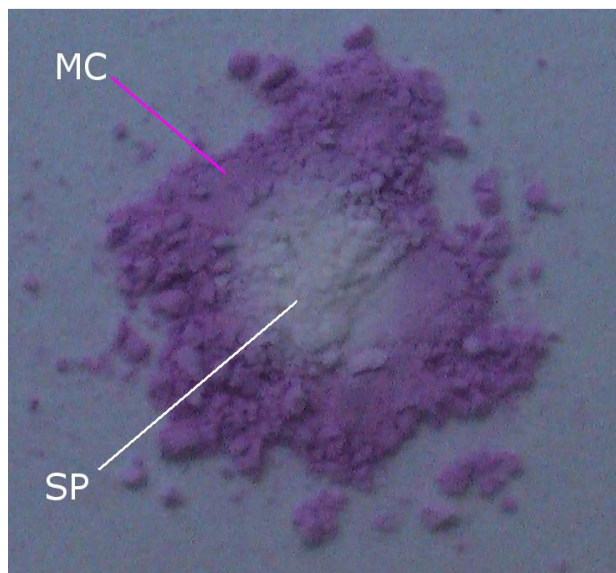
Figure 3.16: *Image of SPCOOH coated-poly(S-co-DVB) bulk polymer after being irradiated with UV (375 nm) LED for 5 min, where the SP form (white) and the MC form (pink) are both clearly visible*

While the colour did appear reduced after three washings with methanol the switching between the two forms was still visible and therefore it was decided that the first attempt to immobilise the spiropyran on the surface of the monolith should be through hydrophobic interaction.

Finally, a short proof of concept study was carried out to determine how well the spiropyran immobilised on the surface of the polymer could retain and release Cu^{2+} in a flow through set-up shown in Fig. 3.3. SPE cartridges packed with SPCOOH coated poly(S-*co*-DVB) were used to simulate the retention and release behaviour of the SPCOOH coating in a flow through set-up. Fig. 3.17 shows the calibration plot of the Cu^{2+} standards from the inductively coupled plasma-atomic emission spectroscopy (ICP-AES) with both the standards and samples displayed.
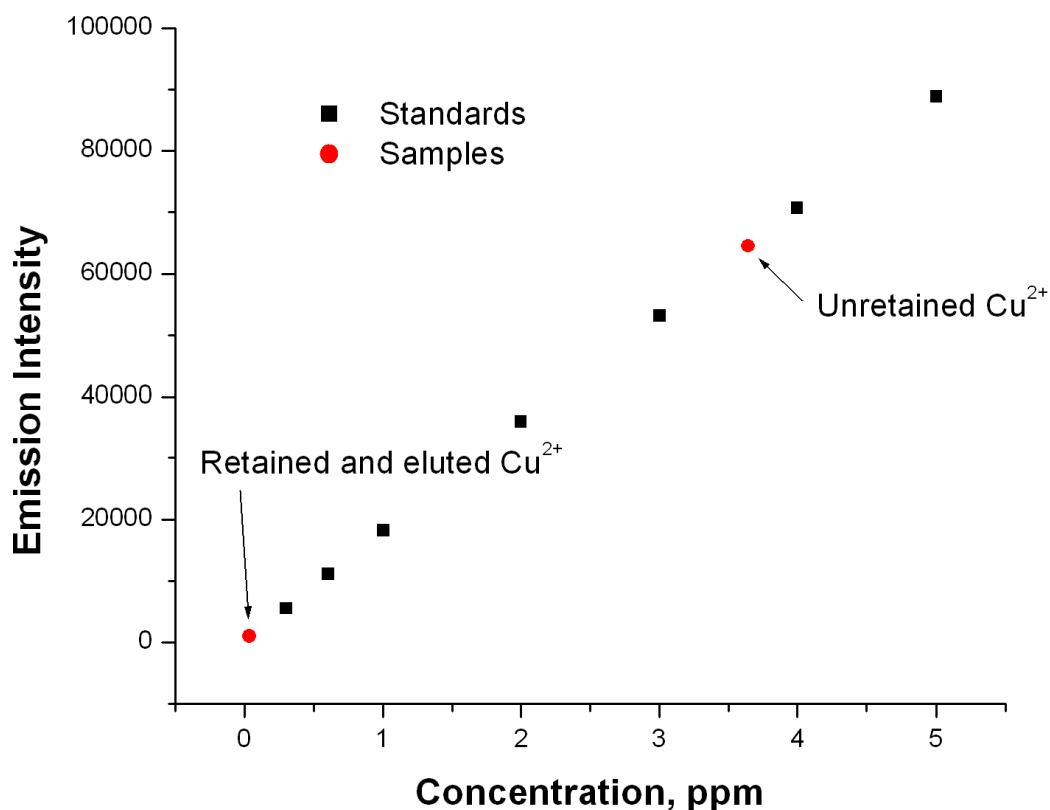
Figure 3.17: *Calibration plot for a range of Cu^{2+} standards from 0.5-5 ppm obtained by inductively coupled plasma-atomic emission spectroscopy, also displaying the results of the samples obtained from the flow through experiments in which Cu^{2+} was retained and released from a SPCOOH coated stationary phase*

It can be seen that the amount of unretained Cu^{2+} (3.64 ppm) relative to the amount of retained Cu^{2+} (0.04 ppm) is quite significant showing that the stationary phase in this case does not retain very much of the copper ions. Nonetheless the amount of Cu^{2+} retained by approximately 100 mg of packing was calculated to be 3-5% of the 4 ppm Cu^{2+} solution. This means that the 120-200 ppb of copper was retained by the stationary phase and of that only 40% (48-80 ppb) was eluted when the stationary phase was irradiated with visible light and washed with water. While this is quite low, it does show the proof of concept that spiropyran coated stationary phases have the potential to retain and release metal ions in a flow through system. It is now necessary to improve the

quality of the stationary phase so that higher percentages of the target analytes can be retained in a flow-through system.

3.3.2. Incorporation of spiropyrans in monolithic materials – Immobilisation by electrostatic interaction

Following on from the experiments carried out in bulk the first method of immobilising the spiropyran on the monolithic column was done by injecting plugs of a solution of the carboxylated spiropyran (SPCOOH) onto the monolith and allowing the dye to stick by electrostatic interactions. This method is quite often used in liquid chromatography [125] to change the surface properties of an underlying stationary phase for a particular separation, often reversibly so that the column can be used again for another purpose.

After the synthesis of the monolithic scaffold, the poly(S-*co*-DVB) monolith was connected to a basic HPLC set up and 5 µl injections of the SPCOOH in ethanol solution were performed onto the column until breakthrough of the dye was recorded on the conductivity detector. This was achieved after 6.5 µl of the 1.5 mM solution of dye had been injected onto the column.

This can be used to calculate the coverage of spiropyran on the surface of the polymer. Firstly, the monolith was prepared in 100 µm fused silica capillary which was 6 cm long. The internal volume of the capillary can then be calculated using the equation for the volume of a cylinder (Eq. 3.7);

$$\pi r^2 l = \pi (0.005 \; cm)^2 \; \times 6 \; cm = 4.714 \; \times \; 10^{-4} \; cm^3 = 0.4714 \; \mu l \qquad (3.7)$$

Where r is the radius of the internal cavity of the capillary, l is the length of the capillary and π is a constant. The entire volume of the capillary is not, however, entirely filled with polymer (Eq. 3.8). As 40% monomers were added to the pre-polymer solution and 100% conversion is achieved, then there can only be 40% polymer in the channels of the capillary, the rest must be pores.

$$V_{pores} = 0.4714 \; \mu l \; \times 0.6 = 0.2828 \; \mu l \qquad (3.8)$$

From the calculations above (Eq. 3.8) the pore volume is 0.2828 µl. As breakthrough was achieved at 6.5 µl injection volume, it took 23 column volumes to coat the monolith surface with spiropyran.

The molarity of the spiropyran solution was 0.0015 M and the molecular weight of the spiropyran is 394.415 g/mol, therefore the mass of the spiropyran on the pore surface of the monolith can be calculated.

No. of moles of spiropyran (Eq. 3.9);

$$(6.5 \times 10^{-6} l) \times (1.5 \times 10^{-3} \, mol/l) = 9.75 \times 10^{-9} \, mol \qquad (3.9)$$

No. of grams of spiropyran (Eq. 3.10);

$$(9.75 \times 10^{-9} \, mol) \times 394.415 \frac{g}{mol} = 3.8 \times 10^{-6} \, g \qquad (3.10)$$

As was calculated above (Eq. 3.7) the volume of the empty capillary was 0.4714 µl, therefore the volume of 40% monolith in the capillary was 0.1884 µl. From the literature it is known that the density of the polymer is approximately 1 g/ml and so the mass of the polymer in the channel is calculated as (Eq. 3.11, 3.12);

$$Density \, (D) = \frac{Mass \, (M)}{Volume \, (V)} \; \therefore M = V \times D \qquad (3.11)$$

$$M = (1.884 \times 10^{-4} \, ml) \times 1 \frac{g}{ml} = 1.884 \times 10^{-4} \, g \qquad (3.12)$$

From the calculations above there is 3.8 µg of spiropyran in the channel and 188.4 µg of the polymer.

$$\frac{3.8 \times 10^{-6} \, g}{1.884 \times 10^{-4} \, g} \times 100 = 2 \, \% \qquad (3.13)$$

We can see that for every 100 g of polymer there are approximately 2 g of spiropyran on the pore surface (Eq. 3.13), a relatively low amount. The monolith was then characterised to determine whether this low % of coverage affects the efficiency of the monolith in its intended application.

To characterise the switching efficiency lateral conductivity profiling was performed along the length of the monolith at three different stages in the coating process. The measurements were taken at 2 mm intervals and the detector was allowed to equilibrate for 5 min between each movement of the detector and the resulting conductivity profiles are shown in Fig. 3.18. The blue line shows the uncoated PS-DVB monolith, the black line shows the monolith directly after coating and it can be seen that the concentration of dye at the head of the column is higher than at the end furthest from the injector showing inhomogeneity of coating. The monolith was then flushed for 6 h with ethanol and the profiling repeated, this time with the spiropyran switched between the two forms, it can be seen that the conductivity at the head of the column is significantly decreased after the flushing indicating that a large amount of the spiropyran has been eluted from the column after washing. There is a visible difference between the SP and MC form of the spiropyran and a more homogeneous distribution of the dye along the monolith length after the flushing.
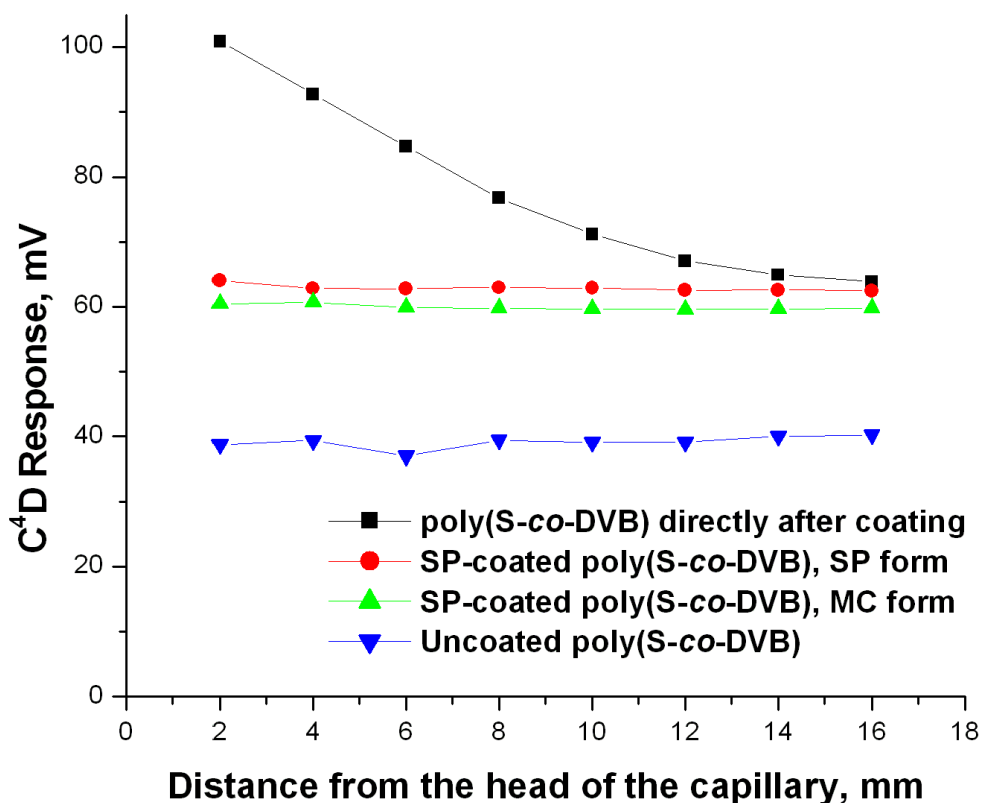
Figure 3.18: *Plot showing distance of the sensor from the head of the capillary (mm) vs. response (mV) obtained from a capacitively coupled contactless conductivity detector (C^4D) which was used to characterise the coating of the PS-DVB stationary phase with SPCOOH. The traces show the conductivity of the poly(S-co-DVB) monolith before coating (blue), directly after coating (black) and after washing for 6 h in both the spiropyran (red) and merocyanine (green) form.*

Despite the ease of coating and the ability of the spiropyran to switch between the two forms while retained on the surface of the monolith, this is not the optimal procedure for immobilising the spiropyran on the surface of the monolith due to the fact that the spiropyran elutes from the pores over time and so the coating is not stable.

3.3.3. Incorporation of spiropyrans in monolithic materials – Immobilisation by covalent linkage

While it is desirable to have the spiropyran immobilised on the surface of the monolith, as this should maximise the interaction between the dye and the mobile phase, it is clear

from the previous section that simple immobilisation through electrostatic interactions is not the most effective method. An immobilisation procedure which provides a permanent link between the dye and the stationary phase would be optimal. Two different methods of obtaining a permanent linkage have been examined, one which incorporates five reaction steps and immobilisation through surface grafted carboxylic acid groups and a second which has a total of three steps and involves immobilisation through surface grafted amine groups.

After the covalent immobilisation of the spiropyran on the surface of the monolith through the carboxylic acid groups the pore surface should resemble the schematic in Fig. 3.19.
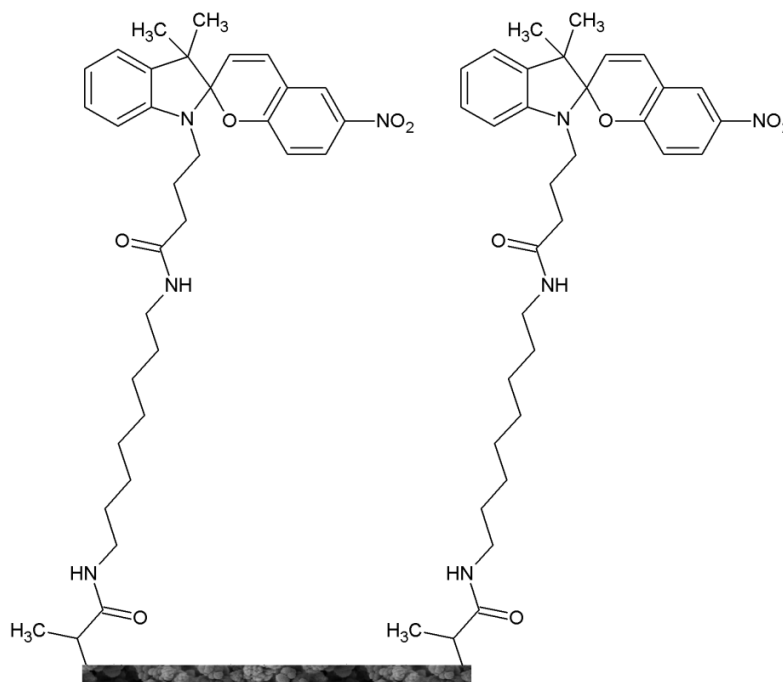
Figure 3.19: *Schematic showing the attachment of the SPCOOH to the monolith pore surface through the immobilised 1,8-diaminooctane linker group [Group I]*

It can be seen that the spiropyran is well spaced from the pore surface and therefore the switching of the molecule should not be hindered as it can be when the molecule is too close to the surface [193]. The immobilisation process is, however, extremely long taking approximately 6 days for completion, additionally there are a large number of

steps involved in the immobilisation process. This is one of the most pressing problems for the utilisation of spiropyran-modified stationary phases, as it can be assumed that with every additional layer there is less coverage than the previous layer, meaning that the more steps involved in getting the spiropyran on the surface the less spiropyran will be on the surface in the end. There is also some potential for this type of stationary phase to be used for the pre-concentration and extraction of heavy metals from samples, but the likelihood of having residual carboxylic acid groups on the surface of the monolith (reactions in Group I) means that parasitic interactions can occur between them and the metals, therefore any retention of metals in the column could be due both the spiropyran and the COOH groups.

Comparing the two methods, there are fewer steps involved when the spiropyran is immobilised through the amine group on the surface of the monolith (reactions in Group II). This indicates that the amount of spiropyran on the surface should be higher. Taking all this into account, it is clear that the immobilisation through the amine group is a more viable approach mostly because of the shorter synthesis. When the immobilisation through the amine group is complete the surface of the pore should resemble the schematic in Fig. 3.20.
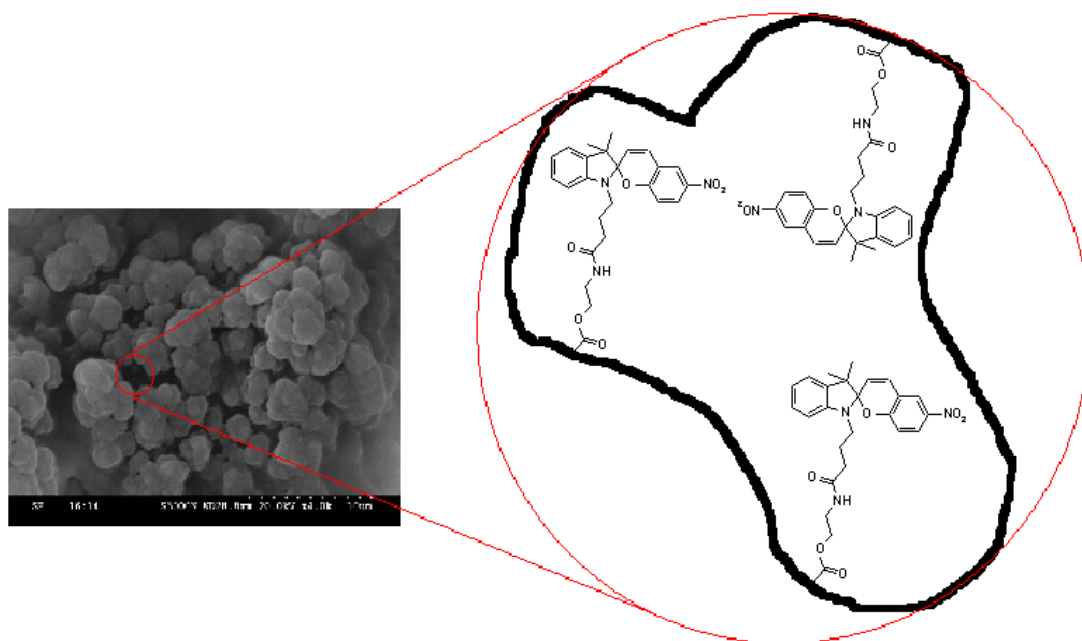
Figure 3.20: *Schematic of the SPCOOH immobilised within the pores of an AEMA-grafted poly(BuMA-co-EDMA) monolith [Group II]*

Even without a spacer molecule the chain length between the spiropyran and the surface is more than nine atoms long and therefore the molecule should not be hindered by the surface during the switching between the two forms. As mentioned previously eight carbons is the optimum linker length to prevent interaction between the dye and the surface [193].

From this point on all discussions relate to the monolith which has SPCOOH immobilised on the surface of the monolith through grafted AEMA. To show visually that there is a colour change when the merocyanine form is produced a photographic image of the capillary, Fig. 3.21, was taken after the capillary had been irradiated for 5 min with a 375 nm LED. The area where the dye was grafted on the surface is dark pink after irradiation showing the presence of the merocyanine. The white edges in the picture are areas which were photo-masked during grafting and so do not have any immobilised AEMA and therefore no SPCOOH will be bound in this area, hence no pink colour. Irradiating with white light will then cause the spiropyran form to be regenerated and the monolith in the capillary appears white again (not shown).
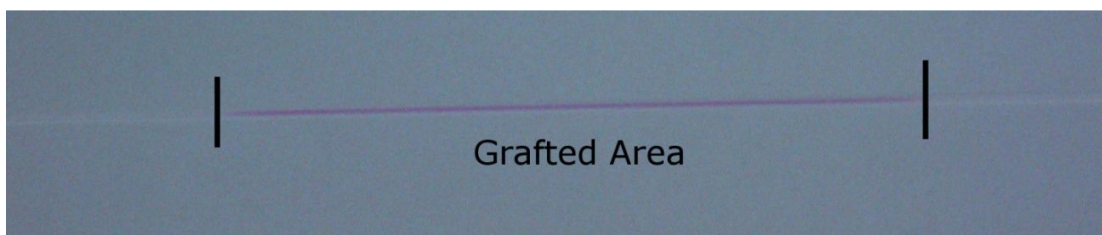
Figure 3.21: *Image of a poly(BuMA-co-EDMA) monolith with SPCOOH covalently immobilised on the pore surface (via amination, Group II) after irradiation at 375 nm to produce the merocyanine form*

After showing the presence of the merocyanine form visually it was also important to show that this change could be detected spectrally. A special reflectance probe was designed as described above (Section 3.2.4.14) and was used to measure the reflective absorbance spectra of the SPCOOH-grafted poly(BuMA-*co*-EDMA) monoliths within PTFE-coated fused silica capillary. The capillaries were irradiated for 5 min with visible light to produce the SP form and then 5 min with UV light to generate the merocyanine. The resulting spectra are shown in Fig. 3.22. As can be seen the spectrum of the SP form is relatively flat as it reflects almost all the light in the visible spectrum equally, in the case of the MC form a band appears in the spectrum at approximately 550 nm, the maximum absorbance of the merocyanine form. Subsequent irradiation of the MC form causes the disappearance of the band as the SP form is regenerated.
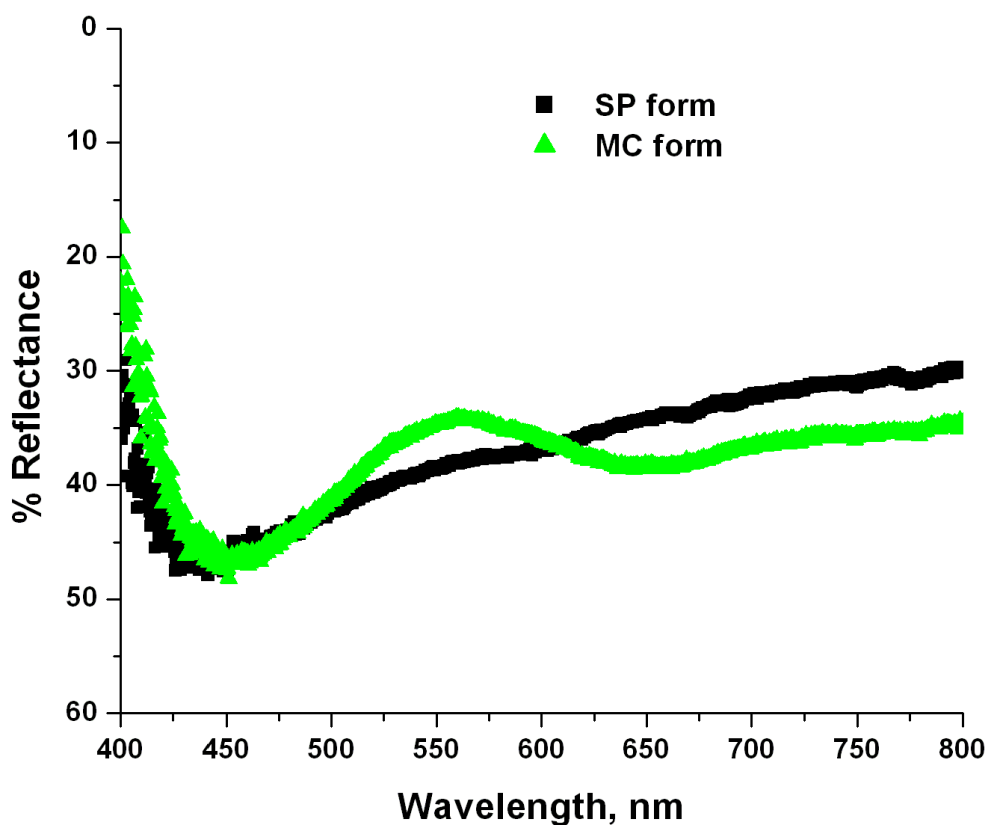
Figure 3.22: *Reflective absorbance spectra of a SPCOOH immobilised AEMA-grafted-poly(BuMA-co-EDMA) monolith in both the SP (black) and the MC (green) forms*

It was necessary also to determine approximately how much time was required to convert the SP to the MC form as this would be important information for future applications of the monolith. The same reflectance probe as before was used to measure the conversion over 5 min with a spectrum of the surface taken every 10 s under constant UV irradiation. The graph in Fig. 3.23 was plotted with the data obtained.
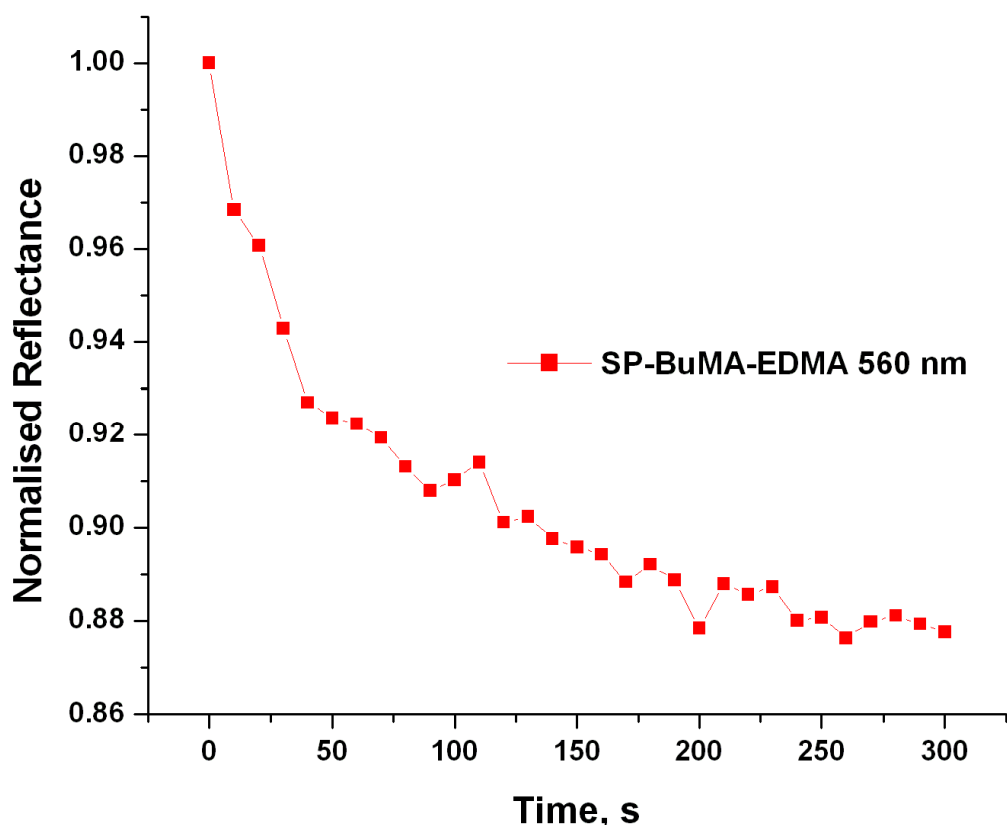
Figure 3.23: *Changes in reflectance at 560 nm of a SPCOOH-AEMA-poly(BuMA-co-EDMA) monolith during conversion of SP to MC form under constant UV irradiation*

It can be seen that in less than 50 s the reflectance changes significantly and then more slowly up to 150 s when it hardly changes at all. This point at 150 s is the plateau point where the maximum conversion of SP to MC has been obtained; however even at 50 s there is already a high amount of conversion. In the context of photo-chemical interconversions this is relatively slow however it has been noted that macrocycles, such as polymers, can retard the conversion between the two forms [207], which is likely what is seen in this case.

From the above characterisation it has been confirmed that the spiropyran immobilised through the amine group is well attached to the surface of the monolith, switches repeatedly while bound to the surface, shows a visual colour change and this colour change can be detected spectrophotometrically and from kinetic data it has been possible to determine the length of time necessary to produce the conversion from the SP to the

MC form. These SPCOOH immobilised-poly(BuMA-*co*-EDMA) monoliths will be incorporated into micro-fluidic devices with an aim to create photo-controllable electroosmotic pumps, as is presented in Section 3.3.5.

3.3.4. Incorporation of spiropyrans in monolithic materials – Copolymerisation with a cross-linking monomer

After much experimentation with the immobilisation of the spiropyran dye on the surface of the monolith, a third approach of copolymerisation was attempted. Previously all the work had been carried out using a carboxylated spiropyran SPCOOH (Fig. 3.2), which is not suited for this approach as it has no double bonds to allow it to copolymerise with a cross-linking monomer. Despite the lack of double bonds it was thought that this SPCOOH could be used as a dopant – added to the pre-polymer solution but not copolymerised - in the polymer solution.

As the spiropyran is hydrophobic, a styrene-divinylbenzene pre-polymer solution was selected and 2% (per weight of monomers) of the SPCOOH was added to the pre-polymer solution along with the initiator and porogen, before placing in a water bath at 60°C for 20 h. The desired end result was that the SPCOOH would become incorporated in the polymer matrix and retains its ability to switch between the SP and MC forms.

After polymerisation the resulting materials were washed thoroughly with methanol to remove all traces of the pre-polymer solution. The polymers were dried overnight at room temperature, the bulk material was then ground into smaller pieces and subjected to alternating periods of irradiation from a 375 nm LED and a 532 nm laser. After each period of irradiation the polymer was photographed to determine whether a colour change could be observed.

The results from this experiment are shown in Fig. 3.24. From bulk experiments, it was seen that when the polymer is doped with the spiropyran dye there is no noticeable colour change of the polymer when irradiated at 375 nm or 532 nm.
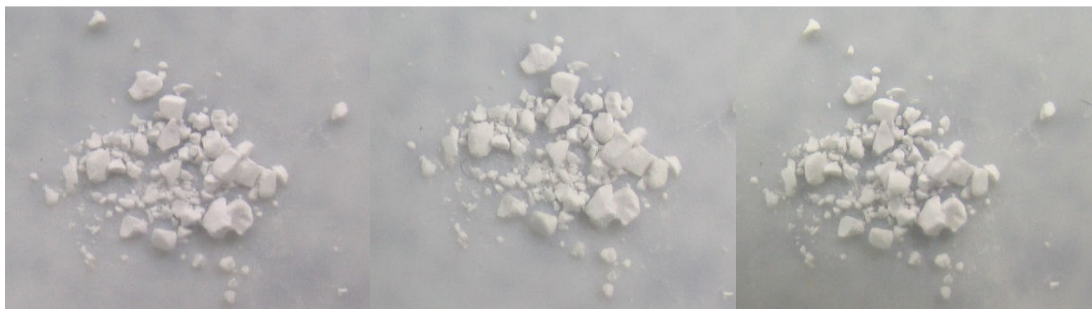
Figure 3.24: *Photographic images showing the spiropyran doped poly(S-co-DVB) after (a) 1 min irradiation with a 375 nm LED, (b) 1 min irradiation with a 532 nm laser and (c) 2 min irradiation with a 375 nm LED*

As the spiropyran is a self-indicating system, changing colours in response to changes in its environment, it is important to be able to see the colour change to ensure the system is functioning correctly. As this method of incorporating the dye within the polymer did not produce a significant colour change it can be assumed that either the dye was not incorporated in the bulk or the switching ability of the dye is hindered when it is trapped within the polymer matrix. In either case this method was deemed unsuitable for the incorporation of the dye within the polymer.

The next stage in this approach was to synthesise a spiropyran derivative with a double bond which would allow it to be copolymerised with a cross-linker to create a monolithic scaffold consisting of the photochromic dye

A reactive monomeric spiropyran (SPM) was synthesised according to the experimental procedure described in Section 3.2.4.9 above. Synthesis of the spiropyran monomer was quite straightforward and was carried out exactly as described in the publication of McCoy *et al.* [201].The SPM was then copolymerised with DVB, according to the procedure outlined in Section 3.2.4.10, resulting in a new photo-switchable monolithic material.

For the synthesis of the spiropyran monolith both ethylene dimethacrylate and divinylbenzene were used as cross-linkers in the preliminary experiments, however only divinylbenzene produced a rigid macroporous copolymer with the spiropyran monomer. Once divinylbenzene was selected three different concentrations of SPM (5%, 10% and

50% w/v) were added to the polymerisation solution but it was found that only the lowest concentration (5% w/v) would dissolve in the mixture, therefore all polymerisations were carried out with the stock solution containing this concentration of spiropyran relative to the divinylbenzene cross-linker.

Scanning electron microscopy was used to examine the morphology of monolith. A SEM image of the poly(spiropyran-*co*-divinylbenzene) [poly(SPM-*co*-DVB)] monolith is shown in Fig. 3.25. As can be seen from the figure, the monolith has the typical globular, porous structure expected from an organic polymeric monolith, with globules approximately 6 µm in diameter. Looking closely the wall attachment can be seen, meaning the column has good mechanical stability.
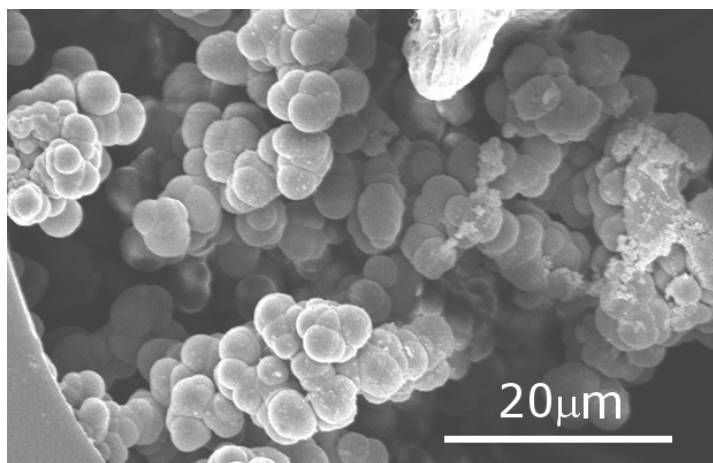
Figure 3.25: *Scanning electron micrograph of a poly(SPM-co-DVB) monolith within 100 µm i.d. PTFE coated fused silica capillary*

After the porous structure was verified the switching ability of the monolithic spiropyran polymer was also characterised. The monolith was irradiated for 2 min with a white (400-750 nm) LED, the monolith was then placed on the observation plate of an optical microscope and optical micrographs of the monolithic material were taken. This was repeated after irradiation with a 375 nm LED for 2 min. The images are shown in Fig. 3.26. The change from the SP to the MC form can clearly be seen in these images. Irradiation with the visible light produces the uncharged SP form which is colourless

(Fig. 3.26A), after irradiation with the UV (375 nm) LED a blue colour appears indicating the transition to the merocyanine (Fig. 3.26B).
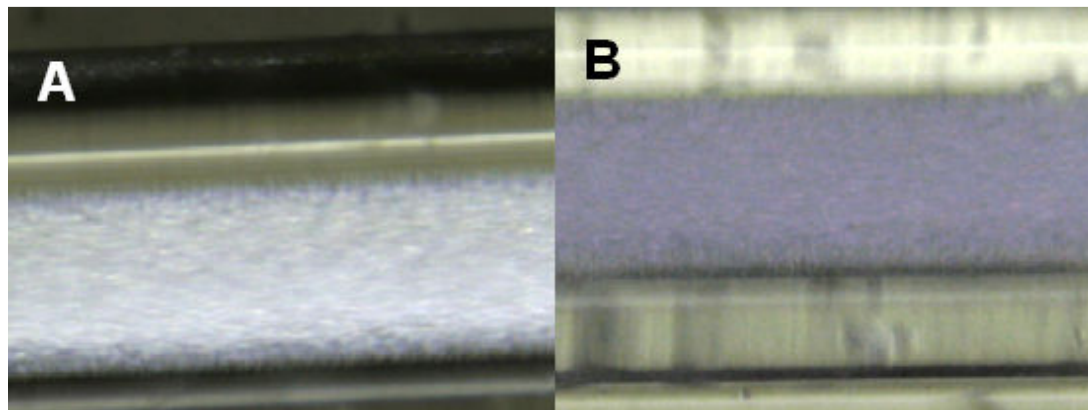
Figure 3.26: *Optical micrographs showing the poly(SPM-co-DVB) monolith in the spiropyran form (A) and the merocyanine form (B)*

The presence of the blue colour of the merocyanine form of the monolith indicates that the copolymerisation was successful; the appearance of blue spiropyrans in non-polar solvents [208] and matrices [209] has been documented previously in the literature. Work carried out previously in this group showed that when spiropyrans are covalently immobilised on poly(styrene) beads they appear pink in the MC form despite the fact that they are in close proximity to a non-polar surface, they are not affected by it. The spiropyran monolith however is blue suggesting that it is affected by the non-polarity of the matrix, and therefore likely to be incorporated in it, this was also noted by Zhu *et al.* after incorporation of a spiropyran derivative in non-polar polymer nano-particles [209]. The spiropyran monolith can be made to appear pink also by flushing with a polar solvent, the surface groups are then in a polar environment and appear pink. This is shown spectrally in Fig. 3.27. The green and blue lines show the open MC and closed SP forms of the spiropyran monolith in the normal state showing the effect of the non-polar matrix by the shift in the wavelength of maximum absorbance 560 nm to 582 nm. The red and black lines show the open MC and closed SP form of the monolith after it has been flushed with ethanol causing a hypsochromic shift in the absorbance maximum to 550 nm, additionally the spiropyran also appears visually pink.
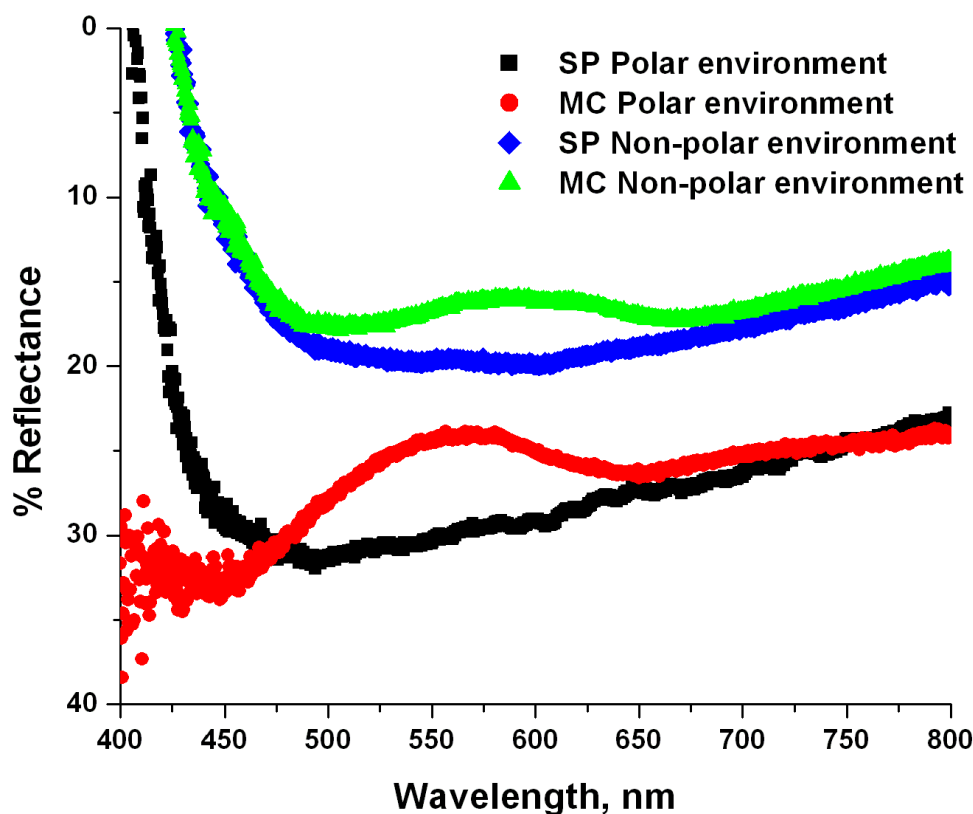
Figure 3.27: *Reflective absorbance spectra of the polar (red, black) and non-polar (green, blue) forms of the poly(SPM-co-DVB) monolith in both the SP (black, blue) and the MC (red, green) forms*

It can be clearly seen from the above spectra that there is a difference between both the SP and MC forms and also between the polar and non-polar environments within the pores of the monolith. Additionally it is necessary to quantify the time necessary to convert the SP to the MC form; this was done in the same way as described in Section 3.3.3 above and the resulting data is presented in Fig. 3.28 below.
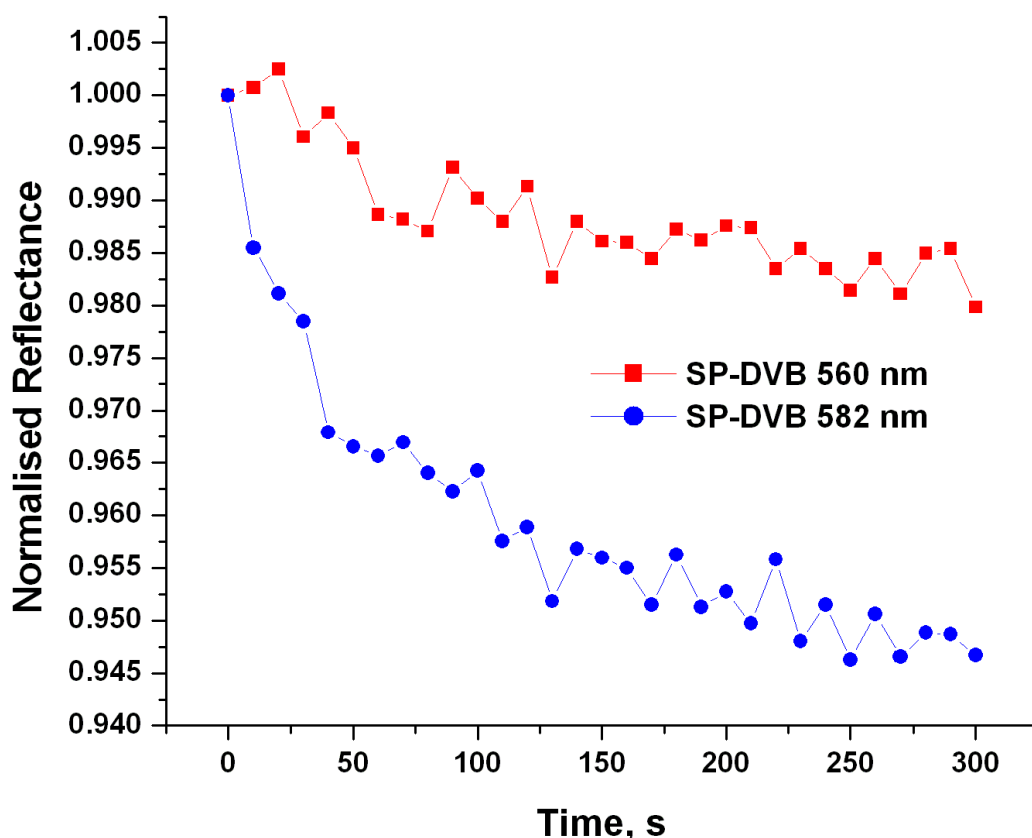
Figure 3.28: *Changes in reflectance at 560 nm and 582 nm of a poly(SPM-co-DVB) monolith during conversion of SP to MC form under constant UV irradiation*

The graph presented here shows the results obtained from the kinetic experiment performed in the natural non-polar state of the monolith. The spectral changes were detected at two wavelengths, 560 nm and 582 nm. The changes at 560 nm correspond to the absorbance maximum of the SPCOOH grafted poly(BuMA-*co*-EDMA) monolith described earlier (Fig. 3.22) and the poly(SPM-*co*-DVB) monolith in the polar form (Fig. 3.28), but 582 nm corresponds to the absorbance maximum of the poly(SPM-*co*-DVB) monolith in the non-polar form. It can clearly be seen that the conversion to the merocyanine form is more dramatic at 582 nm indicating that this really is the wavelength of maximum absorbance of the monolith. The trend of the conversion is comparable to that observed for the grafted monolith SPCOOH-poly(BuMA-*co*-EDMA) (Section 3.3.3) in that the change is very sharp in the first 50 s slowing down to 150 s and then changing only very slightly for the remaining time of the experiment. This

relatively slow switch, compared to the solution kinetics again serves to underline the retardation of the switching caused by the interaction with the polymer structure.

3.3.5. Application of spiropyran modified monoliths as photo-dynamically controllable electroosmotic pumps

At this stage significant progress had been made in another area of this collaborative project using silica beads with SPCOOH covalently bound to the surface [190] as a light modulated stationary phase. This, coupled with the fact that without specific modifications, such as described by Trojer *et al.* [12] or Connolly *et al.* [13], monoliths are not well suited to the separation of small molecules, and the uninspiring preliminary results showing low retention of metal ions on spiropyran coated polymeric stationary phases, it was decided to examine other potential applications of these novel photochromic monoliths.

Due to the ability of the monoliths to retain their photo-switching properties after the grafting and copolymerisation processes, it was decided to exploit this and attempt the development of photo-switchable electroosmotic pumps for micro-fluidics.

This was deemed a more suitable application for the spiropyran monoliths are they can be more easily placed in the channels of micro-fluidic chips than packing beads.

This novel pumping system described provides the ability to modify the flow rate not only by changing the electric field, as is commonly done [210], but also by irradiation with light. To the author's best knowledge, this is the first example of a photo-controllable electroosmotic pumping system.

In the first set of experiments MES-histidine buffer at approximately pH 6 was used as the buffer to try to generate electroosmotic flow (EOF) which could then be modulated by irradiating the spiropyran modified monolith within the micro-fluidic device. The first monolith which was examined was the poly(BuMA-*co*-EDMA) monolith with the SPCOOH immobilised on the surface of the monolith. As the SP form of the monolith should have no surface charge there would, theoretically, be no EOF expected from this form of the monolith and EOF would only be expected from the MC form. It has been

previously reported, however, that organic polymer monoliths produce a weak EOF without further modification [211, 212].

Applying a field ramp of 0-250 kV/m over 15 min produced the plot shown in Fig. 3.29. As can be seen from the plot the flow rate generated by the pump is extremely low even at such high applied fields and the difference between the spiropyran and merocyanine form is insignificant.
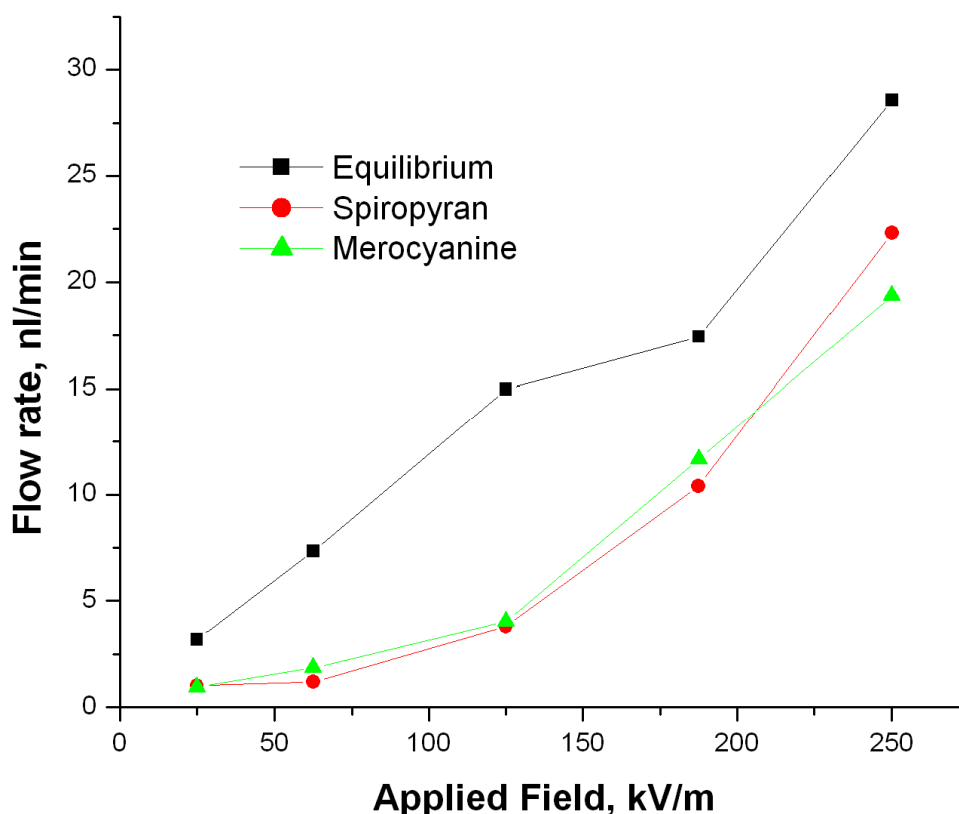
Figure 3.29: *Plot of flow rate vs. applied field for a SPCOOH-poly(BuMA-co-EDMA) monolith, using 2 mM MES-histidine buffer as the background electrolyte.*

It should be noted that during the experiment the electrodes were in the normal position with the current travelling from anode to cathode. This means that, as the flow is towards the negative electrode, the surface of the monolith is negatively charged. The generation of negative charge, and not the lack of charge due to the presence of the zwitterionic stationary phase, is likely caused by the adsorption of charges on the

surface of the stationary phase and also it is possible that there is some complexation between the merocyanine form and the histidine in the buffer.

The difference between the two lines, however, is little more than error and several repetitions of the experiment could not improve the electroosmotic flow generation despite the fact that the monolith had been irradiated for longer than was necessary to affect the conversion between the SP and MC form as shown by the kinetics experiment (Fig. 3.23).

Due to the poor results obtained from the SPCOOH-poly(BuMA-*co*-EDMA) monolith where SPCOOH was grafted on the surface it was decided to repeat the same experiments with the poly(SPM-*co*-DVB) monolith where the monomeric spiropyran, SPM, is copolymerised with divinylbenzene. Here the same buffer and applied field were used but the overall result was different.

In the case of the poly(SPM-*co*-DVB) monolith the EOF is much higher showing a maximum flow rate of approximately 445 nl/min for the spiropyran form of the monolith and just 357 nl/min for the merocyanine form. While the speed of the EOF is significantly higher for the poly(SPM-*co*-DVB) monolith than for the monolith with SPCOOH covalently immobilised on the surface, there is still a relatively small difference between the EOF generated by the SP and MC forms as seen in Fig. 3.30, with a reduction in flow rate of just 20% at the maximum applied field.
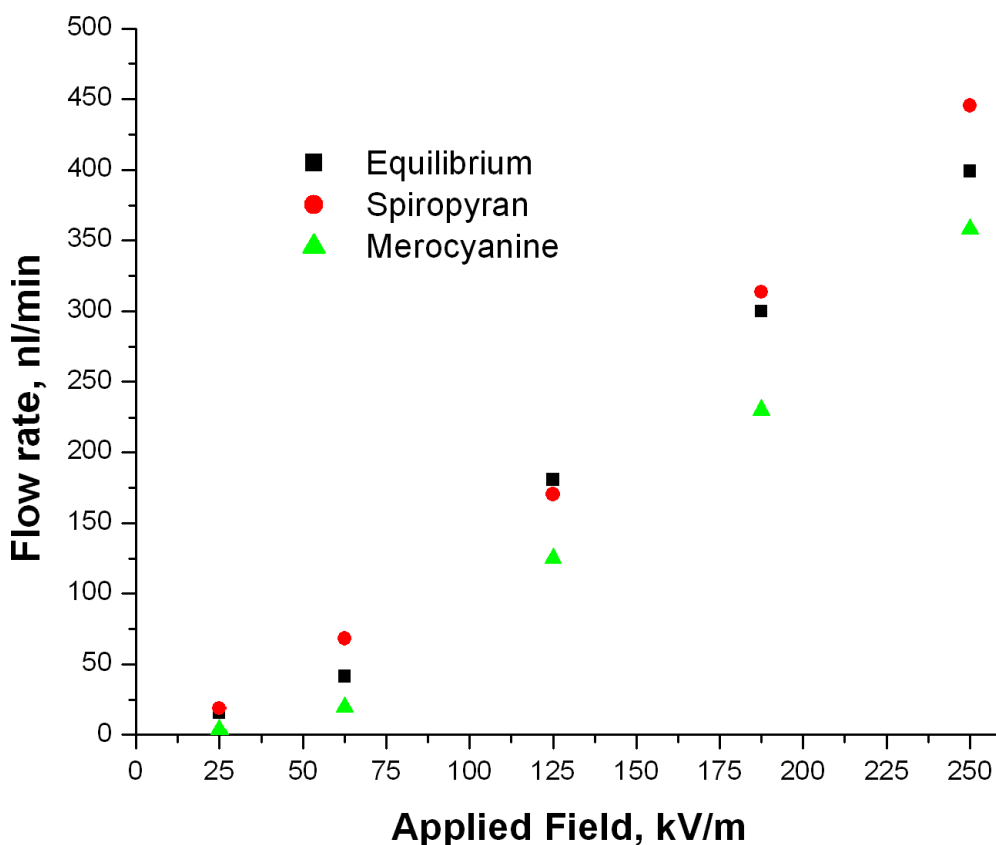
Figure 3.30: *Plot of flow rate vs. applied field for a poly(SPM-co-DVB) monolith, using 2 mM MES-histidine buffer as the background electrolyte*

From measurements the equilibrium pH of the SPM is approximately pH5.68, therefore around this value the SP form is uncharged and the MC form is zwitterionic, outside of this range there can be changes to the electronic configuration, which can then result in the generation of a single charge on one or both forms of the spiropyran [213]. As the MES-histidine buffer is at pH 6, the environment in which the spiropyran monoliths exist is only mildly acidic and close to the equilibrium pH. With a mildly acidic electrolyte some protonation of the stationary phase will occur, however there does not seem to be a large enough difference in the charge density between the two forms to produce a significantly different EOF between the two states. It is therefore difficult to see a significant effect of the light irradiation on the electroosmotic flow.

There is however a large difference between the EOF generated by the SPCOOH-poly(BuMA-*co*-EDMA) monolith and the poly(SPM-*co*-DVB) monolith. Although the

same buffer was used and the same field applied to both monoliths the difference in the maximum flow rates generated by the monoliths under the electric field differ wildly. The grafted monolith produces a very low EOF (max. 30 nl/min) while the poly(SPM-*co*-DVB) monolith produces an EOF which is quite a good deal higher (up to 445 nl/min). It has been questioned whether the incorporation of a charged substance in the bulk of the poly(SPM-*co*-DVB) monolith can generate better electrochromatographic properties than what is observed when the charged substance is immobilised on the surface. What has been seen in this experimental work would suggest that this is the case, as there is more charge in the bulk contributing to the EOF whereas in the grafted monolith the charged layer is relatively small, as it is localised on the surface, compared to the uncharged bulk, which is not contributing to the EOF. While this looks plausible, further experimentation with a range of different electrolytes and stationary phases would be necessary to determine whether this is an actual fact of copolymerisation *vs.* grafting or simply an interesting anomaly.

As was mentioned earlier the SPCOOH grafted poly(BuMA-*co*-EDMA) monolith did not perform very well in the first set of experiments with MES-histidine buffer, either due to low SPCOOH content in the monolith or not enough charge contribution from the bulk of the monolith. For this reason further experiments were carried out only with the poly(SPM-*co*-DVB) monoliths.

Staying within the stable pH range of the spiropyran and using standard electrophoretic buffers does not seem to be enough to generate the effect of the light switchable EOP which is sought after. Looking at the work of Drummond *et al.*, it is possible to generate a stable positive charge on the surface of the MC form using acidic media [213], it seems likely that if the acidic medium is still present when closing the ring to reform the SP that the positive charge would also be present on the SP form. Admittedly the presence of the acid will make the reconversion more difficult due to the possibility of acid mediated reconversion to the MC form [166].

A more substantial difference between the EOF of both forms is required to use these monoliths as photo-controllable electroosmotic pumps. To achieve this, protonation of

the spiropyran monolith was found to be necessary by the means of flushing with 1 mM HCl.

Switching the buffer from 2 mM MES-histidine to 1 mM hydrochloric acid produced a significant change in the results obtained. After irradiating with UV light the electric field was applied to the capillaries in the channels and electroosmotic flow was observed. When this experiment was repeated several times the channel was irradiated again with visible light to produce the SP form and again EOF was observed only this time it was significantly higher than EOF for the MC form. Repetition of these experiments show the same trend that the EOF of the MC form is always approximately 40% lower than that of the SP form (averaged with the exclusion of the first two points obtained at low field). The results can be seen in Fig. 3.31.
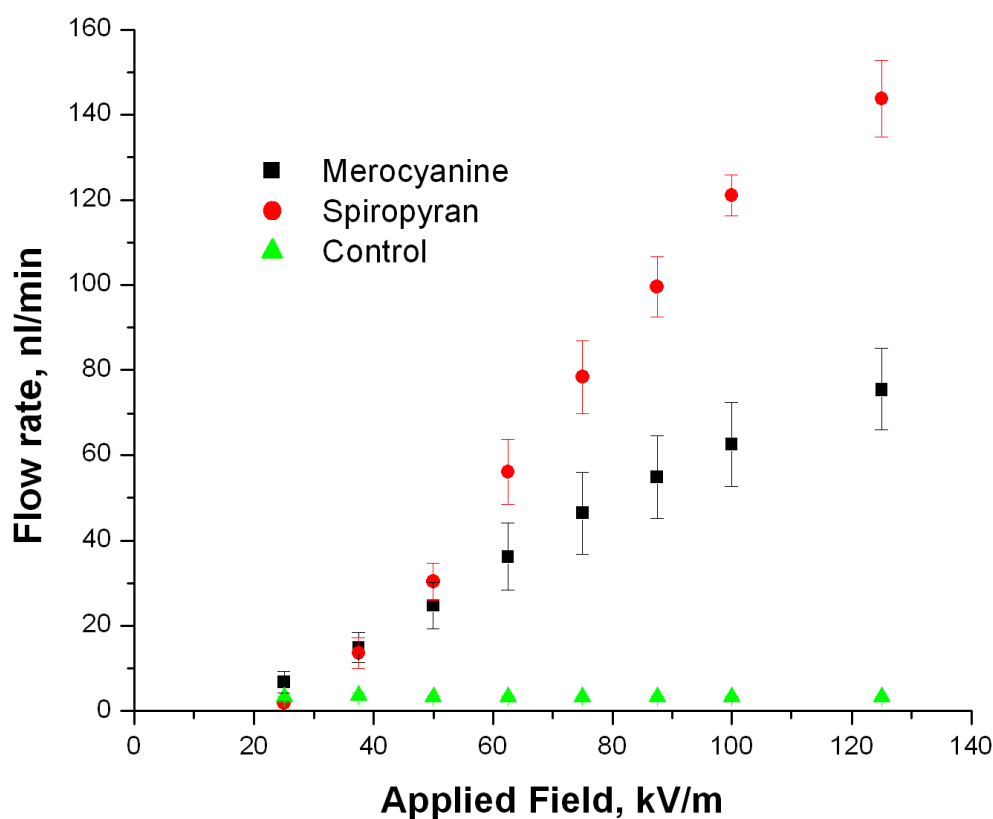
Figure 3.31: *Plot of flow rate vs. applied field for a poly(SPM-co-DVB) monolith, using 1 mM HCl as the background electrolyte*

As can clearly be seen by comparing Fig. 3.31 and Fig. 3.30, the EOF generated using the MES-histidine buffer is greater overall compared to the HCl buffer, which is likely due to the fact that MES-histidine is a better conducting electrolyte than dilute HCl. Despite this the switch from the SP to the MC state is far more significant using the HCl as the electrolyte with a drop in flow rate of approximately 40% at each applied field compared to approximately 25% at each point for the grafted monolith.

What is interesting about both Fig. 3.31 and Fig. 3.30, is that in both cases the SP form shows a greater EOF than the MC form, which is contrary to what may be predicted knowing that the SP is uncharged and the MC is zwitterionic, and therefore electrically neutral. We have proposed an explanation for this phenomenon which is outlined as follows; in the protonated SP-form there is a localised positive charge centred on the N of the indoline ring. In contrast, in the protonated MC form, the phenylate oxygen is protonated, cancelling its negative charge, and the positive charge on the indoline ring is delocalised into the extended π-system (Fig. 3.32). Additionally, the quininoid form of the MC is believed to be present in equilibrium with the protonated form. The presence of the quininoid form, which has no effective charge, in parallel to the protonated MC form reduces the number of charged sites available for generation of the EOF. Hence, under strongly acidic conditions, the SP-form produces a greater number of charged sites than the MC form, and therefore a higher EOF. The suggested mechanism for the switching of the spiropyran between the SP and MC form causing the EOF to increase and decrease accordingly is shown in Fig. 3.32, this is similar to that proposed by Drummond and Furlong for the switching of the molecule in the presence of water/1,4-dioxane mixtures [213].
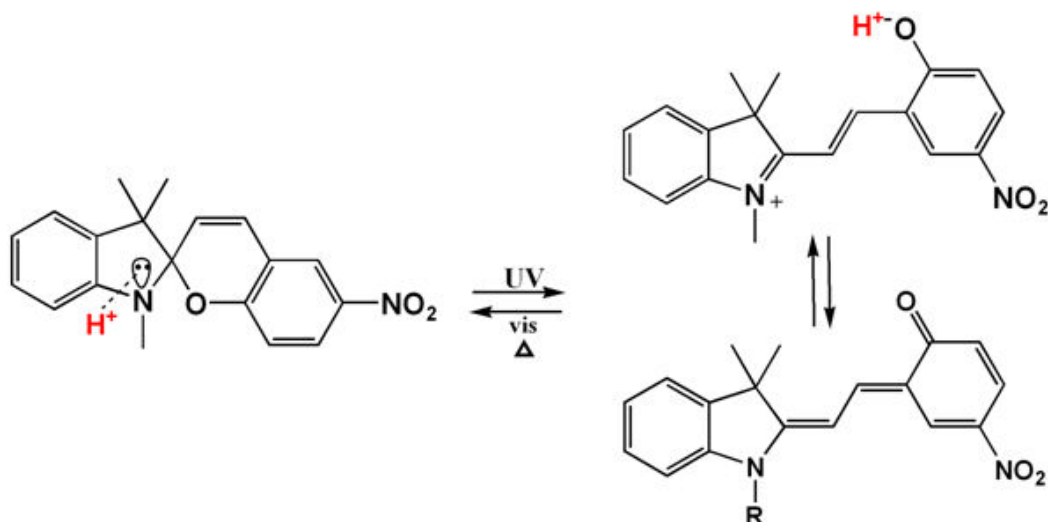
Figure 3.32: *Schematic of the proposed mechanism of switching between the SP and MC form in acidic media, showing the merocyanine equilibrium between the protonated form (above) and the quininoid form (below)*

Experiments have been carried out attempting to pass current in both directions, towards the anode and towards the cathode, however EOF is only observed towards the anode indicating that the surface is always cationic. When the SP is protonated the surface of the monolith is positively charged and so the electrical double layer is made up of negative charges which migrate towards the positive electrode. As the charge migration begins to occur electrolyte flow in the channel, or EOF, begins to occur, which is then measured at the anode. Irradiating the monolith at 375 nm to form the protonated MC form actually results in the formation of a two forms of the MC, a cationic and uncharged form. This reduces the effective surface charge and the electroosmotic flow slows down.

To summarise, irradiating the poly(SPM-*co*-DVB) monolith with a white LED shifts the equilibrium state, in which the spiropyran usually resides, towards the SP form and an increase in the EOF is observed while irradiation with UV light pushes the equilibrium towards the MC form and the EOF is decreased by an average of 40% at all applied fields. The maximum difference in flow rate is observed at the maximum applied field,

in Fig. 3.31, where the measured EOF decreases from around 143 nl/min (SP) to ca. 75 nl/min (MC) at an applied field of 125 kV/m.

It can be noticed in Fig. 3.31 that there is a non-linear character to the EOF which may be caused by inhomogeneous distribution of charges along the length of the column causing the EOF to non-linear fashion. This inhomogeneous charge distribution can be explained by the random nature of the copolymerisation between the spiropyran monomer and the divinylbenzene meaning that the spiropyran monomer molecules and the divinylbenzene are not distributed evenly along the length of the column and therefore, neither is the EOF. It may also be due to the population effect of changing between the two states – eventually as the % in a particular form begins to dominate, the effect will diminish as there is less of the other form around to switch. Both of these possible causes remain to be investigated. With this graph (Fig. 3.31), which is an average of four experiments, it is shown that the flow rate from the spiropyran based electroosmotic pump can be easily modified by irradiation with different wavelengths of light. Under acidic conditions the SP form produces an increase in EOF while the MC form produces a decrease. Switching the wavelength of irradiation means that the flow rate can be increased or decreased without having to change the applied field. The maximum field that could be applied on the poly(SPM-*co*-DVB) in the micro-fluidic chip was 125 kV/m due to the instability of the current and the generation of bubbles in the channels. Despite being lower than the fields previously used, it is still extremely high and so the desired effect could still be observed.

3.4. Conclusions

In this section a number of different methods of immobilising a photochromic spiropyran derivative on or within a monolithic material have been described and the product of each method has been characterised to determine its viability for use in a flow through system such as liquid chromatography and electrophoresis. Immobilisation of the spiropyran by hydrophobic interaction was shown with little success as only 2 % of the dye was immobilised and it can be removed from the surface of the polymer with constant washing with alcoholic solvents. Retention of metal ions on the SPCOOH-coated poly(S-*co*-DVB) monolith was estimated and appeared to be very low (<5%). It

was decided that monoliths with SP adsorbed on the surface are not optimal for separation of small molecules.

Immobilisation of the spiropyran on the monolithic polymer through a layer of methacrylic acid or 2-aminoethyl methacrylate photo-grafted onto the surface provided a photochromic monolith which retained its photochromic properties indefinitely. Covalent linkage of the dye to the surface provides a permanent spiropyran coating. Of the two different methods for the immobilisation of the spiropyran on the surface of the monolithic material, the method involving covalent linkage through a grafted amine group (reactions in Group II) was deemed the most useful for further use. The experimental time is reduced in comparison to the Group I route of immobilisation through surface grafted –COOH groups due to the lower number of stages required to immobilise the dye, this also results in a higher % of dye on the surface. Additionally, choosing the amine groups instead of carboxylate groups, reduces the potential of parasitic interactions from the carboxylate groups with a number of potential analytes including metals and amino acids.

Copolymerisation of a monomeric spiropyran derivative provided another method of obtaining a photochromic monolithic stationary phase permanently modified with the photochromic dye. It was found that the copolymerisation of the spiropyran monomer SPM with DVB does not hinder the ability of the monolith to switch. Irradiation of the monolith with UV light produces a dark blue colour on the monolith indicating the presence of the merocyanine which disappears under irradiation from a white light source.

In general, monoliths are not ideally suited to the separation of small molecules, especially monoliths with high permeability such as those presented in this chapter. For this reason the decision was made to try a different application of the spiropyran monoliths and to use them for electroosmotic pumping due to the charge on the surface which can be changed by irradiation with different wavelengths of light. This gives the potential for photo-controllable EOF.

Encasement of the grafted and copolymerised monoliths into PMMA chips, with reservoirs attached allowed their potential as electroosmotic pumps to be determined. It is clear from the results that the copolymerised monoliths function more effectively as electroosmotic pumps than the spiropyran grafted monoliths. This is likely due to the location of the graft; the copolymerised monolith has the dye molecules dispersed throughout the bulk, while the grafted monolith has only a layer of charge over an uncharged bulk. It seems due to this that copolymerised dye monoliths are more suited to electrophoretic applications. In the case of both monoliths irradiation with visible light, which produces the spiropyran, causes an increase in the EOF while UV light produces the merocyanine form and a decrease in the EOF. This is likely due to the presence of an uncharged merocyanine form in equilibrium with the charged form causing a reduction in the number of surface charges and therefore a reduction in the EOF. A more significant difference between the two states (high and low EOF) can be achieved by protonating the stationary phase.

To conclude, the concept of a photo-switchable electroosmotic pump based on a novel poly(SPM-*co*-DVB) monolithic stationary phase encased in a micro-fluidic chip has been presented. The monolith has been examined in both the stable form and the protonated form and it has been found that while the EOF can be generated in the stable form the conversion between the two forms does not play a role in modulating the EOF. Using the protonated form of the monolith the EOF generated from the monolith can be easily modulated by irradiation with visible or UV light to produce and increase or a decrease in EOF, respectively. The results of spiropyran monolith synthesis and EOF results are submitted for publication.

Using the information obtained from the copolymerisation of spiropyran with divinylbenzene other dyes, with biological importance, are currently being investigated for the synthesis of other dye based monoliths for applications in electrochromatography. Preliminary results garnered from the use of poly(neutral red-*co*-EDMA) monoliths in electrochromatography for the separation of dopamine and ascorbic acid are positive and clearly show interaction of the analytes with the dye even after copolymerisation.

The potential for dye based monolithic stationary phases in capillary electrochromatography is very interesting and it is hoped that more biologically important dyes can be investigated in the future.

4. Red Light Initiated Polymerisation in Polyimide and Polyimide Coated Capillaries

4.1. Introduction

Chapter 2 of this thesis illustrated the benefits of photo-initiated polymerisation over thermally initiated polymerisation methods. Photo-initiated methods allow controlled formation of monolithic materials in a short time in a specific location within the channel. This is very important for applications in industry and micro-fluidics needing speed and spatial control, respectively.

While ultraviolet (UV) light initiated polymerisation has numerous advantages, which have been detailed in Chapter 2, there are two main disadvantages to the procedure. First, it is essential to the success of the polymerisation reaction that the mould is UV transparent. While UV transparent poly(tetrafluoroethylene) (PTFE) coated fused silica capillary is commercially available it does not possess the durability and ease of handling of the polyimide coated fused silica capillaries commonly used in capillary electrophoresis and chromatography. UV-transparent micro-fluidic chips are also available which are more durable that the UV-transparent capillaries, however it is still extremely useful to develop a method whereby organic polymer monoliths can be synthesised within the cavity of polyimide coated capillaries.

The second disadvantage of UV-light initiated polymerisation is that it is also necessary to use UV-transparent monomers and porogens which excludes the styrenes and the majority of chromophoric monomers. The solution to this problem developed during the course of this thesis, which is the synthesis of styrenic monoliths with blue light initiated polymerisation, is detailed in Chapter 5.

In this chapter red light initiated polymerisation is developed and suggested as an alternative method of photo-initiated polymerisation which will allow the user to overcome some of the drawbacks of UV-initiated polymerisation.

Dulay *et al.* [59] have carried out some preliminary work in this field with the synthesis of silica sol-gel monolithic stationary phases in polyimide coated capillary using blue light at 470 nm to initiate the polymerisation. As described in Section 1.4.2.1, the polymerisation was an example of a cationic polymerisation using the commercially available photo-initiator Irgacure 784 as the photo-sensitiser and diphenyliodonium chloride as the initiator with a cool fluorescent lamp filtered to emit light at 470 nm as the initiating light source.

While light at 470 nm may pass through the polyimide coating without it having to be removed, as suggested by Dulay *et al.* [59], it should be easier to pass red light through the polyimide coated capillary, as wavelengths in the red region of the electromagnetic spectrum are less likely to be absorbed by a brown coloured material than blue light. This is due to its colour, brown will absorb complementary colours more than similar ones, therefore light in the blue/green region of the spectrum will be more strongly absorbed than red light. During the course of this investigation the spectra of a number of polyimide sheets were taken and it was confirmed that red light passes easily through the polyimide. These results are presented in Section 4.3.

For polymerisation in the visible region a common approach is to use a combination of dye sensitiser and radical initiator [59]. The initiation then works by a process called photo-induced electron transfer from the sensitiser to the radical generator as was described previously in Section 1.4.2.1. As the dyes are coloured they will absorb at various wavelengths in the visible region, the radical generators on the other hand usually form colourless solutions and therefore will absorb more strongly in the UV region of the spectrum. The dye absorbs a photon from the light source and transfers an electron to the radical initiator which causes a radical-ion pair to be formed. The radical can then initiate the polymerisation by attacking the double bond of the monomers in solution and the polymerisation reaction can propagate [70, 78].

Throughout the course of this research the work of the group of Kabatc and Paczkowski was important as they have studied in detail the synthesis of visible light photo-initiators which absorb light in the red region of the spectrum. They have done much work on visible light initiated synthesis of polymers in bulk using cyanine dyes as sensitisers

with a range of radical co-initiators, in particular borate anions [214]. These dyes generally absorb in the region of 500-700 nm although the exact absorbance can be tailored by increasing and decreasing the number of methylene spacers between the aromatic ring systems and by varying the substituents on the aromatic rings themselves. Noting the usefulness of cyanine dye/borate initiator complexes from the work of Kabatc and Paczkowski, a commercially available cyanine dye, 3-butyl-2-[5-(1,3-dihydro-3,3-dimethyl-1-propyl-2H-indol-2-ylidene)-penta-1,3-dienyl]-1,1-dimethyl-1H-benzo[e]-indolium (CyB), which absorbs at 660 nm, complexed together with a borate radical generator, triphenyl butyl borate was selected. This system was used as the starting point for the development of an initiating system for the photo-initiated polymerisation reaction investigated in this thesis. Fig. 4.1 shows the structure of the cyanine dye/borate radical generator used for these experiments.
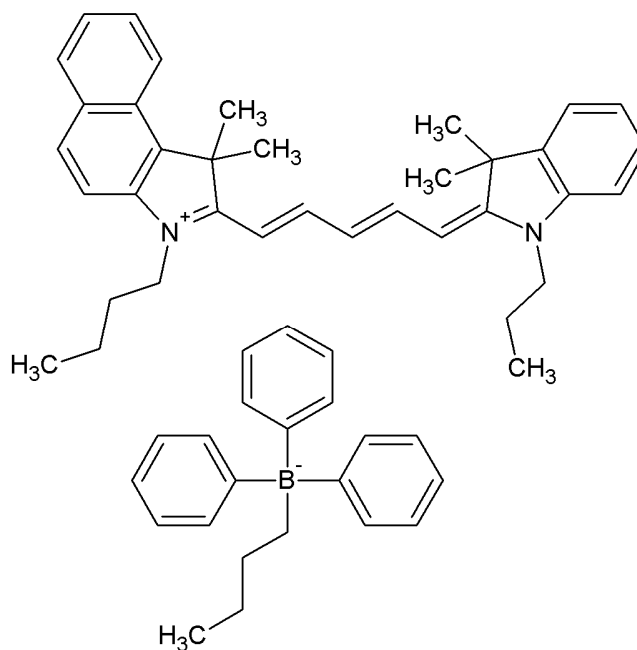
Figure 4.1: *Structure of 3-butyl-2-[5-(1,3-dihydro-3,3-dimethyl-1-propyl-2H-indol-2-ylidene)-penta-1,3-dienyl]-1,1-dimethyl-1H-benzo[e]-indolium triphenyl butyl borate (CyB)*

Throughout this work two different types of mould were used to house the monolithic polymers, these were standard polyimide coated fused silica capillaries purchased from

Polymicro Technologies (AZ, U.S.A.) and specially designed polyimide micro-fluidic chips from Agilent Technologies (Santa Clara, U.S.A.). In the case of the capillaries it is known from the product data sheet that the thickness of the polyimide coating is 20 µm while the micro-fluidic chips have a layer of polyimide 150 µm thick on both sides of the channel [215].

All the work on visible light initiated polymerisation of methacrylate monomers within polyimide coated moulds was done using this dye/salt complex as the base initiating system, modifications were made to the initiating system to increase the efficiency of the polymerisation reaction and these will be discussed in more detail in the experimental section of this chapter.

The main focus of this Chapter is the photo-initiated polymerisation of methacrylate monomers within polyimide coated fused silica capillary and polyimide micro-fluidic chips, within this the optimisation of the pre-polymer solution and the polymerisation reaction conditions are also described. Finally, an additional application of this method, which allows the photo-initiated grafting of chromophoric monomers onto pre-existing polymer monoliths, is also presented.

4.1.1. Aims

The main aims for the work carried out in this chapter were;

1. To investigate a method by which monolithic stationary phases could by synthesised by photo-initiated mechanisms within polyimide coated fused silica capillary without the need to remove the polyimide coating to allow light to pass into the capillary,

2. To determine if this method can also be used to synthesise monoliths in polyimide moulds of any shape and diameter, for example, polyimide micro-fluidic chips,

3. To examine if this photo-initiation method can also be used for photo-initiated grafting of monomers onto pre-existing monolithic scaffolds.

4.2. Experimental

4.2.1. Reagents

1-Decanol (Reagent grade, 99%), 1-propanol (HPLC grade), 3-(trimethoxysilyl)propyl methacrylate (>98%, TMSPM), acetic acid (ACS Reagent 99.7%), acetone (HPLC grade), acetonitrile (HPLC grade), basic alumina (~150 mesh), butyl methacrylate (99%, BuMA), cytochrome C from bovine heart, ethanol (HPLC grade), ethylene dimethacrylate (98%, EDMA), formic acid (ACS Reagent 88%), glycidyl methacrylate (97%, GMA), methanol (HPLC grade), methyl methacrylate (99%, MMA), myoglobin from equine skeletal muscle, *N*-methoxy-4-phenylpyridinium tetrafluoroborate (MPPB), ovalbumin from chicken egg white, potassium phosphate dibasic (98%), potassium phosphate monobasic (99%) and ribonuclease A from bovine pancreas were all purchased from Sigma-Aldrich Chemical Co. (Wicklow, Ireland and St.Louis, MO, U.S.A.). All chemicals were used as received with the exception of monomers which were purified before use by passing over a bed of basic alumina.

3-Butyl-2-[5-(1,3-dihydro-3,3-dimethyl-1-propyl-2H-indolylidene)-penta-1,3-dienyl]-1,1-dimethyl-1H-benzo[e]-indolium triphenyl butyl borate (CyB) was purchased from Spectra Group Limited, Inc. (Millbury, OH, U.S.A.).

Monomeric spiropyran, 1',(9-decenyl)-3',3'-dimethyl-6-nitrospiro[2H-1]-benzopyran-2,2'-indoline, was synthesised from a procedure described by McCoy *et al.* [201] (Section 3.2.4.9). Water used in these experiments was obtained from a Milli-Q Ultrapure water filtration system from Millipore (Billarica, MA, U.S.A.).

4.2.2. Materials

660 nm Light emitting diodes (LEDs) were purchased from Roithner LASER Technik (Vienna, Austria). 660 nm LEDs were also obtained from MCD Electronics Ltd. (Albuquerque, NM, U.S.A.) and Soanar Electronics (New Zealand).

Stripboard, for constructing LED arrays, was purchased from Maplin Electronics (Dublin, Ireland). A motor with variable speed of rotation was used at low speeds (approximately 34 rpm) for the polymerisation of full monoliths in capillary and for

photo-initiated grafting. This motor was purchased from Peats Electronics (Dublin, Ireland). A second motor was used for the polymerisation of the poly(methyl methacrylate-*co*-ethylene dimethacrylate) monoliths with a higher rotation speed, this was fabricated in-house by a post-doctoral researcher in our group (A. Yavorski)

Sheets of Kapton ®, a variety of polyimide, of four different thicknesses - 25 μm, 50 μm, 75 μm and 125 μm - were purchased from DuPont (Circleville, OH, USA).

Polyimide coated fused silica capillaries, with internal diameter in the range of 10-100 μm, were obtained from Polymicro Technologies (Phoenix, AZ, USA) and their internal walls were silanised prior to use with 3-(trimethoxysilyl)propyl methacrylate using the same procedure as described in Section 2.2.4.1. Polyimide micro-fluidic chips, with an internal channel 0.2 mm x 0.2 mm x 68 mm, were provided by Agilent Technologies (Santa Clara, CA, USA) and fabricated by the procedure described by Yin *et al.* [215]. Poly(methyl methacrylate) (PMMA) micro-fluidic chips with three internal channels each 0.4 mm x 0.4 mm x 8 mm were prepared in-house by F-Q. Nie according to procedures described in his own work [27, 28].

4.2.3. Instrumentation

Flow resistance measurements and the separation of proteins in monolithic capillary moulds were carried out on an Ultimate 3000 nano-HPLC (Dionex Corporation, Sunnyvale, CA, USA) or using a S-120 HPLC pump (Knauer, Berlin, Germany) at flow rate range 1-10 μl/min.

Separations on monoliths in polyimide micro-fluidic chips were carried out on a modified 1100 Series LC from Agilent Technologies (Santa Clara, CA, USA). The modified set-up included an on-chip diode array detector customised for the micro-fluidic chips which had been provided for this work.

Electroosmotic flow measurements on the poly(glycidyl methacrylate-*co*-ethylene dimethacrylate) [poly(GMA-*co*-EDMA)] monoliths were carried out using an in-house built CE system consisting of a 0-30 kV power supply with platinum electrodes from Unimicro Technologies (Pleasanton, CA, USA) and a nano-flow sensor from Upchurch Scientific (Oak Harbor, WA, USA).

The decomposition of the dye sensitiser in the presence of different co-initiators was monitored using a Shimadzu 1600 UV-Vis spectrometer (Kyoto, Japan), while simple UV-Vis absorbance spectra were taken on either a Cary 50 UV-Vis spectrometer (Varian Inc., Palo Alto, CA, USA) or a Lambda 900 UV/Vis/NIR spectrometer (Perkin-Elmer Corp. Waltham, MA, USA).

Optical micrographs of capillaries were taken with a TE200 optical microscope from Nikon (Tokyo, Japan), a LabView Synchronized Video Microscope SVM-340 from National Instruments (Austin, TX, USA) or an EMZ-8TR video microscope (Meiji Techno, Saitama, Japan), while scanning electron micrographs were taken with an S-3000N or S-3400N Variable Pressure Scanning Electron Microscope from Hitachi (Tokyo, Japan) or an Ultra-55 analytical scanning electron microscope from Carl Zeiss (Jena, Germany).

A Tracedec$^{®}$ capacitively coupled contactless conductivity detector (C^4D) with a 375 µm sensor head from Istech (Vienna, Austria) was used for lateral conductivity profiling. A low pressure infusion pump (KDScientific, Holliston, MA, USA) with a 250 µl syringe (Hamilton, Bonaduz, Switzerland) was used to provide a constant flow of water through the capillary during conductivity profiling.

4.2.4. Procedures

4.2.4.1. Preparation of the polyimide moulds.

Polyimide coated fused silica capillaries were pre-treated (silanised) using the procedure described in Section 2.2.4.1.

The preparation of the micro-fluidic chips was much simpler than that used to prepare the capillaries. Firstly, the channels were flushed with acetone and dried under nitrogen, then flushed with water and dried under air and, finally, flushed with methanol and dried under nitrogen before filling the channels with the pre-polymer solution.

4.2.4.2 Initiator spectra and decomposition

The initiator decomposition experiment was carried out on a photochemical optical bench which was designed and built in the lab of Prof. Petr Klán in Masaryk University,

Czech Republic. The set-up consisted of a xenon lamp with a built in multi-wavelength filter which allows the generation of a specific wavelength of light from the source. This light is passed through a series of infrared filters and optical lenses, which remove the heat and focus the light into a glass cuvette, respectively. The glass cuvette holds the initiator mixture along with a stirring bar, which mixes the solution continuously during the reaction, to ensure homogeneous decomposition. At certain intervals during the irradiation the cuvette was removed from the holder and the UV-Vis absorbance spectrum of the initiator was taken to monitor the decrease in absorbance and therefore the decrease in the amount of initiator remaining that can generate radicals. This gives an idea of how long it will take for the initiator to decompose. This experiment was carried out using light at 635 nm, the shoulder peak of the initiator as a 660 nm filter was not available for the light source used. In the polymerisation reactions in capillary a 660 nm LED was used as the initiating light source as it is at this wavelength that the maximum absorbance of the dye occurs. The solutions of initiator were 3.33 mM of the cyanine dye/borate initiator complex dissolved in the desired solvent.

4.2.4.3. Synthesis of poly(glycidyl methacrylate-*co*-ethylene dimethacrylate) monoliths in polyimide coated capillary using light at 660 nm

The typical pre-polymer solution consisted of 80 μl GMA (0.59 mmol), 80 μl EDMA (0.42 mmol), 60 μl acetonitrile, 80 μl 1-propanol, 100 μl decanol, 4.2 mg *N*-methoxy-4-phenylpyridinium tetrafluoroborate (MPPB) (2.5% per weight of monomer) and 0.42 mg CyB (0.25% per weight of monomer). All solutions were prepared in amber vials and sonicated for 30 min, to aid dissolution and mixing of reagents, and purged with nitrogen to remove dissolved oxygen. The resulting aquamarine-coloured solution was then filled into polyimide coated capillaries, the ends were sealed with rubber septa and the capillary was masked with black electrical tape. A single 660 nm LED was positioned at 60° to the capillary and the capillary was placed in the grip of a small motor which was rotating at a constant speed of 17 rpm. The forward current through the LED was set at 30 mA and the polymerisation reaction was allowed to proceed for 30-40 min. The polymerisation reactions were then carried out in the dark to eliminate interference from ambient light. After polymerisation was complete the capillary was

flushed with several column volumes of methanol to remove traces of unreacted initiators and monomers.

4.2.4.4. Fabrication of the poly(methyl methacrylate) micro-fluidic chip and encasement of the poly(glycidyl methacrylate-*co*-ethylene dimethacrylate) monoliths

Fabrication of the PMMA chip was carried out by a co-worker, F-Q. Nie, by a procedure described in previous publications [27, 28] and in detail in Section 3.2.4.12 above.

In brief, after the channels were milled in the PMMA sheet, the capillaries containing monolithic poly(GMA-*co*-EDMA) (prepared as in Section 4.2.4.3) were encased in the channels and then sealed into the chip with another layer of unmilled PMMA. The procedure is as outlined in the bullet points below and shown schematically in Fig. 3.10, with the exception of the presence of the LED;

1. 8 mm lengths of the poly(GMA-*co*-EDMA) filled polyimide coated fused silica capillaries were cut using a capillary cutter;

2. A drop of epoxy resin was put in each channel to ensure that the capillary remains fixed in the channel;

3. Once the epoxy has dried (5-10 min), a layer of pressure sensitive adhesive (PSA) was placed over the entire chip covering the capillaries in the channels;

4. A sheet of unmilled PMMA of the same dimensions as the sheet holding the capillaries was placed above the PSA and pressed down tightly;

5. The entire chip was placed in a vice grip for 10 min to ensure a liquid tight seal before the chip can be fitted with connections and used for electroosmotic flow (EOF) experiments.

4.2.4.5. Synthesis of poly(butyl methacrylate-*co*-ethylene dimethacrylate) monoliths in polyimide coated capillary using light at 660 nm

A solution containing 0.25 mg CyB in 10 µl acetonitrile and 20 µl 1-propanol was prepared and sonicated to dissolve the initiator. A second solution containing 2.5 mg

MPPB in 13 µl acetonitrile and 26 µl 1-propanol was also prepared and sonicated. These two solutions were mixed together in an amber vial along with 42 µl butyl methacrylate, 28 µl ethylene dimethacrylate and 61 µl 1-decanol. The mixture was sonicated for 30 min to remove dissolved oxygen and ensure full mixing of all components of the pre-polymer solution.

The pre-treated polyimide coated fused silica capillaries were filled with the pre-polymer solution by capillary action and the ends were sealed with rubber septa. After sealing, the capillaries were connected to a motor and rotated at 34 rpm while irradiating with a red LED positioned at 60° to the capillary for 2 h.

After polymerisation the monoliths were flushed with methanol to remove unreacted initiator and then dried with nitrogen before being stored in water.

4.2.4.6. Fabrication of an LED array

An LED array was fabricated from a piece of stripboard and 5 660 nm LEDs. Using two parallel strips on the board, the LEDs were positioned with the anode leg through one strip and the cathode leg though the adjacent strip with a 2 hole gap between each LED. The legs of the LEDs were then cut to a length of 2-3 mm and bent over taking care not to have them touching the adjacent strip. Using lead-free solder the legs of the LEDs were soldered into their respective strips, once again taking care not to accidentally join adjacent strips as this would result in a short in the circuit and the array would not function. Finally the two of the cut legs of the LEDs were soldered at opposite ends of the array, one in the anode strip and the other in the cathode strip, to function as connections to the power supply. This is shown schematically in Fig. 4.2.
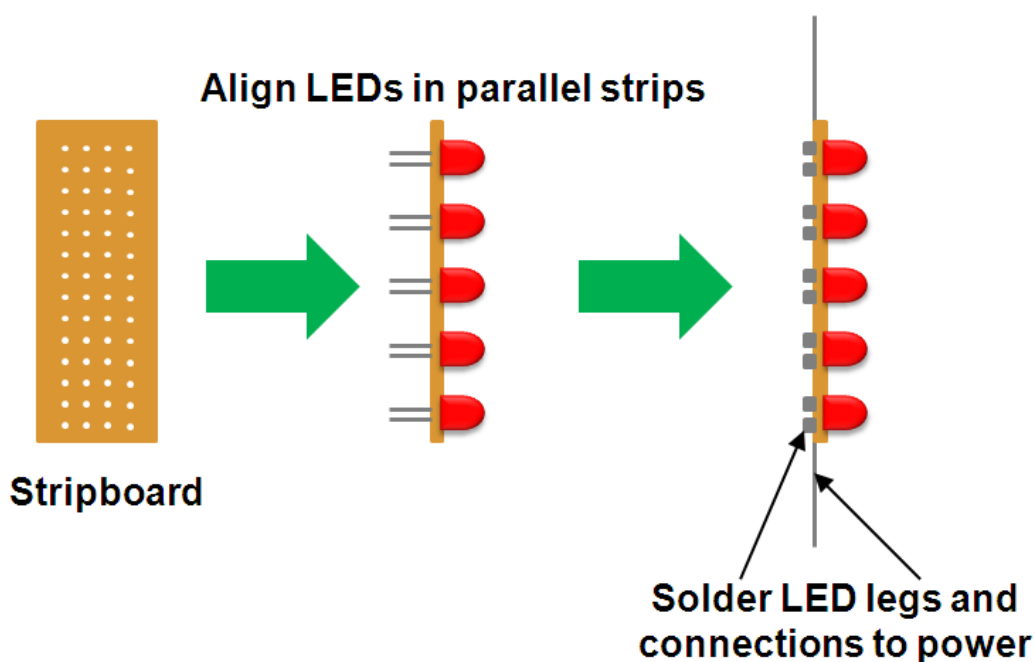
Figure 4.2: *Schematic of the LED array fabricated in-house*

4.2.4.7. Synthesis of poly(methyl methacrylate-*co*-ethylene dimethacrylate) monoliths in capillary

0.2 mg of CyB initiator were dissolved in 10 µl acetonitrile (ACN) and 10 µl 1-propanol and 2 mg of MPPB were dissolved in 13 µl ACN and 36 µl 1-propanol, both solutions were shaken well in order to dissolve the initiators. The solutions were mixed together in a vial along with 56 µl of 1-decanol, 48 µl of MMA and 32 µl of EDMA. The solution was sonicated for 30 min to ensure mixing and removal of dissolved oxygen present in the sample. 10 cm Lengths of 100 µm. 75 µm and 50 µm i.d. capillaries which had been pre-treated (Section 2.2.4.1) were filled with the pre-polymer solution and irradiated with an in-house made LED array, which was positioned directly underneath the capillary at a distance of 2 cm, for 1.5 h, 1.5 h and 1 h, respectively. After the polymerisation was complete the capillaries were flushed with methanol to remove any unreacted initiators and the porogens and then stored for further use.

4.2.4.8. Synthesis of poly(butyl methacrylate-*co*-ethylene dimethacrylate) monoliths in micro-fluidic chips

In the case of the micro-fluidic chips the pre-polymer solution was identical to that used for the capillary polymerisation, however the filling procedure involved connecting the chip to a special platform which consisted of a metal plinth on which position markers had been incorporated. These were small pieces of metal which were raised out of the plate, they were used to keep the chip in place while the injection valve was fitted. A standard 6 port injection valve, with all but the port leading to the channel of the chip stoppered, was placed on top of the chip and through this valve the polymerisation solution was introduced into the channel, as was methanol for washing the channel prior to use. The polymerisation solution was filled into a syringe, taking care to introduce as little air as possible, and then injected into the channel through the 6-port valve. The outlet of the channel was sealed with a rubber septum held in place by a standard stationery clip. As removing the valve could introduce air into the channel the valve was left in place during polymerisation. After polymerisation the monoliths were flushed with methanol to remove unreacted initiator and then dried with nitrogen before being stored in water.

4.2.4.9. Photo-initiated grafting of monomeric spiropyran onto the surface of poly (butyl methacrylate-*co*-ethylene dimethacrylate) in poly(tetrafluoroethylene) coated fused silica capillary

0.02 wt % (0.2 mg/ml) of the CyB was weighed into a vial along with 2 mg MPPB. These initiators were dissolved in 180 µl ACN, 360 µl 1-propanol and 460 µl 1-decanol. Finally, 1 wt % (1 mg/ml) of the spiropyran monomer, (1'-(9-decenyl)-3',3'-dimethyl-6-nitrospiro-[2H-1]-benzopyran-2,2'-indoline), was added to the mixture and sonicated to ensure dissolution of all reagents and to remove dissolved oxygen in the mixture. The mixture was flushed through a poly (BuMA-*co*-EDMA) monolith and the ends of the capillaries were sealed with rubber septa. The capillary monolith was then connected to a motor and rotated while being irradiated with a 660 nm LED for 2 h. After irradiation the monolith was flushed with methanol to remove any unreacted reagents.

4.2.4.10. Characterisation of the monolithic stationary phases

4.2.4.10.1. Flow resistance measurements

The resistance to flow of the monolithic columns was measured using a Knauer S-120 HPLC pump (poly(GMA-*co*-EDMA) or a Dionex Ultimate 3000 nano-LC (poly(BuMA-*co*-EDMA) and poly(MMA-*co*-EDMA)). The flow was measured with 100% deionised water with 0.1% formic acid as the eluent. The flow measurements were carried out over a specific range, which depending on the permeability of the monoliths, in a step-wise manner.

4.2.4.10.2. Optical microscopy

After synthesis the porogens were removed from the monolith by flushing with acetonitrile and then drying with air or nitrogen. This approach emphasises the contrast between the empty and filled parts of the capillary in optical microscopy. Optical microscopy was carried out on all samples from the sides, and not on the cross-section, regardless of the microscope used. Examination of the cross-section was done by scanning electron microscopy. A variety of different magnifications were used to visualise the void free monoliths within the channels.

4.2.4.10.3. Scanning electron microscopy

5-8 mm lengths of the capillary were cut from different places along the length of the capillary. These pieces were then held upright with the surface to be imaged facing upwards. Before imaging the capillaries were sputter coated with a thin layer of gold as the polymer, which is non-conducting, generates significant surface charge under the electron beam during imaging, which can distort the quality of the micrographs. To image the micro-fluidic chips a scalpel was used to score a line across the centre of the chip, the chip was broken and the uneven edges were shaved down using a microtome to obtain a flat surface where the monolith was not damaged for imaging. The chip was then placed in a special holder from Agar Scientific (Essex, U.K.) with the exposed channel facing upwards, and then sputter coated with a thin layer of gold before imaging.

4.2.4.10.4. Lateral conductivity profiling

An on-column C^4D cell was placed on the capillary filled with water and moved down the length of the filled capillary at 1 mm increments, the conductivity value was recorded at each interval. While the stationary phase bears no charge, voids in the columns result in an increase in conductivity. The capillaries were flushed constantly with water during the measurement.

4.2.4.10.5. Monolithic Electroosmotic pumps

8 mm lengths of poly(GMA-*co*-EDMA) monoliths were encased in the PMMA micro-fluidic chips as described in Section 4.2.4.4. The monoliths were flushed with 1 M NaOH to produce O⁻ groups on the surface of the monolith. The reservoirs were then filled with 2 mM phosphate buffer at pH 11. The channels, reservoirs and inlet/outlet tubing were all flushed and then filled with the electrolyte before immersing the electrodes into the reservoirs. An electric field ramp from 0-250 kV/m was applied over the channel and the flow generated by the electric field was measured by a nano-flow sensor positioned at the same height as the electrolyte level in the reservoir, which prevents gravity generated flow.

4.2.4.10.6. Separation of proteins

Analyses on monoliths in capillary were carried out at a flow rate of 1 μl/min, with an injected sample volume of 50 nl and a detection wavelength of 210 nm. The gradient elution profile consisted of 0.1% formic acid in water (mobile phase A) for 1 min, 5 min to go from 0-60% mobile phase B in A (0.1% formic acid in acetonitrile), 10 min hold, return to A in 5 min followed by 5 min conditioning before the next injection. Each separation was run three times on each column.

For the protein analysis carried out on the monoliths in micro-fluidic chips the gradient profile consisted of 0.1% formic acid in water (mobile phase A) for 1 min, 10 min to go from 0-60% mobile phase B in A (0.1% formic acid in acetonitrile), 10 min hold, return to A in 5 min followed by 5 min conditioning before the next injection. A length of 25 μm i.d. tubing had to be connected between the pump and injector in order to generate enough pressure to run at such a low flow rate (1 μl/min) due to high permeability of the monoliths in the channels.

4.3. Results and Discussion

After optimisation of the synthesis of monoliths within polyimide capillaries a range of different methacrylate based monoliths were synthesised using the same basic procedure with minor modifications tailored to the specific pre-polymer solution. Methacrylate monomers were the focus of this study as they are easily polymerised by photo-initiated means, although up to this point this has only been with UV light in the area of monolith synthesis. Styrenic monomers, while popular for thermally initiated monolith synthesis, are very stable due to the resonance stabilised structure of the benzene ring and need much more energy to start forming polymer chains than can be provided by this initiating system, discovered from countless hours of unsuccessful experimentation. The failure of this method with regard to styrene was what encouraged the development of the blue light initiated polymerisation method which is described in detail in Chapter 5.

4.3.1. Optimisation of the polymerisation conditions

4.3.1.1. Estimation of light transmission through the polyimide layers

Before the initiating system could be decided upon, it was necessary to determine which part of the UV-Visible-Near Infrared spectrum would be the most easily transmitted through the polyimide coating of the fused silica capillary into the cavity. As the exact composition of the polyimide coating of the fused silica capillaries produced by Polymicro Technologies is not freely available some estimation of the transmission was necessary. The UV-Vis spectra of four sheets of Kapton$^®$ polyimide of different thicknesses (25 µm, 50 µm, 75 µm and 125 µm) were taken and these are shown in Fig. 4.3.
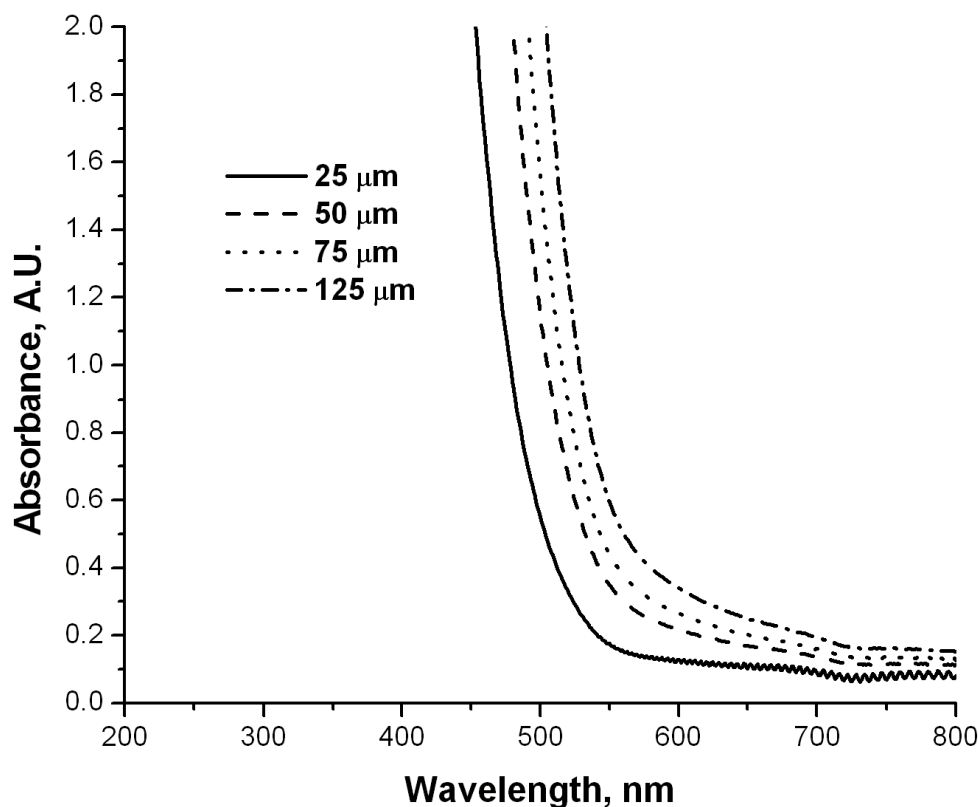
Figure 4.3: *Plot of wavelength (nm) vs. absorbance for polyimide films of four different thicknesses*

Once the spectra were recorded, the absorbance value at several points above 550 nm were taken from the graph and used to calculate the absorbance of a range of different thicknesses of polyimide at these wavelengths. The experimental results were taken from the obtained spectra by drawing a line through the spectra at certain wavelength values and noting the absorbance at the intersecting point. Using the linear equation of the line, obtained by passing a trendline through the experimental points taken from Fig. 4.3 the absorbance values were calculated for all thicknesses of polyimide in the range 20-150 µm, this is shown in Fig. 4.4.
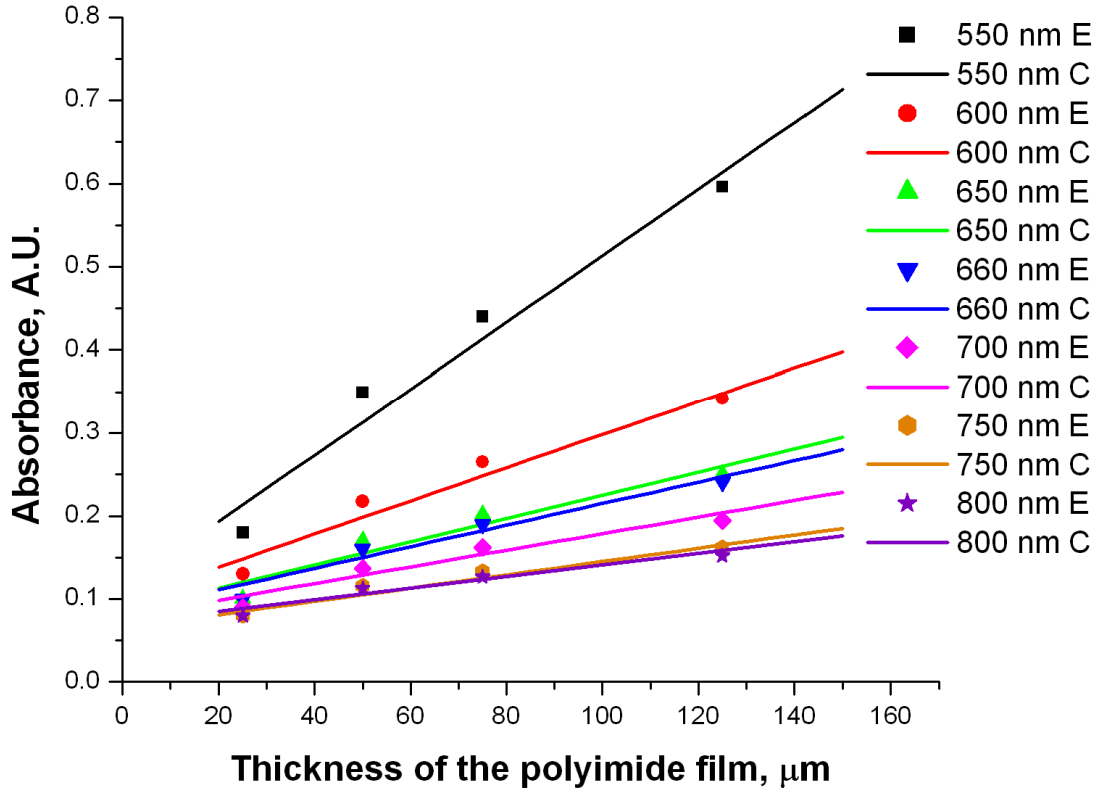
Figure 4.4: *Plot of thickness of the polyimide film (μm) vs. the absorbance of the film at 6 different wavelengths: 550 nm, 600 nm, 650 nm, 700 nm, 750 nm and 800 nm. Experimental values (E) are overlaid with extrapolated absorbance values (C) calculated from the spectra in Fig. 4.3*

The transmission values were was then calculated from the absorbance values using Eq. 4.1 and 4.2;

$$A = Log_{10}T \qquad (4.1)$$

$$\% T = 10^{-A} \times 100 \qquad (4.2)$$

Where A is the absorbance of and T is the transmission through the polyimide layer.

The transmission of light at wavelengths from 550-800 nm through the polyimide at thicknesses between 20-150 μm is plotted in Fig. 4.5.
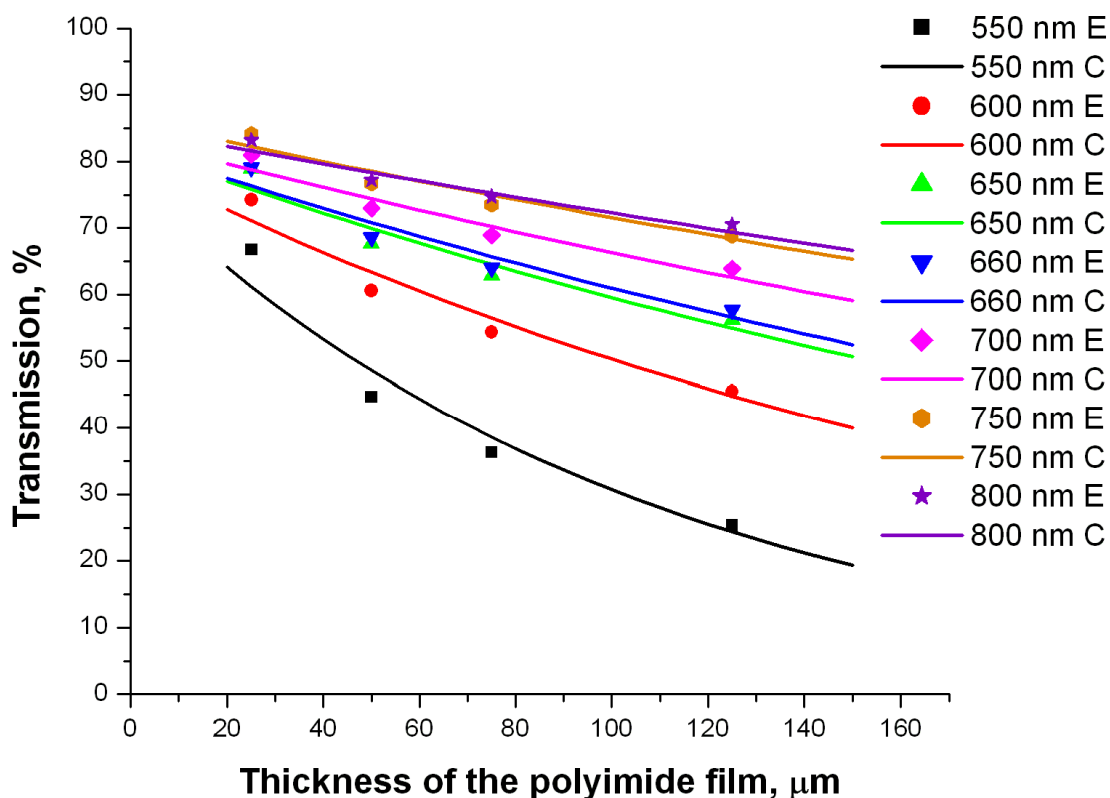
Figure 4.5: *Plot of thickness of the polyimide film (µm) vs. % transmission of light through the film at 6 different wavelengths: 550 nm, 600 nm, 650 nm, 700 nm, 750 nm and 800 nm. Experimental values (E) are overlaid with extrapolated absorbance values (C). Transmission data was calculated from the absorbance values in Fig. 4.4*

From Fig. 4.3 it is clear that light below 550 nm is absorbed by the polyimide (capillary outside coating), therefore light above 550 nm has to be used to initiate the polymerisation in polyimide moulds.

In order to be able to polymerise successfully within the cavity using light initiated polymerisation the initiator for the reaction must absorb strongly above 550 nm. In Fig. 4.5, it can be seen clearly that, as the wavelength of the irradiation light increases the transmission of light through the polyimide layer also increases. With small thicknesses the difference between all the wavelengths is not significant (approximately 10%), however, as the thickness of the polyimide increases this difference becomes more important. Using a wavelength in the region of 650-700 nm would be optimal as more

than half of the incident light is transmitted through the layer along the whole range of thicknesses. Looking to longer wavelengths; while the transmission above 700 nm appears to be greater, the longer the wavelength is, the lower in energy the light will be which may be a problem for the generation of radical species in a reasonable amount of time.

In the work of Kabatc *et al.* [214, 216, 217], it was noted that cyanine dyes are efficient photo-sensitisers for free radical polymerisations initiated in the red region of the spectrum. They are commonly paired with a borate radical initiator, to which they transfer electrons in a process known as photo-induced electron transfer. Efficient single electron transfer to the borate anion from the excited cyanine sensitiser is known to generate the cyanine radical and the butyl radical, along with phenyl borane [218-220]. The butyl radical species are then able to initiate chain polymerisation.

A commercially available cyanine dye/borate salt complex, the triphenyl butyl borate salt of 3-butyl-2-[5-(1,3-dihydro-3,3-dimethyl-1-propyl-2H-indol-2-ylidene)-penta-1,3-dienyl]-1,1-dimethyl-1H-benzo[e]-indolium (CyB), which has an absorbance maximum at 660 nm was selected. The structure of this dye is shown in the introduction, Fig. 4.1.

The plots of absorbance and transmission were then recalculated for irradiation at 660 nm; the results are shown in Fig. 4.6A and Fig. 4.6B, respectively.
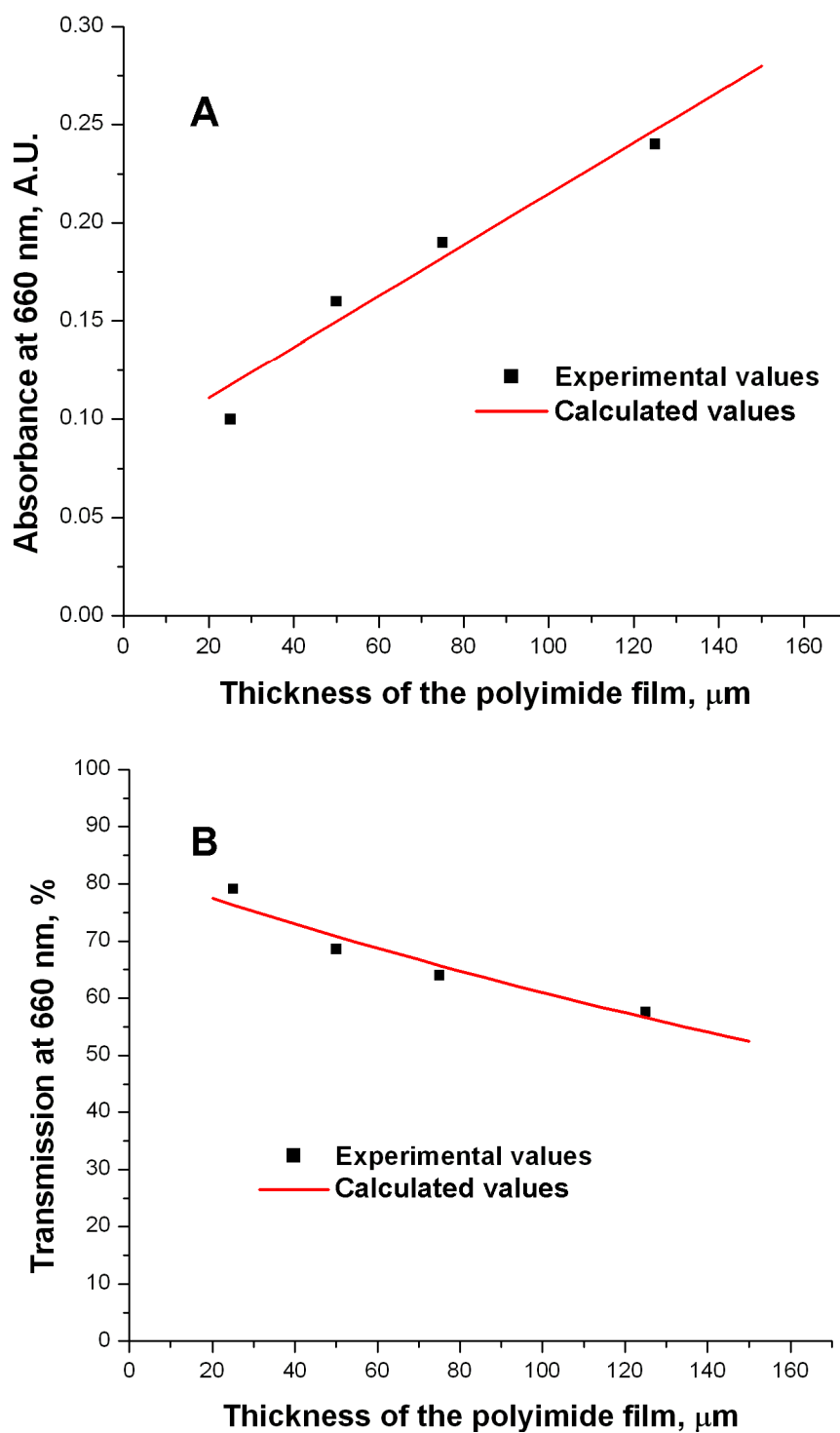
Figure 4.6: *Plots of thickness of the polyimide film (µm) vs. (A) calculated absorbance of the film at 660 nm, and (B) % transmission of light through the film at 660 nm. Values were calculated from the spectra in Fig. 4.3 and absorbance values in Fig. 4.4*

It can be seen from Fig. 4.6A that as the thickness of the layer increases the absorbance also increases; however, even at 150 µm the absorbance value does not exceed 0.26 AU at 660 nm, which means there is still a large amount of light passing into the cavity. Fig. 4.6B allows for the estimation of the actual amount of light which passes into the cavity. When the polyimide layer is 20 µm thick the transmission of light is 77.5% (660 nm) and this decreases to 55.6% (660 nm) when the thickness is increased to 150 µm. These two thicknesses are very important as, from the data sheets; it is known that the thickness of the polyimide coating around the fused silica capillary is 20 µm thick, while the layer above the channel in the polyimide chip is 150 µm thick. If both of these moulds are to be used for polymerisation it is very important that a large amount of the light directed at the mould actually passes into the cavity. In both cases the light transmission is more than half the light irradiation which was deemed sufficient to proceed with the optimisation of polymerisation conditions.

660 nm light emitting diodes (LEDs) were used as the light sources to initiate the synthesis of the methacrylate monoliths within the polyimide coated moulds. There are numerous advantages to the use of LEDs, discussed in Chapter 2, in particular their negligible heat generation and the ease with which they can be positioned around the capillary if monoliths of a particular shape are required. The quasi-monochromatic nature of LEDs means that the absorbance maxima of initiators and emission maxima of initiating light sources can be easily matched with one another to increase the efficiency of the polymerisation, as can be seen in Fig. 4.7.
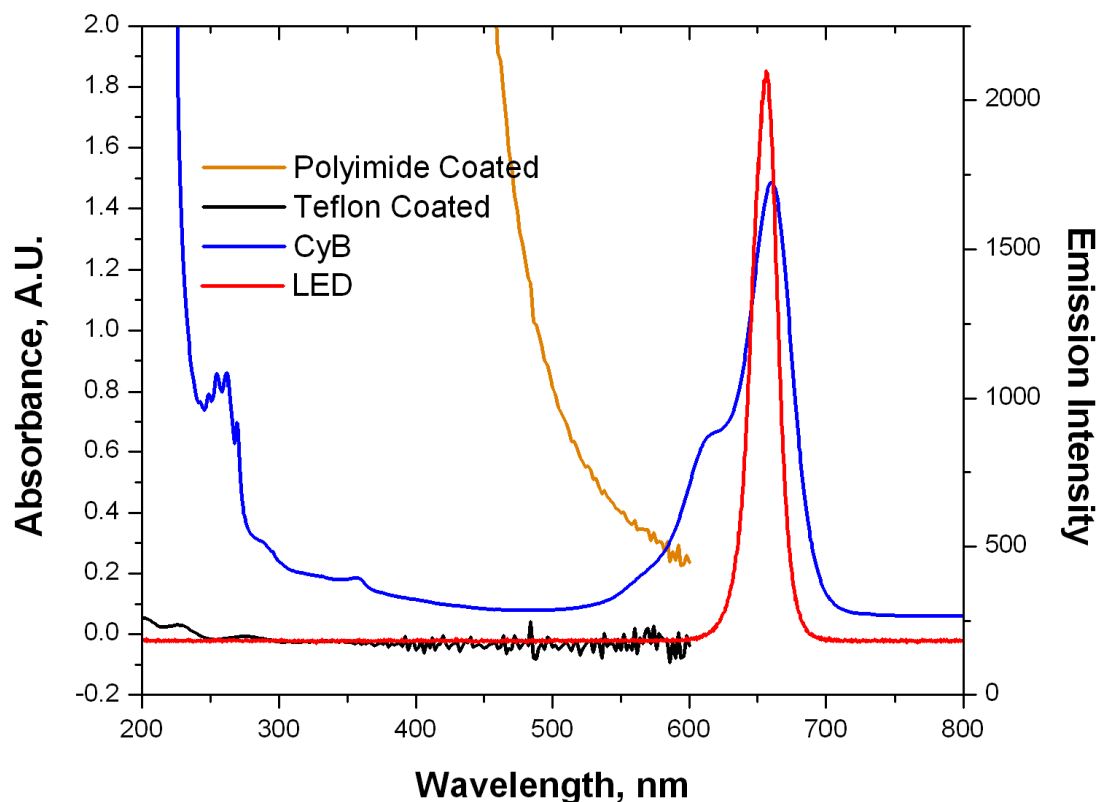
Figure 4.7: *Absorbance spectrum of the CyB initiator in ethanol/1-propanol, a polyimide coated fused silica capillary and a poly(tetrafluoroethylene) coated fused silica capillary and overlaid with the emission spectrum of a 660 nm LED. The spectra of the capillaries were taken on an Agilent CE instrument which has a detection limit of 600 nm (limitation of deuterium lamp), all capillaries were filled with deionised water during measurement*

4.3.1.2. Choice of Initiator Concentration

To determine the optimum concentration of initiator relative to monomer to be used in the pre-polymer solution, the absorbance spectra of known concentration of the dye sensitiser/radical generator was taken (3.33 mM in ethanol/1-propanol, as shown in Fig. 4.7). Knowing the approximately % transmission of light through the polyimide coating, it was possible to construct a graph to see how much light is remaining in the capillary at different distances from the wall. This graph is shown in Fig. 4.8.
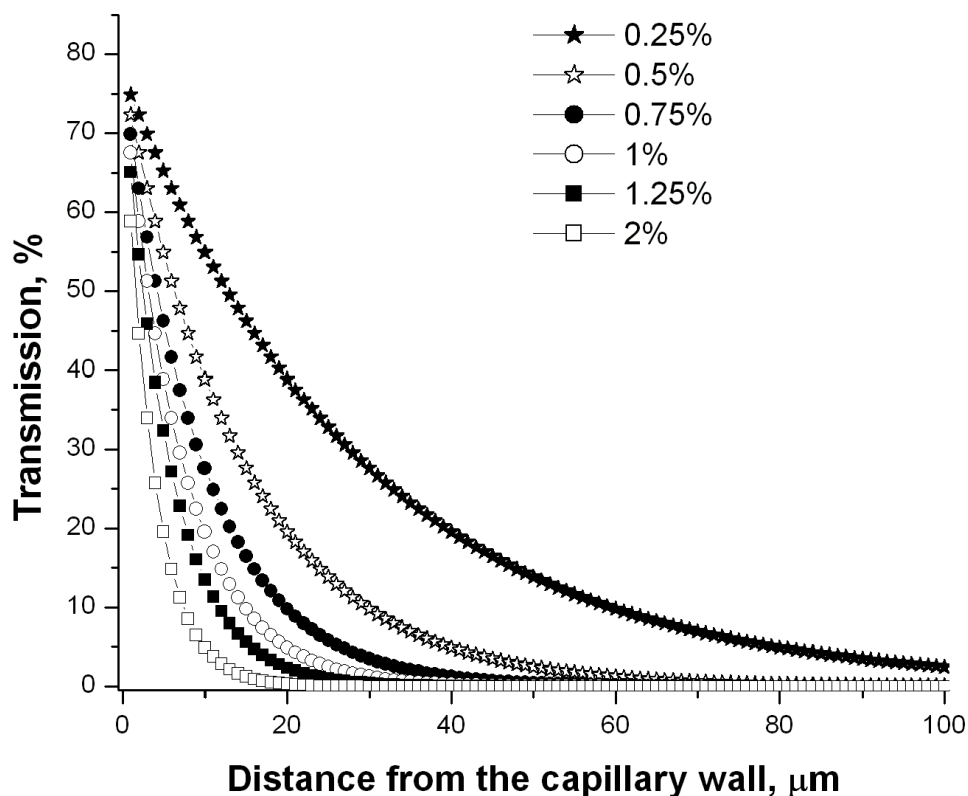
Figure 4.8: *Plot of distance from the wall of the capillary on the cross-section (μm) vs. light transmission showing how much can penetrate into the capillary when different % of dye sensitiser/radical generator are used relative to the weight of the monomer*

From Fig. 4.6B the transmission through the 20 µm layer of polyimide surrounding the capillary was estimated to be 77.5%. Using the factor 0.775, the molar extinction coefficient of the dye (ε^{660} = 230,000 L/mol/cm) and the Beer-Lambert law (Eq. 4.3), the light penetration into the capillary can be estimated at all depths of the capillary cross-section from the wall adjacent to the LED;

$$A = \varepsilon c l \qquad (4.3)$$

Where A is the absorbance of the dye, ε is the molar extinction coefficient, c is the concentration of the dye solution within the cavity and l is the diameter of the cavity in the fused silica capillary. Using the distance into the capillary cavity as the path length the absorbance is calculated and then multiplied by the factor 0.775 to account for the shielding by the polyimide coating.

176

In the case of the higher concentrations of initiator (1%, 1.25%, 2%) it can be seen that the light penetration is almost zero before the light has reached 30 µm into the capillary. If the light penetration to the opposite wall is very weak there will be less and less polymer formation the further into the capillary one looks, meaning inhomogeneously formed monoliths. For the 0.75% and 0.5% initiator the light transmission is almost zero at approximately 50 µm and 70 µm, respectively, however using 0.25% of the initiator allows light to be transmitted through the capillary all the way to the opposite wall. When the monomers are present there will be light scattering effects caused by the formation of polymer chains during the polymerisation, however if the light would not penetrate sufficiently anyway, this problem would be even worse.

For the majority of polymerisations 0.25% was the concentration used, in the case of the poly(BuMA-*co*-EDMA) monoliths the concentration of the initiator had to be increased to 0.375% due to incomplete formation of the polymer in a reasonable amount of time. In this case increasing the concentration of the initiator relative to the weight of the monomer greatly improved the polymerisation efficiency.

4.3.1.3. Optimisation of the polymerisation mixture composition

The majority of the synthesis optimisation was carried out using GMA and EDMA in the pre-polymer solution. GMA-EDMA pre-polymer solutions are easy to prepare and can be polymerised using a large variety of initiating methods and therefore it was believed that this pre-polymer solution would allow for more time to be spent optimising the polymerisation method. When transferring the method for use with other monomers more optimisation was required.

Starting with a pre-polymer solution containing 20% GMA, 20% EDMA, 24% methanol, 36% v/v 1-decanol (all v/v) and 0.25% CyB (per total weight of monomers), the pre-treated capillaries were filled with the mixture and the capillary was placed on a flat surface with the LED positioned perpendicular to it at a distance of 15 mm (Fig. 4.9A). A 660 nm LED with a forward current of 30 mA was used and the polymerisation was allowed to proceed for 30 min.
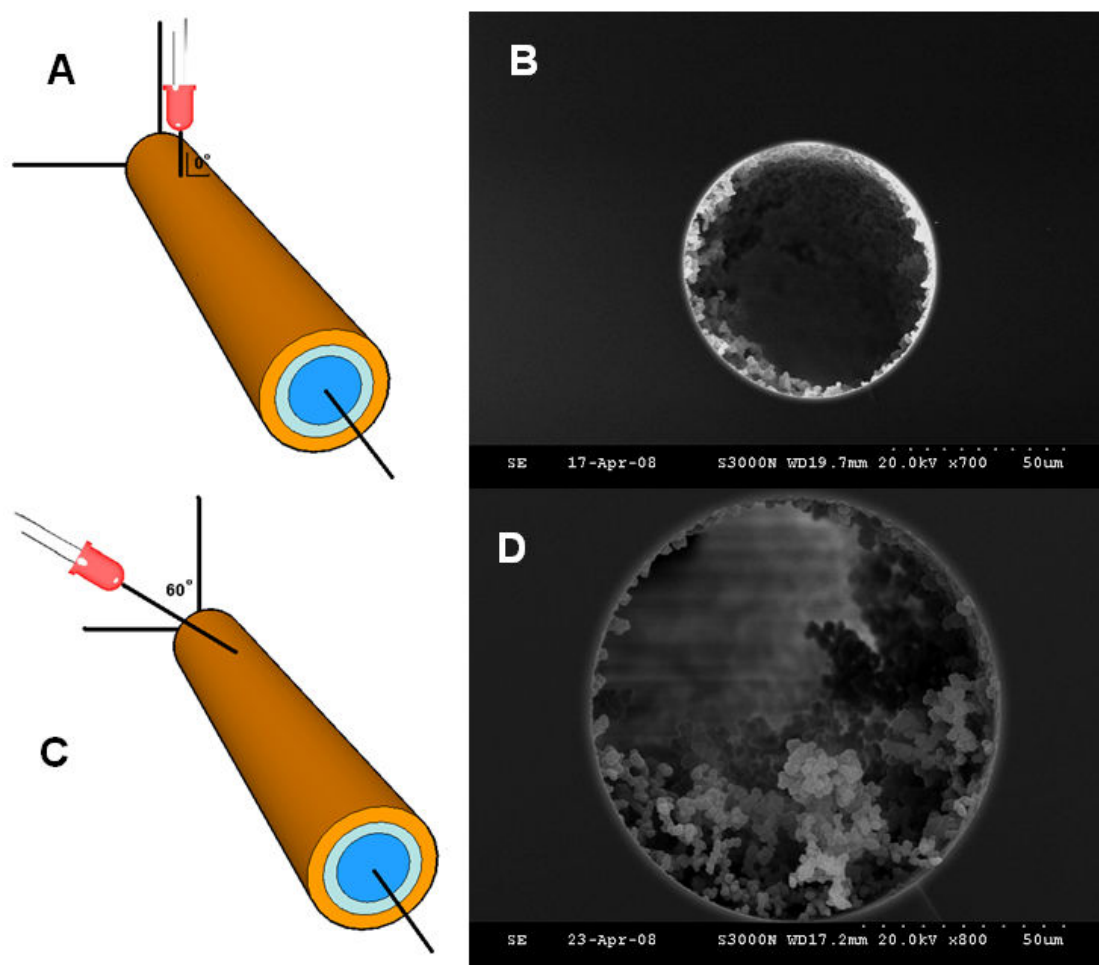
Figure 4.9: *Schematics showing different ways to position the LED relative to the capillary during polymerisation, (A) the LED is positioned perpendicular to the capillary, (C) the LED is at 60° to the capillary. (B) and (D) show SEM images of the monoliths obtained from positioning the LEDs in this manner, (B) corresponds with (A) and (D) with (C)*

The resulting monolithic polymer had a thin layer of polymer formed all along the walls of the capillary (Fig. 4.9B). When the LED is positioned at 60° a thick layer of polymer is formed on one side (the side adjacent to the LED) but overall there is very little polymer formation within the channel. The lens-like properties of the capillary walls and the high absorptivity of the dye sensitiser (ε^{660}= 230 000 L/mol/cm) are believed to be the reason for this occurrence.

When the LED is perpendicular to the capillary the majority of light passes through the polyimide coating and the fused silica wall in a straight line with little scattering of the light rays. On reaching the cavity, the transmission of light through the polymerisation solution is hindered by the high absorptivity of the dye. From Fig. 4.8 above it is estimated that while approximately 79% of light is absorbed at the adjacent wall (within 1 µm of the wall) only 2.6% can be absorbed at the opposite wall (100 µm distance). While diffusion of radicals and some light scattering does occur, the more common outcome is an inhomogeneous wall coating. Keeping all other conditions constant, the LED was shifted incrementally towards the parallel.

Moving the LED away from the perpendicular significantly improved the quantity and homogeneity of the polymer formed within the cavity. The optimum degree of polymerisation was achieved when the LED was positioned at approximately 60° to the normal (Fig. 4.9C). At this angle there is increased light scattering within the walls of the capillary, which allows more radicals to be generated, giving a more homogeneous monolith. This increase in the polymer formation can be seen in Fig. 4.9D, it can be seen that there is a very thick layer of polymer formed at the wall adjacent to the LED but not on the opposite side. Despite improving the quantity of polymer formed, the problem that the polymer formation was concentrated in one area remained to be solved. The problem was solved by employing a small motor to rotate the capillary at a rate of 17 rpm, so that light could penetrate more evenly through the capillary; this has previously been discussed by Eeltink *et al.* [221].

4.3.1.4. Optimisation of the composition of the porogenic solvent

One issue that may have contributed to the unsuccessful polymerisations observed in the previous section (Section 4.3.1.3), was that the porogen composition was not perfectly suited to the dissolution of the initiator, it took excessively long to dissolve the CyB initiator complex in the porogens prior to mixing with the monomers, up to 1 h of sonication was often necessary. After this was noted, a number of different solvents were tested and it was found that acetonitrile dissolved the initiator within minutes, without the need for sonication.

In order to produce radicals, however, hydrogen is abstracted by the initiator from the monomer or solvent to produce radicals, once the initiator is decomposing into radicals the absorbance band of the initiator should begin to decrease to the point where the maximum amount of hydrogen has been abstracted or all the initiator has been used. When the radicals are generated the absorbance spectrum of the dye/initiator complex should change as the concentration of the dye is reduced to form new radical species. As acetonitrile has no abstractable H atoms, an initiator decomposition experiment was performed (as described in Section 4.2.4.2) to see if any change in the absorbance spectrum would be observed after prolonged irradiation, which would indicated the formation of radicals.

It can be seen from Fig. 4.10 below, there is no decomposition of the initiator after 98 min of irradiation with red light at (635 nm) in the presence of pure acetonitrile. ACN is not a good source of abstractable hydrogen and therefore it will not promote the decomposition of the initiator. Additionally, ACN as a single porogen is not suitable due to the extreme polarity of the solvent. Growing polymer chains are not soluble in pure acetonitrile and short chains will drop out quickly after formation leaving a monolith with small pores and small globules as no swelling of the globules has occurred. As the pores of the monolith would be extremely small it would, therefore, be difficult to flush solvents through such a dense structure. It appears necessary to add an additional source of H to the porogen.
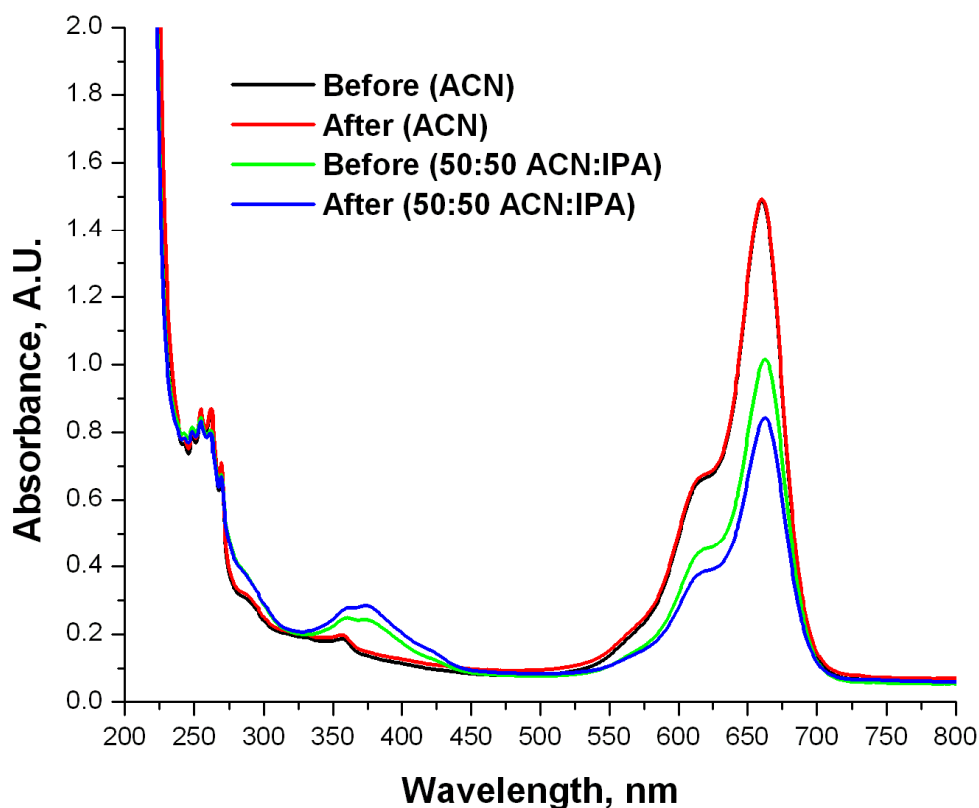
Figure 4.10: *Plot of wavelength (nm) vs. absorbance (A.U.), before and after irradiation, for the commercially available cyanine borate initiator in the presence of two different porogen solvent mixtures: acetonitrile and acetonitrile/1-propanol. Each solution contains 3.33 mM of the cyanine borate complex and is irradiated at 660 nm with a light emitting diode over a period of 98 min*

Adding 1-propanol increases the concentration of available hydrogen, therefore there is a clear difference between the absorbance of the initiator before and after irradiation for 98 min. The 1-propanol promotes the decomposition of the initiator and therefore allows the polymerisation to proceed more efficiently. Despite this monoliths synthesised with a 50:50 mixture of ACN and 1-propanol, while an improvement on pure ACN, would also suffer from poor flow through properties due to similar, although less severe, incompatibility with the growing polymer chains.

Finally it was decided that it would be necessary to add a macro-porogen, such as decanol, to achieve better flow through properties and increase the amount of abstractable hydrogen to encourage further decomposition of the initiator. From this point it was decided that the most suitable porogen composition was a ternary mixture of acetonitrile, 1-propanol and 1-decanol.

4.3.1.5. Introducing the three-component initiating system

Although the preliminary experiments (in Section 4.3.1.3) were originally carried out with only 30 min irradiation, the polymerisation time was increased to 3 h when it was noted that the entire capillary was not filled with polymer. Even at this increased polymerisation time, using the 0.25% dye sensitiser/radical generator complex in the pre-polymer solution gave incompletely filled capillaries even after 3 h of direct irradiation with 660 nm LEDs. It is well-known that the advantage of photo-initiated polymerisation is that the reaction times are short, however short reaction times were to this point unattainable with the initiator system used.

In addition to changing the porogenic solvent it was realised that it was also necessary to modify the initiating system. Going back to the literature it was found that Kabatc and Paczkowski [222] used *N*-methoxy-4-phenylpyridinium tetrafluoroborate (MPPB, Fig. 4.11) to accelerate the polymerisation of 2-ethyl-2-(hydroxymethyl)-1,3-propanediol triacrylate when a hemi-cyanine dye/borate salt was used as the initiating system.
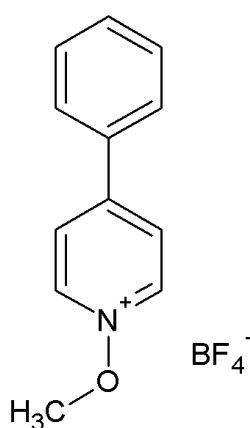
Figure 4.11: *Structure of N-methoxy-4-phenylpyridinium tetrafluoroborate*

This second initiator can abstract an electron from the excited state of the cyanine dye to produce a methoxy radical and pyridine *via* reductive cleavage of the N–O bond [223]. This three-component initiating system is more efficient because it is capable of releasing two radical species as polymerisation initiators upon absorption of a single photon, while the overall rate of free radical formation is not controlled by the reverse electron transfer [222], this is shown in Fig. 4.12.
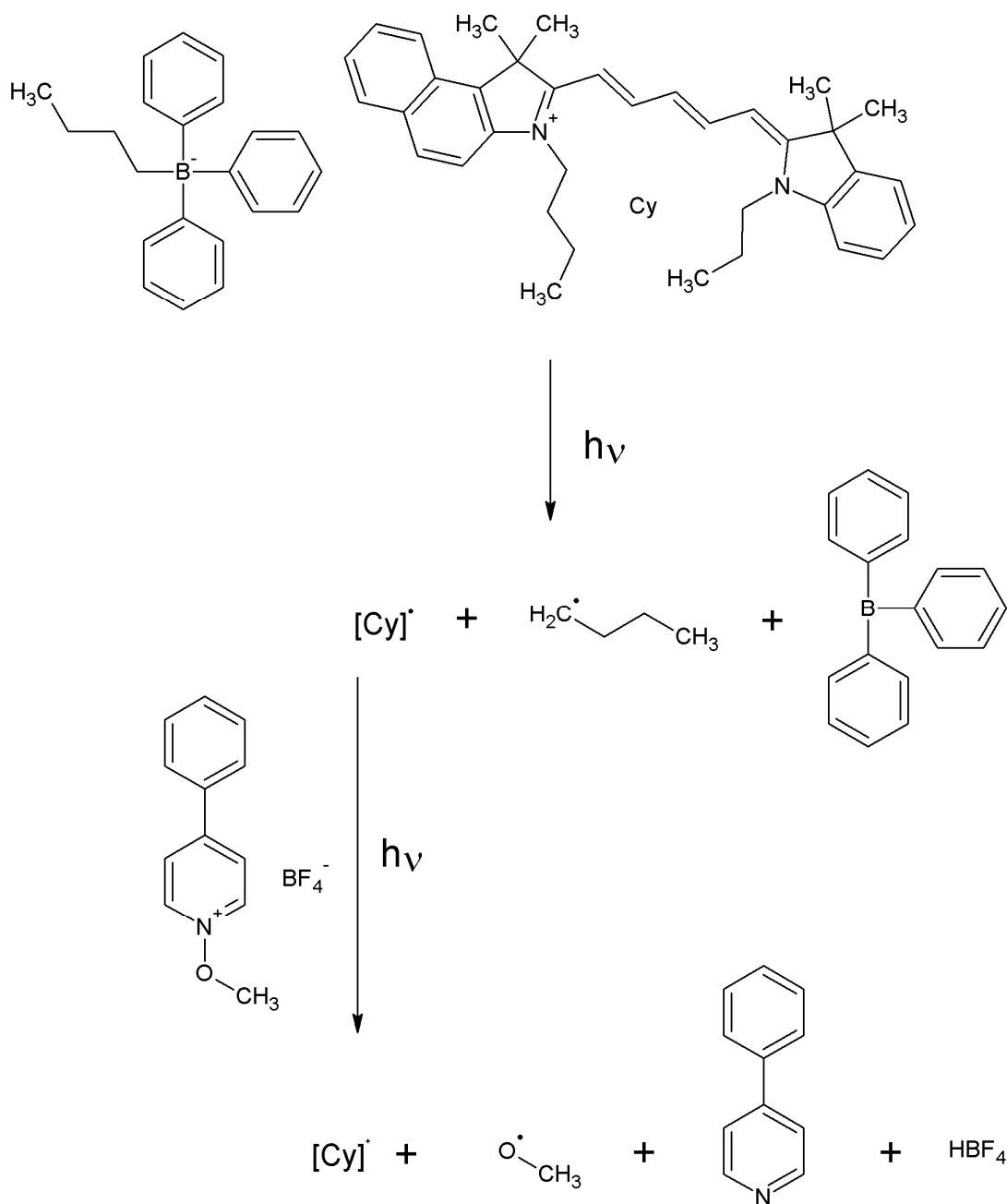
Figure 4.12: *Schematic of the electron transfer from the cyanine dye and the formation of the butyl and methoxy radicals from the initiators to start the polymerisation*

Referring to the work of Kabatc and Paczkowski [222], 10-fold molar excess of the alkoxypyridinium salt was used in this study to ensure that the photo-initiated polymerisation of the monolithic stationary phases was as efficient as possible. The

modification to the porogen made in the previous section (Section 4.3.1.4), also suited this modified initiating system allowing both components to be dissolved fully without the need for sonication. Sonication was still employed, however, to ensure removal of dissolved oxygen from the pre-polymer solution.

Even in low concentrations, sixty times lower than the optimised concentration for the polymerisation, it can be seen that the absorbance of the initiating complex is improved by the presence of the MPPB, Fig. 4.13. In these spectra the concentration of the cyanine borate complex is 0.01 mM while the MPPB is 0.32 mM.
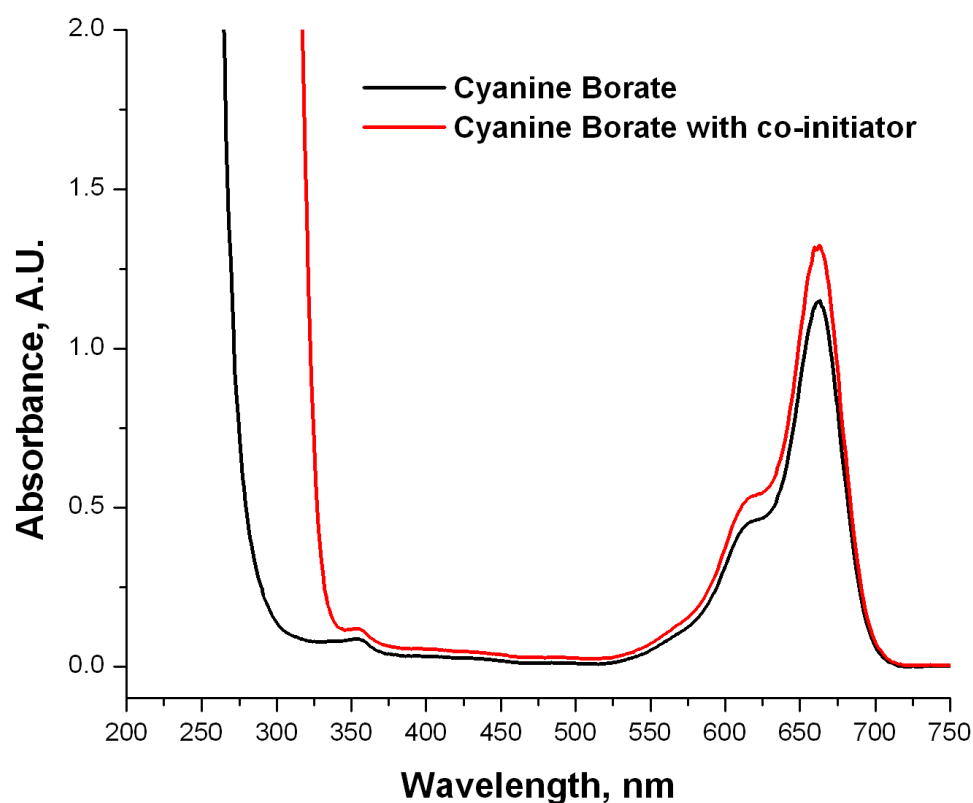
Figure 4.13: *UV-Vis absorbance spectra of the CyB initiator (black line) and the CyB initiator plus a 10-fold excess of the MPPB salt (Red line) taken in an 18:36:46 volume ratio of acetonitrile:1-propanol:1-decanol*

Increased absorbance of light increases the number of radicals, which can be generated by photo-induced electron transfer; this in turn improves the efficiency of the polymerisation. Additionally, the presence of the MPPB introduces a more efficient,

relative to the butyl radical, methoxy radical into the system. The presence of this second radical species is the likely cause for the improvement in polymer formation within the capillary.

Using a combination of this novel three-component initiating system and rotation of the capillary during polymerisation it was possible to obtain capillary moulds entirely filled with polymer monolith stationary phase within 30-40 min. This can be seen in Fig. 4.14.

The optimised pre-polymer solution now consists of 40% monomers and 60% porogens, of which the three porogens - acetonitrile, 1-propanol and 1-decanol - are in a ratio of 18:36:46, all % are v/v. The initiator consists of 0.25% CyB and 2.5% MPPB dissolved in the porogen prior to mixing with the monomers.
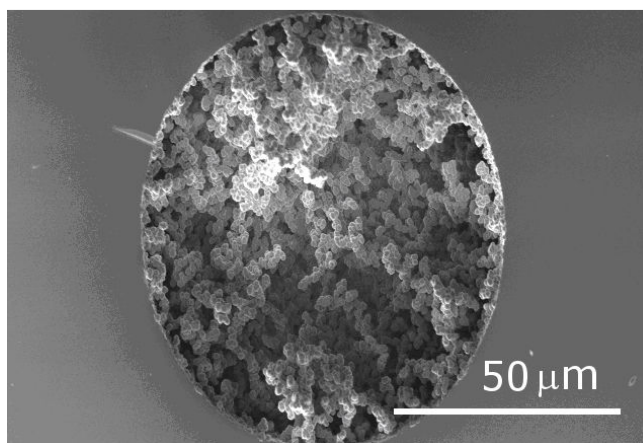
Figure 4.14: *Scanning electron micrograph of a poly(glycidyl methacrylate-co-ethylene dimethacrylate) monolith in polyimide coated capillary after 40 min of polymerisation with red light and a novel three component initiating system. Capillary was irradiated at an angle of 60º and rotated at approximately 17 rpm during polymerisation*

Once it had been shown that monolithic stationary phases could be repeatedly synthesised within polyimide capillaries, by irradiation through the coating, the range of moulds and applications of this system were expanded. During the course of this research project the photo-initiated polymerisation of monolithic stationary phases in polyimide coated fused silica capillaries and polyimide micro-fluidic chips and the photo-initiated grafting of chromophoric monomers onto pre-existing monolithic

scaffolds were investigated using this novel three component initiating system and red LEDs as the initiating light source.

4.3.2. Poly(methacrylate) monoliths in capillary

The three stationary phases synthesised using this method were poly(glycidyl methacrylate-*co*-ethylene dimethacrylate) [poly(GMA-*co*-EDMA)], poly(methyl methacrylate-*co*-ethylene dimethacrylate) [poly(MMA-*co*-EDMA)] and poly(butyl methacrylate-*co*-ethylene dimethacrylate) [poly(BuMA-*co*-EDMA)]. All have different levels of hydrophobicity ranging from hydrophilic (GMA) to hydrophobic (BuMA), this section shows the synthesis, characterisation and application of each of the different monolithic stationary phases.

It can be seen from Table 4.1 that as the hydrophobicity of the monomers used in the pre-polymer solution increase the polymerisation time and the amount of initiator required to start the polymerisation increase also. It is not only the hydrophobicity of the monomers which is increasing, the stability of the monomers is also increasing meaning that more energy is required to bring the polymerisation reaction to completion, hence the increase in the amount of initiator required and the lengthening of the polymerisation reaction time.

Table 4.1: *Synthesis conditions for three different monolithic stationary phases produced by red light initiated polymerisation*

	Poly(GMA-*co*-EDMA)	Poly(MMA-*co*-EDMA)	Poly(BuMA-*co*-EDMA)
LED Power	0.06 W	0.2 W (1.278 lm/W)	0.06 W (0.079 lm/W)
Polymerisation Time	30-40 min	1-1.5 h	2 h
Initiator Concentration (per weight monomers)	0.25 % CyB/2.5 % MPPB	0.25 % CyB/2.5 % MPPB	0.375 % CyB/3.75 % MPPB
Monomer/Porogen concentrations (% v/v)	40%/60%	40%/60%	35%/65%
LED Position	60°	0°	60°

A significant advantage of polyimide-coated over PTFE-coated capillary is the fact that the polyimide coating prevents the capillary from acting as a wave-guide. This also means that the need for photo-masking is less important when polyimide coated capillary is used. Light will not travel along the capillary so if the light is focussed on one point of the capillary and other parts are in darkness, with or without masking; no polymer will be formed in these sections. To be sure of very sharp edges, however, masking of the capillary with, for example, black electrical tape is recommended.

During the polymerisation of the poly(GMA-*co*-EDMA) and poly(BuMA-*co*-EDMA) monoliths with single LEDs it was important that the LED was positioned at an angle of 60° to the capillary to maximise the light transmitted into the cavity. Synthesis of the poly(MMA-*co*-EDMA) monoliths was done using an LED array and therefore it was not as important to position the array at a certain angle to the capillary and so the array was

placed directly beneath the capillary at a distance of 2 cm. As there are 5 LEDs in the array with overlapping cones of emittance there is not one single focal point of the light within the capillary but many and therefore enough light is transmitted into the capillary to start the polymerisation. For this reason, LED position is only important when a single LED is employed.

In the following sections the characterisation of the three different types of monolith, synthesised by the optimised polymerisation procedure, are described and compared with one another. These characterisations and comparisons show that with minor modifications relating to the pre-polymer solution composition the method is usable and reproducible on a range of methacrylate monomers.

4.3.2.1. Optical microscopy

As in previous chapters the first stage of the characterisation was to examine the monoliths using optical microscopy to ensure the formation of sharp edges, this reduces peak tailing once the monoliths are used in chromatographic applications.

While not extremely important for the synthesis of monoliths in capillaries, as they can be cut to the remove diffuse ends without damaging the usability of the stationary phase mould, it is important when the monolith is to be synthesised in a mould which cannot be cut to size, for example micro-fluidic chips. In Fig. 4.15 it can be seen that the synthesis of monolithic polymers with sharp edges can be done with easily.
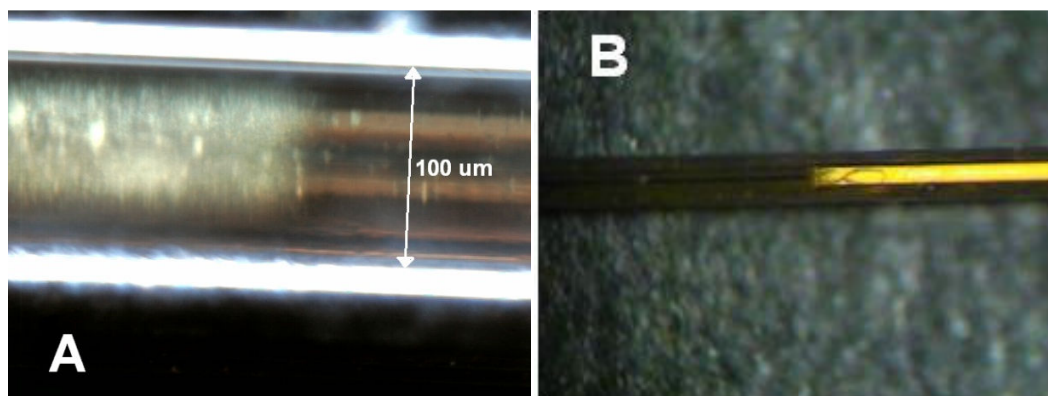
Figure 4.15: *Optical micrographs of (a) a poly(GMA-co-EDMA) monolith and (b) a poly(BuMA-co-EDMA) monolith, synthesised within 100 μm i.d. polyimide coated fused silica capillary. Ends were masked with black electrical tape to show formation of sharp edges on the monolithic stationary phase*

In all cases it is clearly seen the edges are sharp and that there are no obvious voids in the filling of the capillary. Some mould studies were carried out using the poly(MMA-*co*-EDMA) pre-polymer solution to show that with the same conditions and a reduction in the polymerisation time monolithic polymers of a reproducible standard can be synthesised in smaller moulds than the standard 100 µm i.d. capillary. Fig. 4.16 shows optical micrographs of poly(MMA-*co*-EDMA) in 75 µm and 50 µm i.d. moulds and it can be seen that the edges of the monoliths are sharp in the capillary and that there are no voids in the filling of the cavity.
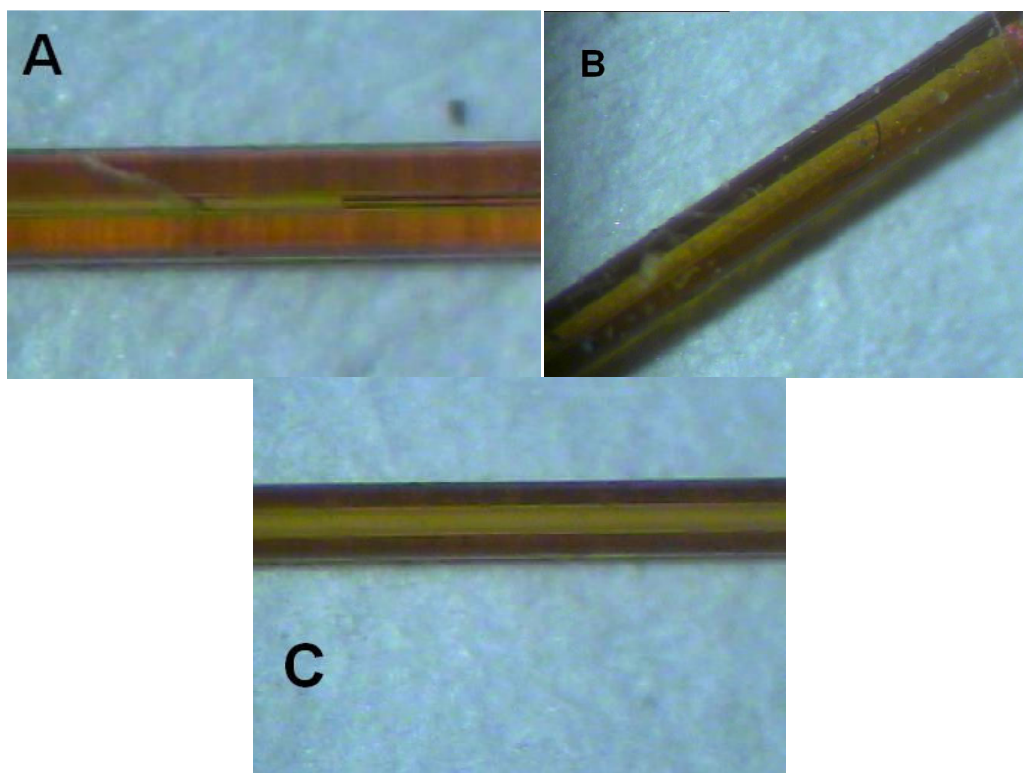
Figure 4.16: *Optical micrographs of poly(MMA-co-EDMA) monoliths in (A) 50 µm, (B) 75 µm and (C) 100 µm i.d. polyimide coated fused silica capillary*

4.3.2.2. Scanning electron microscopy

Previously, with the use of the optical microscope examining the monolith within the capillary through the wall of the capillary, it appeared that there were no obvious voids in the polymer monolith held within the mould. For further confirmation of this fact, the use of scanning electron microscopy was necessary. Although this is a destructive technique, that is by preparing the sample for analysis it is destroyed, it is the best available for examining the whether the cavity of the capillary is adequately filled with stationary phase and if this stationary phase is bound to the wall.

Fig. 4.14 (above) shows an SEM image of poly(GMA-*co*-EDMA) and Fig. 4.17 shows that of a poly(BuMA-*co*-EDMA) monolith both within 100 µm i.d. polyimide coated fused silica capillaries. While the method of polymerisation was similar for both monoliths (Table 4.1) it can be seen from the images that the structures of the two different polymers are different. The poly(GMA-*co*-EDMA) monoliths were formed in a

191

shorter time and so the monolith appears less dense with larger pores evident in Fig. 4.14. Additionally the increased hydrophobicity of the BuMA will cause the polymer chains to precipitate from the polymer solution earlier, shorter chains result in smaller pores and globules. The polymerisation reaction to form the poly(BuMA-*co*-EDMA) monolith (Fig. 4.17) was allowed to proceed for 2 h, instead of 40 min as for the poly(GMA-*co*-EDMA) monolith, so more short chains are formed and therefore the polymer is denser within the mould with smaller pores and more tightly clustered globules. It is evident from these images that polymerisation time and hydrophobicity of the monomer are important factors in the structure of the polymer monolith.
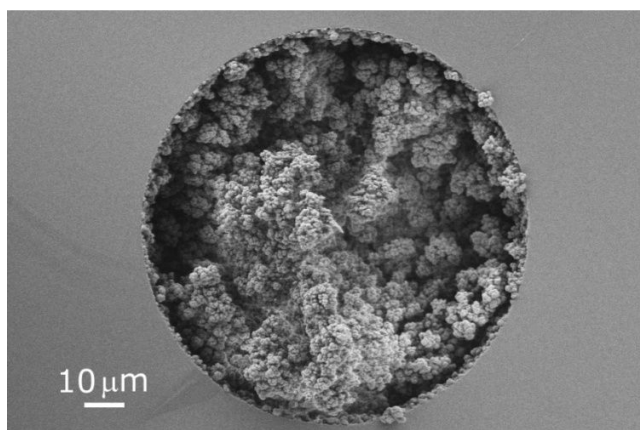
Figure 4.17: *Scanning electron micrograph of a poly(BuMA-co-EDMA) monolith, in 100 μm i.d. polyimide coated fused silica capillary*

Importantly, as can be seen from the SEM images, the capillaries are fully filled with monolith and these monoliths are well attached to the walls of the capillaries giving them good mechanical stability. This will allow them to be more resistant to high pressure flow through the column and will ensure that stationary phase compression is minimal once they are used in chromatography.

Looking again at the poly(MMA-*co*-EDMA) monoliths within polyimide capillaries of different sizes, Fig. 4.18, it can be seen that regardless of the size of the mould it is possible to synthesise monoliths within the cavity in less than 2 h. Additionally, the monoliths fill the entire cavity and are well attached to the walls, indicating their suitability for use as stationary phases in chromatographic applications. The reduction in

size of the mould and therefore the stationary phase is quite useful when analysing samples of low abundance and high cost. Smaller stationary phases mean using lower sample volumes, to avoid overloading of the stationary phase, therefore allowing the conservation of more of the sample.
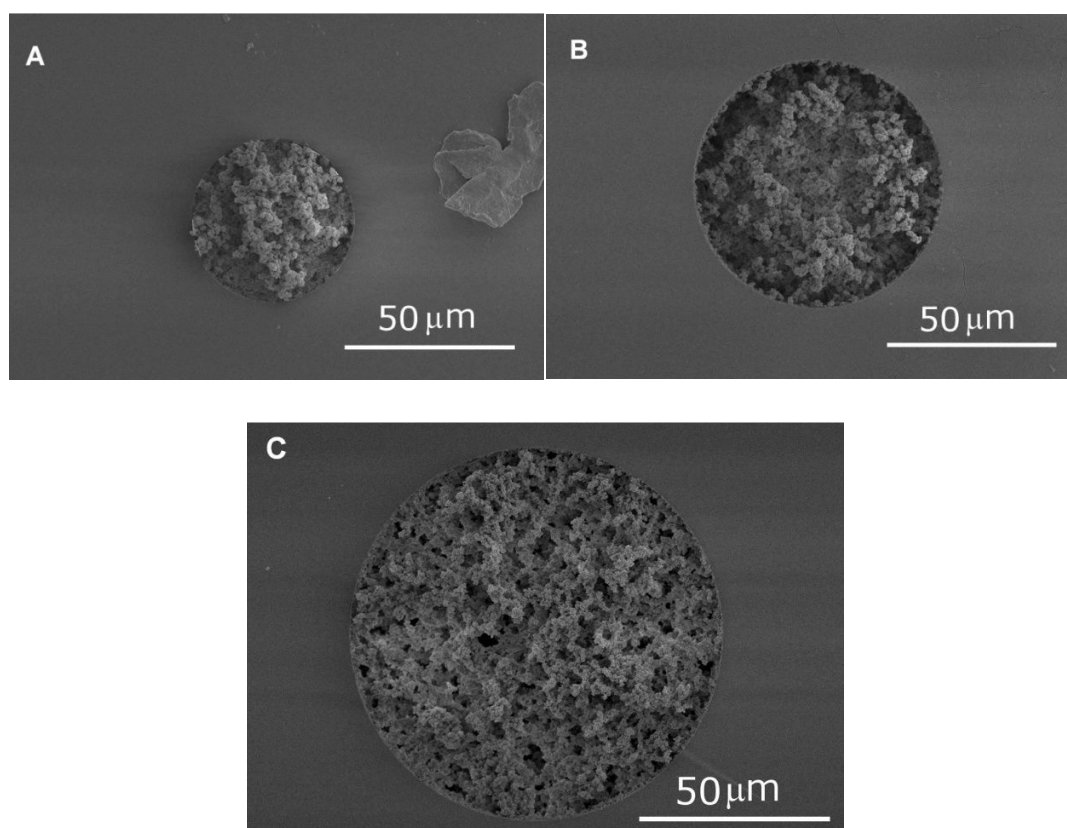
Figure 4.18: *Scanning electron micrographs of poly(MMA-co-EDMA) monoliths in (A) 50 µm, (B) 75 µm and (C) 100 µm i.d. polyimide coated fused silica capillaries*

4.3.2.3. Flow resistance measurements

Measurements of the flow resistance of the poly(GMA-*co*-EDMA) and poly(BuMA-*co*-EDMA) monoliths confirmed what had been identified in the SEM images, that the poly(BuMA-*co*-EDMA) monoliths were significantly denser than the poly(GMA-*co*-EDMA) monoliths due to the elongation in polymerisation time and increased hydrophobicity of the BuMA compared to the GMA. These back pressure measurements are shown in Fig. 4.19. In all cases water was used to measure the flow resistance.

A

B
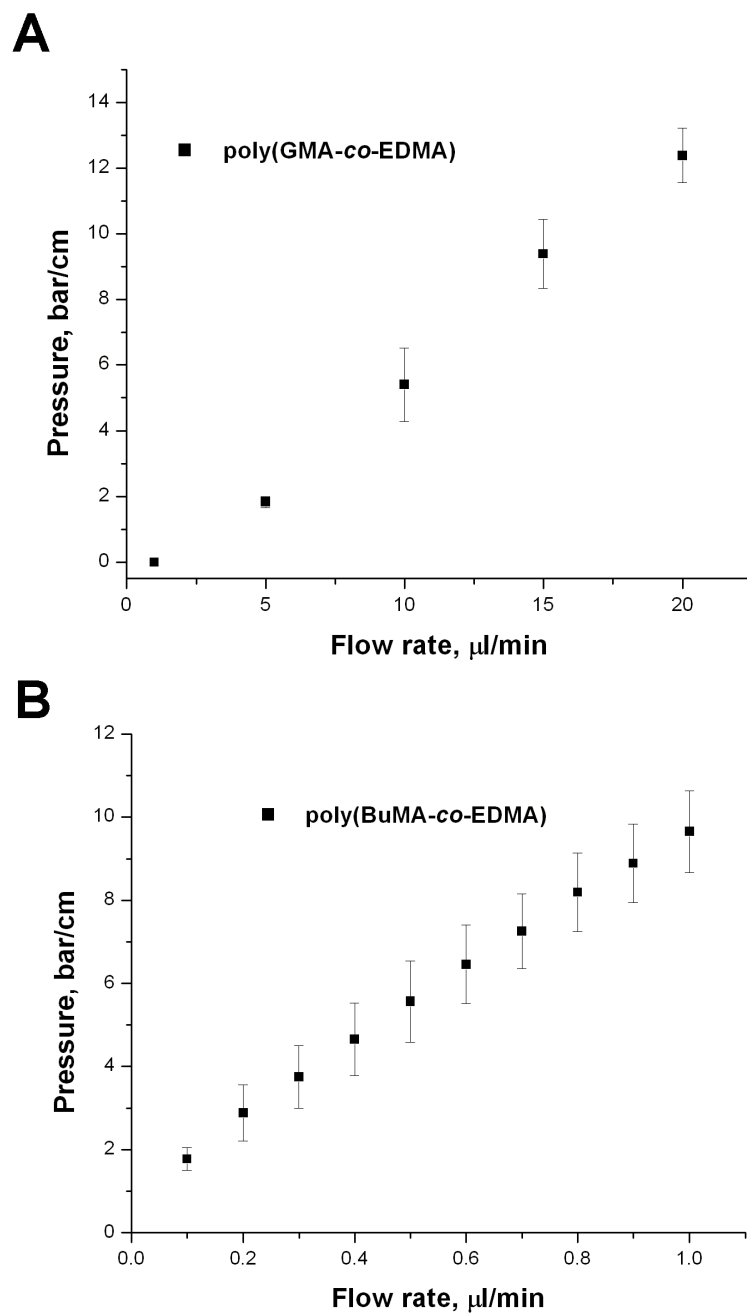
Figure 4.19: *Plot of flow rate (µl/min) vs. flow resistance (bar/cm) for (A) a batch of poly(GMA-co-EDMA) monoliths and (B) a batch of poly(BuMA-co-EDMA) monoliths, n=3 in each batch, in 100 µm i.d. polyimide coated fused silica capillary*

Looking at Fig. 4.19 it can be seen that the average back pressure of the poly(BuMA-*co*-EDMA) monolith at 1 µl/min was approximately 10 bar/cm, while in the case of the

poly(GMA-*co*-EDMA) monolith the pressure did not approach 10 bar/cm until the flow rate was 15 µl/min.

In the case of the poly(MMA-*co*-EDMA) monoliths in moulds ranging from 50 µm to 100 µm i.d. Fig. 4.20 shows the back pressure measured for the three different i.d. columns plotted against the volumetric flow rate. It can be seen that similar back pressures can be obtained for all three different columns although polymerisation time and capillary i.d are different. One interesting point to note is that, while the pressures are similar, to carry out separations of comparable efficiency on each of the three types of monolith, the flow rate would have to be reduced by a factor of two from the 100 µm to the 75 µm column and by a factor of four to the 50 µm column to achieve similar linear flow rates through the column and similar mass transfer efficiency. It must be admitted that the polymerisation time was reduced for the 50 µm column from 1.5 h to 1 h as the columns were difficult to flush. A more accurate comparison would be presented if all polymerisations were carried out for the same length of time but it is important to balance this with ability to use the columns produced and this was done here. What can be seen here, however, is that by modifying the polymerisation time and sometimes the prepolymer concentration monoliths of similar density can be obtained in mould of different diameters.
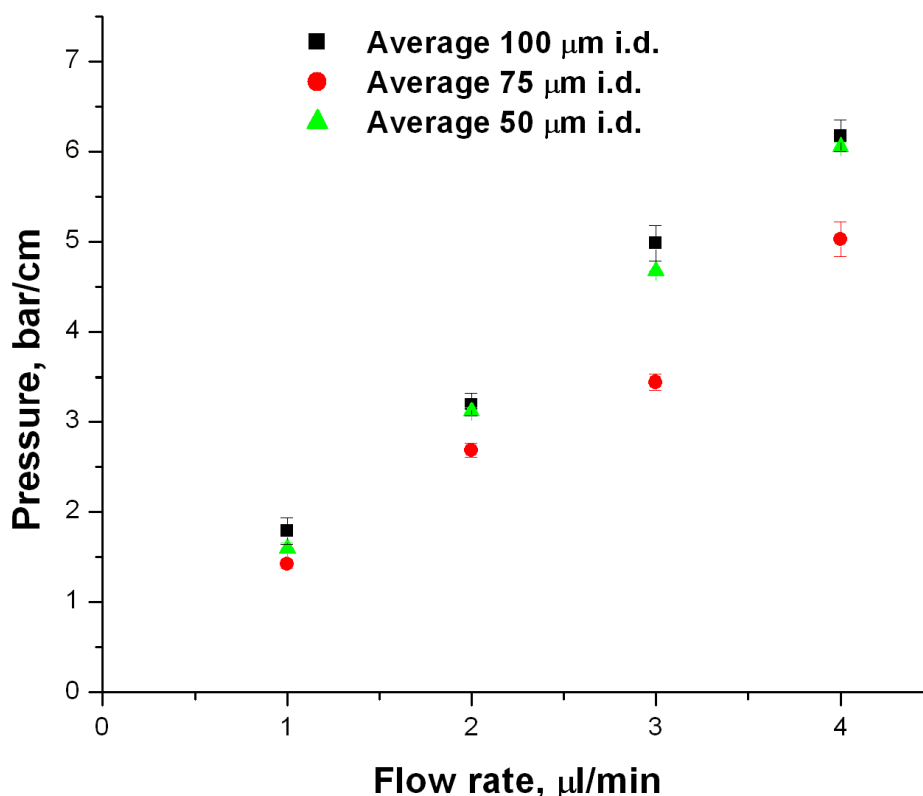
Figure 4.20: *Plots of flow rate (µl/min) vs. flow resistance (bar/cm) for batches of poly(MMA-co-EDMA) monoliths, n=3 for each batch, made in 100 µm, 75 µm and 50 µm i.d. polyimide coated fused silica capillary*

In all cases, both Fig. 4.19 and 4.20, the pressure increases linearly with increasing flow rate, there are no significant increases in back pressure over the flow rate range indicating there is no bed compression or detachment from the walls of the capillary. The relative standard deviation (RSD) of the back pressures of the monoliths is useful in determining the repeatability of the monolith synthesis. For the poly(MMA-*co*-EDMA) monoliths the RSDs were 3.86%, 5.35% and 1.43% for the 100 µm, 75 µm and 50 µm i.d. capillaries, respectively. As this is within an acceptable range (i.e. less than 10%) it can be said that the synthesis of these polymers was quite reproducible. For the poly(GMA-*co*-EDMA) the RSD was slightly higher, 9.53%, however it still showed a good degree of repeatability of the synthesis. In the case of the poly(BuMA-*co*-EDMA) the repeatability was out of the desired range and showed a lower degree of repeatability compared to the other monoliths with a RSD of 15.49%. Due to the random nature of

copolymerisation the formation of the globules within the cavity will often be different resulting in small to large differences in the back pressure measured from the capillary. This can often have little to no effect on the separating ability of the monolith as will be shown later.

4.3.2.4. Lateral conductivity profiling

Lateral conductivity profiling is an excellent method for determining the quality of the polymer within the capillary, whether or not it is homogeneous and free from voids.

Fig. 4.21 shows the conductivity profile of a batch of poly(GMA-*co*-EDMA) monoliths synthesised under the optimum conditions.
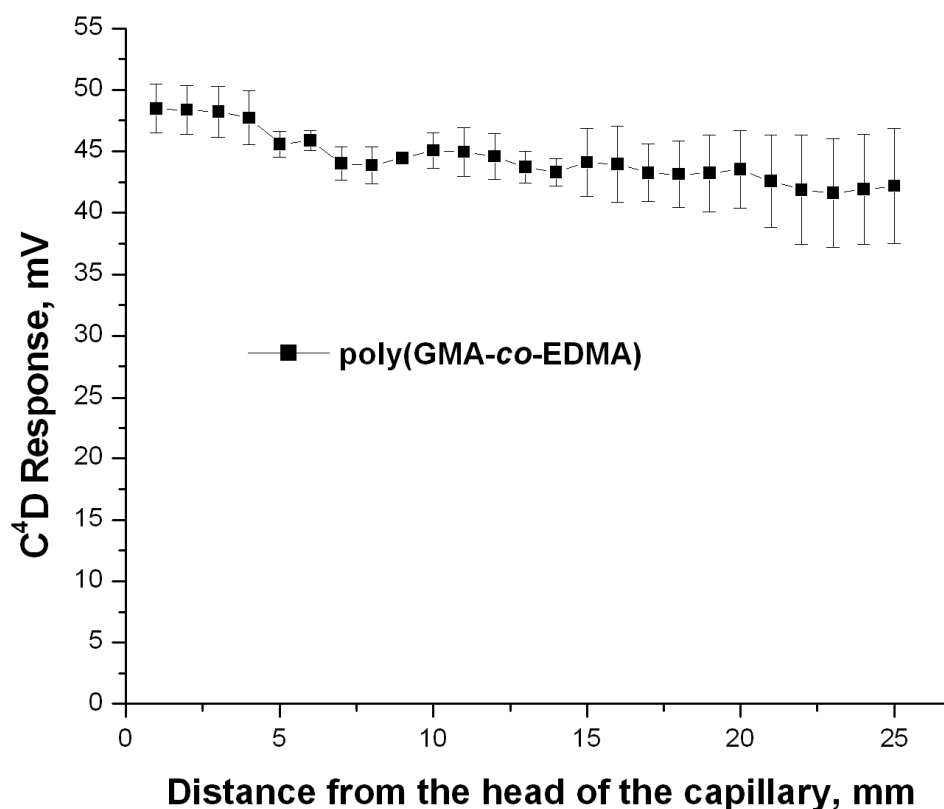
Figure 4.21: *Average lateral conductivity profiles of a batch of poly(GMA-co-EDMA) monoliths, n=3, made in 100 μm i.d. polyimide coated fused silica capillary*

It can be seen clearly from Fig. 4.21 that the monoliths are homogeneous along the length, the % RSD calculated from the values obtained from all columns in the batch

show that the deviation along the length of the monoliths from batch to batch is 5.5%. This is well below the acceptable maximum value of 10%. From these results it can be said that the polymers are homogeneous along the length of the rod and that this homogeneity is reproducible from column to column.

The poly(MMA-*co*-EDMA) monoliths in capillaries of differing internal diameters were also examined. Fig. 4.22 shows the conductivity profiles for three batches each containing three monoliths and each batch being synthesised in a capillary of different internal diameters.
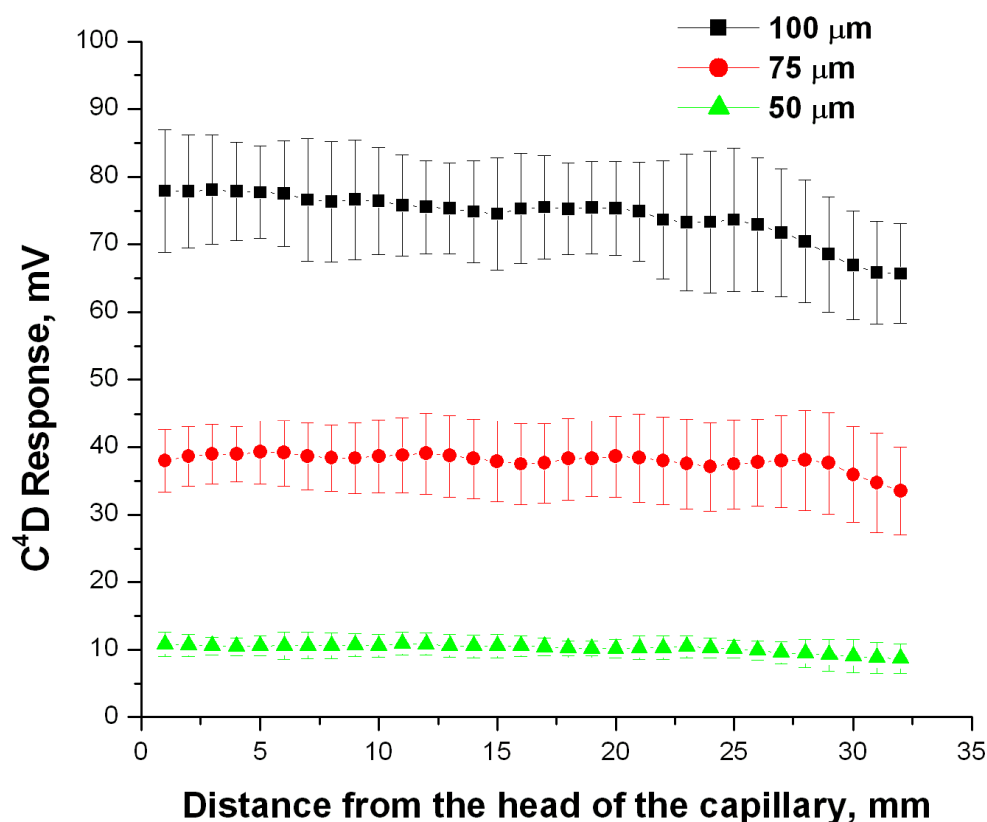
Figure 4.22: *Average lateral conductivity profiles of batches of poly(MMA-co-EDMA) monoliths, n=3 in each batch, made in 100 µm, 75 µm and 50 µm i.d. polyimide coated fused silica capillary*

It is quite clearly seen from the plot that the monoliths were homogeneous along their length with the RSD for the batch being 4.62% for the 100 µm i.d. capillaries, 3.23% for

the 75 µm i.d. capillaries and 5.83% for the 50 µm i.d. capillaries. All batches showed homogeneous monolith synthesis which was reproducible from column to column. It is also clear from the plot that as the internal diameter decreases so does the response from the detector, indicating an increase in the density of the stationary phase. As the same concentration of monomer (40%) is growing in capillaries of decreasing diameter, the monolith is likely to be more dense as the capillary diameter gets smaller, which is shown clearly in Fig. 4.22.

With the lateral conductivity profiling of the monolithic stationary phases, the preliminary characterisation is complete. The final part of the characterisation is the most important and shows the application of the three different stationary phases.

4.3.2.5. Applications of synthesised monolithic materials

Poly(GMA-*co*-EDMA) can often be a charged polymer due to the ease of cleavage of the epoxy ring on the surface to generate a diol in acidic media and an O$^-$ group in basic media. This can be problematic for separations applications as a change in pH can cause a change in surface charge. This type of polymer is more often used as a base monolith for further modification as the epoxy ring is easily modified by a number of wet chemical methods to impart a range of different functionalities on the monolithic stationary phase, as was described in the Section 1.5.

In this study the surface of the poly(GMA-*co*-EDMA) was not modified further but, keeping a constant pH, the surface was hydrolysed to produce negative charges in the form of O- groups and the stationary phase was applied as an electroosmotic pump. For this purpose, lengths of the hydrolysed poly(GMA-*co*-EDMA) monoliths were encased in PMMA micro-fluidic chips as was described in Section 4.2.4.4.

After the chip was fabricated and the capillaries encased in the channels, PEEK tubing was glued into the reservoirs which were milled on the chip. The PEEK tubing served as inlet and outlet tubing. This was then connected *via* peristaltic tubing (inlet) and a three-way adapter (outlet) to homemade solvent reservoirs consisting of a 2 ml vial with a 1 cm length of PEEK tubing inserted in the bottom of the vial. The third arm of the three-way adapter was connected again *via* peristaltic tubing to a nano-flow sensor. The

tubing height was kept at the same level as the solvent in the reservoirs so no gravity driven flow can occur. Finally two platinum electrodes were placed in the vial caps so that the platinum was fully immersed in the electrolyte. A schematic of the chip after all the connections had been made is shown in Fig. 4.23.
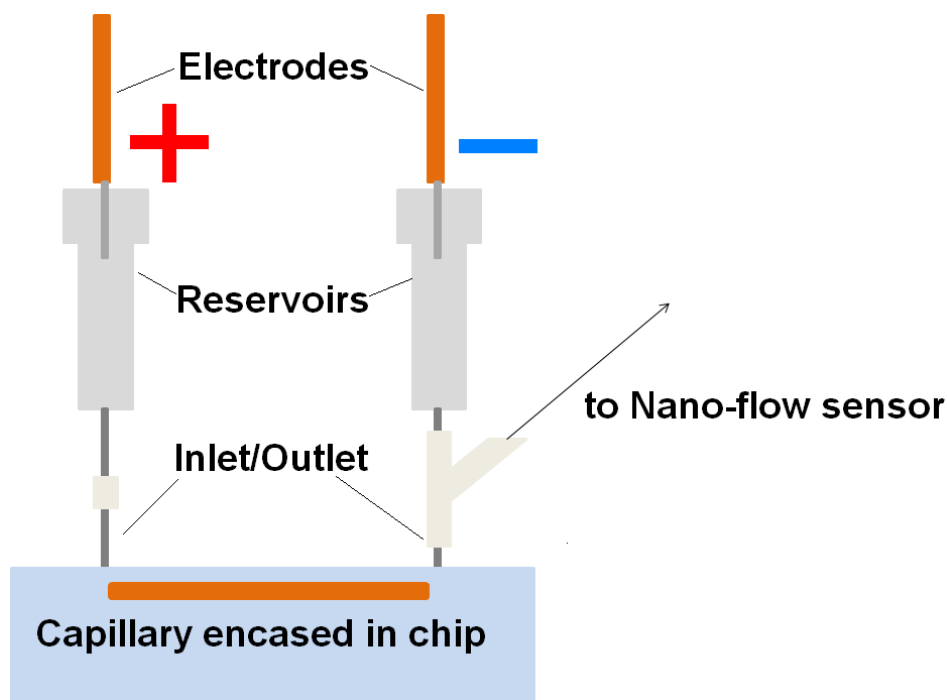
Figure 4.23: *Schematic of the electroosmotic pump after all the capillaries had been encased and the necessary connections had been attached for generation of electroosmotic flow within the channels*

The electrodes were connected in the normal manner (for generation of normal electroosmotic flow, EOF), that is the current passes from the positive to the ground electrode, denoted in the schematic by the negative symbol (Fig. 4.23).

The monolith was flushed with 1 M NaOH for 3 h to attack the epoxy ring of the GMA and produce negative charges on the surface which should create electroosmotic flow. As the surface has been hydrolysed the monolith holds a negative charge on the pore surface, the counter-ions, i.e. positive ions, in the phosphate buffer used for the generation of the EOF move towards the negative electrode and generate cathodic

electroosmotic flow. The pH of the phosphate buffer is 11, keeping the monolith in basic media and therefore maintaining the negative charge.

An electric field ramp was applied to the monoliths encased in the micro-fluidic chip in the range 0-250 kV/m over 15 min. With each increase in the applied field the rate of electrolyte flow generated by the poly(GMA-*co*-EDMA) monolith increased also up to a maximum flow rate of 274 nl/min, (Fig. 4.24). For comparison, an unmodified commercial silica C18 monolith as EOP has been shown to give a flow rate of approximately 160 nl/min with 2 mM NaCl buffer at 2 kV [27], therefore the value obtained with the modified poly(GMA-*co*-EDMA) monolith shows an acceptable performance as an EOP. When the flow rate was measured without modification of the monolith, a negligible flow rate was obtained regardless of the voltage applied.
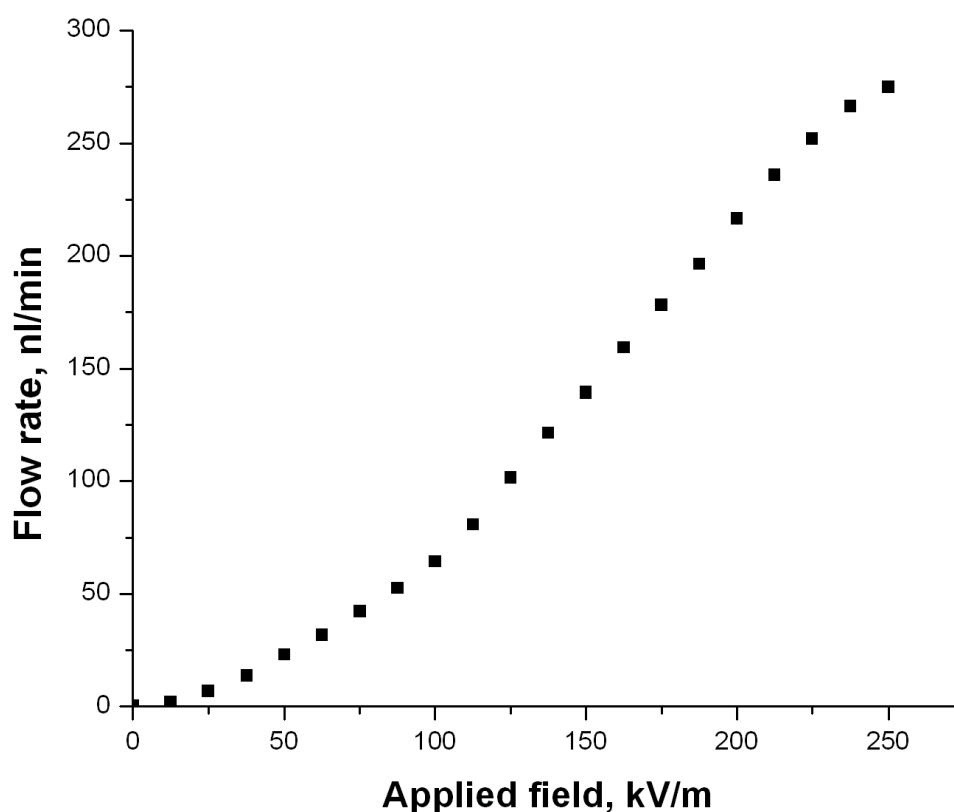
Figure 4.24: *Plot of applied voltage (kV/m) vs. flow rate (nl/min) for a poly(GMA-co-EDMA) monolith in polyimide coated fused silica capillary*

The ability to generate electroosmotic flow using the poly(GMA-*co*-EDMA) monoliths encased within PMMA micro-fluidic chips is a positive step and shows that not only can the monoliths be synthesised but they can also be applied in electrochromatography.

The next step would be to see if the monoliths synthesised by this visible polymerisation method can be used chromatographically also. Despite their usefulness as a base for further functionalisation to create tailored monoliths for specific separations, poly(GMA-*co*-EDMA) monoliths are generally not used themselves in chromatography due to unsuitable surface chemistry for a number of separations methods. For this reason the poly(MMA-*co*-EDMA) monoliths and poly(BuMA-*co*-EDMA) monoliths were synthesised, these monoliths can be more easily used as chromatographic stationary phases due to their increasingly hydrophobic surfaces which can be used in reversed phase chromatography.

4.3.2.6. Application of poly(MMA-*co*-EDMA) and poly(BuMA-*co*-EDMA) monoliths for the separation of proteins

The poly(MMA-*co*-EDMA) monoliths were tested for their ability to separate a mixture of test proteins as the final characterisation of the monolithic stationary phases, The test protein mixture used consisted of ribonuclease A, cytochrome C, myoglobin and ovalbumin. This protein mixture is typically separated using a more hydrophobic stationary phases, however poly(MMA-*co*-EDMA) has a slightly hydrophobic character and therefore it should be possible to determine four peaks even if they are not fully baseline resolved.

An example of the separation of a 0.1 mg/ml mixture of the test proteins is shown in Fig. 4.25. This separation is carried out on a 100 µm i.d. poly(MMA-*co*-EDMA) monolith to give a demonstration of the ability to use these monoliths in separation science. The 75 µm and 50 µm capillaries are not shown here; however, having the same surface chemistry their separation efficiency will be the same assuming some simple modifications are made to the separation conditions. The flow rate must be scaled down when smaller i.d. capillaries are used in order to ensure the same linear velocity through the column, along with a reduction in sample volume, which prevents sample overloading.
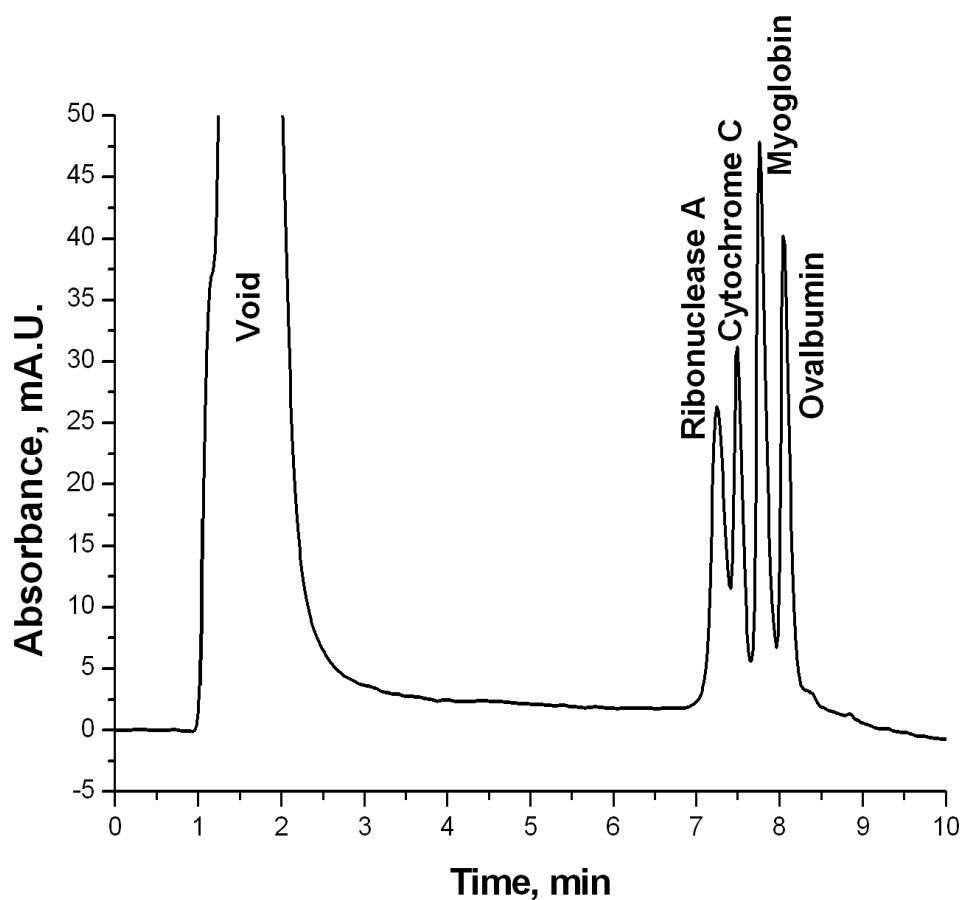
Figure 4.25: *Example of a separation of a mixture of proteins using a poly(MMA-co-EDMA) monolith in 100 μm i.d. capillary. Peaks (in order of elution) are ribonuclease A, cytochrome C, myoglobin and ovalbumin. Separation was carried out at a flow rate of 0.774 μl/min, a gradient of 0-60% 0.1 vol.% formic acid in acetonitrile was performed in 3 min and peaks were detected at 210 nm*

To determine the repeatability of the separation from run to run and column to column the k, or retention factor, is calculated using Eq.4.4;

$$k = \frac{t_m - t_0}{t_0} \qquad (4.4)$$

Where t_m is the elution time of the peak in question and t_0 is the elution time of the void marker.

This equation allows the calculation of the time necessary for the peak to elute after the void marker. This should be similar for separations of the same type on columns of the same surface chemistry. The average k, along with standard deviation and RSD, for each of the peaks is shown in Table 4.2. It is clear from the tabulated data that the separation is repeatable over the entire batch of columns as the maximum RSD observed is 3.69% for the ovalbumin peak.

Table 4.2: *Comparison of retention factors with SDs and RSDs for a batch of poly (MMA-co-EDMA) monoliths, n=3, in 100 μm i.d. polyimide coated fused silica capillaries*

Peak	k ± SD	% RSD
Ribonuclease A	5.8 ± 0.063	1.08
Cytochrome C	6.05 ± 0.084	1.38
Myoglobin	6.44 ± 0.228	3.54
Ovalbumin	6.74 ± 0.249	3.69

Looking back at Fig. 4.25, as was expected four individual peaks can be seen on the chromatogram, however the peaks are not completely resolved from one another. The actual resolution of each of the peaks from their nearest neighbour was calculated using Eq.4.5;

$$R_s = \frac{2(t_{r1} - t_{r2})}{1.7(W_{h,1} + W_{h,2})} \qquad (4.5)$$

Where t_r is the adjusted retention time ($t_r = t_m - t_0$) for each of the two peaks and W_h is the full width at half the peak maximum (FWHM).

FWHM was obtained for each peak using the peak integration function in the data analysis software, Origin 8.1. The values obtained from these calculations are presented in Table 4.3 along with standard deviation and RSD values. It is clear from both the chromatogram (Fig. 4.25) and the calculated resolution that the ribonuclease A and cytochrome C peaks are not sufficiently resolved, with an average resolution of 0.896.

The resolution of the cytochrome C/myoglobin and myoglobin/ovalbumin peaks is more acceptable being above 1 at 1.204 and 1.151 respectively.

Table 4.3: *Comparison of peak resolution with SDs and RSDs for a batch of poly (MMA-co-EDMA) monoliths, n=2, in 100 μm i.d. polyimide coated fused silica capillaries*

Peaks	Average Rs
Ribonuclease A/Cytochrome C	0.896
Cytochrome C/Myoglobin	1.204
Myoglobin/Ovalbumin	1.151

Despite being able to identify four individual peaks from the chromatogram, it is clear that this is not the optimal stationary phase for this separation or at least not the optimal elution conditions. The proteins that have been chosen as the test analyte are more suited to a more hydrophobic stationary phase such as the poly(BuMA-co-EDMA) monoliths. This separation was carried out on a poly(MMA-co-EDMA) monolith simply to give a comparison with the poly(BuMA-co-EDMA) and show that the poly(BuMA-co-EDMA) was better suited to the separation of proteins under the test conditions used.

The elution profile used for the poly(MMA-co-EDMA) monoliths was modified slightly for the separation on the poly(BuMA-co-EDMA) monoliths in order to optimise the separation and have the best resolution possible. An example of a separation of the same mixture of test proteins is shown in Fig. 4.26. It is quite clear from the chromatogram presented here that using poly(BuMA-co-EDMA) monoliths is a distinct improvement on the use of poly(MMA-co-EDMA) monoliths (Fig. 4.25) for the separation of the proteins.
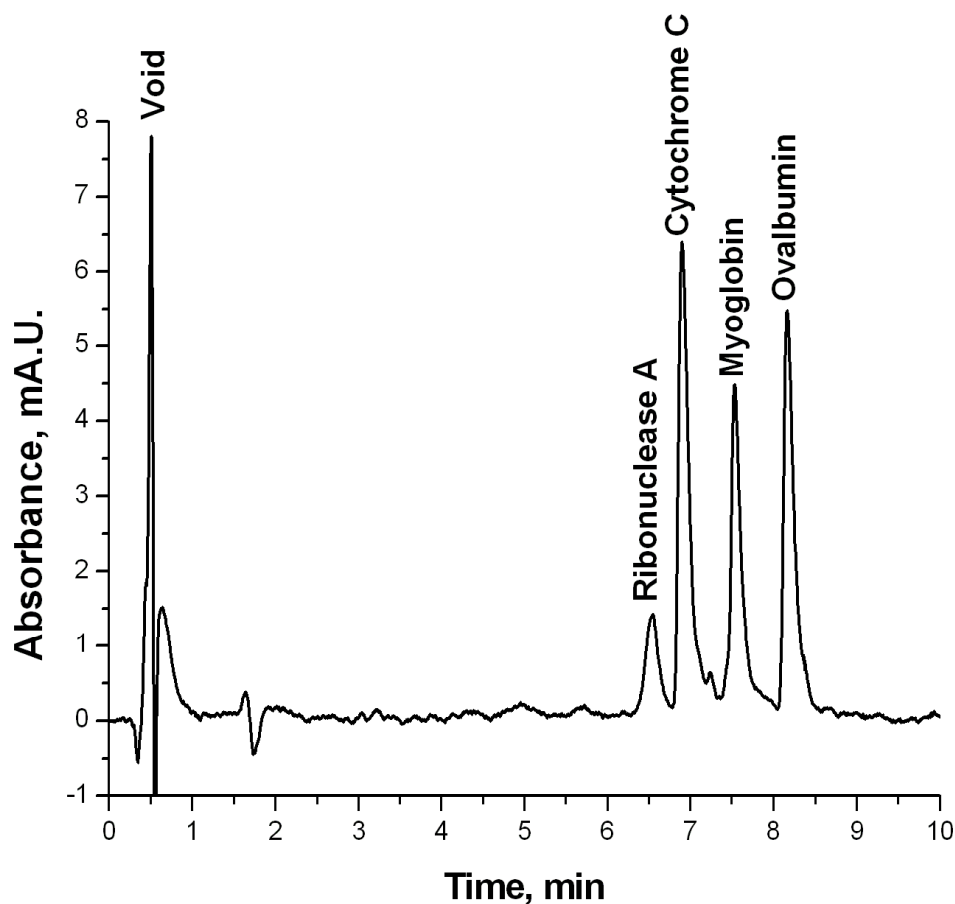
Figure 4.26: *Example of a separation of a mixture of proteins using a poly(BuMA-co-EDMA) monolith in capillary. Peaks (in order of elution) are ribonuclease A, cytochrome C, myoglobin and ovalbumin. Separation was carried out at a flow rate of 1 µl/min, gradient of 0-60% 0.1 vol.% formic acid in acetonitrile in 5 min, UV detection was at 210 nm*

Again retention factors were calculated and are presented in Table 4.4. It can be seen from this table that this separation has a very high repeatability between runs and between columns with the maximum variance at only 0.53%. Nischang *et al.* [224] have performed the separation of the same mixture of proteins on poly(BuMA-*co*-EDMA) monoliths synthesised by thermal initiated polymerisation and the retention order of the proteins shown in Fig. 4.26 correlates very well with the retention data they presented in

their paper. This indicates that this is a robust method which can produce similar results to the well studied methods already presented in the literature.

Table 4.4: *Comparison of retention factors with SDs and RSDs for a batch of poly (BuMA-co-EDMA) monoliths, n=4, in 100 μm i.d. polyimide coated fused silica capillaries*

Peak	k ± SD	% RSD
Ribonuclease A	6.01 ± 0.024	0.39
Cytochrome C	6.41 ± 0.034	0.53
Myoglobin	7.00 ± 0.032	0.45
Ovalbumin	7.67 ± 0.039	0.51

It is quite clear from the chromatogram in Fig. 4.26 that the peaks are well resolved, however, for comparison with the poly(MMA-*co*-EDMA) monoliths the resolution of each of the peaks from their nearest neighbour was calculated and is presented in Table 4.5. All of the values are higher than 1.5 confirming that each of the peaks is fully baseline resolved, the variance of the resolution is also lower than 10% indicating sufficient repeatability of the resolution of the peaks.

Table 4.5: *Comparison of peak resolution with SDs and RSDs for a batch of poly (BuMA-co-EDMA) monoliths, n=4, in 100 μm i.d. polyimide coated fused silica capillaries*

Peaks	Rs ± SD	% RSD
Ribonuclease A/Cytochrome C	1.71 ± 0.159	9.28
Cytochrome C/Myoglobin	2.96 ± 0.146	4.94
Myoglobin/Ovalbumin	2.94 ± 0.158	5.38

Clearly from the data obtained from the separation of the proteins on these two types of monolithic stationary phase show that the poly(BuMA-*co*-EDMA) is more suited to the separation of proteins than the poly(MMA-*co*-EDMA) monolith. As these separations

were carried out in gradient mode it is not possible to calculate and compare column efficiency values however from the elution profile and the resolution it can be seen that it is possible to separate this mixture of 4 proteins on a poly(BuMA-*co*-EDMA) monolith within 8 min with full baseline resolution which is a short run time in which to achieve well separated peaks. In the case of the poly(MMA-*co*-EDMA) monoliths, while their suitability for this type of separation is lower, the peaks are symmetrical and the resolution is, for the most part, within the acceptable range, showing that in principle the quality of the stationary phase is suited to separations applications. They may also be well suited to use as an underlying scaffold for grafting layers of biologically active compounds, an application that is becoming more popular in the literature, due to their lower hydrophobicity, which can prevent non-specific interactions.

Having shown that the polymerisation of methacrylate monoliths within polyimide coated fused silica capillaries of a variety of internal diameters is possible using red light and a specially tailored initiating system and that the resulting monoliths are of a high quality and can be applied in both chromatography and electrochromatography, it was decided to investigate this method of polymerisation in alternative polyimide moulds. In the following section the examination of the polymerisation of poly(BuMA-*co*-EDMA) monoliths within the channels of a specially designed polyimide micro-fluidic chip is presented.

4.3.3. Monoliths in the channel of polyimide micro-fluidic chips

After it had been shown that full methacrylate monolithic stationary phases could be produced in polyimide coated fused silica capillaries in relatively short times with high reproducibility, it was decided to try this method using different moulds. For this a limited number of polyimide micro-fluidic chips were designed and provided for use with the Agilent 1100 series Chip-LC. These chips are made entirely of polyimide with no other substrate beneath the polyimide. The polyimide layers above and below the channel are approximately 150 µm thick and the channel itself is 200 µm square. From the plot of transmission *vs.* thickness (Fig. 4.5 and Fig. 4.6B) it can be estimated that with this thickness of polyimide approximately 55% of the light from the LED will be able to pass into the channel to initiate polymerisation. Following the procedure

described in the experimental section above two 660 nm LEDs were placed above a 1 cm length of exposed channel filled with BuMA-EDMA pre-polymer solution, which had been masked with black tape to obtain sharp edges of the polymer within the channel. An optical micrograph of the channel after polymerisation is shown in Fig. 4.27.
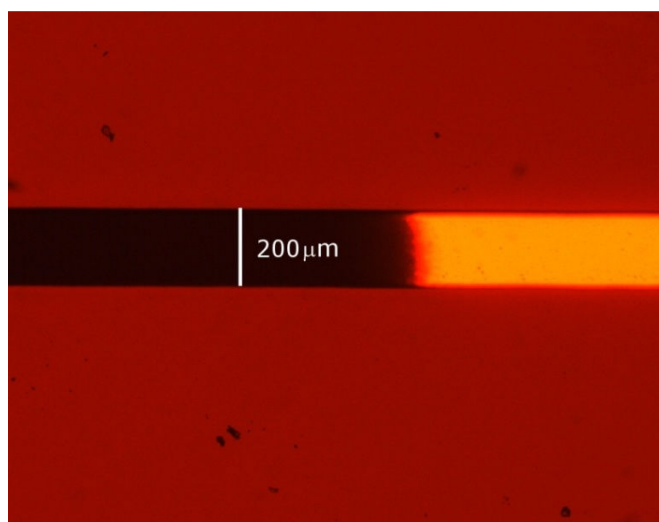
Figure 4.27: *Optical micrograph of poly(BuMA-co-EDMA) monoliths in a polyimide micro-fluidic chip*

The optical micrograph of the channel in Fig. 4.27 shows that sharp edged monoliths are easily obtainable within the channel using this simple photo-mask allowing short plugs of the desired stationary phase to be formed. It can also be seen that the un-masked part of the channel is completely filled with the monolith, there are no apparent voids indicating a good quality stationary phase.

Scanning electron microscopy allowed confirmation of the good quality of the monolith within the channel. Fig. 4.28 shows the poly(BuMA-*co*-EDMA) monolith within the channel, the monolith possesses the characteristic macroporous, globular morphology associated with monolithic stationary phases. The monolith is also well attached to the walls and the channel is completely filled. This indicates that the stationary phases should be suited to applications in LC.
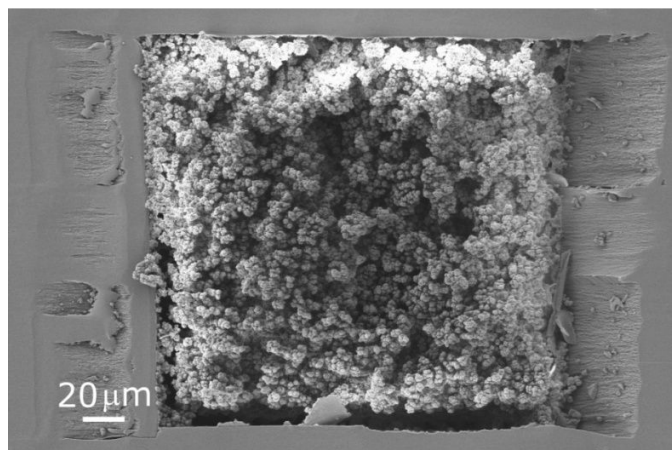
Figure 4.28: *Scanning electron micrographs of poly(BuMA-co-EDMA) monoliths in the channel of a polyimide micro-fluidic chip*

To determine the homogeneity and the suitability for separations applications the chip was attached directly to the LC instrument and the separation of mixtures of standard proteins was attempted. Fig. 4.29 shows an example of a separation obtained on this stationary phase and it can be seen that it is an example of a protein separation with poor efficiency, especially compared to the higher quality separations obtained in capillaries and presented previously. While peaks for the four different proteins are visible on the chromatogram, the peak shapes are very poor. This peak tailing and spreading is likely due to voids in the stationary phase.
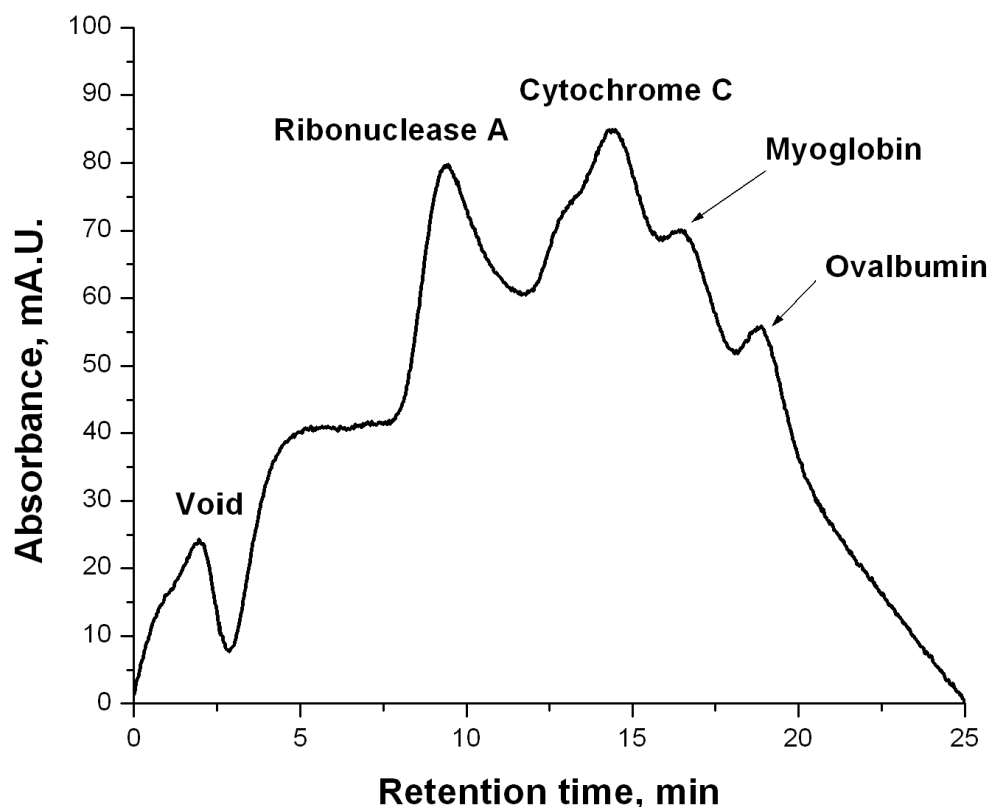
Figure 4.29: *Example of a separation of a mixture of proteins using a poly(BuMA-co-EDMA) monolith in a polyimide micro-fluidic chip. Peaks (in order of elution) are ribonuclease A, cytochrome C, myoglobin and ovalbumin. Separation was carried out at a flow rate of 1 µl/min, gradient of 0-60% 0.1 vol.% formic acid in acetonitrile in 20 min, UV detection was at 210 nm*

Examination of the channel using optical microscopy did not show evidence of voids in the channel however the method of sealing the channel for polymerisation so that there is no evaporation of solvent during the polymerisation does mask approximately 1mm of channel just before the outlet to the detector. While 1 mm is a relatively small amount in general terms, compared to the size of the channel this is quite a substantial gap for chromatographic separations and would be enough space to allow the peaks to begin to disperse before reaching the detector. This dispersion of the separation bands would then cause the peak shapes clearly observable on the chromatogram in Fig. 4.29. Due to limited time and a limited number of chips available, this problem was understood but could not be corrected before this research project was finished. It is hoped that there

will be further collaboration with the chip producer in the future and other methods of solving this problem can be examined.

At this stage, what can be concluded from this work is that it is possible to synthesise good quality monolithic stationary phases within the channels of polyimide micro-fluidic chips, with further modifications these monoliths should be well suited to applications in the separation of bio-molecules.

4.3.4. Photo-initiated grafting onto monolithic scaffolds using visible light

The final application of this initiation method investigated during this research project and one of its most useful advantages is the ability to graft chromophoric monomers onto the surface of pre-existing monolithic scaffolds. Dyes are often used in chromatography for the creation of affinity stationary phases and they are immobilised on the surface through a number of methods including wet chemical methods and a combination of photo-grafting and wet chemical immobilisation techniques. Due to the strong absorbance of the majority of dyes in the UV region it is not possible to photo-graft monomeric dyes onto monolithic scaffolds directly using the current state of the art, as this is done with UV light. Using this novel three-component initiating system it has been possible to photo-graft a monomeric spiropyran dye (shown previously in Chapter 3, Fig. 3.9) onto the surface of a poly(BuMA-*co*-EDMA) monolith using a one step procedure. The spiropyran in its coloured, merocyanine form has a maximum in the visible region at 540 nm and no specific absorbance above 600 nm. The initiating system absorbs at 660 nm and therefore there will be no competition between the initiator and the monomer for the photons from the initiating light source, Fig. 4.30.
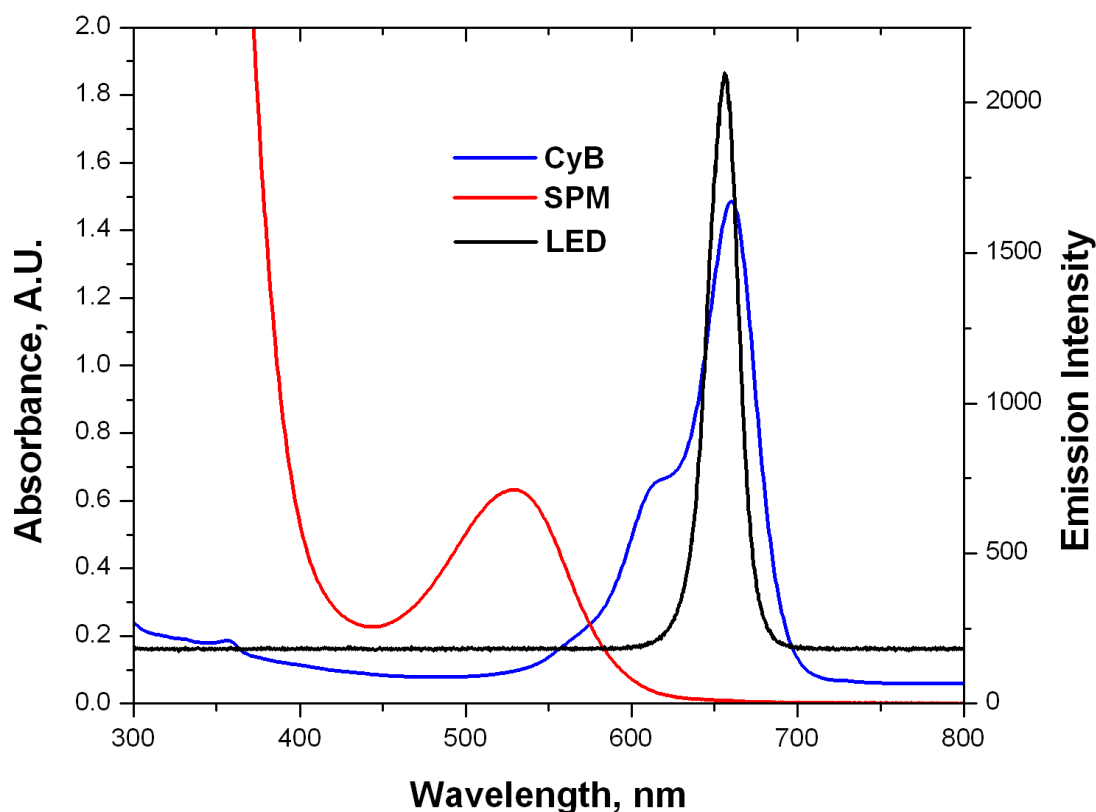
Figure 4.30: *Absorbance spectra of a monomeric spiropyran dye (SPM) and the initiator (CyB) overlaid with the emission spectrum of a 660 nm LED*

A one-step procedure was used to photo-graft a layer of spiropyran monomer onto the surface, unlike the process described in Section 2.2.4.7, where the grafting involved two steps. In this one-step procedure the spiropyran monomer, initiator and solvent were mixed together and filled into the pores of a poly(BuMA-*co*-EDMA) monolith in PTFE coated fused silica capillary and irradiated for 2 h with a 660 nm LED. After flushing with methanol to remove the grafting solution the monolith was flushed for another hour with methanol to see if the faint pink colour on the surface of the monolith could be removed. Copious washings with polar solvents are known to remove non-covalently bound spiropyran from the monolith surface (spiropyrans were covered in great detail in Chapter 3), however the faint pink colour remained indicating that the spiropyran is covalently bound to the monolith surface (Fig. 4.31). Due to the faintness of the pink colour it was difficult to pick it up in a photographic image, however under irradiation

with UV light the merocyanine form of the spiropyran fluoresces strongly and a clear photographic image could be obtained, Fig. 4.32.
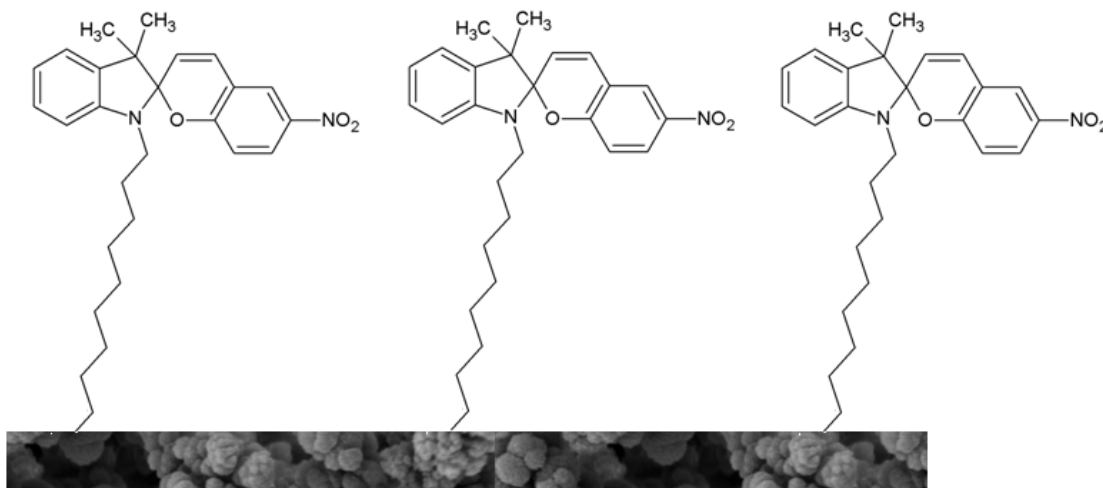
Figure 4.31: *Schematic of the grafting of the spiropyran monomer onto the surface of a poly(BuMA-co-EDMA monolith*
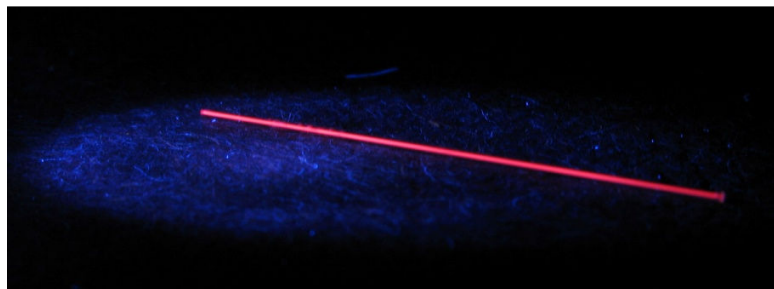
Figure 4.32: *A photographic image of a poly(BuMA-co-EDMA) monolith in a poly(tetrafluoroethylene) coated fused silica capillary after photo-initiated surface grafting of a monomeric spiropyran dye using 660 nm LEDs*

As mentioned in the introduction (Section 1.6.1), spiropyrans are photochromic molecules which change their colour in response to irradiation with different wavelengths of light. In the spiropyran form the molecule is colourless and in the merocyanine form it is intensely coloured. In polar solvents the merocyanine form is a strong pink colour. After photo-grafting the spiropyran monomer onto the surface of the monolith reflective absorbance spectroscopy was carried out to see if the grafted dye

still retains its ability to switch. The reflective absorbance spectra were taken using the same procedure and the same instrumentation as described in Section 3.2.4.14.
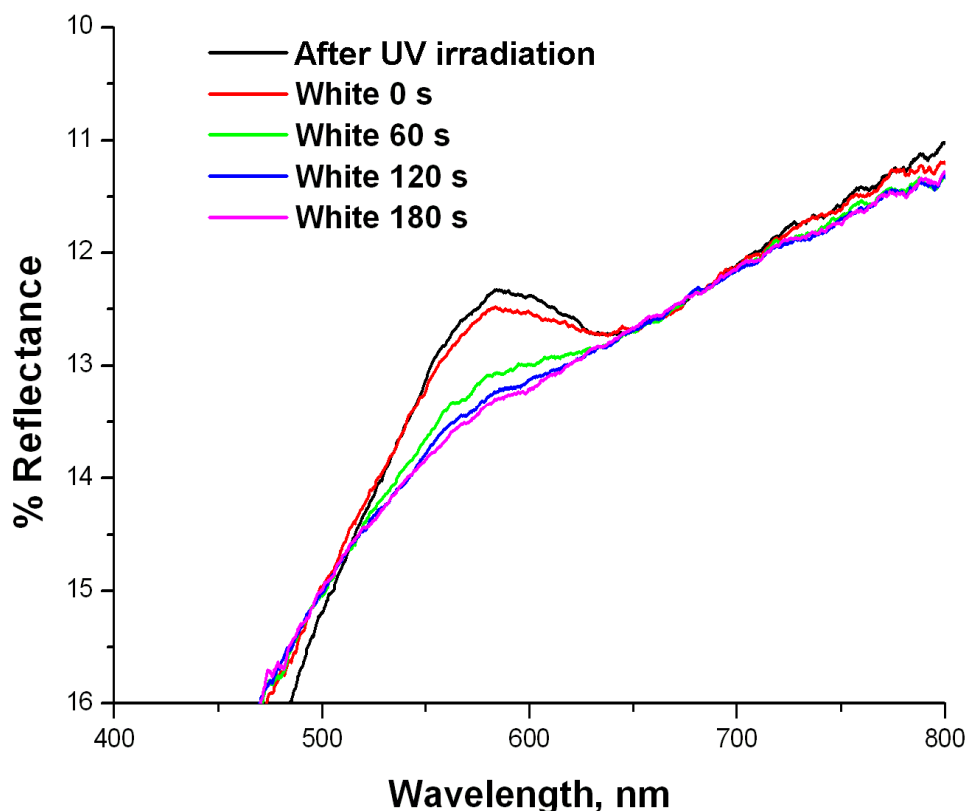
Figure 4.33: *Reflective absorbance spectra of a poly(BuMA-co-EDMA) monolith in a poly(tetrafluoroethylene) coated fused silica capillary after photo-initiated surface grafting of a monomeric spiropyran dye using 660 nm LEDs. Measurements were taken by S. Scarmagnani*

Fig. 4.33 shows the reflective absorbance spectra of the monolith with the grafted layer of monomeric dye. The black line shows the surface response after 2 min irradiation with UV light, it can be seen that an absorbance band is present at 560 nm, which is approximately the same as the absorbance maximum of the dye in solution before the grafting. The other four spectra show the response of the modified monolith surface after turning of the UV light (0 sec) and then 60 s, 120 s and 180 s of irradiation with white light. As the irradiation time increases the absorbance band decreases until all the

merocyanine form has been reconverted to the spiropyran. This experiment was repeated three times and similar results were seen each time.

From these preliminary results it can be seen that it is now possible to photo-graft monomers which absorb strongly in the UV region with ease if an initiating system outside the absorbance range of the monomer is found. As this initiation system used in this work absorbs at 660 nm, quite at the far end of the visible spectrum it should be possible to use it for the photo-initiated grafting of a large number of monomers which have absorbance bands less than approximately 600 nm. It has been seen however, from attempts to photo-initiate the polymerisation of styrene's using this method that, despite absorbing strongly in the UV and not in the red region, the photo-initiated polymerisation and grafting of the styrene's using this initiator complex is not possible yet.

4.4. Conclusions

A fully reproducible method for the synthesis of methacrylate monoliths within polyimide coated fused silica capillaries without the need to remove the polyimide coating in order to allow more light penetration was developed during this project. The selection of an initiator, which absorbs at the point in the spectrum where the polyimide is almost transparent to light, was essential in achieving this goal.

By simply modifying the polymerisation time one can obtain similar quality monoliths in moulds of different internal diameters. These monoliths can then be used as electroosmotic pumps, in the case of the poly(GMA-*co*-EDMA) monoliths and for the separation of proteins in the case of the poly(MMA-*co*-EDMA) and poly(BuMA-*co*-EDMA) monoliths with some success.

Once the optimisation of the polymerisation had been carried out in capillary, the polymerisation of poly(BuMA-*co*-EDMA) monoliths within the channels for Chip-LC separations of proteins was investigated. The polyimide layer of the chip is much thicker than that around the fused silica capillaries; yet with an extension in polymerisation time it was possible to fill the channels with monolith which was well attached to the walls.

The monoliths possess the desired porous globular structure and optical micrographs do not show any obvious voids along the channel length. Despite the quality of the monolithic phase there were voids present at the outlet of the channel which in turn contributed to the poor peak shape observed in the chromatographic separations on the chip. A topic for future work resulting from this thesis will aim to improve the filling of the channels at the outlet which should improve the peak shapes and separation ability of the monolith.

As a final application of this initiating technique, the initiator was used to photo-graft a monomeric dye onto the surface of a poly(BuMA-*co*-EDMA) monolith which had been synthesised within PTFE-coated fused silica capillary. The application was deemed successful as permanent light pink photo-switchable layer was obtained on the surface, as this is how the spiropyran dye behaves when immobilised on surfaces.

In the future, the investigation of usefulness of this method for the polymerisation of different types of monomers and for the grafting of other monomeric dyes will also be carried out. Optimisation of the polymerisation in chip to improve peak shape for separations is also an important future tasks.

To summarise, this is the first report in the literature of the synthesis of organic polymer monoliths with visible light initiated polymerisation. The results presented in this chapter show the development of an initiating system which was used to successfully synthesise methacrylate monoliths in a range of polyimide coated capillaries and polyimide chips. From the characterisation carried out these monoliths were of a high enough quality for use in chromatography and electrochromatography. Additionally this method can also be used for the photo-initiated grafting of chromophoric monomers onto monolithic scaffolds.

5. Visible Light Initiated Polymerisation of Styrenic Monoliths Using Blue Light Emitting Diodes

5.1. Introduction

The previous chapter showed one of the advantages of using visible light to initiate polymerisation of monolithic stationary phases. There is one additional disadvantage of photo-initiated polymerisation related to the use of UV light. While there are a large number of UV transparent monomers, for example, the whole range of acrylates and methacrylates, styrenes absorb strongly in the UV region and therefore cannot be polymerised very effectively using UV light. This is illustrated by the scheme in Chapter 2 (Fig. 2.13). Poly(styrene-*co*-divinylbenzene) [poly(S-*co*-DVB)] monoliths are frequently described in the literature and are widely used in chromatography, therefore it would be advantageous to develop a synthesis method whereby styrenic monoliths could be prepared using visible light in place of UV light.

Poly(S-*co*-DVB) stationary phases were first introduced by Horváth *et al.* [225, 226] when they copolymerised styrene (S) and divinylbenzene (DVB) on the surface of pellicular glass beads for the separation of nucleotides. This was followed by Maa and Horváth in 1988 [226, 227] by the synthesis of non-porous particles made entirely of poly(S-*co*-DVB), which were used for the separation of proteins. Today, commercially available porous poly(S-*co*-DVB) beads are largely used in size exclusion chromatography and adsorption processes. A recent development in polymer stationary phases was the introduction of monolithic porous polymers in 1992 [6]. The first poly(S-*co*-DVB) monoliths were prepared using thermally initiated polymerisation to achieve a rigid, macroporous, interconnected polymer structure [6, 15].

Chapter 4 has already introduced the concept of photo-initiated polymerisation in the visible region in order to obtain monolithic stationary phases within non-UV transparent capillaries. A second limitation of photo-initiated polymerisation with UV light is that the monomers must also be UV transparent to avoid competition between the initiators and monomers for photons from the initiating light source. Fig. 5.1 shows the

absorbance spectra of styrene and divinylbenzene in solutions of acetonitrile/1-propanol/1-decanol overlaid with the emission spectra of a 255 nm, a 365 nm and a 470 nm light emitting diode (LED). The concentration of the monomers is approximately 20% of the concentration used in the typical pre-polymer solution for monolith synthesis.
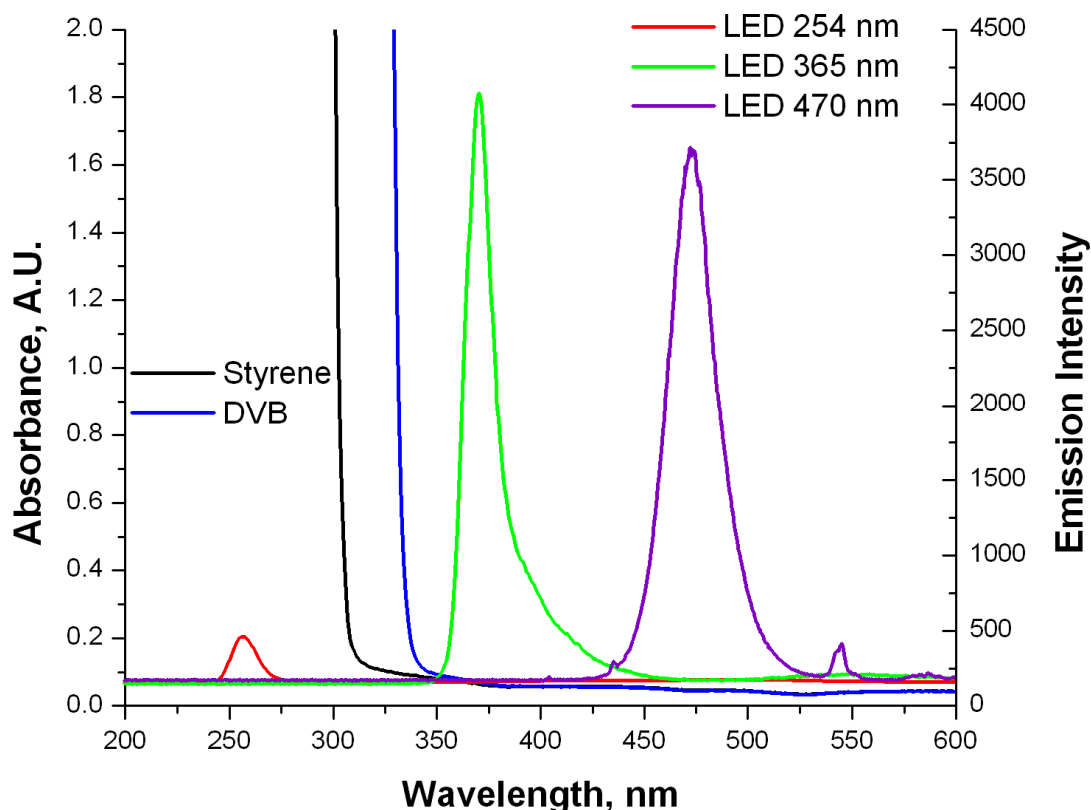
Figure 5.1: *Plot showing the absorbance spectra of styrene (0.51 M) and divinylbenzene (0.41 M) in a solution of acetonitrile/1-propanol/1-decanol (18:36:46) at 20% of the concentration used for the pre-polymer solutions. Overlaid are the emission spectra of a 254 nm, 365 nm and 470 nm light emitting diodes*

It is obvious in Fig. 5.1 that the monomers absorb very strongly in the UV region, up to 330 nm, fully absorbing the emission of the 254 nm LED and, although it is not seen from Fig. 5.1, will show a substantial overlap with the emission of the 365 nm LED when present in the concentrations required for monolith synthesis. This overlap, or potential overlap, can then result in a reduction in initiation efficiency. In contrast, the

emission of the 470 nm LED is sufficiently spectrally resolved from the absorbance of the monomers and therefore is a suitable wavelength at which to initiate the polymerisation of styrenic monomers, provided a suitable initiating system can be exploited.

Theoretically it would be possible to polymerise styrenes using the red light (660 nm) initiated polymerisation method described previously (Chapter 4) as styrenes do not absorb in the red region of the spectrum, however, some practical considerations have to be noted, which hinder the polymerisation of styrenes by this method. Methacrylate monomers, due to their lack of resonance stabilisation, are very easily attacked, leading to the initiation and propagation of polymer chain growth. In Chapter 4 the butyl and methoxy radicals generated on decomposition of the initiator, are of a low and high efficiency, respectively, with both having a low rate of radical transfer [228]. While this is not optimal, in that particular case the limiting factor was the available initiators which absorb in the red region of the spectrum, additionally are reactive enough that even low energy radicals are sufficient to start polymer chain growth. Due to the resonance stabilised structure of the benzene ring, both styrene and divinylbenzene are less reactive than methacrylate monomers. Due to this property higher efficiency radicals, such as AIBN, whose efficiency can be increased with increasing temperature [228], are more suitable for the polymerisation of styrenes. The most commonly available photo-initiators absorb ultraviolet light, however as mentioned previously styrenes absorb strongly in the UV region of the spectrum. Limé and Irgum have previously described the use of AIBN with light at 365 nm to photo-initiate the polymerisation of poly(S-*co*-DVB) beads, however the polymerisation times are unfeasibly long ranging from 24-163 h [229]. This demonstrates why a new initiating system for the more efficient polymerisation of poly(S-*co*-DVB) using light initiated polymerisation is necessary. As one moves further away from the UV region the availability of photo-initiators becomes less, generally most photo-initiating complexes which are activated at longer wavelengths are composed of a dye sensitiser to absorb the light and a co-initiator which receives electrons from the dye by a process called photo-induced electron transfer allowing radicals to be generated. In this case, as we are not limited by the wavelength at which the coating of the capillary absorbs and simply by

the wavelength at which the monomer absorbs, it is possible to examine the blue region of the spectrum when looking for potential initiating systems.

Looking at Fig. 5.1 it can be seen that the spectra of the monomers are well removed from the emission spectrum of a blue light emitting diode with wavelength of maximum emission at 470 nm. Using an initiating system activated at 470 nm combined with a LED at this wavelength would be the most suitable for the polymerisation of styrenes as there would be no competition between the monomers and initiators.

As was mentioned previously most initiating systems in the visible region consist of a dye sensitiser and a radical initiator and generate radicals by photo-induced electron transfer [230]. This case is no different so a search of the literature was performed to determine which dye sensitiser would absorb at 470 nm and would be the most suited to this polymerisation. It is known, particularly in the field of dentistry, that *S*-(+)-camphorquinone (CQ, Fig. 5.2) is an excellent photo-sensitiser for the initiation of free radical polymerisation *via* photo-induced electron transfer when irradiated at 470 nm [231-236]. Oxman *et al.* have studied the use of this sensitiser with a variety of radical co-initiators and found that ethyl 4-dimethylaminobenzoate (EDAB, Fig. 5.2) was the most efficient giving the highest conversion of monomer to polymer in the shortest time [235].
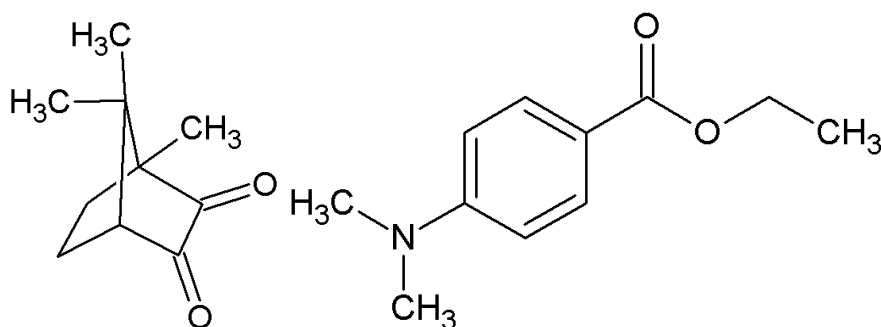
Figure 5.2: *Structure of S-(+)-camphorquinone (left) and ethyl 4-dimethylaminobenzoate (right)*

In this chapter the use of a CQ/EDAB based initiating system for the synthesis of poly(S-*co*-DVB) monoliths using blue LEDs as the photo-initiating light source was

investigated. This investigation involved the optimisation of the initiating system, including the examining of additional co-initiators, optimisation of the porogenic solvent and monomer composition were also important in achieving the end result, that being the successful synthesis of poly(S-*co*-DVB) monoliths in capillary and micro-fluidic chips using light initiated polymerisation. Once the optimisation of the pre-polymer solution has been completed, characterisation of the resulting monolithic stationary phases and their application as stationary phases were investigated and the results are presented in the following sections.

5.1.1. Aims

The main aims for the work carried out in this chapter were;

1. To develop an initiating system with which poly(styrene-*co*-divinylbenzene) monoliths can be synthesised by photo-initiated mechanisms,

2. To characterise the synthesised monoliths and show that they are applicable for bio-molecule separations like poly(styrene-*co*-divinylbenzene) monoliths synthesised by other mechanisms,

3. To show that the method developed can be transferred to other moulds, such as micro-fluidic chips, and that the polymerisation is not confined to fused silica capillaries.

5.2. Experimental

5.2.1. Reagents

1-Decanol (Reagent grade, 99%), 1-propanol (HPLC grade), 3-(trimethoxysilyl)propyl methacrylate (>98%, TMSPM), acetic acid (ACS Reagent 99.7%), acetone (HPLC grade), basic alumina (~150 mesh), cytochrome C from bovine heart, divinylbenzene (80%, DVB), ethanol (HPLC grade), ethyl 4-dimethylaminobenzoate (EDAB), formic acid (ACS Reagent 88%), acetonitrile (HPLC grade), methanol (HPLC grade), myoglobin from equine skeletal muscle, *N*-methoxy-4-phenylpyridinium tetrafluoroborate (MPPB), ovalbumin from chicken egg white, ribonuclease A from bovine pancreas, *S*-(+)-camphorquinone (CQ), styrene (>99%, S) and tetrahydrofuran

(HPLC grade, THF) were all purchased from Sigma-Aldrich Chemical Co. (St.Louis, MO, U.S.A.). All chemicals were used as received with the exception of monomers which were purified before use by passing over a bed of basic alumina.

Water used in these experiments was obtained from a Milli-Q Ultrapure water filtration system from Millipore (Billarica, MA, U.S.A.).

5.2.2. Materials

470 nm Single LEDs and a 470 nm LED array (RLT-MIL470-12B-30) consisting of 12 LEDs emitting at 470 nm with 20 mW of power each were purchased from Roithner LASER Technik (Vienna, Austria).

A motor with variable speed of rotation was used at low speeds (approximately 34 rpm) for the polymerisation of full monoliths in capillary. This motor was purchased from Peats Electronics (Dublin, Ireland).

Poly(tetrafluoroethylene) (PTFE)-coated fused silica capillary, with internal diameter of 100 μm, was obtained from Polymicro Technologies (Phoenix, AZ, USA) and the internal walls were silanised prior to use with 3-(trimethoxysilyl)propyl methacrylate using the same procedure as described in Section 2.2.4.1.

Cyclic olefin copolymer (COC) micro-fluidic chips, with an internal channel of dimensions 0.15 mm x 0.15 mm x 60 mm, were prepared by a collaborator (T. Stachiowak) at the Lawrence Berkeley National Laboratory using procedures described by Mair *et al.* [113, 237].

5.2.3. Instrumentation

Flow resistance measurements and the separation of proteins on monoliths in capillary moulds and in COC micro-fluidic chips were carried out on an Ultimate 3000 nano-HPLC (Dionex Corporation, Sunnyvale, CA, USA).

The decomposition of the dye sensitiser in the presence of different co-initiators was monitored using a Cary 50 UV-Vis spectrometer (Varian Inc., Palo Alto, CA, USA).

Optical micrographs of capillaries were taken with a TE200 optical microscope from Nikon (Tokyo, Japan) or a DM4000 optical microscope from Leica (Wetzlar, Germany), while scanning electron micrographs were taken with an S-3400N Variable Pressure Scanning Electron Microscope from Hitachi (Tokyo, Japan) or an Ultra-55 analytical scanning electron microscope from Carl Zeiss (Jena, Germany).

A Tracedec® capacitively coupled contactless conductivity detector (C^4D) with a 375 µm sensor head from Istech (Vienna, Austria) was used for lateral conductivity profiling. A low pressure infusion pump (KDScientific, Holliston, MA, USA) with a 250 µl syringe (Hamilton, Bonaduz, Switzerland) was used to provide a constant flow of water through the capillary during conductivity profiling. For the micro-fluidic chips, lateral conductivity profiling was carried out with a C^4D from e-Daq (New South Wales, Australia) fitted with a micro-fluidic sensor head. For the profiling, the channels of micro-fluidic chips were filled with water and then sealed.

5.2.4. Procedures

5.2.4.1. Pre-treatment of the PTFE-coated capillaries and COC micro-fluidic chips

PTFE-coated fused silica capillaries were pre-treated using the procedure described in Section 2.2.4.1.

The COC micro-fluidic chips were prepared using the procedure described by Chen *et al.* [26] by first washing the channels with methanol, drying them with nitrogen and then filling them with a solution of 0.2% benzophenone in *t*-butanol:water, which was sonicated for 10 min prior to use. The channels were then irradiated for 5 min at a dose of 11 mW/cm^2. This procedure generates radicals on the walls of the channel, which allow attachment of the growing polymer chains. After irradiation the channels were washed with methanol and dried with nitrogen before filling with the S-DVB pre-polymer solution.

5.2.4.2. Synthesis of poly(styrene-*co*-divinylbenzene) monoliths in PTFE-coated capillary

0.64 mg (3.86 µmol) of *S*-(+)-camphorquinone, 3.2 mg (16.57 µmol) of ethyl 4-dimethylaminobenzoate and 3.2 mg (17.18 µmol) of *N*-methoxy-4-phenylpyridinium tetrafluoroborate were weighed into a vial and dissolved in 130 µl of a mixture of acetonitrile, 1-propanol and 1-decanol in a ratio 18:36:46. The vial was shaken to dissolve all components of the initiator system. 35 µl (305 µmol) of styrene and 35 µl (246 µmol) of divinylbenzene were then added and the solution was sonicated for 20-30 min to ensure complete mixing of the solutions and to remove dissolved oxygen which can interfere with the polymerisation process. All pre-polymer solutions were prepared in amber vials and the polymerisations were carried out in a dark room to ensure no interference by ambient light with the polymerisation reaction. Capillaries were filled with the pre-polymer solution by capillary action. The ends of the capillaries were sealed with rubber septa and black vinyl tape. A combination of black vinyl tape and rubber septa was used to mask the capillaries for polymerisation as rubber septa are very effective in stopping evanescent wave polymerisation and black vinyl tape was necessary as the rubber septa are not long enough to mask the entire length of the capillary where polymerisation should not occur. Capillaries were placed beneath the LED array at a distance of 1 cm and irradiated for a period of 2 h with rotation at approximately 34 rpm. After polymerisation, the capillary was flushed with methanol to remove any remaining pre-polymer solution.

5.2.4.3. Synthesis of poly(styrene-*co*-divinylbenzene) monoliths in COC micro-fluidic chips

The pre-polymer solution used here was identical to that for the polymerisation within the capillary mould. The channels of the chip were filled using a glass syringe connected to a length of 100 µm i.d. capillary which was fitted to one of the nano-ports using micro-tight nuts. The chips were placed 1 cm above the LED array and irradiated for 2 h with blue light. The channels were then flushed using the same syringe as before filled with methanol to remove traces of the pre-polymer solution.

5.2.4.4. Characterisation of the monolithic stationary phases

5.2.4.4.1. Optimisation of the pre-polymer solution

Before polymerisation could be carried out in the capillaries or micro-fluidic chips, which is the ultimate goal of this work, an experimental design programme (MODDE 8.0.2, trial licence, Umetrics, Umea, Sweden) together with a standard data analysis software (Origin 6.0, OriginLab Corporation, MA, USA) was used to determine the optimum composition of initiators and monomers in the polymerisation solution. A series of parameters were input into the programme and a set of experiments were drawn up. The results of these experiments were then input back into the programme and the output was a range of graphical plots which show the conditions that improved the experimental results and those that had a detrimental effect. To simplify the data obtained, the final results from the MODDE software were input into the Origin software and the output was given as a bar chart which is displayed in Section 5.3 below. This format makes the data easier to interpret.

5.2.4.4.2. Initiator decomposition study

After the optimal composition of initiator had been determined the speed of decomposition of the initiator in the porogens was measured. A 20% solution of the sensitiser alone and then with each of the initiators was made up and the spectra were taken with no irradiation and then every 30 min up to 2 h while irradiating constantly with blue light to see the speed of the decomposition and how the decomposition changes when different compounds are present.

5.2.4.4.3. Determination of % conversion

The conversion of monomers was determined by a simple weighing method. The polymerisations were carried out in bulk in clear glass vials, which were weighed empty, then again when the pre-polymer solution had been added and finally when the polymerisation reaction had been terminated and the product had been washed with methanol to remove any unreacted components of the pre-polymer solution. The difference between the weight of the monomer and the weight of the polymer was calculated and the total conversion is recorded as a % of the weight of the dried solid polymer relative to the weight of the monomers. For verification of the process several

samples were selected and the polymerisation was carried out in capillary. When the reaction had been terminated the capillary was flushed with dichloromethane (DCM) into an auto-sampler vial and diluted with 1 ml DCM. GC-FID analysis was performed on the samples to determine whether styrene and divinylbenzene still remained unreacted. The separation was carried out on an Agilent 6890N GC-FID with a temperature ramp of 150-280ºC over 2 min, with separation time of 10 min on a silica-C18 wall coated column 25 m in length.

5.2.4.4.4. Flow resistance measurements

In preliminary experiments the back pressure of the monolithic columns was measured using an Agilent 1200 series HPLC. The flow was measured over the range 5-20 μl/min in increments of 5 μl/min in a step pattern with 100% deionised water with 0.1% formic acid as the eluent. In later experiments it was done with a Dionex Ultimate 3000 nano-LC using the same procedure and increments of 100 nl/min.

5.2.4.4.5. Optical microscopy

After synthesis of the monoliths the porogens were removed from the polymer by flushing with acetonitrile and then air or nitrogen. This approach emphasises the contrast between the empty and filled parts of the capillary in optical microscopy. Optical microscopy was carried out on cuts from all the samples using a Leica DM4000 optical microscope. Most samples were imaged at 20x and 10x magnification. Some samples were also imaged at 50x magnification although with lower resolution.

5.2.4.4.6. Scanning electron microscopy

5-8 mm lengths of the capillary were cut from different places along the length of the capillary. These pieces were then held upright with the surface to be imaged facing upwards. Before imaging the capillaries were sputter coated with a thin layer of gold as the polymer, which is non-conducting, generates a lot of surface charge under the electron beam during imaging which can distort the quality of the micrographs.

To image the channels of the micro-fluidic chips a box knife was used to score a line across the centre of the chip, the chip was then dipped in liquid nitrogen and then snapped along the scored line. The chip was then placed in a special holder from Agar

Scientific (Essex, U.K.) with the exposed channel facing upwards, and then sputter coated with a thin layer of gold before imaging.

5.2.4.4.7. Lateral conductivity profiling

An on-column C^4D cell was placed on the capillary, which is flushed continuously with water during measurement, and moved down the length of the filled capillary at 1 mm increments, the conductivity value was recorded at each interval. A schematic outlining the procedure is shown in Fig. 2.2. While the stationary phase bears no charge, voids in the columns result in an increase in conductivity. The capillaries were flushed constantly with water during the measurement.

The profiling procedure for the micro-fluidic chips was similar to that carried out on the capillaries in that the conductivity in the channel was measured at 1 mm increments. An exception to this was that the capillary detector was replaced with a micro-fluidic chip C^4D platform (Fig. 5.3). The chips were filled with water and then sealed for the duration of the measurements.
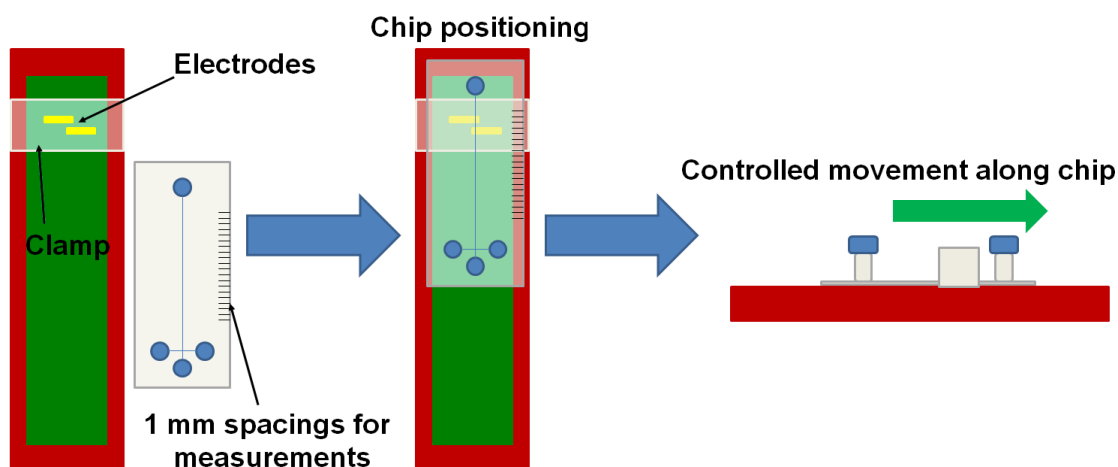
Figure 5.3: *Schematic of the micro-fluidic chip C^4D platform and the conductivity profiling procedure*

5.2.4.4.8. Separation of proteins

Analyses were carried out at a flow rate of 1 μl/min, with an injected sample volume of 50 nl and a detection wavelength of 210 nm. The gradient elution profile consisted of 0.1% formic acid in water (mobile phase A) for 1 min, then 10 min to go from 0-60%

mobile phase B (0.1% formic acid in acetonitrile), 5 min hold, return to mobile phase A in 5 min followed by 5 min conditioning before the next injection. Each separation was run three times on each column.

5.3. Results and Discussion

After fully examining the use of red light to initiate the polymerisation of methacrylates in polyimide moulds and the photo-initiated grafting of chromophoric monomers, and finding that this method was not applicable to the polymerisation of styrenic monomers, the investigation of a method which would allow the photo-initiated polymerisation of styrenic monoliths, using blue light as the initiating light source, was suggested.

5.3.1. Optimisation of polymerisation conditions

5.3.1.1. Binary initiator system - experimental design and conversion study

As mentioned previously, from the literature a photo-initiating system consisting of *S*-(+)-camphorquinone (CQ) as the photo-sensitiser and ethyl 4-dimethylaminobenzoate (EDAB) as the co-initiator was selected as a starting point. A pre-polymer solution consisting of 20% v/v styrene, 20% v/v DVB, 55% v/v 1-decanol and 5% v/v tetrahydrofuran (THF) was chosen from the literature as a starting point for the optimisation procedure, this system is commonly used for the synthesis of poly(S-*co*-DVB) monoliths [6].

Experimental design software is commonly used in industry for the optimisation of chemical processes where more than one variable contributes to the outcome of the polymerisation. Investigations are carried out to determine the effect of each parameter on the outcome of the process. The software used in this study allows the changing of a number of parameters simultaneously, which speeds up the optimisation process. Using more traditional methods, that is without the help of experimental design software, it was necessary to vary each parameter individually. Within the software there are a number of different models which can be used each with a different number of variables which can be investigated at one time. A simple experimental plan was drawn up using the MODDE software. While the percentage of the dye sensitiser was kept constant at

1%, the percentage of the co-initiator was varied from 1-5%, the distance from the LED was varied for 1-5 mm and the time of bulk polymerisation was varied from 20-60 min. The experimental plan took the form shown schematically in Fig. 5.4.
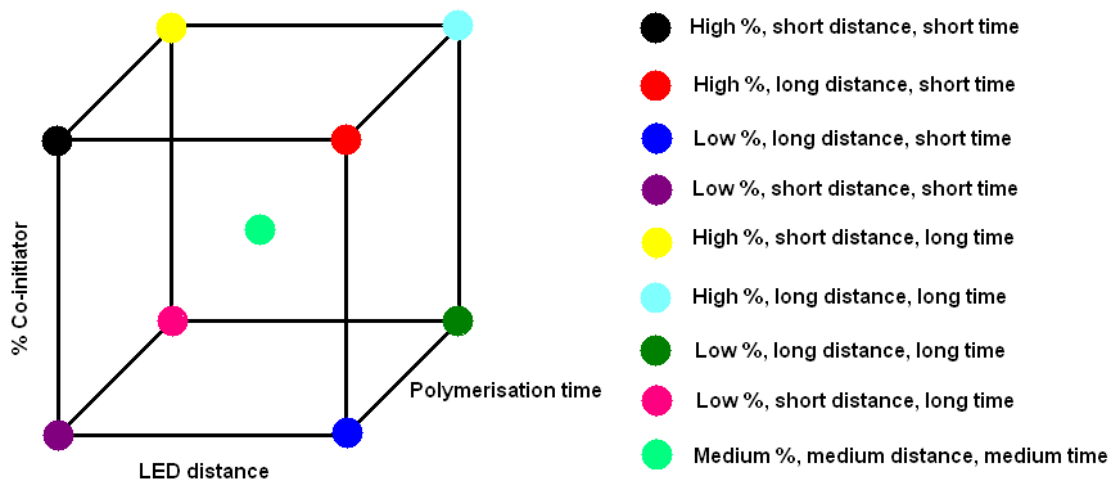
Figure 5.4: *Schematic showing the experimental design scheme*

Each of the experiments was performed using the extremes of the ranges as the high and low values and the mid-point as the medium values. The median point experiment was performed 3 times to get an average of the centre point values. The experimental plan is a simple cube design, with three variable axes. This is the most complicated plan that can be represented graphically in the data analysis software without the help of experimental design software. The parameter used to monitor the optimisation process is the % conversion of monomer to polymer as each contributing factor of the polymerisation process is varied.

The results of the polymerisation experiments are shown as a bar chart with experiment number plotted against % conversion from monomer to polymer. The conversion was calculated using the method described above (Section 5.2.4.4.3). The experiments were carried out in a random nature to avoid batch error by experiments solutions being made from the same batch but irradiated for different times. The results of the experiments are shown in Fig. 5.5.
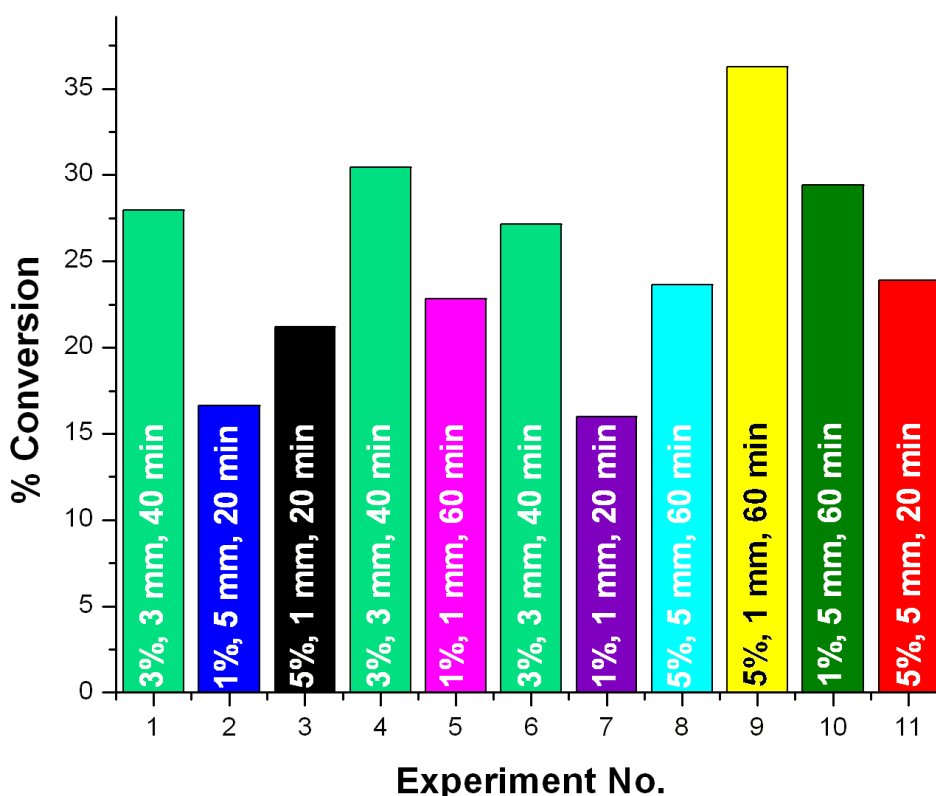
Figure 5.5: *Bar chart showing the % conversion of monomer to polymer for each set of experimental conditions*

The highest conversion of monomers was obtained when 5% of the co-initiator was used and the LED was positioned 1 mm from the vial with the polymerisation allowed to continue for 60 min, however at 35% this is still quite a low conversion. To improve monomer conversion some of the parameters will still need to be optimised. The difference in monomer conversion by increasing the concentration of co-initiator EDAB from 1% to 5% is approximately 13% (23% - 36%). Although this is purely speculative, if every 4% increase of the co-initiator produces a 13% increase in % conversion, 25 wt% EDAB would be necessary to give 100% conversion, meaning 18.25 mg of the initiator would need to be dissolved in the 200 µl pre-polymer solution, which is not feasible. Putting the LED closer than 1 mm to the vial is also quite impossible therefore it was decided that reaction time would be the only variable in the next stage of the polymerisation optimisation. The polymerisation reaction was then carried out at four different times; 60 min, 120 min, 180 min and 240 min. The disadvantage of increasing

the polymerisation time is that this will make it more difficult to control the location of the polymer in PTFE-coated fused silica capillary as this type of mould suffers from a wave-guiding effect described previously in Section 2.3.3.2. With this wave-guiding effect the light tends to travel underneath the photo-mask meaning the monoliths can have diffuse instead of sharp edges, however using rubber septa as photo-masks is sufficient to halt to propagation of light waves along the length of the capillary ensuring the sharp edges are maintained.

Using the optimised pre-polymer mixture (20% styrene, 20% DVB, 55% 1-decanol, 5% THF, 0.73 mg CQ and 3.65 mg EDAB) the polymerisation was once again carried out in clear vials at the four different time periods with the LED array positioned 1 mm and 10 mm from the vial for comparison. The monomer conversion was determined by weighing as before and the values were graphed against polymerisation time (Fig. 5.6).
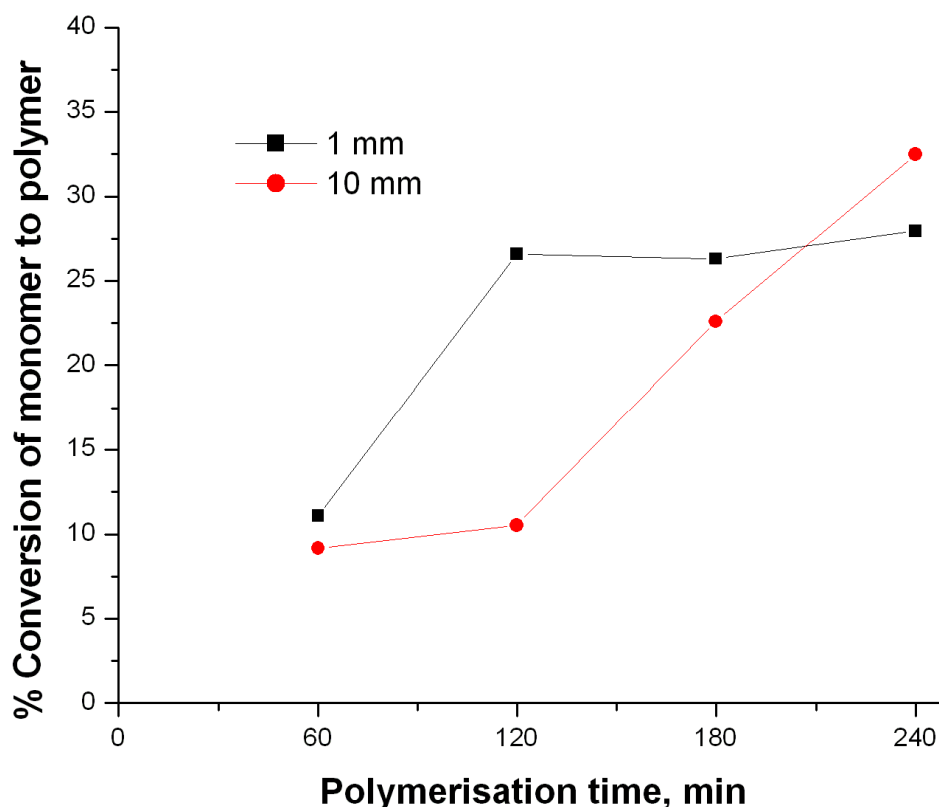
Figure 5.6: *Plot showing the conversion of styrene and divinylbenzene monomers to poly (S-co-DVB) when the polymerisation was carried out in batch in glass vials with 5% EDAB over different time ranges both 1 mm and 10 mm from the LED array*

When the LED is positioned at 10 mm the maximum conversion is 32% while at 1 mm it is 27%, this is even lower than the previous experiments and significantly less than the desired conversion. Additionally, it is contrary to what is expected in that the conversion, within the vials further from the LED, is higher at longer polymerisation times. Nothing definitive can be gauged from the polymerisation in vials; however it does give an indication of the effectiveness of the initiating system and therefore performs a purely qualitative role.

The most important information will only be derived later from the polymerisation within the capillary and eventually chip moulds. To confirm that the polymerisation was not going to completion the pre-polymer solution, which was up to this point the optimal composition, was prepared and filled into pre-treated PTFE coated fused silica

capillaries. The polymerisation was carried out for 30 min, 60 min, 120 min, 180 min and 240 min, with the capillaries held 1 mm and 10 mm from the light source. Using optical microscopy and back pressure measurements as the methods of analysis it was possible to see that the polymerisation was not complete and that the method was not reproducible.

Looking first at the optical microscopy data, it is evident that the results obtained are less then optimal when the two-component initiator was used with 1-decanol and THF as the porogens (Fig. 5.7).
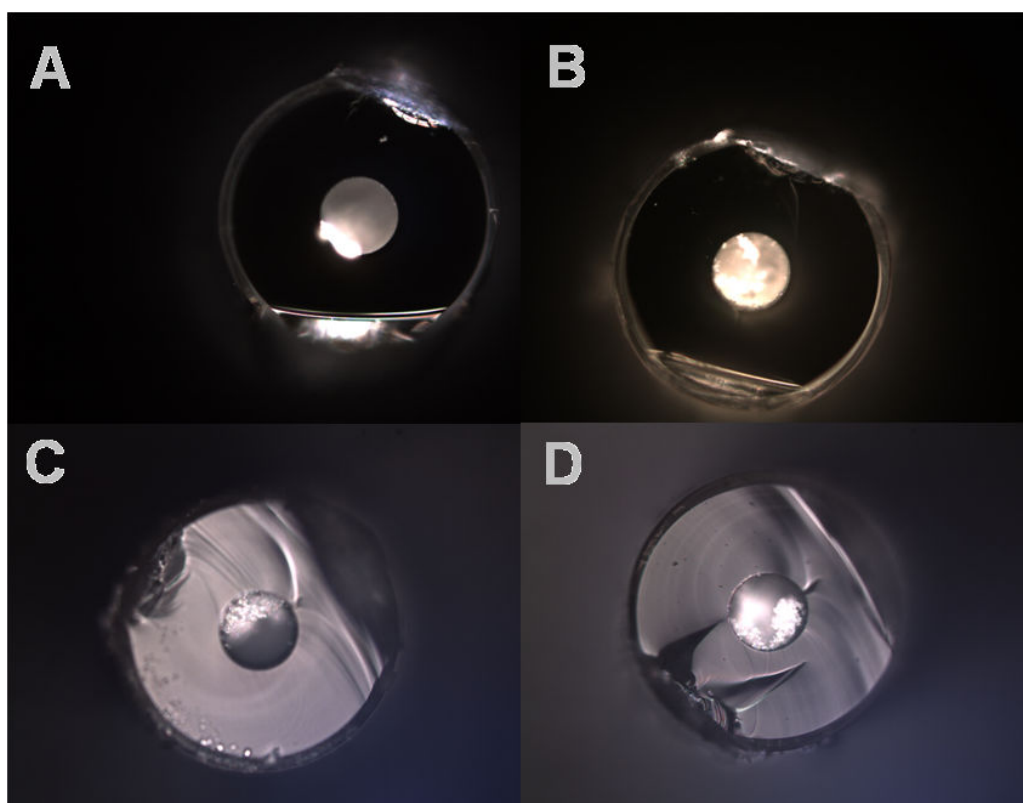
Figure 5.7: *Optical microscope images of monoliths synthesised (a) for 60 min LED 10 mm away, (b) for 240 min LED 10 mm away, (c) for 60 min LED 1 mm away, (d) for 240 min LED 1 mm away*

For the 60 min polymerisations (Fig. 5.7A, C) less than half the visible area of capillary is filled with polymer, while after 240 min (Fig. 5.7B, D) a larger amount of polymer is visible in the cavity, although they are still not completely filled. It is also evident from

the microscope images that rotation of the capillary will be necessary to obtain homogeneous monoliths as in all the images it can be seen that the polymer is mainly on one side of the capillary with little formation on the opposite wall. Rotation of the capillary will allow even distribution of light and radicals throughout the internal cavity and allow for a more homogeneous filling. Some flow resistance measurements of the different monoliths in capillary further highlight the inhomogeneity of the stationary phases obtained so far (Fig. 5.8). The flow resistance measurements for the monoliths synthesised 10 mm from the LED array are shown as an example of the poor quality of the monoliths obtained.
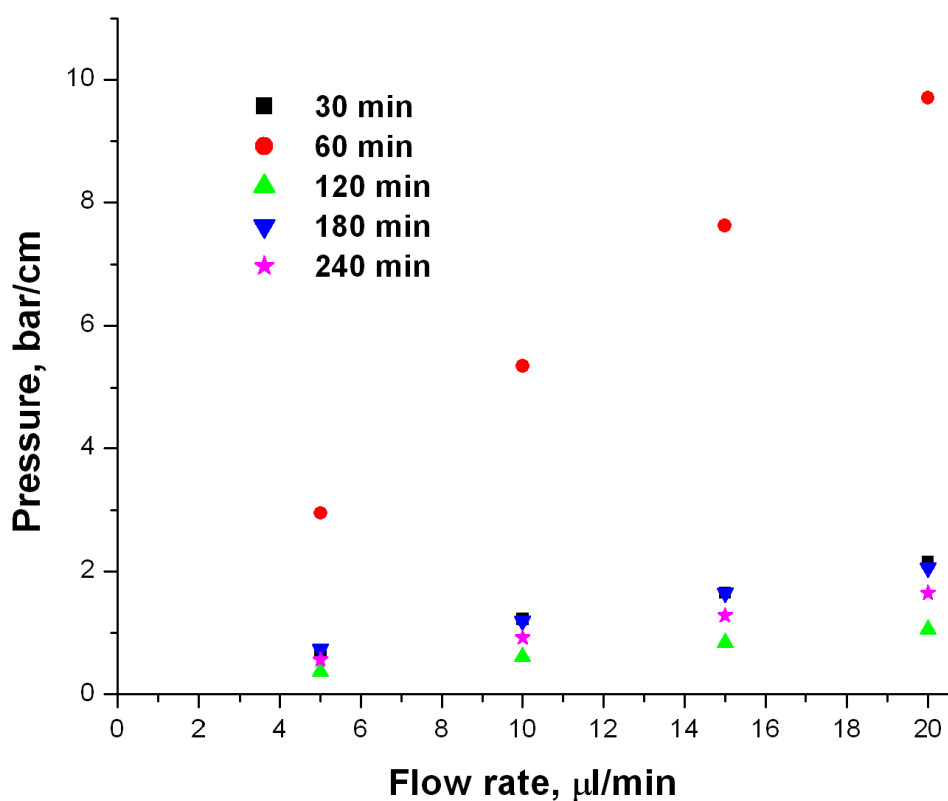
Figure 5.8: *Graph showing the flow resistance vs. polymerisation time for all the monoliths which were polymerised 10 mm from the LED array*

With the exception of the 60 min polymerisation (Fig. 5.8), all the monoliths have quite low back pressures indicating high permeability which in turn confirms what was seen in the optical microscope images, that the capillaries are not completely filled.

Additionally, there is no trend to the increase in back pressure indicating that the synthesis is not very reproducible. Finally to further verify the incomplete polymerisation a batch of monoliths were prepared in capillaries again and after polymerisation the remaining pre-polymer solution was flushed from the capillary using dichloromethane into an auto-sampler vial and then this sample was diluted further with 1 ml of DCM. The samples were analysed by gas chromatography with flame ionisation detection and compared to a standard 1 mg/ml sample of both styrene and divinylbenzene. The results are shown in Fig. 5.9.
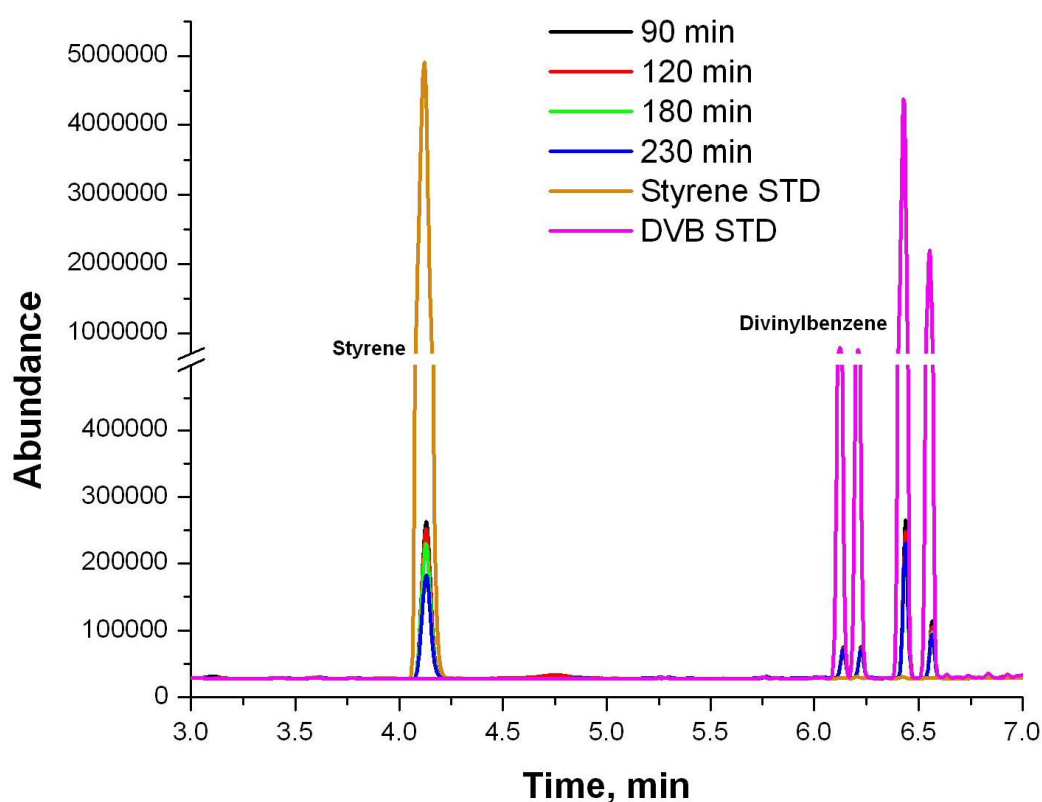
Figure 5.9: *Example of a GC separation of mixtures of styrene and divinylbenzene in dichloromethane before and after polymerisation in capillary. Separation is carried out on a 25 m column with 250 μm i.d. and detection is done with a flame ionisation detector. Separation conditions: temperature ramp of 150-280ºC over 2 min, with separation time of 10 min on a silica-C18 wall coated column.*

In Fig.5.9 four peaks are noted for the divinylbenzene as it is a mixture of four isomers (1,4-divinylbenzene, 1,3-divinylbenzene, 1,4-diethylvinylbenzene and 1,3-diethylvinylbenzene, all of which are shown in Table 0.1). It is clear from the chromatogram that, while the styrene and divinylbenzene peaks are far smaller than the standard peaks they are still present, indicating that the polymerisation does not go to completion. This data along with conversion calculations, optical microscopy and back pressure measurements further confirms that this two-initiator system discussed up to this point is not the most suitable for the polymerisation of S-DVB monomers.

5.3.1.2. Three-component initiator system

In a paper by Oxman *et al.* [235], nine different initiating systems comprising camphorquinone, a tertiary amine electron donor and a cationic diaryliodonium salt were studied for their ability to initiate the polymerisation of epoxides and acrylates. In one example EDAB was used as the electron donor while in a second example THF was used. When EDAB was present the polymerisation was reported to occur within 15 s while no polymerisation was reported when THF was used. It was believed, the presence of the THF was having a detrimental effect on the polymerisation efficiency and the length of time necessary for the polymerisation to go to completion. It is possible that the two electron donors are competing with one another for the electron transfer from the photo-sensitiser or donate electrons between one another and so generate fewer radicals for polymerisation.

Taking these literature results into account THF was removed from the solvent mixture in this work in order to stop this competition between the two electron donors. In addition to changing the composition of the porogenic solvent, a second co-initiator was investigated to see whether the polymerisation time could be brought down from 4 h to less than 2 h. In the previous chapter (Chapter 4) red light was used to initiate the polymerisation of methacrylates within polyimide coated capillary using a cyanine/borate initiator complex along with a second co-initiator, *N*-methoxy-4-phenylpyridinium tetrafluoroborate (MPPB, Fig. 4.11). MPPB has been observed to be very effective in speeding up the polymerisation reaction. This second initiator

decomposes easily to a methoxy radical by electron transfer from a photo-sensitiser and the presence of a second radical species further promotes the polymerisation.

Clearly the CQ/EDAB initiator does initiate the polymerisation of the styrenic monomers to a certain extent, however not enough for the reaction to proceed to completion or even allow the capillary to be completely filled with monolithic stationary phase. Noting from Chapter 4, that MPPB makes a significant improvement to the rate of polymerisation, it was decided to use this salt as an additive to the CQ/EDAB initiating system to try to improve the efficiency of the polymerisation. In Chapter 4, it was discovered that the MPPB does not dissolve in all solvents easily, and as the THF had to be replaced from the previous mixture due to competition with the EDAB, it was decided to replace it with a mixture of acetonitrile and 1-propanol as had already been used in Chapter 4.

Before going too far in the optimisation stage and finding that the composition of the pre-polymer solution was still not optimal an initiator decomposition study was performed. This was done in 3 stages; (1) camphorquinone, (2) camphorquinone/EDAB and (3) camphorquinone/EDAB/MPPB, were all dissolved in the correct weight ratios in mixtures of ACN/1-propanol/decanol, the new porogen system, and their spectra were taken at intervals over a period of 2 h of irradiation at 470 nm. In each case 10 mM camphorquinone was used, in (2) and (3) 47 mM EDAB was added and in (3) 30.5 mM MPPB was also added. While all components of the initiator system are in the correct ratio amounts they are present in a 50% lower amount than usual in the polymerisation solution. The results of the study are shown in Fig. 5.10.
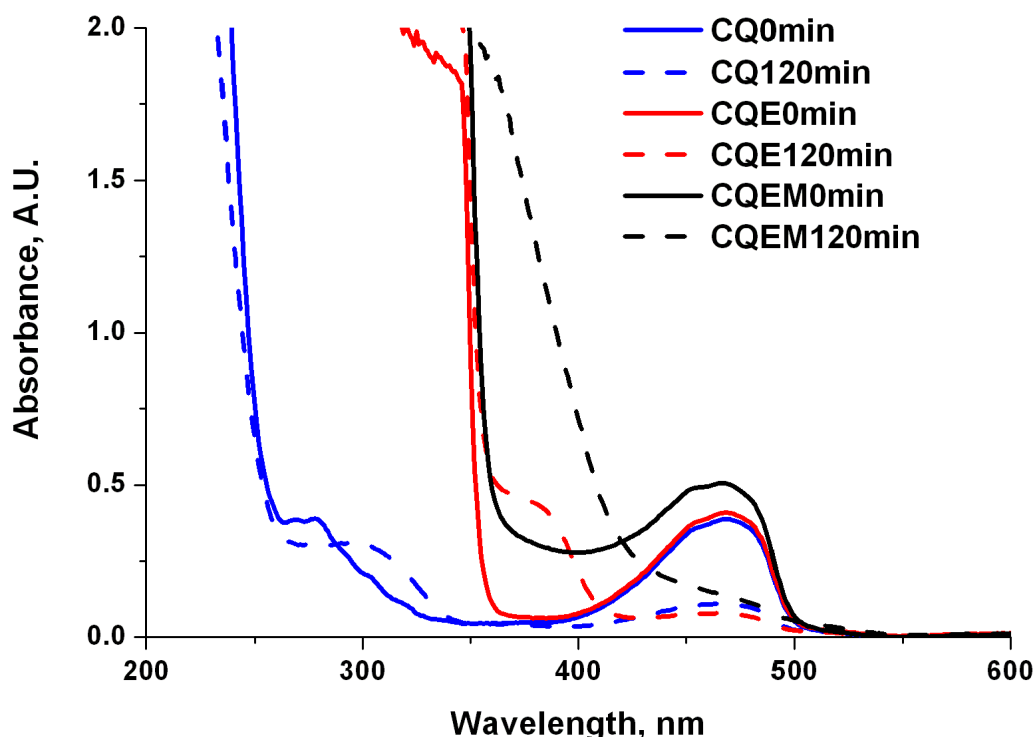
Figure 5.10: *Plot showing the effect of the addition of components of the initiator complex on the absorbance of the dye sensitiser and the rate of initiator decomposition. The lines represented on the legend by CQ (0 min, 120 min) are the spectra of a solution containing 1 wt% CQ only, the lines represented by CQE (0 min, 120 min) have 5 wt% EDAB added to the original CQ solution and the lines represented by CQEM (0 min, 120 min) have 5 wt% EDAB and 5 wt% MPPB added to the original CQ solution*

Looking at the decomposition study in Fig. 5.10, three different decompositions are shown. The decomposition of the dye sensitiser (CQ, blue lines) and a combination of the CQ and EDAB (red lines) over a 2 h period of irradiation show very little difference from one another. Before irradiation there is little difference in the absorbance of the two and within 2 h the absorbance is approaching zero meaning that in either case the effectiveness of the initiating system has been exhausted within 2 h. The addition of the MPPB, while it does not increase the decomposition time, does produce one important benefit. The absorbance of the initiating system before irradiation is increased by over 0.1 AU. This means that the initiator can absorb more light, which in turn means that more radicals can be generated by photo-induced electron transfer increasing the overall

efficiency of the initiating system, as shown in Fig. 5.11. The decomposition time is dictated by the lifetime of the photo-sensitiser, which appears to be 2 h. This indicates that it is not worth continuing the polymerisation beyond 2 h as there will be no more radicals generated after this time due to extinction of the sensitiser.
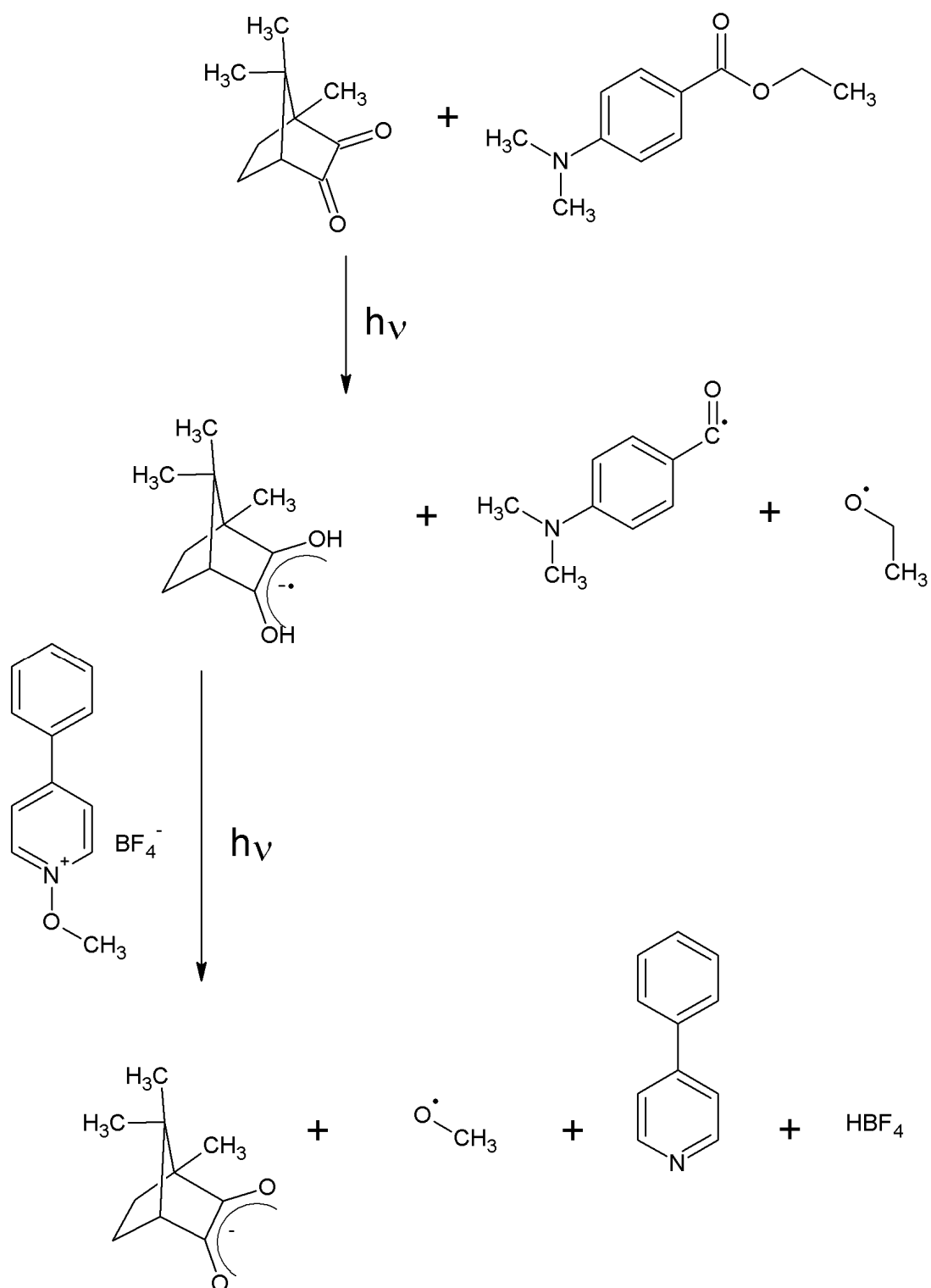
Figure 5.11: *Schematic of the generation of radicals using the three component initiating system*

After the study of the decomposition of the initiator the next stage was to monitor the conversion of the monomers to polymer using the new porogenic solvent composition.

Firstly control experiments were carried out to determine the time necessary to initiate polymerisation under ambient light conditions. The polymerisation mixture was placed in clear vials, labelled and placed in the bright lab without specific irradiation, after 4 h polymer formation was observed in the bottom of the vial and within 24 h the solution was fully polymerised. Knowing this, all solutions for polymerisation were then made up in amber vials and polymerisation was carried out in the dark as a precaution to ensure that the polymerisation mixture was not exposed to any ambient light which may interfere with the LED initiated polymerisation.

The monomer conversion experiments were then carried out in the standard way, polymerising the solution in clear vials and weighing the final product after washing and drying. Three sets of polymerisations were carried out, in the first batch all vials contained CQ only in the new porogen system, the second batch contained CQ and EDAB in the new porogen and the third contained CQ, EDAB and MPPB in the new porogen. For all the measurements the vials were positioned at 1 mm from the LED array and a current of 4 A was passed through the LEDs. Results from this experiment show that using the sensitiser on its own the maximum conversion is 28%, using the sensitiser and EDAB it is 28% and with the three-component initiator system the maximum conversion achieved is 56%, after 3 h of polymerisation. This is a significant improvement on the values obtained from the values obtained when using the former system of 1-decanol/THF as the porogen. Despite an improvement the conversion is still below 100%, again this is believed to be a problem of the vials as the light diffusion through the vial is not as good as through the capillary as the distance (the walls of vials) that the light needs to penetrate is far greater than in a capillary mould. Additionally, it is more of a qualitative technique as due to the nature of the production the glass vials are not identical to one another and this can have some effect on the dynamics of the polymerisation within the vial. The results can therefore not give a definitive value for the monomer conversion but more of an idea what can improve and hinder the polymer synthesis.

In order to be sure that it was the addition of the third initiator which produced the increase in the conversion of monomer and not just an increase in the total percentage of monomers another series of polymerisations were carried out in vials containing 1% CQ and 10% EDAB or 1% CQ and 10% MPPB. The total conversion in both cases was less than when the three-component system was used (5% of each were mixed with the CQ), confirming the action of the MPPB in accelerating the polymerisation reaction.

This polymerisation method was then transferred into capillaries and, although the polymerisation in vials gave the optimum time as 3 h the initiator decomposition experiment showed that there is no initiator remaining after 2 h therefore it was decided that 2 h would be the most suitable length of time for the polymerisation reaction. In the previous section (Section 5.3.1.1) it was noted that the % monomer was 40%, however keeping this % produced monomers which were too dense to be used on the HPLC system. The pressure approached the maximum that the system could handle and several times caused the column to become disconnected from the system. As it was important not to damage the detector it was decided to reduce the concentration of the monomer in the pre-polymer solution. The % monomer was reduced to 35% and this produced monoliths which were sufficiently porous to allow them to be used with the HPLC system available. The final composition of the pre-polymer solution was 17.5% v/v styrene, 17.5% v/v divinylbenzene, 11.5% v/v acetonitrile, 23% v/v 1-propanol, 30% v/v 1-decanol, 1 wt% CQ, 5 wt% EDAB and 5 wt% MPPB, with the capillary held 10 mm from the LED array, which had 4 A of current driven through it.

5.3.1.3. Study of LED position

When working on visible light initiated polymerisation using red light it was noted that the angle at which the LED was placed relative to the capillary was an important factor in the quality of the monolithic product. As described above (Chapter 4) this was likely due to the shielding effect of the polyimide coating on the capillary, which makes light penetration more difficult when the LED is perpendicular to the capillary due to fewer focal points for the light within the walls. In the case of blue light initiated polymerisation, as PTFE coated fused silica capillary is used and not polyimide it was found that regardless of the angle at which the LED is placed a good quality monolith

can be obtained. This is likely a result of the wave-guiding properties of the PTFE coating which allow light at all angles to pass through the coating into the capillary. As the position of the LED is not important to the result the LED was placed perpendicularly to the capillary as shown in Fig. 5.12.
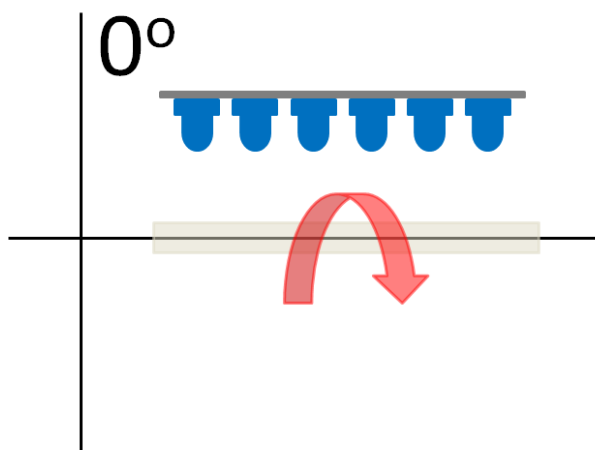
Figure 5.12: *Position of the LED array relative to the capillary during polymerisation*

What is important, however, is the rotation of the capillary during the polymerisation, indicated by the arrow in Fig. 5.12. It is even more important when the LED array is used for polymerisation. The LED array used here for polymerisation consisted of two rows of LEDs 1 cm apart (Fig. 5.13), there are points of high and low light intensity along the length of the capillary, which can result in alternating plugs of dense and permeable monolith.
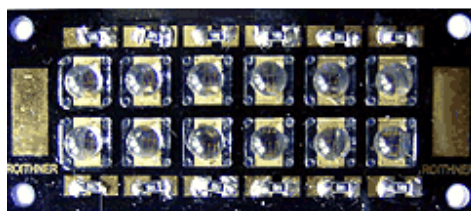
Figure 5.13: *Photographic image of 470 nm LED array, reprinted from www.roithner-laser.com*

Axial rotation of the capillary during polymerisation was therefore found to be very important to the preparation of homogeneous monoliths. As the capillary filled with the pre-polymer solution is constantly rotated during the polymerisation, these dense/permeable bands disperse (when the LED array is used) and the monolith is more homogeneous along its length.

Conductivity profiling along the length of the column was used to determine the homogeneity of the poly(S-*co*-DVB) monoliths. The homogeneity of monoliths prepared by two different methods was measured and plotted in Fig. 5.14. The insets in Fig. 5.14 show scanning electron micrographs of the two different monoliths, one of which was left stationary during polymerisation (Fig. 5.14A) and the other which was rotated continuously during the polymerisation reaction (Fig. 5.14B). Visually there are no obvious differences between the two images; in contrast, the conductivity profiles show another story. The profiles of the monoliths which were rotated during polymerisation are quite smooth and homogeneous along the length, whereas the monolith which was left stationary shows clear inhomogeneities along the length corresponding to patches of dense and permeable monolith in the capillary. The spacing between these peaks and troughs in the profile is quite regular and roughly corresponds to the spacing of the LEDs in the array which indicates that differences in light output along the length of the capillary can cause these types of inhomogeneities.
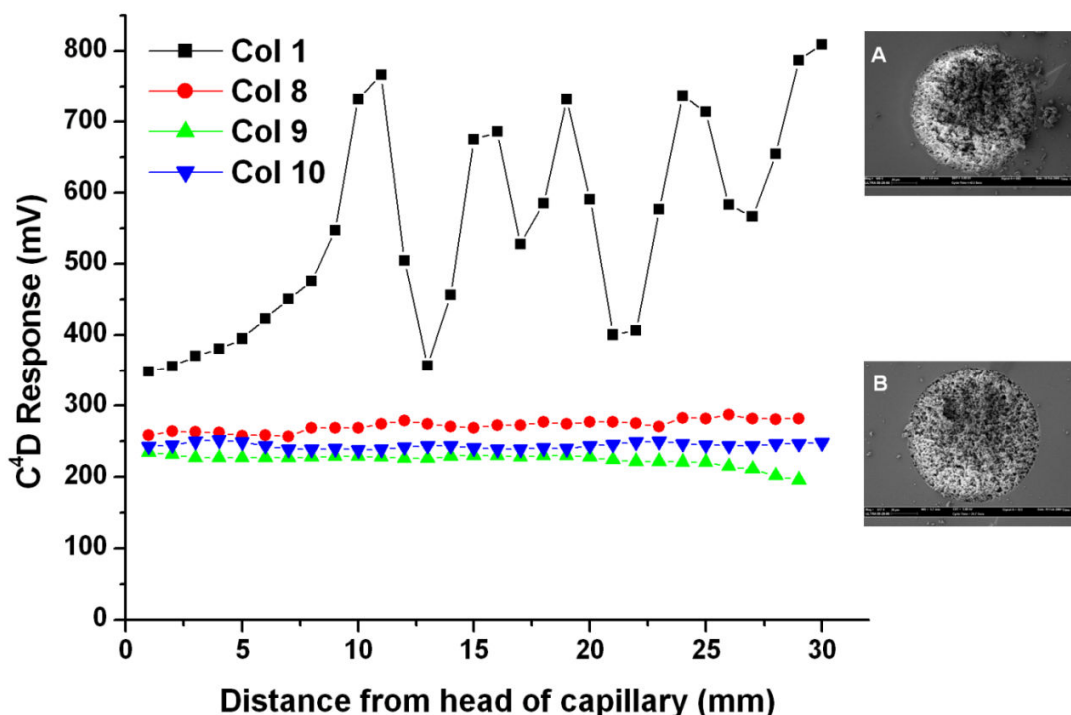
Figure 5.14: *Lateral conductivity profiling of four different poly(S-co-DVB) monoliths in PTFE coated fused silica capillaries, Columns 8, 9, 10 were rotated during polymerisation and Column 1 remained stationary. Insets show a scanning electron micrograph of a poly(S-co-DVB) monolith which has been (A) left stationary and (B) rotated during polymerisation*

5.3.2. Characterisation of monoliths in capillary

Photo-initiated polymerisation is a useful tool to control diffusion of polymer at the ends of the monolithic capillary column. Using a simple photo-mask the location of the monolith within the capillary can be controlled very easily. As PTFE-coated fused silica capillary is an effective light wave-guide, as described previously in Section 2.3.3.2, a more efficient mask than simply using black vinyl tape must be employed. For this reason, rubber septa were placed at the ends of the capillary to block light from propagating along the length that would lead to polymerisation even in the masked parts. The rubber septa more effectively absorb the light as they form a tighter seal around the capillary than the black vinyl tape. Fig. 5.15 shows the edge of a poly(S-*co*-DVB) monolith formed within a PTFE-coated fused silica capillary by the method described

above. The image confirms that the edges of the polymer monolith within the capillary are acceptably sharp.
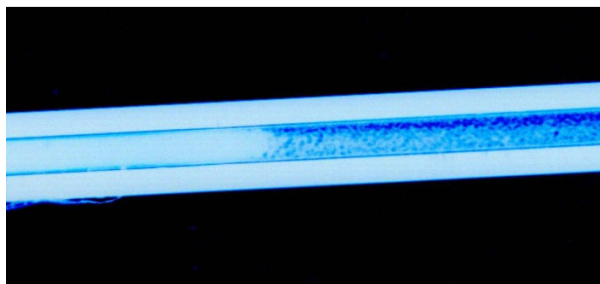
Figure 5.15: *Optical micrograph of a poly(S-co-DVB) monolith in the channel of a PTFE-coated fused silica capillary*

Scanning electron microscopy was also used to characterise the monoliths within the capillary as has been described previously. The images in Fig. 5.16 show that the optimised polymerisation procedure results in the expected polymer monolith structure, with a well developed globular, macroporous arrangement. The images also confirm that the capillary is completely filled with monolith and that it is firmly attached to the walls.
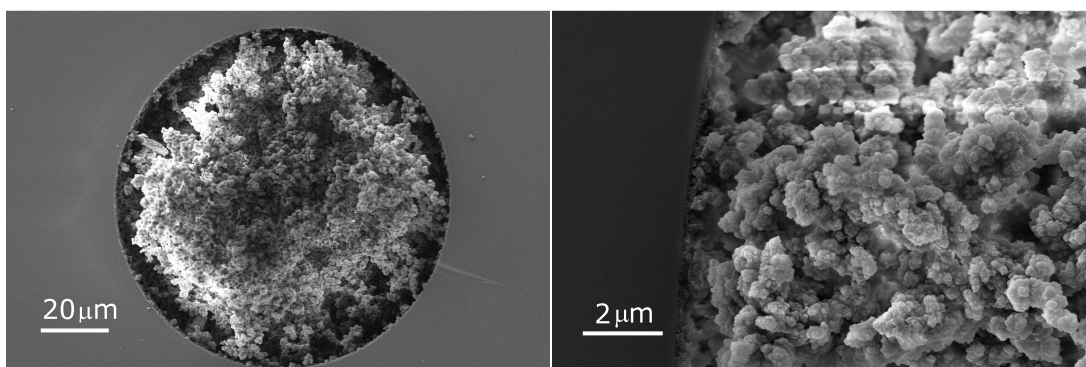
Figure 5.16: *Scanning electron micrographs of a poly(S-co-DVB) monolith in the channel of a PTFE coated fused silica capillary*

The pressure drop of a batch of three columns prepared using the optimised conditions was measured using water as the eluent (Fig. 5.17). The relative standard deviation calculated from the three columns shows a variance in the synthesis method of 12%. Although this is higher than expected, the chromatograms obtained (an example of which is shown in Fig. 5.18) do show a high degree of repeatability with low % RSD.
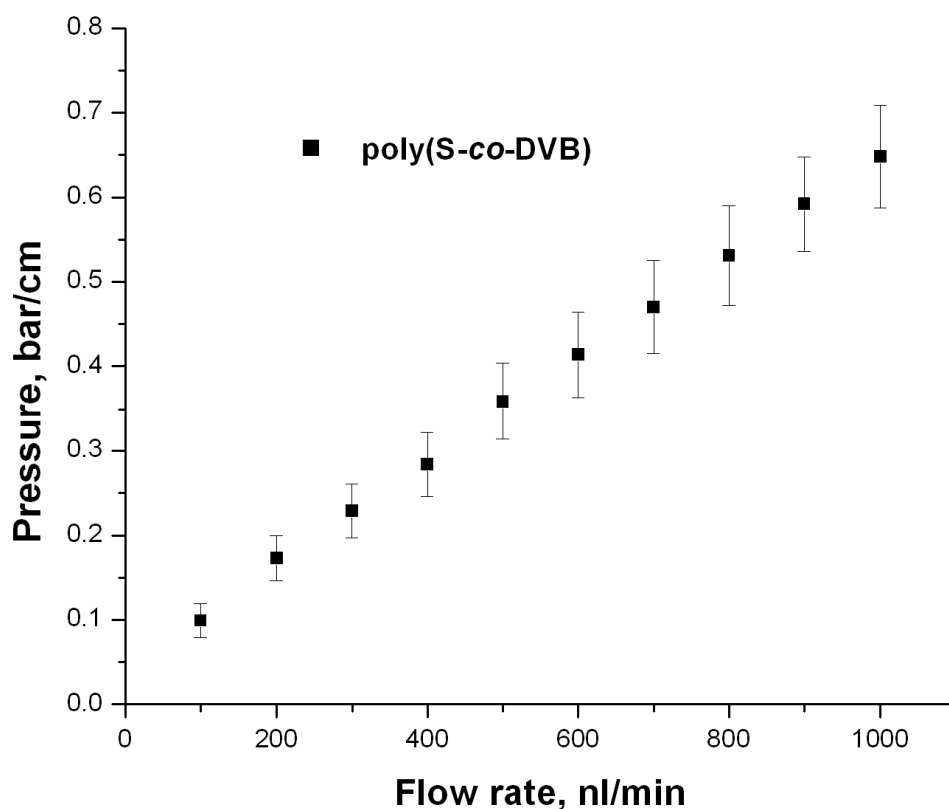
Figure 5.17: *Plot of flow rate (μl/min) vs. flow resistance (bar/cm) for a batch (n=3) poly(S-co-DVB) monoliths in PTFE-coated fused silica capillaries*

From the literature it is well-known that poly(S-*co*-DVB) monoliths are suitable for the separation of bio-molecules such as proteins and peptides [111, 238-240]. The monoliths synthesised in this section were examined for the separation of a mixture of standard proteins; ribonuclease A, cytochrome C, myoglobin and ovalbumin. An example of a baseline separation of this mixture on a poly(S-*co*-DVB) monolith synthesised by blue light initiated polymerisation is shown in Fig. 5.18.
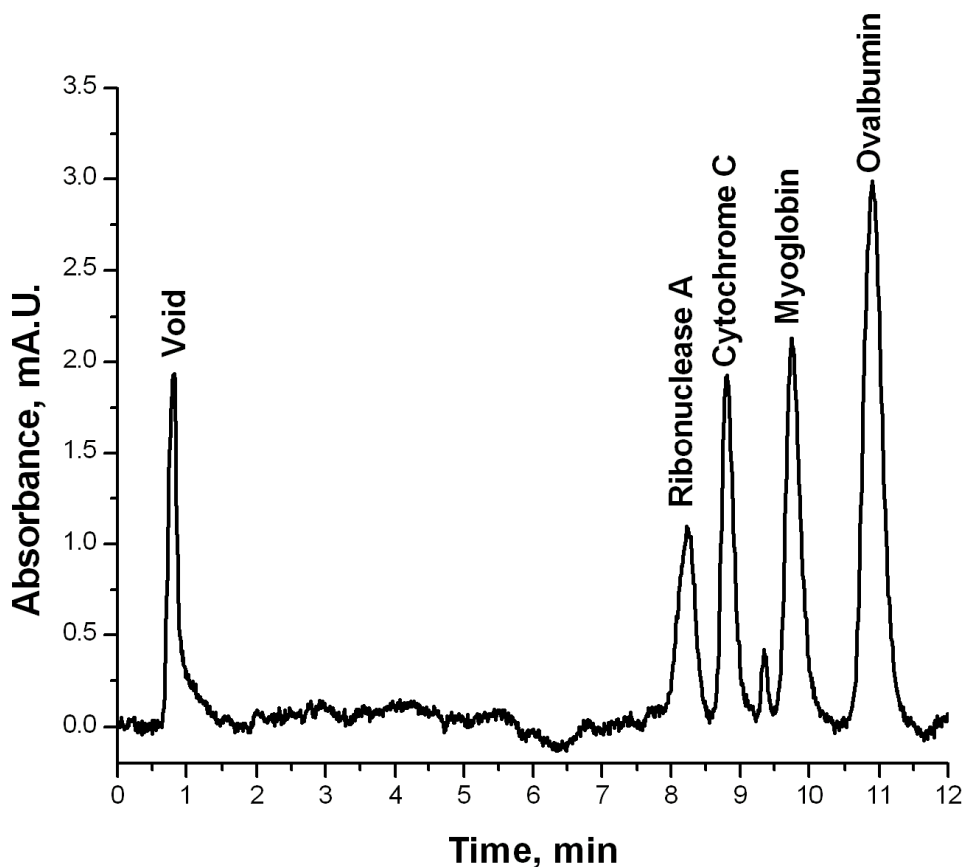
Figure 5.18: *Example of a separation of a mixture of proteins using a poly(S-co-DVB) monolith in capillary. Peaks (in order of elution) are ribonuclease A, cytochrome C, myoglobin and ovalbumin. Separation was carried out at a flow rate of 1 µl/min, gradient of 0-60% 0.1 vol.% formic acid in acetonitrile in 10 min, UV detection at 210 nm*

The separations were run three times on a batch of three different columns synthesised under the optimum conditions outlined in Section 5.3.1.2. Table 5.1 shows the average retention factors for each protein run on each of the three columns. The relative standard deviation for the retention factors was all less than 2.58%.

Table 5.1: *Comparison of retention factors (k) for a batch (n=3) of poly(S-co-DVB) monoliths in capillary columns with SDs and % RSDs*

Peak	k ± SD	% RSD
Ribonuclease A	9.48 ± 0.24	2.53
Cytochrome C	10.14 ± 0.25	2.43
Myoglobin	11.36 ± 0.28	2.46
Ovalbumin	12.90 ± 0.33	2.58

The selectivity for the proteins separated as shown in Fig. 5.18 was the same as that observed by Levkin *et al.* [111] using poly(S-*co*-DVB) monoliths synthesised by thermally initiated polymerisation in a micro-fluidic chip. This confirms that the monoliths synthesised in this work exhibited a very similar selectivity based on their hydrophobic character. The resolution of ribonuclease A and cytochrome C was 1.07. The cytochrome C/myoglobin and myoglobin/ovalbumin peaks were even better resolved with an average of 2.11 and 2.56, respectively.

Now that a method of polymerisation of styrenic monomers using light has been developed and optimised, the next stage is to examine whether this can be transferred into different moulds. Transfer being possible would indicate that this method is a robust method for the light induced polymerisation of styrenic monolithic stationary phases for separation science.

5.3.3. Characterisation of monoliths in micro-fluidic chips

After optimisation of the blue light initiated polymerisation procedure within PTFE coated fused silica capillary, some investigations were done using cyclic olefin copolymer (COC) micro-fluidic chips as the mould instead of capillary. There are some limitations on the mould that should be taken into account, in particular, the ability to withstand damage in the presence of acetonitrile, as this is present in the porogenic solvent. This ruled out the use of poly(methyl methacrylate) chips which turn opaque in the presence of acetonitrile and polydimethylsiloxane (PDMS) which are also damaged

by this solvent. Glass chips and COC chips were then examined, COC chips being chosen for use due to their ease of fabrication in comparison with glass chips.

Fig. 5.19 shows a photographic image and an optical micrograph of poly(S-*co*-DVB) monoliths within the channels of a COC micro-fluidic chip. It can be seen that the edges of the polymer within the channel are very sharp due to photo-masking of the channel during polymerisation. It was much easier to photo-mask the channels of the micro-fluidic chip in comparison with the PTFE coated fused silica capillaries as COC chips are not waveguides like the UV-transparent capillaries. Using black vinyl tape as the photo-mask, sharp plugs of monolith were obtained within the channels.
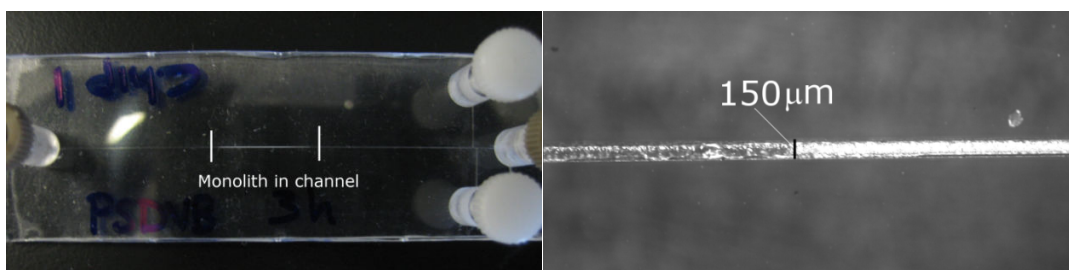
Figure 5.19: *(left) Photographic image and (right) optical micrograph of a poly(S-co-DVB) monolith in the channel of a COC micro-fluidic chip with dimensions 0.15 mm x 0.15 mm x 60 mm*

The morphology of the monolith obtained in the channel of the COC micro-fluidic chips was also examined. Fig. 5.20 shows a scanning electron micrograph of a poly(S-*co*-DVB) monolith within the channel of a COC chip. The chip was prepared for the SEM by making a score mark across the centre of the channel and then immersing the chip in liquid nitrogen before breaking the chip along the score mark. The bending of the chip while breaking it caused some deformation of the channel and therefore the channel appears as a slightly deformed rectangle. Despite this it can still be seen that the channel is well-filled with monolith and that this monolith is attached to the COC walls. Both of these characteristics are essential for the use of these monoliths in chromatographic applications. It can also be seen that the monolith possesses the porous, globular structure of poly(S-*co*-DVB) monoliths, which is also important.
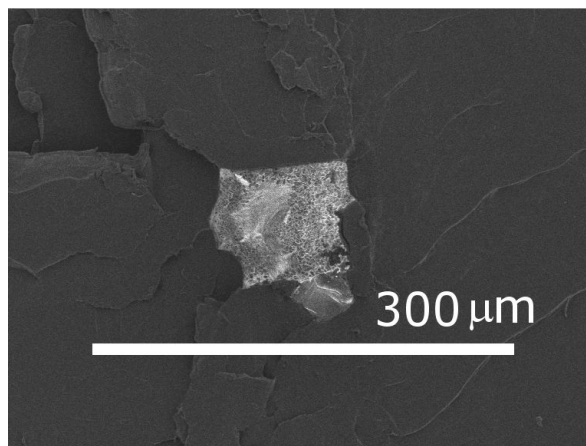
Figure 5.20: *Scanning electron micrograph of a poly(S-co-DVB) monolith in the channel of a COC micro-fluidic chip*

In the previous section it was noted that rotation of the capillary is important to ensure that the monolith is formed homogeneously within the channel. Using micro-fluidic chips, where there is approximately 1 cm of COC on either side of the channel makes rotation quite difficult as the channel will spend a large amount of time outside the light, therefore the polymerisation efficiency may be reduced. It was then decided not to rotate the channel during the polymerisation but to simply place the channel over the length of the array and then after the polymerisation to use conductivity profiling to determine whether this method produced monoliths of the required degree of homogeneity. As these monoliths were synthesised within the channels of micro-fluidic chips, it was necessary to replace the capillary C^{4}D with a micro-fluidic platform. A ruler was used to mark 1 mm increments along the edge of the chip and a layer of epoxy glue was poured over the surface of the chip to ensure the contact between the channel and the electrodes was as tight as possible to get the best signal. The chip was then moved over the electrodes in 1 mm increments and the conductivity values were recorded and plotted in Fig. 5.21.
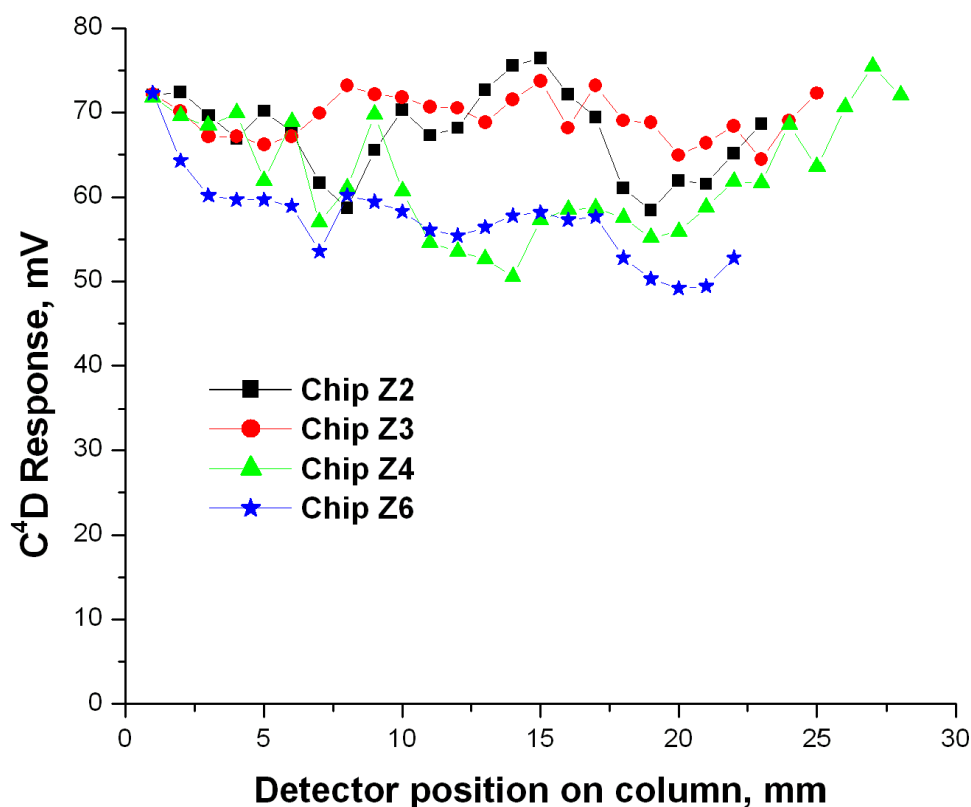
Figure 5.21: *Lateral conductivity profiling of poly(S-co-DVB) monolith within the channels of COC micro-fluidic chips*

As the chip cannot be rotated during polymerisation the homogeneity profiles (determined by lateral conductivity profiling) of the monoliths within the channels were not expected to be as smooth as those of the monoliths within the channels of the PTFE-coated capillaries. Despite this fact the %RSD along the lengths of all the channels and between the four different channels is less than 10% showing an acceptable level of homogeneity of these monoliths. It is quite unusual that the unrotated capillary would show such a bad profile while the unrotated chip, while not excellent, is still acceptable. This may be due to the geometry of the channels; light is dispersed more easily in channels which are square or rectangular than in cylindrical channels as there is only one focal point for the light. Additionally with the capillaries there are two layers through which the light must pass before reaching the cavity. This means that in the cylindrical capillaries the light is reflected and refracted many times within the channel giving rise to more intense areas of high and low light intensity which may cause further

inhomogeneities. For this reason rotation of the capillary during polymerisation seems to be more important than the rotation of the chip.

The final necessary characterisation of these monoliths will be the application of the stationary phases within the channels for the separation of bio-molecules., for example, this stationary phase could be used to separate a mixture of proteins as was shown for the monoliths in capillary in Fig. 5.18.

Due to a design flaw the nano-ports on the micro-fluidic cannot withstand long periods of light irradiation despite covering them with black tape to protect them from the light, they become over exposed and effectively over-cured. Prolonged irradiation causes the nano-ports to crack and break when connecting fittings for attachment to an LC system. Up to this point this problem has not been rectified and therefore no useful separations have been achieved on these micro-fluidic chips. It is hoped that this can be continued in the near future and that some remedy to this problem can be found so that these micro-fluidic chips can be applied for micro-fluidic separations.

5.4. Conclusions

For the first time poly(S-*co*-DVB) monolithic stationary phases have been synthesised using light initiated polymerisation. Finding that the red light initiated polymerisation procedure presented in Chapter 4 did not easily polymerise styrenic monomers, the use of blue light to initiate the polymerisation of styrenes was investigated. The results presented in this chapter show the first successful light initiated polymerisation of styrenic monoliths which have, up to this point, not been polymerised by light initiated methods. Initiation with visible light at 470 nm could be conveniently achieved with an LED array. The physical and chromatographic characterisation of the monoliths prepared in the PTFE coated fused silica capillary verified that this procedure affords monolithic columns of comparable characteristics to those produced by thermally initiated polymerisation. Separations of proteins were carried out and shown to be comparable to literature separations of proteins on similar stationary phases. The synthesis of poly(S-*co*-DVB) monoliths in COC micro-fluidic chips were also successfully carried out and the characterisation of these stationary phases showed that they would be suitable for use in separations applications. This new development in the

area of visible light initiated polymerisation will now allow more flexibility with regards to the monomers which can be used for photo-initiated monolith synthesis.

6. General Conclusions and Outlook

It is clear that the field of monolithic stationary phase synthesis and modification is large and varied and includes not only the most common rigid macroporous silica and organic polymers but also hydrogels, cellulosic beds, acrylamide beds, cryogels and polymeric foams to name a few. Even focusing solely on rigid, macroporous, organic polymer monoliths, there are a large variety of different methods of initiation - free radical, anionic, RAFT - and initiation sources - heat, light, microwaves - for this relatively small field, although free radical thermal and UV-light initiated polymerisation clearly dominate.

There are also a large number of methods by which the monolithic scaffold can be functionalised either before or after polymerisation, in order to provide a monolith with a particular surface chemistry for a specific separation. Examples of modification include the ter-polymerisation of butyl methacrylate, ethylene dimethacrylate and 2-acrylamido-2-methylpropane sulphonic acid which produces a monolithic with cation exchange functionality, or the grafting of enzymes onto a monolithic scaffold to produce an enzymatic reactor for protein digestion.

Despite all the work that has been carried out in the field of monolith synthesis and modification, there are still certain areas where more development is necessary, such as the photo-initiated polymerisation of UV absorbing monomers for example, and it is in these places where this thesis makes its contribution.

Chapter 2 presents work carried out on the synthesis of monolithic stationary phases by thermally and photo-initiated means from methods described in the literature, which have been modified slightly to suit certain applications, such as changing a porogen to create a more/less dense stationary phase, etc.

After fully investigating the literature methods some experimentation with photo-initiated polymerisation using alternate light sources was carried out and the main novelty in this chapter was the development of a low-pressure method of packing particulate stationary phases using short plugs of monolith as retaining frits. The

retaining frits were synthesised using UV-light initiated polymerisation with light emitting diodes as the initiating light source. The ability to synthesise short monolithic frits, which can withstand high pressures and the ability to pack particulate columns using a low pressure method while still achieving homogeneously packed columns is very useful in separation science. Traditional column-packing equipment, including stainless steel retaining frits, can be costly and the packing time is lengthy as the column packer needs to depressurise slowly. Packing at low pressure without the need for retaining frits is a distinct advantage for many types of column packing particularly if a particulate stationary phase is required in a micro-fluidic chip where it would not be possible to employ traditional retaining frits.

This chapter also presented the usefulness of photo-initiated surface modification in the form of photo-initiated grafting. It was shown that with the aid of simple photo-masks specific areas of localised functionalisation could be achieved in less than 20 min. This was very useful in further work where more detailed functionalisation of monolithic stationary phases is studied.

Chapter 3 shows the functionalisation of methacrylate monoliths with spiropyran, a photochromic dye, along with the copolymerisation of a monomeric spiropyran derivative with divinylbenzene in order to achieve photochromic monoliths. Regardless of the method of immobilisation or incorporation into the monolithic material the spiropyran retains its switching functionality allowing it to be present as both an uncharged and zwitterionic moiety depending on the wavelength of light used to irradiate the stationary phase. In this chapter the potential of copolymerised spiropyran monoliths as photo-controllable electroosmotic pumps has been demonstrated, meaning that flow in a micro-fluidic device could be controlled by light rather than increase or decreasing the voltage as is the normal method. Further work is necessary to improve the switching times so that in the future it may be possible to achieve flow rate gradients by simply switching the molecule back and forth between different states. As the spiropyran shows high fatigue resistance this pump could be used more than 100 times before photo-bleaching may occur indicating a relatively long lifetime. Although the spiropyran grafted monoliths were shown to underperform the copolymerised monoliths

as photo-controllable electroosmotic pumps, it was noted from experimentation that organic polymer monoliths with a functional dye layer grafted on the pore surface perform better in liquid chromatographic separations than in electrochromatographic separations. In the original idea for these dye grafted stationary phases it was decided to examine their potential for the photo-controlled retention and release of divalent metal ions, in the mean time their use as photo-controlled electroosmotic pumps was also examined and work in this area dominated as the high permeability of the monoliths made them unsuited to the analysis of small molecules. Modification of the underlying scaffold to reduce the pore size may be the best option to allow these dye grafted monoliths suitable for pre-concentration and separation of divalent metal ions.

The most promising use of this type of column would be for sample clean-up or pre-concentration, where one analyte would need to be extracted from the mixture and analysed while other analytes would either be passed onto another separating column or sent to waste. This method would take advantage of the affinity of the merocyanine form for divalent metal ions and amino acids. By injecting the sample onto the column with the MC form present the analyte which has the most affinity for the MC form would be retained while all others would pass out of the column. Once the other analytes were removed from the column the SP form could be regenerated releasing the retained analyte which would pass to the detector. As the spiropyran modified materials can be switched over 100 times before any degradation in the switching ability can be seen [170, 241], this type of stationary phase could be used for on-line sample concentration before a normal separation column in a standard capillary LC system. The potential of this type of stationary phase, using spiropyran coated silica micro-beads, was demonstrated recently by this group [190].

It is important to note that while UV-initiated polymerisation is very common, only one group have ever described the use of light in the visible region to initiate the polymerisation of monolithic materials. Despite the advantages of UV-initiated polymerisation there are two principle disadvantages, the first being that only moulds, which are transparent to UV light, can be used to hold the pre-polymer solution during polymerisation. This means that polyimide coated fused silica capillaries, by far the

most popular type of capillary used in capillary separations, cannot be used for photo-initiated polymerisation of monolithic stationary phases using the current state of the art. During this project, and detailed in Chapter 4, a method of initiating the synthesis of methacrylate monolithic stationary phases within polyimide coated capillary without having to remove the coating prior to initiation of the polymerisation was developed. The visible light initiated polymerisation of methacrylates within polyimide coated fused silica capillary presents a significant contribution to monolith synthesis as it increases the number of moulds which can be used to contain monolithic stationary phases polymerised by photo-initiated means. Additionally this allows for the photo-initiated synthesis of monoliths in polyimide micro-fluidic chips and potentially in glass moulds which absorb in the UV.

Another novel point about this new method of polymerisation is that the method can also be used for the photo-initiated grafting of chromophoric monomers. In the past monomers absorbing in the UV could not be photo-grafted as all the light energy would be absorbed by the monomer and not by the initiator, however using the three component initiator system developed in Chapter 4 a spiropyran monomer was successfully grafted onto the surface of a poly(butyl methacrylate-*co*-ethylene dimethacrylate) stationary phase. This has great potential for use in the functionalisation of monolithic scaffolds as the choice of molecule to graft on the surface of the scaffold is no longer limited by its absorbance in the UV region of the electromagnetic spectrum.

Throughout Chapter 4, the development of the initiator and its use in the synthesis of full monolithic stationary phases in both polyimide coated fused silica capillary and polyimide micro-fluidic chips, along with the photo-initiated grafting of chromophoric monomers onto a monolithic scaffold was shown. Further work for this initiating system will be to show that it is possible to synthesise longer, porous layer open tubular monoliths within polyimide coated fused silica capillary, which can then be applied in gas chromatographic applications, another major user of polyimide coated fused silica capillaries. Further work is also necessary to improve the polymerisation within the polyimide micro-fluidic chips which will result in an improvement in the separation ability of the stationary phase. With modification to the initiating system, it should also

be possible to synthesise styrenic monoliths within polyimide coated fused silica capillaries. This initiating system is a great improvement on the current state of the art of photo-initiated monolith synthesis, by increasing the number of moulds and monomers that can be used for the synthesis and modification of monolithic stationary phases.

In the meantime, the synthesis of styrenic monoliths by photo-initiated mechanism is still highly desirable due to the fact that the production of styrenic monoliths using photo-initiated polymerisation was never reported in the literature, another limitation of UV-light initiated polymerisation. Styrenes, absorbing strongly in the UV region of the spectrum, compete with the initiator in photo-initiated polymerisation, which makes their synthesis by this method impossible or very lengthy depending on the wavelength chosen.

Taking guidance from the polymer chemistry applied in dentistry, a common initiating system for the curing of dental resins using blue light was investigated and with the addition of a second co-initiator and the change of the porogenic solvents, it was possible to achieve the synthesis of poly(styrene-*co*-divinylbenzene) monolith within poly(tetrafluoroethylene) coated fused silica capillary and cyclic olefin copolymer micro-fluidic chips and the results are presented in Chapter 5.

The ability to photo-initiate the synthesis of styrenic monomers has great potential in the field of monolith synthesis due to the popularity of styrenic monoliths in bio-separations.

Combining the development of initiating systems activated by red and blue light, this presents a large addition to the field of photo-initiated polymerisations of monolithic stationary phases. Using one of these two systems will allow either the polymerisation within polyimide coating and UV absorbing moulds or the synthesis of styrenic monoliths or even the photo-grafting of chromophoric molecules onto the surface of pre-existing monolithic scaffolds. There is great potential for further development of these techniques, using different second co-initiators to change the speed of the reaction and also for which monomers the systems is suitable. There are also many areas where these techniques may be applied to improve the field of monolith synthesis and modification.

Overall several novel and significant contributions have been made to the field of monolith synthesis. It is envisaged that with further investigation they can make an improvement on many different areas of monolith synthesis, modification and application in the years to come.

7. References

[1]   M. Kubin, P. Spacek, R. Chromecek, Collection of Czechoslovak Chemical Communications, 32 (1967) 3881.

[2]   F. Svec, Journal of Separation Science, 27 (2004) 747.

[3]   W.D. Ross, R. Jefferson, Journal of Chromatographic Science, 8 (1970) 386.

[4]   H. Schnecko, O. Bieber, Chromatographia, 4 (1971) 109.

[5]   S. Hjerten, J.L. Liao, R. Zhang, Journal of Chromatography, 473 (1989) 273.

[6]   F. Svec, J.M.J. Frechet, Analytical Chemistry, 64 (1992) 820.

[7]   T.B. Tennikova, B.G. Belenkii, F. Svec, Journal of Liquid Chromatography, 13 (1990) 63.

[8]   K. Nakanishi, N. Soga, Journal of the American Ceramic Society, 74 (1991) 2518.

[9]   H. Minakuchi, K. Nakanishi, N. Soga, N. Ishizuka, N. Tanaka, Analytical Chemistry, 68 (1996) 3498.

[10]   L.S. Ettre, Journal of Chromatographic Science, 41 (2003) 225.

[11]   Z.G. Shi, Y.Q. Feng, L. Xu, M. Zhang, S.L. Da, Talanta, 63 (2004) 593.

[12]   L. Trojer, C.P. Bisjak, W. Wieder, G.K. Bonn, Journal of Chromatography A, 1216 (2009) 6303.

[13]   D. Connolly, B. Paull, Journal of Separation Science, 32 (2009) 2653.

[14]   A.E. Rodrigues, V. Mata, G., M. Zabka, L. Pais, in: F. Svec, T.B. Tennikova, Z. Deyl (Eds.), Monolithic materials: Preparation, properties and applications (Journal of Chromatography A Library, Vol. 67), Elsevier, Amsterdam, 2003, p. 325.

[15]   Q.C. Wang, F. Svec, J.M.J. Frechet, Analytical Chemistry, 65 (1993) 2243.

[16]   J.E. MacNair, K.D. Patel, J.W. Jorgenson, Analytical Chemistry, 71 (1999) 700.

[17]   N.W. Smith, Z. Jiang, Journal of Chromatography A, 1184 (2008) 416.

[18]   D.C. Harris, Quantitative Chemical Analysis, W.H. Freeman and Company, New York, 2003.

[19]   Q.Z. Luo, S. Mutlu, Y.B. Gianchandani, F. Svec, J.M.J. Frechet, Electrophoresis, 24 (2003) 3694.

References

[20]   G. Proczek, V. Augustin, S. Descroix, M.C. Hennion, Electrophoresis, 30 (2009) 515.

[21]   C. O Riordain, E. Gillespie, D. Connolly, P.N. Nesterenko, B. Paull, Journal of Chromatography A, 1142 (2007) 185.

[22]   E.C. Peters, M. Petro, F. Svec, J.M.J. Frechet, Analytical Chemistry, 70 (1998) 2288.

[23]   B.H. Gu, J.M. Armenta, M.L. Lee, Journal of Chromatography A, 1079 (2005) 382.

[24]   Y.B. Wu, J.H. Wu, Z.G. Shi, Y.Q. Feng, Journal of Chromatography B-Analytical Technologies in the Biomedical and Life Sciences, 877 (2009) 1847.

[25]   M. Chen, Y. Lu, Q. Ma, L. Guo, Y.Q. Feng, Analyst, 134 (2009) 2158.

[26]   G.F. Chen, F. Svec, D.R. Knapp, Lab on a Chip, 8 (2008) 1198.

[27]   F.Q. Nie, M. Macka, B. Paull, Lab on a Chip, 7 (2007) 1597.

[28]   F.Q. Nie, M. Macka, L. Barron, D. Connolly, N. Kent, B. Paull, Analyst, 132 (2007) 417.

[29]   in: D. Hoiberg (Ed.), Encyclopedia Britannica, Encyclopaedia Britannica Inc., New York, 1985-Present.

[30]   J.W. Nicholson, The Chemistry of Polymers, Royal Society of Chemistry, Cambridge, U.K., 2006.

[31]   F. Svec, J.M.J. Fréchet, in: F. Svec, T.B. Tennikova, Z. Deyl (Eds.), Monolithic Materials: Preparation, Properties and Applications (Journal of Chromatography Library), Elsevier, Amsterdam, 2003, p. 19.

[32]   T.J. Causon, R.A. Shellie, E.F. Hilder, Analyst, 134 (2009) 440.

[33]   A. Nordborg, E.F. Hilder, Analytical and Bioanalytical Chemistry, 394 (2009) 71.

[34]   F. Svec, J.M.J. Frechet, Science, 273 (1996) 205.

[35]   X.F. Sun, Z.K. Chai, Journal of Chromatography A, 943 (2002) 209.

[36]   M.R. Buchmeiser, Polymer, 48 (2007) 2187.

[37]   J.M.G. Cowie, Polymers: Chemistry and Physics of Modern Materials, Chapman and Hall, Dordrecht, 1991, p. 52.

[38]   I.C. Liu, H.M. Huang, C.Y. Chang, H.C. Tsai, C.H. Hsu, R.C.C. Tsiang, Macromolecules, 37 (2004) 283.

[39]   T. Nakano, Y. Okamoto, Macromolecular Rapid Communications, 21 (2000) 603.

[40]   S. Camerlynck, P.A.G. Cormack, D.C. Sherrington, European Polymer Journal, 42 (2006) 3286.

[41]   R. Vijayaraghavan, D.R. MacFarlane, Chemical Communications (2004) 700.

[42]   T. Krasia, R. Soula, H.G. Borner, H. Schlaad, Chemical Communications (2003) 538.

[43]   D. Seifert, M. Kipping, H.-J.P. Adler, D. Kuckling, Macromolecular Symposia, 254 (2007) 386.

[44]   E. Khosravi, L.R. Hutchings, M. Kujawa-Welten, Designed Monomers and Polymers, 7 (2004) 619.

[45]   A. Patel, S. Fouace, J.H.G. Steinke, Analytica Chimica Acta, 504 (2004) 53.

[46]   J. Chiefari, Y.K. Chong, F. Ercole, J. Krstina, J. Jeffery, T.P.T. Le, R.T.A. Mayadunne, G.F. Meijs, C.L. Moad, G. Moad, E. Rizzardo, S.H. Thang, Macromolecules, 31 (1998) 5559.

[47]   M. Turson, X.L. Zhuang, H.N. Liu, P. Jiang, X.C. Dong, Chinese Chemical Letters, 20 (2009) 1136.

[48]   H.N. Liu, X.L. Zhuang, M. Turson, M. Zhang, X.C. Dong, Journal of Separation Science, 31 (2008) 1694.

[49]   M.R. Buchmeiser, in: F. Svec, T.B. Tennikova, Z. Deyl (Eds.), Monolithic materials: Preparation, properties and applications (Journal of Chromatography A Library), Elsevier, Amsterdam, 2003, p. 103.

[50]   F.M. Sinner, M.R. Buchmeiser, Angewandte Chemie-International Edition, 39 (2000) 1433.

[51]   P. Vana, C. Barner-Kowollik, T.P. Davis, K. Matyjasewski, Encyclopedia of polymer science and technology, John Wiley and Sons, Inc., Hoboken, New Jersey, 1988, p. 359.

[52]   U. Meyer, F. Svec, J.M.J. Frechet, C.J. Hawker, K. Irgum, Macromolecules, 33 (2000) 7769.

[53]   C. Yu, M.C. Xu, F. Svec, J.M.J. Frechet, Journal of Polymer Science Part a-Polymer Chemistry, 40 (2002) 755.

[54]   C. Viklund, F. Svec, J.M.J. Frechet, K. Irgum, Chemistry of Materials, 8 (1996) 744.

[55]   C. Viklund, E. Ponten, B. Glad, K. Irgum, P. Horstedt, F. Svec, Chemistry of Materials, 9 (1997) 463.

[56]   B. Beiler, A. Vincze, F. Svec, A. Safrany, Polymer, 48 (2007) 3033.

[57]   E.A. Moschou, A.D. Nicholson, G.Y. Jia, J.V. Zoval, M.J. Madou, L.G. Bachas, S. Daunert, Analytical and Bioanalytical Chemistry, 385 (2006) 596.

[58]   K. Chuda, J. Jasik, J. Carlier, P. Tabourier, C. Druon, X. Coqueret, Radiation Physics and Chemistry, 75 (2006) 26.

[59]   M.T. Dulay, H.N. Choi, R.N. Zare, Journal of Separation Science, 30 (2007) 2979.

[60]   I. Mihelic, M. Krajnc, T. Koloini, A. Podgornik, Industrial & Engineering Chemistry Research, 40 (2001) 3495.

[61]   O.G. Potter, M.C. Breadmore, E.F. Hilder, Analyst, 131 (2006) 1094.

[62]   J.K. Adu, S.S. Lau, D.G. Watson, M.R. Euerby, G.G. Skellern, J.N.A. Tettey, Electrophoresis, 26 (2005) 3445.

[63]   M. Lammerhofer, F. Svec, J.M.J. Frechet, W. Lindner, Journal of Chromatography A, 925 (2001) 265.

[64]   M. Lammerhofer, E.C. Peters, C. Yu, F. Svec, J.M.J. Frechet, W. Lindner, Analytical Chemistry, 72 (2000) 4614.

[65]   S. Abele, F.Q. Nie, F. Foret, B. Paull, M. Macka, Analyst, 133 (2008) 864.

[66]   H. Aoki, N. Tanaka, T. Kubo, K. Hosoya, Journal of Polymer Science Part a-Polymer Chemistry, 46 (2008) 4651.

[67]   V. Pucci, M.A. Raggi, F. Svec, J.M.J. Frechet, Journal of Separation Science, 27 (2004) 779.

[68]   T. Rohr, E.F. Hilder, J.J. Donovan, F. Svec, J.M.J. Frechet, Macromolecules, 36 (2003) 1677.

[69]   E. Gillespie, D. Connolly, B. Paull, Analyst, 134 (2009) 1314.

[70]   M.B. Smith, J. March, in: M.B. Smith, J. March (Eds.), March's Advanced Organic Chemistry: Reactions, Mechanisms and Structure, John Wiley and Sons, Inc., Hoboken, New Jersey, 2007, p. 328.

[71]   C. Yu, M.H. Davey, F. Svec, J.M.J. Frechet, Analytical Chemistry, 73 (2001) 5088.

[72]   X.C. Wang, X.H. Yang, X.M. Zrang, Analytical Sciences, 22 (2006) 1099.

[73]   D. Connolly, V. O'Shea, P. Clark, B. O'Connor, B. Paull, Journal of Separation Science, 30 (2007) 3060.

[74]   J. Gu, Z. Lei, Q.Z. Yao, Journal of Membrane Science, 287 (2007) 271.

[75]   D. Bandilla, C.D. Skinner, Journal of Chromatography A, 1004 (2003) 167.

[76]   J. Wen, C. Guillo, J.P. Ferrance, J.P. Landers, Analytical Chemistry, 79 (2007) 6135.

[77]   D.S. Peterson, T. Rohr, F. Svec, J.M.J. Frechet, Analytical Chemistry, 74 (2002) 4081.

[78]   G.J. Kavarnos, N.J. Turro, Chemical Reviews, 86 (1986) 401.

[79]   F.A. Rueggeberg, S.W. Twiggs, W.F. Caughman, S. Khajotia, Journal of Dental Research, 75 (1996) 2897.

[80]   S.L. McDermott, J.E. Walsh, R.G. Howard, Optics and Laser Technology, 40 (2008) 487.

[81]   R.N. Hall, R.O. Carlson, T.J. Soltys, G.E. Fenner, J.D. Kingsley, Physical Review Letters, 9 (1962) 366.

[82]   N. Holonyak, S.F. Bevacqua, Applied Physics Letters, 1 (1962) 82.

[83]   P.N. Johnson, D.W.L. Tolfree, Nuclear Instruments & Methods, 134 (1976) 29.

[84]   H. Amano, T. Asahi, I. Akasaki, Japanese Journal of Applied Physics Part 2-Letters, 29 (1990) L205.

[85]   M.A. Haase, J. Qiu, J.M. Depuydt, H. Cheng, Applied Physics Letters, 59 (1991) 1272.

[86]   R.F. Rutz, Applied Physics Letters, 28 (1976) 379.

[87]   E.F. Schubert, Light Emitting Diodes, Cambridge University Press, Cambridge, U.K., 2003.

[88]   P.K. Dasgupta, I.Y. Eom, K.J. Morris, J.Z. Li, Analytica Chimica Acta, 500 (2003) 337.

[89]   K.T. Lau, S. Baldwin, M. O'Toole, R. Shepherd, W.J. Yerazunis, S. Izuo, S. Ueyama, D. Diamond, Analytica Chimica Acta, 557 (2006) 111.

[90]   R.W. Mills, British Dental Journal, 178 (1995) 169.

[91]   M.G. Neumann, W.G. Miranda, C.C. Schmitt, F.A. Rueggeberg, I.C. Correa, Journal of Dentistry, 33 (2005) 525.

[92]   M.G. Neumann, C.C. Schmitt, G.C. Ferreira, I.C. Correa, Dental Materials, 22 (2006) 576.

[93]   Z. Tarle, A. Meniga, A. Knezevic, J. Sutalo, M. Ristic, G. Pichler, Journal of Oral Rehabilitation, 29 (2002) 662.

[94]   W. Teshima, Y. Nomura, N. Tanaka, H. Urabe, M. Okazaki, Y. Nahara, Biomaterials, 24 (2003) 2097.

[95]   A. Uhl, R.W. Mills, A.E. Rzanny, K.D. Jandt, Dental Materials, 21 (2005) 278.

[96]   F. Stahl, S.H. Ashworth, K.D. Jandt, R.W. Mills, Biomaterials, 21 (2000) 1379.

[97]   R. Bandari, W. Knolle, A. Prager-Duschke, H.R. Glasel, M.R. Buchmeiser, Macromolecular Chemistry and Physics, 208 (2007) 1428.

[98]   R. Bandari, C. Eisner, W. Knolle, C. Kuhnel, U. Decker, M.R. Buchmeiser, Journal of Separation Science, 30 (2007) 2821.

[99]   M.R. Buchmeiser, Journal of Polymer Science Part a-Polymer Chemistry, 47 (2009) 2219.

[100]   Y.P. Zhang, L.Q. Fan, K.P. Lee, Y.J. Zhang, S.H. Choi, W.J. Gong, Microchimica Acta, 158 (2007) 353.

[101]   A. Safrany, B. Beiler, K. Laszlo, F. Svec, Polymer, 46 (2005) 2862.

[102]   G.W. Kang, W.J. Cheong, Bulletin of the Korean Chemical Society, 27 (2006) 1459.

[103]   Y.P. Zhang, W. Li, X.J. Wang, L.B. Qu, G.L. Zhao, Y.X. Zhang, Analytical and Bioanalytical Chemistry, 394 (2009) 617.

[104]   S. Barlow, S.R. Marder, Advanced Functional Materials, 13 (2003) 517.

[105]   J. Urban, V. Skerikova, P. Jandera, R. Kubickova, M. Pospisilova, Journal of Separation Science, 32 (2009) 2530.

[106]   J. Krenkova, A. Gargano, N.A. Lacher, J.M. Schneiderheinze, F. Svec, Journal of Chromatography A, 1216 (2009) 6824.

[107]   Q.Z. Luo, H.F. Zou, X.Z. Xiao, Z. Guo, L. Kong, X.Q. Mao, Journal of Chromatography A, 926 (2001) 255.

[108]   X.A. Huang, S. Zhang, G.A. Schultz, J. Henion, Analytical Chemistry, 74 (2002) 2336.

[109]   T.B. Tennikova, M. Bleha, F. Svec, T.V. Almazova, B.G. Belenkii, Journal of Chromatography, 555 (1991) 97.

[110]   M. Barut, A. Podgornik, M. Merhar, A. Strancar, in: F. Svec, T.B. Tennikova, Z. Deyl (Eds.), Monolithic materials: Preparation, properties and applications (Journal of Chromatography A, Vol. 67), Elsevier, Amsterdam, 2003, p. 51.

[111]   P.A. Levkin, S. Eeltink, T.R. Stratton, R. Brennen, K. Robotti, H. Yin, K. Killeen, F. Svec, J.M.J. Frechet, Journal of Chromatography A, 1200 (2008) 55.

[112]   I.M. Lazar, L.J. Li, Y. Yang, B.L. Karger, Electrophoresis, 24 (2003) 3655.

[113]   D.A. Mair, E. Geiger, A.P. Pisano, J.M.J. Frechet, F. Svec, Lab on a Chip, 6 (2006) 1346.

[114]   M.F. Bedair, R.D. Oleschuk, Analytical Chemistry, 78 (2006) 1130.

[115]   P.L. Wang, D.Y. Tao, L.H. Zhang, Z. Liang, Y.K. Zhang, Journal of Separation Science, 32 (2009) 2629.

[116]   Z. Altun, L.G. Blomberg, E. Jagerdeo, M. Abdel-Rehim, Journal of Liquid Chromatography & Related Technologies, 29 (2006) 829.

[117]   Z. Altun, A. Hjelmstrom, M. Abdel-Rehim, L.G. Blomberg, Journal of Separation Science, 30 (2007) 1964.

[118]   I.Y. Galaev, M.B. Dainiak, F.M. Plieva, R. Hatti-Kaul, B. Mattiasson, Journal of Chromatography A, 1065 (2005) 169.

[119]   J.R.E. Thabano, M.C. Breadmore, J.P. Hutchinson, C. Johns, P.R. Haddad, Journal of Chromatography A, 1175 (2007) 117.

[120]   F. Wei, M. Zhang, Y.Q. Feng, Journal of Chromatography B-Analytical Technologies in the Biomedical and Life Sciences, 850 (2007) 38.

[121]   X.L. Dong, J. Dong, J.J. Ou, Y. Zhu, H.F. Zou, Electrophoresis, 27 (2006) 2518.

[122]   M. Lammerhofer, F. Svec, J.M.J. Frechet, Analytical Chemistry, 72 (2000) 4623.

[123]   X.Y. Wei, L. Qi, G.L. Yang, F.Y. Wang, Talanta, 79 (2009) 739.

[124]   H.M. Ma, R.H. Davis, C.N. Bowman, Macromolecules, 33 (2000) 331.

[125]   E. Gillespie, M. Macka, D. Connolly, B. Paull, Analyst, 131 (2006) 886.

[126]   F. Svec, Journal of Separation Science, 27 (2004) 1419.

[127]   F. Svec, Journal of Separation Science, 28 (2005) 729.

[128]   M. Bedair, Z. El Rassi, Electrophoresis, 25 (2004) 4110.

[129]   S.D. Chambers, K.M. Glenn, C.A. Lucy, Journal of Separation Science, 30 (2007) 1628.

[130]   E.F. Hilder, F. Svec, J.M. Frechet, Journal of Chromatography A, 1044 (2004) 3.

[131]   A.Y. Kanatyeva, A.A. Kurganov, E.N. Viktorova, A.A. Korolev, Uspekhi Khimii, 77 (2008) 393.

[132]   M. Kato, K. Sakai-Kato, T. Toyo'oka, Journal of Separation Science, 28 (2005) 1893.

[133]   R. Mallik, D.S. Hage, Journal of Separation Science, 29 (2006) 1686.

[134]   K. Miyabe, G. Guiochon, Journal of Separation Science, 27 (2004) 853.

[135]   L. Rieux, H. Niederlander, E. Verpoorte, R. Bischoff, Journal of Separation Science, 28 (2005) 1628.

[136]   M.J. Benes, D. Horak, F. Svec, Journal of Separation Science, 28 (2005) 1855.

[137]   M. Wilchek, I. Chaiken, in: P. Bailon, G.K. Ehrlich, W.-J. Fung, W. Berthold (Eds.), Affinity Chromatography: Methods and Protocols (Methods in Molecular Biology, Vol. 147), Humana Press, Totowa, New Jersey, 2000.

[138]   P.-E. Gustavsson, P.-O. Larsson, in: F. Svec, T.B. Tennikova, Z. Deyl (Eds.), Monolithic materials: Preparation, properties and applications (Journal of Chromatography A Library, Vol. 67), Elsevier, Amsterdam, 2003, p. 121.

[139]   S. Fisichella, G. Alberghina, M.E. Amato, M. Fichera, A. Palermo, N.E. Pogna, A. Savarino, Journal of Cereal Science, 36 (2002) 103.

[140]   M. Odabasi, A. Denizli, Polymer International, 53 (2004) 332.

[141]   M. Odabasi, A. Denizli, Journal of Applied Polymer Science, 93 (2004) 719.

[142]   H. Yavuz, E. Duru, O. Genc, A. Denizli, Colloids and Surfaces a-Physicochemical and Engineering Aspects, 223 (2003) 185.

[143]   F. Qu, Y.P. Guan, Z.Y. Ma, Q. Zhang, Polymer International, 58 (2009) 888.

References

[144]   D.C. Nash, H.A. Chase, Journal of Chromatography A, 776 (1997) 55.

[145]   C. Garcia-Diego, J. Cuellar, Chemical Engineering Journal, 143 (2008) 337.

[146]   F. Li, P.J. Dong, Q.F. Zhuang, Journal of Chromatography A, 1216 (2009) 4383.

[147]   M.Y. Arica, M. Yilmaz, E. Yalcin, G. Bayramoglu, Journal of Chromatography B-Analytical Technologies in the Biomedical and Life Sciences, 805 (2004) 315.

[148]   M. Karakisla, G. Bayramoglu, M.Y. Arica, Journal of Applied Polymer Science, 108 (2008) 3313.

[149]   G. Bayramoglu, B. Kaya, M.Y. Arica, Chemical Engineering Science, 57 (2002) 2323.

[150]   A. Ouyang, P. Bennett, A. Zhang, S.T. Yang, Process Biochemistry, 42 (2007) 561.

[151]   G. Alberghina, S. Fisichella, E. Renda, Journal of Chromatography A, 840 (1999) 51.

[152]   M. Yilmaz, G. Bayramoglu, M.Y. Arica, Food Chemistry, 89 (2005) 11.

[153]   G. Bayramoglu, M. Yilmaz, M.Y. Arica, Biochemical Engineering Journal, 13 (2003) 35.

[154]   M.Y. Arica, G. Bayramoglu, Process Biochemistry, 40 (2005) 1433.

[155]   S. Fisichella, G. Alberghina, M.E. Amato, D. Lafiandra, D. Mantarro, A. Palermo, A. Savarino, G. Scarlata, Journal of Cereal Science, 38 (2003) 77.

[156]   T. Nakagama, K. Hirasawa, K. Uchiyama, T. Hobo, Analytical Sciences, 17 (2001) 119.

[157]   E. Fischer, Y. Hirshberg, Journal of the Chemical Society (1952) 4522.

[158]   R. Guglielmetti, in: H. Durr, H. Bouas-Laurent (Eds.), Photochromism: Molecules and Systems, Elsevier, Amsterdam, 2003.

[159]   H. Zollinger, Color Chemistry: Syntheses, Properties and Applications of Organic Dyes and Pigments, Wiley-VCH, Weinheim, Germany, 2003.

[160]   F.M. Raymo, S. Giordani, Proceedings of the National Academy of Sciences of the United States of America, 99 (2002) 4941.

[161]   M.A. Suzuki, T. Hashida, J. Hibino, Y. Kishimoto, Molecular Crystals and Liquid Crystals Science and Technology Section a-Molecular Crystals and Liquid Crystals, 246 (1994) 389.

References

[162] J. Hibino, T. Hashida, M.A. Suzuki, Y. Kishimoto, K. Kanai, Molecular Crystals and Liquid Crystals Science and Technology Section a-Molecular Crystals and Liquid Crystals, 255 (1994) 243.

[163] J.D. Winkler, C.M. Bowen, V. Michelet, Journal of the American Chemical Society, 120 (1998) 3237.

[164] P. Bamfield, Chromic Phenomena: Technological applications of colour chemistry, Royal Society of Chemistry, Cambridge, U.K., 2001.

[165] B.S. Lukyanov, M.B. Lukyanova, Chemistry of Heterocyclic Compounds, 41 (2005).

[166] C.J. Roxburgh, P.G. Sammes, Dyes and Pigments, 27 (1995) 63.

[167] P.M.S. Monk, R.J. Mortimer, D.R. Rosseinsky, Electrochromism and electrochromic devices, Cambridge University Press, Cambridge, U.K., 2007.

[168] Y. Liu, M. Fan, S. Zhang, X. Sheng, J. Yao, New Journal of Chemistry, 31 (2007) 1878.

[169] N. Shao, Y. Zhang, S.M. Cheung, R.H. Yang, W.H. Chan, T. Mo, K.A. Li, F. Liu, Analytical Chemistry, 77 (2005) 7294.

[170] R.J. Byrne, S.E. Stitzel, D. Diamond, Journal of Materials Chemistry, 16 (2006) 1332.

[171] L.S. Atabekyan, A.K. Chibisov, Journal of Photochemistry, 34 (1986) 323.

[172] H. Sakamoto, T. Yokohata, T. Yamamura, K. Kimura, Analytical Chemistry, 74 (2002) 2522.

[173] J. Filley, M.A. Ibrahim, M.R. Nimlos, A.S. Watt, D.M. Blake, Journal of Photochemistry and Photobiology a-Chemistry, 117 (1998) 193.

[174] M. Bedair, Z. El Rassi, Journal of Chromatography A, 1079 (2005) 236.

[175] R. Mallik, J. Tao, D.S. Hage, Analytical Chemistry, 76 (2004) 7013.

[176] J. Krenkova, Z. Bilkova, F. Foret, Journal of Separation Science, 28 (2005) 1675.

[177] J. Krenkova, N.A. Lacher, F. Svec, Analytical Chemistry, 81 (2009) 2004.

[178] T.C. Logan, D.S. Clark, T.B. Stachowiak, F. Svec, J.M.J. Frechet, Analytical Chemistry, 79 (2007) 6592.

References

[179] K. Amatschek, R. Necina, R. Hahn, E. Schallaun, H. Schwinn, D. Josic, A. Jungbauer, Hrc-Journal of High Resolution Chromatography, 23 (2000) 47.

[180] W.C. Yang, X.H. Sun, T. Pan, A.T. Woolley, Electrophoresis, 29 (2008) 3429.

[181] M. Bedair, Z. El Rassi, Journal of Chromatography A, 1044 (2004) 177.

[182] Q. Zhao, X.F. Li, X.C. Le, Analytical Chemistry, 80 (2008) 3915.

[183] J.P. Hutchinson, M. Macka, N. Avdalovic, P.R. Haddad, Journal of Chromatography A, 1106 (2006) 43.

[184] U. Daņiļēvičs, Z. Walsh, P. Smejkal, J. Křenková, S. Abele, F. Foret, M. Macka, 32nd International Symposium on Capillary Chromatography and Electrophoresis, Riva del Garda, Italy, 2008.

[185] K.J. Yao, J.X. Yun, S.C. Shen, L.H. Wang, X.J. He, X.M. Yu, Journal of Chromatography A, 1109 (2006) 103.

[186] M. Rainer, H. Sonderegger, R. Bakry, C.W. Huck, S. Morandell, L.A. Huber, D.T. Gjerde, G.K. Bonn, Proteomics, 8 (2008) 4593.

[187] F.M. Okanda, Z. El Rassi, Electrophoresis, 27 (2006) 1020.

[188] J.R. Chen, M.T. Dulay, R.N. Zare, F. Svec, E. Peters, Analytical Chemistry, 72 (2000) 1224.

[189] J.P. Ma, M.Y. Ding, Y. Xu, L.X. Chen, Analytical Sciences, 23 (2007) 371.

[190] S. Scarmagnani, Z. Walsh, F. Benito Lopez, C. Slater, M. Macka, B. Paull, D. Diamond, e-Journal of Surface Science and Nanotechnology, 7 (2009) 649.

[191] B. Ranby, International Journal of Adhesion and Adhesives, 19 (1999) 337.

[192] B. Ranby, W.T. Yang, O. Tretinnikov, 3rd International Symposium on Ionizing Radiation and Polymers (IRaP 98), Weinbohla, Germany, 1998, p. 301.

[193] S. Scarmagnani, Z. Walsh, C. Slater, N. Alhashimy, B. Paull, M. Macka, D. Diamond, Journal of Materials Chemistry, 18 (2008) 5063.

[194] W.L. Zhao, E.M. Carreira, Organic Letters, 7 (2005) 1609.

[195] R. Bertelson, Organic Photochromic and Thermochromic Compounds, Plenum Press, New York, 1999.

[196] G. Such, R.A. Evans, L.H. Yee, T.P. Davis, Journal of Macromolecular Science-Polymer Reviews, C43 (2003) 547.

[197]   A. Radu, S. Scarmagnani, R. Byrne, C. Slater, K.T. Lau, D. Diamond, Journal of Physics D-Applied Physics, 40 (2007) 7238.

[198]   R. Matsushima, M. Nishiyama, M. Doi, Journal of Photochemistry and Photobiology A:Chemistry, 139 (2001) 7.

[199]   F. Benito-Lopez, S. Scarmagnani, Z. Walsh, B. Paull, M. Macka, D. Diamond, Sensors and Actuators B-Chemical, 140 (2009) 295.

[200]   A.A. Garcia, S. Cherian, J. Park, D. Gust, F. Jahnke, R. Rosario, Journal of Physical Chemistry A, 104 (2000) 6103.

[201]   C.P. McCoy, L. Donnelly, D.S. Jones, S.P. Gorman, Tetrahedron Letters, 48 (2007) 657.

[202]   S. Yoshioka, S. Kinoshita, Journal of the Optical Society of America a-Optics Image Science and Vision, 23 (2006) 134.

[203]   L.M. Mathger, R.T. Hanlon, Biology Letters, 2 (2006) 494.

[204]   A. Pauw, American Journal of Botany, 93 (2006) 917.

[205]   A. Radu, R. Byrne, N. Alhashimy, M. Fusaro, S. Scarmagnani, D. Diamond, Journal of Photochemistry and Photobiology a-Chemistry, 206 (2009) 109.

[206]   R.H. Yang, K.A. Li, K.M. Wang, F.L. Zhao, N. Li, F. Liu, Analytical Chemistry, 75 (2003) 612.

[207]   V.A. Krongauz, A. Golinelli, Polymer Bulletin, 6 (1982) 259.

[208]   Y. Kalisky, T.E. Orlowski, D.J. Williams, Journal of Physical Chemistry, 87 (1983) 5333.

[209]   M.Q. Zhu, L.Y. Zhu, J.J. Han, W.W. Wu, J.K. Hurst, A.D.Q. Li, Journal of the American Chemical Society, 128 (2006) 4303.

[210]   K.D. Bartle, M.G. Cikalo, M.M. Robson, in: K.D. Bartle, P. Myers (Eds.), Capillary Electrochromatography, Royal Society of Chemistry, Cambridge, 2001, p. 1.

[211]   L. Zhang, G. Ping, L. Zhang, W. Zhang, Y. Zhang, Journal of Separation Science, 26 (2003) 6.

[212]   J. Dong, C.H. Xie, R.J. Tian, R.N. Wu, J.W. Hu, H.F. Zou, Electrophoresis, 26 (2005) 3452.

[213]   C.J. Drummond, D.N. Furlong, Journal of the Chemical Society-Faraday Transactions, 86 (1990) 3613.

[214]   J. Kabatc, B. Jedrzejewska, J. Paczkowski, Journal of Polymer Science Part a-Polymer Chemistry, 41 (2003) 3017.

[215]   N.F. Yin, K. Killeen, R. Brennen, D. Sobek, M. Werlich, T.V. van de Goor, Analytical Chemistry, 77 (2005) 527.

[216]   J. Kabatc, B. Jedrzejewska, J. Paczkowski, Journal of Polymer Science Part a-Polymer Chemistry, 38 (2000) 2365.

[217]   J. Kabatc, B. Jedrzejewska, J. Paczkowski, Journal of Applied Polymer Science, 99 (2006) 207.

[218]   S. Chatterjee, P. Gottschalk, P.D. Davis, G.B. Schuster, Journal of the American Chemical Society, 110 (1988) 2326.

[219]   S. Murphy, X.Q. Yang, G.B. Schuster, Journal of Organic Chemistry, 60 (1995) 2411.

[220]   G.B. Schuster, X.Q. Yang, C.F. Zou, B. Sauerwein, Journal of Photochemistry and Photobiology a-Chemistry, 65 (1992) 191.

[221]   S. Eeltink, F. Svec, J.M.J. Frechet, Electrophoresis, 27 (2006) 4249.

[222]   J. Kabatc, J. Paczkowski, Journal of Photochemistry and Photobiology a-Chemistry, 184 (2006) 184.

[223]   I.R. Gould, D. Shukla, D. Giesen, S. Farid, Helvetica Chimica Acta, 84 (2001) 2796.

[224]   I. Nischang, F. Svec, J.M.J. Frechet, Journal of Chromatography A, 1216 (2009) 2355.

[225]   C.G. Horvath, B.A. Preiss, S.R. Lipsky, Analytical Chemistry, 39 (1967) 1422.

[226]   C.W. Huck, G.K. Bonn, Chemical Engineering & Technology, 28 (2005) 1457.

[227]   Y.F. Maa, C. Horvath, Journal of Chromatography, 445 (1988) 71.

[228]   G. Moad, D.H. Soloman, The Chemistry of Radical Polymerization, Elsevier, Amsterdam, 2005, p. 49.

[229]   F. Lime, K. Irgum, Macromolecules, 40 (2007) 1962.

[230]   Z. Walsh, S. Abele, B. Lawless, D. Heger, P. Klan, M.C. Breadmore, B. Paull, M. Macka, Chemical Communications (2008) 6504.

[231]   T. Corrales, F. Catalina, C. Peinado, N.S. Allen, Journal of Photochemistry and Photobiology a-Chemistry, 159 (2003) 103.

[232]   N. Emami, K.J.M. Soderholm, Journal of Materials Science-Materials in Medicine, 16 (2005) 47.

[233]   J. Jakubiak, J. Nie, L.A. Linden, J.F. Rabek, Journal of Polymer Science Part a-Polymer Chemistry, 38 (2000) 876.

[234]   V.K. Krishnan, V. Yamuna, Journal of Oral Rehabilitation, 25 (1998) 747.

[235]   J.D. Oxman, D.W. Jacobs, M.C. Trom, V. Sipani, B. Ficek, A.B. Scranton, Journal of Polymer Science Part a-Polymer Chemistry, 43 (2005) 1747.

[236]   Q. Yu, S. Nauman, J.P. Santerre, S. Zhu, Journal of Materials Science, 36 (2001) 3599.

[237]   D.A. Mair, M. Rolandi, M. Snauko, R. Noroski, F. Svec, J.M.J. Frechet, Analytical Chemistry, 79 (2007) 5097.

[238]   A.R. Ivanov, L. Zang, B.L. Karger, Analytical Chemistry, 75 (2003) 5306.

[239]   A. Premstaller, H. Oberacher, W. Walcher, A.M. Timperio, L. Zolla, J.P. Chervet, N. Cavusoglu, A. van Dorsselaer, C.G. Huber, Analytical Chemistry, 73 (2001) 2390.

[240]   S. Xie, R.W. Allington, F. Svec, J.M.J. Frechet, Journal of Chromatography A, 865 (2000) 169.

[241]   S. Stitzel, R. Byrne, D. Diamond, Journal of Materials Science, 41 (2006) 5841.

8. Appendix

List of Publications and Conference Proceedings from the Thesis

1. Silvia Scarmagnani, Zarah Walsh, Nameer Alhashimy, Aleksandar Radu, Brett Paull, Mirek Macka and Dermot Diamond, *Beads-based system for optical sensing using spiropyran photoswitches*, 2007 ANNUAL INTERNATIONAL CONFERENCE OF THE IEEE ENGINEERING IN MEDICINE AND BIOLOGY SOCIETY, VOLS 1-16, (2007) 4096-4097

2. Silvia Scarmagnani, Zarah Walsh, Conor Slater, Nameer Alhashimy, Brett Paull, Mirek Macka and Dermot Diamond, *Polystyrene bead-based system for optical sensing using spiropyran photoswitches*, Journal of Materials Chemistry, 2008, 18, 5063-5071

3. Zarah Walsh, Silvija Abele, Brian Lawless, Dominik Heger, Petr Klán, Michael C. Breadmore, Brett Paull and Mirek Macka, *Photoinitiated polymerisation of monolithic stationary phases in polyimide coated capillaries using visible region LEDs*, Chemical Communications, 2008, 48, 6504-6506

4. Fernando Benito-Lopez, Silvia Scarmagnani, Zarah Walsh, Brett Paull, Mirek Macka and Dermot Diamond, *Spiropyran modified micro-fluidic chip channels as photonically controlled self-indicating system for metal ion accumulation and release*, Sensors and Actuators B: Chemical, 2009, 140, 295-303

5. Silvia Scarmagnani, Zarah Walsh, Fernando Benito López, Conor Slater, Mirek Macka, Brett Paull and Dermot Diamond, *Photoswitchable Stationary Phase Based on Packed Spiropyran Functionalized Silica Microbeads*, e-Journal of Surface Science and Nanotechnology, 2009, 7, 649-652

6. Silvia Scarmagnani, Conor Slater, Fernando Benito-Lopez, Dermot Diamond, Zarah Walsh, Brett Paull and Mirek Macka, *Photoreversible ion-binding using*

spiropyran modified silica microbeads, International Journal of Nanomanufacturing, 2010, 5, 38-52

7. Zarah Walsh, Pavel A. Levkin, Vijay Jain, Brett Paull, Frantisek Svec and Mirek Macka, *Visible light initiated polymerisation of styrenic monoliths using blue light emitting diodes*, Journal of Separation Science, 2010, 33, 61-66

8. Zarah Walsh, Mercedes Vázquez, Fernando Benito-López, Brett Paull, Mirek Macka, Frantisek Svec and Dermot Diamond, *The Use of Scanning Contactless Conductivity Detection for the Characterisation of Stationary Phases in Micro-Fluidic Chips*, Lab on a Chip, submitted

9. Zarah Walsh, Silvia Scarmagnani, Fernando Benito-Lopez, Silvija Abele, Conor Slater, Fu-Qiang Nie, Robert Byrne, Dermot Diamond, Brett Paull and Mirek Macka, *Photochromic spiropyran monolithic polymers: molecular photo-controllable electroosmotic pumps for micro-fluidic devices*, Sensors and Actuators B: Chemical, Submitted

List of Conference Posters Presented or Contributed to by Author

Presenting Author is italicised.

1. *Silvia Scarmagnani*, Zarah Walsh, Nameer Alhashimy, Aleksandar Radu, Mirek Macka, Brett Paull, Dermot Diamond, *Beads-Based System for Optical Sensing Using Spiropyran Photoswitches*, Proc. 29[th]Annual International Conference of the IEEE Engineering in Medicine and Biology Society, August 23rd-26th 2007, Lyon, France.

2. *Zarah Walsh*, Silvija Abele, Brett Paull, Mirek Macka., *UV, Visible and NIR-LEDs for photopolymerisations and photografting of monoliths*, 32nd International Symposium on Capillary Chromatography, May 27th-June 2nd 2008, Riva del Garda, Italy.

3. Silvia Scarmagnani, Zarah Walsh, Fernando Benito-López, Conor Slater, Mirek Macka, Brett Paull, Dermot Diamond, *Spiropyran functionalised microbeads for photodynamic separation science*, 5th International Symposium on Surface Science and Nanotechnology, November 9th-13th 2008, Tokyo, Japan.

4. Zarah Walsh, Silvija Abele, Marketá Ryvolová, Tomasz Piasecki, Jan Preisler, Pavel Krásenský, František. Foret, Peter C. Hauser, Brett Paull, Brian Lawless, Dermot Brabazon, Michael Oelgemoeller, Mirek Macka, *Shedding LED light on synergies between analytical science, miniaturisation, photochemistry, and photonics*, CECE 2008, November 24th- 25th 2008, Brno, Czech Republic.

5. Zarah Walsh, Silvija Abele, Marketá Ryvolová, Tomasz Piasecki, Jan Preisler, Pavel Krásenský, František. Foret, Peter C. Hauser, Brett Paull, Brian Lawless, Dermot Brabazon, Michael Oelgemoeller, Mirek Macka, *Shedding LED light on synergies between analytical science, miniaturisation, photochemistry, and photonics*, ASASS 2008, December 8th- 10th 2008, Hobart, Australia.

6. Zarah Walsh, Uğis Daŋiļēvičs, Tomasz Piasecki, Silvija Abele, Brett Paull, Mirek Macka, *Monoliths in Capillary and Microfluidic Chip Formats for Bioseparations: Examples of Fabrication and Modifications*, International Conference on Trends in Bioanalytical Sciences and Biosensors (ICTBSB 2009), January 26th-27th 2009, Dublin, Ireland.

7. Fernando Benito-López, Silvia Scarmagnani, Zarah Walsh, Brett Paull, Mirek Macka, Dermot Diamond, *Spiropyran Modified PDMS Micro-Fluidic Chip Device for Photonically Controlled Sensor Array Detection of Metal Ions*, International Conference on Trends in Bioanalytical Sciences and Biosensors (ICTBSB 2009), January 26th-27th 2009, Dublin, Ireland.

8. Zarah Walsh, Silvija Abele, Pavel A. Levkin, Brett Paull, František Švec, Mirek Macka, *Visible Light Initiated Polymerisation of Monolithic Stationary Phases using Light Emitting Diodes*, 33rd International Symposium on Capillary Chromatography & Electrophoresis, May 18th-21st 2009, Portland, OR, USA.

9. Silvija Abele, Zarah Walsh, Oksana Yavorska, Mirek Macka, *New Formats of Photoinitiated Polymerisations Utilising LEDs as Light Sources*, 33rd International Symposium on Capillary Chromatography & Electrophoresis, May 18th-21st 2009, Portland, OR, USA

10. Silvia Scarmagnani, Zarah Walsh, Fernando Benito-López, Silvija Abele, Mirek Macka, Brett Paull, Dermot Diamond, *Incorporation of Spiropyran Photochromic Compounds and Spiropyran Modified Substrates in Flow Systems*, Royal Society of Chemistry Analytical Research Forum, July 13th-15th 2009, Canterbury, UK.

11. Zarah Walsh, Pavel A. Levkin, Dominik Heger, Michael Norton, Silvija Abele, František Švec, Petr Klán, Brett Paull, Mirek Macka, *Making monoliths with visible LED light sources*, Vitamins 2009, August 31st-September 2nd 2009, Brno, Czech Republic.

12. Uğis Daņiļēvičs, Zarah Walsh, Silvija Abele, Brett Paull, Mirek Macka, *Exotic monolith: gold-coated silica and polymer monoliths*, 21st International Ion Chromatography Symposium, September 21st-24th 2009, Dublin, Ireland.

13. Zarah Walsh, Silvia Scarmagnani, Michael Norton, Fernando Benito-López, Fu-Qiang Nie, Silvija Abele, František Švec, Dermot Diamond, Brett Paull, Mirek Macka, *Dye Based and Dye Functionalised Monolithic Materials for Chromatography and Electroosmotic Pumps*, 21st International Ion Chromatography Symposium, September 21st-24th 2009, Dublin, Ireland.

List of Conference Talks Presented or Contributed to by Author

First Author is italicised.

1. Zarah Walsh, Damian Connolly, Silvija Abele, Nameer Alhashimy, Silvia Scarmagnani, Brett Paull, Dermot Diamond, Mirek Macka, *Elution with light: Photochromic monolithic stationary phase with light switchable retention*, 31st International Symposium on High Performance Liquid Phase Separations and Related Techniques (HPLC 2007), June 17th-21st 2007, Gent, Belgium.

2. Zarah Walsh, Marco Grundmann, Damian Connolly, Silvija Abele, Fu-Qiang Nie, Brett Paull, Mirek Macka, *Exotic monoliths for separation science and beyond*, 31st International Symposium on High Performance Liquid Phase Separations and Related Techniques (HPLC 2007), June 17th-21st 2007, Gent, Belgium.

3. Zarah Walsh, Damian Connolly, Silvija Abele, Nameer Alhashimy, Dermot Diamond, Brett Paull, Mirek Macka, *Monolithic photochromic stationary phase with light switchable retention*, Royal Society of Chemistry Analytical Research Forum, July 16th-18th 2007, Glasgow, UK.

4. Emma Harvey, Silvija Abele, Zarah Walsh, Damian Connolly, Fu-Qiang Nie, Brett Paull, Mirek Macka, *Porous monoliths for separation science and beyond*, Royal Society of Chemistry Analytical Research Forum, July 16th-18th 2007, Glasgow, UK.

5. Silvija Abele, Anna Stjernlöf, Sebastien Mehlen, Mark Loane, Zarah Walsh, Thomas Kelly, Fu-Qiang Nie, Leon Barron, Nigel Kent, Brian Lawless, Brett Paull, Mirek Macka, *Light emitting diodes and Diode Lasers in Analytical and Separation Science*, Photonics Ireland 2007, September 23rd-26th 2007, Galway, Ireland.

6. Zarah Walsh, Silvia Scarmagnani, Silvija Abele, Nameer Alhashimy, Dermot Diamond, Brett Paull, Mirek Macka, *Monolithic photochromic stationary phase with light switchable retention: Study of covalent linkage to the underlying monolithic scaffold*, 59th Pittsburgh Conference on Analytical Chemistry and Applied Spectroscopy (Pittcon), March 2nd-7th 2008, New Orleans USA.

7. Silvia Scarmagnani, Zarah Walsh, Nameer Alhashimy, Silvija Abele, Damian Connolly, Brett Paull, Mirek Macka, Dermot Diamond, *Beads-based system for optical sensing using molecular photoswitches*, 59th Pittsburgh Conference on Analytical Chemistry and Applied Spectroscopy (Pittcon), March 2nd-7th 2008, New Orleans USA.

8. Silvia Scarmagnani, Zarah Walsh, Nameer Alhashimy, Silvija Abele, Damian Connolly, Brett Paull, Mirek Macka, Dermot Diamond, *Beads-based system for optical sensing using spiropyran photoswitches,* 29th Annual International Conference of the Institute of Electrical and Electronics Engineering: Engineering in Medicine and Biology Society, August 22nd-26th 2007, Lyon, France.

9. Fernando Benito-López, Silvia Scarmagnani, Zarah Walsh, Brett Paull, Mirek Macka, Dermot Diamond, *Spiropyran Modified Microfluidic Chip Channels for Photonically Controlled Sensor Array Detection of Metal Ions*, 3rd International Conference on Smart Materials, Structures And Systems (CIMTEC'08), June 9th-13th 2008, Acireale, Sicily.

10. Zarah Walsh, Silvija Abele, Brett Paull, Mirek Macka, *Photo-Initiated Polymerisation of Monolithic Stationary Phases using Visible Light Emitting LEDs*, 32nd International Symposium on Capillary Chromatography, May 27th-June 2nd 2008, Riva del Garda, Italy

11. Uǧis Daņiḷēvičs, Zarah Walsh, Silvija Abele, Sebastien Cueff, Barry S. O'Connell, Brett Paull, Mirek Macka, *Preparation and Characterisation of a Gold Nano-layer Coated Silica 'Exotic' Monolith*, 32nd International Symposium on Capillary Chromatography, May 27th-June 2nd 2008, Riva del Garda, Italy

12. Uǧis Daņiḷēvičs, Zarah Walsh, Petr Smejkal, Jana Křenková, Silvija Abele, František Foret, Mirek Macka, *Approaches to creating gold nano-layer modified monoliths by deposition of Au-nanoparticles from solutions*, 32nd International Symposium on Capillary Chromatography, May 27th-June 2nd 2008, Riva del Garda, Italy

13. Zarah Walsh, Silvija Abele, Brian Lawless, Dominik Heger, Petr Klán, Silvia Scarmagnani, Michael C. Breadmore, Dermot Diamond, Brett Paull, Mirek Macka, *Visible Light Initiated Polymerisation of Monolithic Stationary Phases in Polyimide Coated Capillaries using Light Emitting Diodes*, 20th International Ion Chromatography Conference, September 21st-24th 2008, Portland, OR, USA.

14. Uģis Daņiļēvičs, Silvija Abele, Zarah Walsh, Brett Paull, Mirek Macka, *Layer-By-Layer (LbL) Method – New Approach In Creating Gold Nano-Particle Modified Monolithic Columns*, International Conference on Trends in Bioanalytical Sciences and Biosensors, January 26th-27th 2009, Dublin, Ireland.

15. Zarah Walsh, Silvija Abele, Brian Lawless, Dominik Heger, Petr Klán, Silvia Scarmagnani, Michael C. Breadmore, Dermot Diamond, Brett Paull, Mirek Macka, *Use of light emitting diodes in the visible region to initiate polymerisation leading to monolithic stationary phases*, 33rd International Symposium on Capillary Chromatography & Electrophoresis, May 18th-21st 2008, Portland, OR, USA.

16. Zarah Walsh, Silvia Scarmagnani, Fernando. Benito-López, Silvija Abele, Dermot Diamond, Brett Paull, Mirek Macka, *Photo-controllable electroosmotic pumps based on spiropyran polymeric monoliths for micro-fluidic devices*, 34th International Symposium on High-Performance Liquid Phase Separations and Related Techniques (HPLC 2009), June 28th-July 2nd 2009, Dresden, Germany.

17. Zarah Walsh, Pavel A. Levkin, Brett Paull, František Švec, Mirek Macka, *Preparation of styrenic monoliths using initiation with visible light emitting diodes at 470 nm*, 34th International Symposium on High-Performance Liquid Phase Separations and Related Techniques (HPLC 2009), June 28th-July 2nd 2009, Dresden, Germany.

18. Mirek Macka, Zarah Walsh, Silvija Abele, Pavel A. Levkin, František Švec, Brett Paull, Dominik Heger, Petr Klán, *Photoinitiated Polymerisations of Monoliths with UV and Visible LED Light Sources*, 34th International Symposium on High-Performance Liquid Phase Separations and Related Techniques (HPLC 2009), June 28th-July 2nd 2009, Dresden, Germany.

19. Uģis Daņiļēvičs, Silvija Abele, Zarah Walsh, Brett Paull, Mirek Macka, *Layer-by-Layer (LbL) method as an approach for creating gold nano-particle modified polymer monolithic columns*, Euroanalysis 2009, September 6th-10th 2009, Innsbruck, Austria.

20. Uǧis Daņiļēvičs, Silvija Abele, Zarah Walsh, Brett Paull, Mirek Macka, Lenka Krčmová, *Gold nanoparticle modified monolithic silica columns: preparation and characterisation*, 21st International Ion Chromatography Symposium, September 21st-24th 2009, Dublin, Ireland.

21. Silvia Scarmagnani, Zarah Walsh, Fernando Benito-López, Mirek Macka, Brett Paull, Dermot Diamond, *Immobilisation and incorporation of photochromic spiropyran dyes in polymeric substrates for metal ion sensing and micro-fluidics*, 21st International Ion Chromatography Symposium, September 21st-24th 2009, Dublin, Ireland.